Peabody Museum of Natural History
Yale University
Bulletin 22

Shell Structure of Patelloid and Bellerophontoid Gastropods (Mollusca)

by
Copeland MacClintock

SHELL STRUCTURE OF PATELLOID AND BELLEROPHONTOID GASTROPODS (MOLLUSCA)

Bulletins published by the Peabody Museum of Natural History at Yale University embody research carried out under the auspices of the Museum. The issues are numbered consecutively as independent monographs and appear at irregular intervals. Shorter papers are published at frequent intervals in the Peabody Museum *Postilla* Series.

Communications concerning purchase or exchange of publications should be addressed to the Editor, Peabody Museum of Natural History, Yale University, New Haven, Connecticut 06520, U.S.A.

Issued 21 February, 1967

PEABODY MUSEUM OF NATURAL HISTORY
YALE UNIVERSITY
BULLETIN 22

Shell Structure of Patelloid and Bellerophontoid Gastropods (Mollusca)

BY
COPELAND MacCLINTOCK

Division of Invertebrate Paleontology
Peabody Museum, Yale University
New Haven, Connecticut

NEW HAVEN, CONNECTICUT
1967

Printed in the United States of America

ERRATA

MacClintock, Copeland, 1967, Shell structure of patelloid and bellerophontoid gastropods (Mollusca): Peabody Museum of Natural History, Yale University, Bull. 22.

Page 4, Text-fig. 2: . . . . . location number 1 should not include margin of shell

Page 39, line 8 from bottom: . . "Fig. 19" should read "Fig. 1"

Page 82, line 18 from bottom . . "Figs. 18, 19" should read "Figs. 1, 2"

Page 86, Table 7: . . . . . *"Nomeopelta"* should read *"Nomaeopelta"*

CONTENTS

ILLUSTRATIONS

TEXT-FIGURES

ILLUSTRATIONS

TEXT-FIGURES

PLATES

TABLES

KEY

YALE UNIVERSITY PEABODY MUSEUM OF NATURAL HISTORY BULLETIN
NO. 22, 140 P., 32 PLS., 128 TEXT-FIGS., 1967

SHELL STRUCTURE OF PATELLOID AND BELLEROPHONTOID GASTROPODS (MOLLUSCA)

BY COPELAND MACCLINTOCK

ABSTRACT

The currently accepted suprageneric classification of Recent patelloid archaeogastropods is based largely on radula and gill morphology, with relatively little consideration given to the shell. Because variations of the simple conical shell shape are repeated in each of the major taxa, accurate systematic evaluation of fossil patelloids is extremely difficult. Existing phylogenies have been based primarily on soft-part relations among living forms. Given in the present study are detailed descriptions and analyses of the microstructure and shell-layer relationships of Recent and fossil gastropods of the primitive superfamilies Patelloidea and Bellerophontoidea.

Of all the molluscan groups of comparable taxonomic size, the patelloids have the most complex and diverse shell structures and yet the simplest shell form (low conical). Shells of 121 patelloid species from around the world were examined. Four basic types of patelloid shell structures are recognized here: (1) *Prismatic*—major and minor crystals oriented at an angle greater than 10° to growth surfaces; (2) *Foliated*—thin sheets of calcium carbonate intersecting growth surfaces at an angle less than 10°; (3) *Crossed*—crossed-lamellar of Bøggild and crossed-foliated, here defined as similar to crossed-lamellar but with a lower angle of cross of second-order lamellae and wider first-order lamellae; (4) *Complex crossed*—complex crossed-lamellar of Bøggild and complex crossed-foliated, here defined as similar to complex crossed-lamellar but with a much lower dip angle of conical second-order lamellae.

Individual patelloid shells are composed of from four to six shell layers, depending on the species. Shell layers become thicker with growth and cut across growth layers. Each shell layer is characterized by either a structure different from that of adjacent layers or, where the structure is the same, by corresponding major structural elements oriented at right angles to each other. Variations of these structures and different sequential combinations of layers, relative to the myostracum (muscle-scar shell layer), are the basis for the recognition of 17 taxonomically informal shell-structure groups. Most of these groups conform to previously accepted taxonomic boundaries, although some do not. In general, shells of the two major patelloid families (Acmaeidae and Patellidae) can be recognized by the presence of certain diagnostic shell structures: acmaeids have a fibrillar (variety of prismatic) layer in the sequence of layers between the myostracum and the dorsal surface of the shell; whereas patellids have foliated or crossed-foliated layers in the sequence dorsal to the myostracum. Because the present systematic study of patelloid shell structure has provided the information necessary for establishing relationships between fossil and Recent forms, it now seems probable that, given enough well-preserved shells throughout the post-Ordovician fossil history of the patelloids, a more accurate phylogeny of the group can be developed.

Several species of Paleozoic bellerophontoid gastropods have been described previously as having nacreous, foliated, and prismatic shell structures. In the present study, crossed-lamellar structure, previously unrecorded in the suborder Bellerophontina, has been observed for the first time in shells of *Euphemites,* and complex crossed-lamellar structure has been observed in the inner layer of shells of *Bellerophon* (*Pharkidonotus*). These are the earliest (Pennsylvanian) recorded occurrences of crossed and complex crossed structures in the Gastropoda. Taken alone, the structures in these two distantly related bellerophontoids indicate that they are more closely related to the fissurelloids (with inner crossed-lamellar and outer prismatic layers) than they are to the pleurotomarioids (with inner nacreous and outer prismatic layers). If with further study the structures of the three species examined are found to be representative of the group as a whole, then the suborder Bellerophontina should be subjected to a systematic re-evaluation.

SHELL STRUCTURE OF PATELLOID AND BELLEROPHONTOID GASTROPODS (MOLLUSCA)*

COPELAND MACCLINTOCK

INTRODUCTION

The microstructure of the mollusk shell is a neglected but potentially useful feature in molluscan systematic and evolutionary studies. In one of the few examples of a thorough integration of shell-structures into formal systematic descriptions and a classification of a group of fossil mollusks, Newell (1938, 1942) successfully employed shell structures in his studies of late Paleozoic pectinoid and mytiloid pelecypods.

In the absence of soft parts and systematically significant external morphologic features in fossil patelloid shells, it appears that shell structures will provide the only reliable clues to accurate systematic evaluations of fossil patelloids. In his classification of the patelloids, Pilsbry (1891) made use of the texture and luster of the inner surface of the shell. Such terms as porcelaneous, fibrous, pellucid, opalescent, metallic and micaceous were used in his suprageneric descriptions. For obvious reasons these terms can be misleading. In some cases shells having different kinds of shell structure may appear to have the same texture or luster. Shells having identical structure may have different textures because of surficial weathering or internal clouding of the organic matrix of the shell. Fossil shells which may have lost their organic matrix or which have been partially recrystallized will lose the texture or luster characteristic of Recent shells having an identical shell structure. Thiem (1917b) used shell structures in his systematic descriptions of several species of the family Acmaeidae. However, the work was of limited value because he studied shells from only three of the presently recognized 17 patelloid shell-structure groups. Bøggild (1930), in his classic monograph on molluscan shell structure, described the structure of 15 patelloid species representing eight of the 17 presently recognized groups. He made no attempt, however, to incorporate the information into a classification of patelloids, and concluded that only after intensive work on the group would shell structures be useful in their classification. The main purposes of the present study are to add to Bøggild's basic data on adult shells, to determine also if there is a correlation between groups based on shell structures and those based on soft parts, and then to discuss the phylogenetic implications. Although no attempt is made to determine the mineralogy of the shell layers, it is assumed that the inorganic material in the shell is either calcite or aragonite. A short part of this report is devoted to the shell structure of bellerophontoid gastropods.

Recent and fossil shells on which this study is based are in the collections of the University of California Museum of Paleontology (abbreviated as UCMP) in Berkeley, the Department of Geology, California Academy of Sciences (CAS) in San Francisco, the Division of Invertebrate Zoology, Peabody Museum, Yale University (YPM) in New Haven, Connecticut, the invertebrate type collection of the San Diego Natural History Museum (SDNHM) in San Diego, California, and the Division of Invertebrate Paleontology, United States National Museum (USNM) in Washington, D. C. Identification of all shells was checked before study. As defined here, a *hypotype* is any figured, or individually mentioned or

*Published with the aid of a National Science Foundation Publication Grant, No. GN-528.

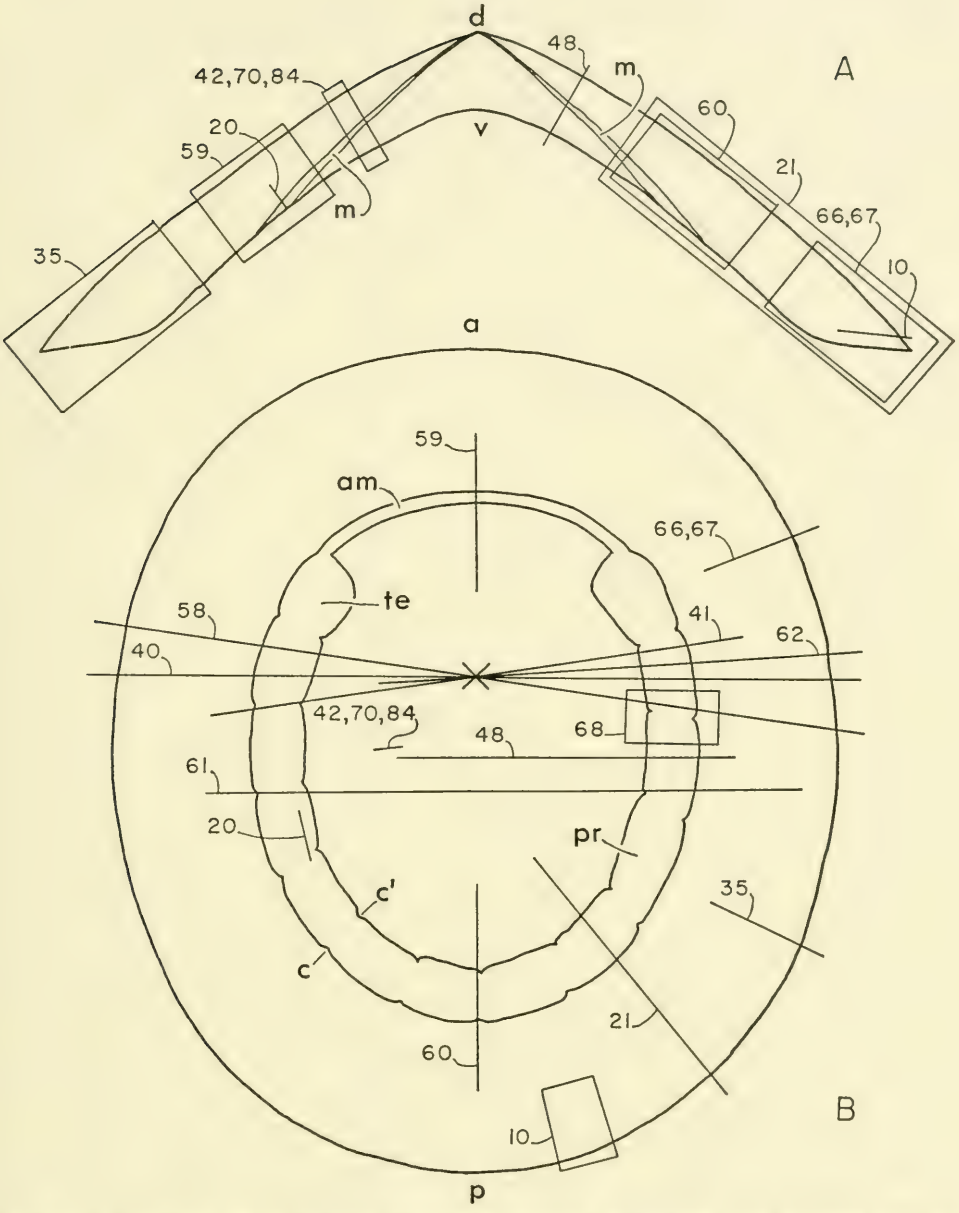

Text-fig. 1.—Location of all patelloid text-figures requiring description. The numbers refer directly to text-figures. A, generalized cross section indicating vertical, radial sections anywhere in the shell. B, ventral view. Explanation of symbols: a, anterior; am, anterior mantle-attachment scar; cc′, constriction in scar; d, dorsal; m, myostracum; p, posterior; pr, pedal-retractor scar; te, terminal enlargement of pedal-retractor scar; v, ventral; ×, position of apex on dorsal surface.

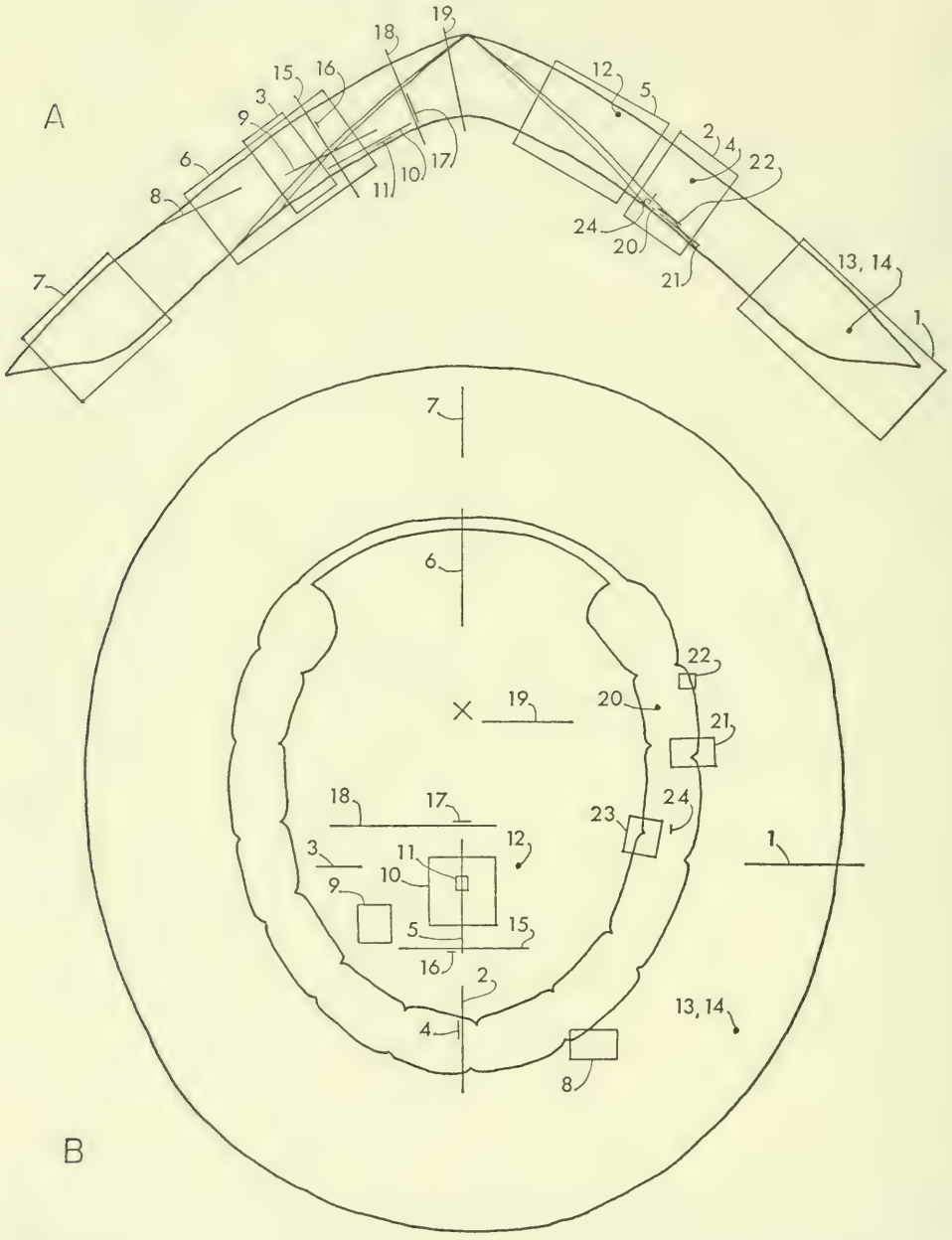
A
19
18
15
16
3
9
6
8
11
10
17
12
5
2
4
22
24
20
21
13, 14
1
7
B
7
6
22
19
20
21
18
17
23
24
3
11
12
1
10
9
5
15
16
2
13, 14
4
8

Text-fig. 2.

Text-fig. 2.—Location of patelloid figures on plates 1-26. Location numbers (1-24 on Text-fig. 2) given on the cross-sectional and ventral views are cross referenced with the plate-figure numbers in the conversion table below. The location numbers are the numbers of the original photographic negatives. A, generalized cross sections indicating vertical, radial sections anywhere in shell. B, ventral view.

Plate	Figure	Location no.
1	1	7
	2	14
	3	107
	4	12
	5	16
	6	8
	7	13
2	1	87
	2	88
	3	86
	4	9
3	1	29
	2	30
	3	22
	4	89
4	1	6
	2	5
	3	17
5	1	18
	2	15
	3	19
6	1	10
	2	11
7	1	26
	2	27
	3	28
8	1	25
	2	24
	3	20
	4	21
9	1	53
	2	55
	3	54
10	1	52
	2	111
11	1	59
	2	58
	3	90
	4	91
	5	91
12	1	60
	2	61
	3	62
13	1	41
	2	51
	3	57
	4	56
14	1	71
	2	72
	3	73
	4	110
15	1	70
	2	74
16	1	68
	2	69
17	1	83
	2	82
18	1	42
	2	43
19	1	44
	2	45
	3	63
	4	64
20	1	85
	2	84
21	1	79
	2	80
	3	81
	4	67
	5	93
	6	94
	7	76
	8	77
	9	75
	10	78
22	1	65
	2	66
	3	95
23	1	36
	2	37
	3	34
	4	33
24	1	2
	2	4
	3	35
25	1	38
	2	39
	3	40
26	1	1
	2	3
	3	23
32		112

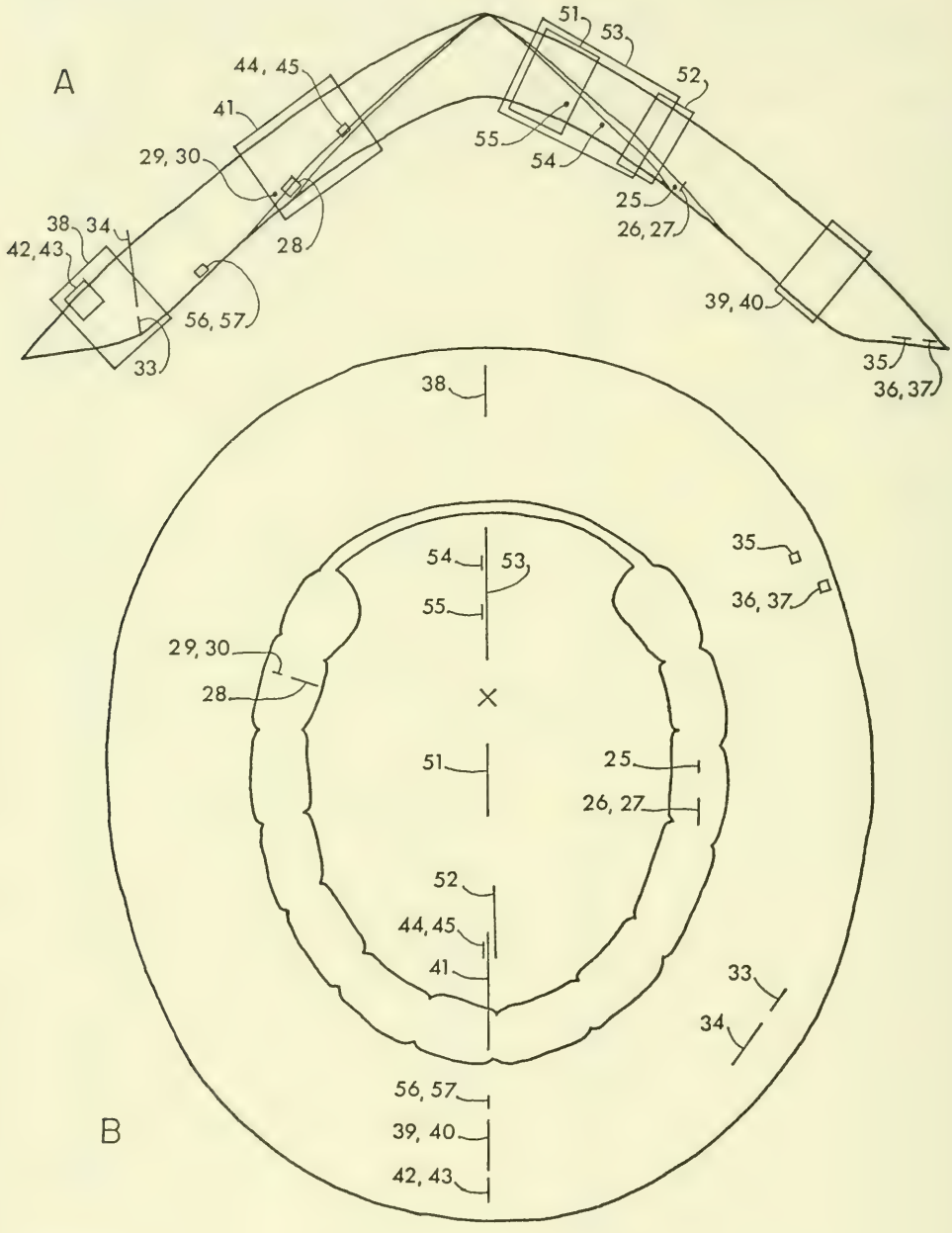
A
51
53
52
44, 45
41
55
54
29, 30
25
26, 27
38
34
42, 43
28
39, 40
56, 57
35
33
36, 37
B
38
35
54
53
36, 37
55
29, 30
28
51
25
26, 27
52
44, 45
41
33
34
56, 57
39, 40
42, 43

Text-fig. 3.

Text-fig. 3.—Location of patelloid figures on plates 1-26. Location numbers (25-57 on Text-fig. 3) given on the cross-sectional and ventral views are cross referenced with the plate-figure numbers in the conversion table below. The location numbers are the numbers of the original photographic negatives. A, generalized cross sections indicating vertical, radial sections anywhere in shell. B, ventral view.

Plate	Figure	Location no.
1	1	7
	2	14
	3	107
	4	12
	5	16
	6	8
	7	13
2	1	87
	2	88
	3	86
	4	9
3	1	29
	2	30
	3	22
	4	89
4	1	6
	2	5
	3	17
5	1	18
	2	15
	3	19
6	1	10
	2	11
7	1	26
	2	27
	3	28
8	1	25
	2	24
	3	20
	4	21
9	1	53
	2	55
	3	54
10	1	52
	2	111
11	1	59
	2	58
	3	90
	4	91
	5	91
12	1	60
	2	61
	3	62
13	1	41
	2	51
	3	57
	4	56
14	1	71
	2	72
	3	73
	4	110
15	1	70
	2	74
16	1	68
	2	69
17	1	83
	2	82
18	1	42
	2	43
19	1	44
	2	45
	3	63
	4	64
20	1	85
	2	84
21	1	79
	2	80
	3	81
	4	67
	5	93
	6	94
	7	76
	8	77
	9	75
	10	78
22	1	65
	2	66
	3	95
23	1	36
	2	37
	3	34
	4	33
24	1	2
	2	4
	3	35
25	1	38
	2	39
	3	40
26	1	1
	2	3
	3	23
32		112

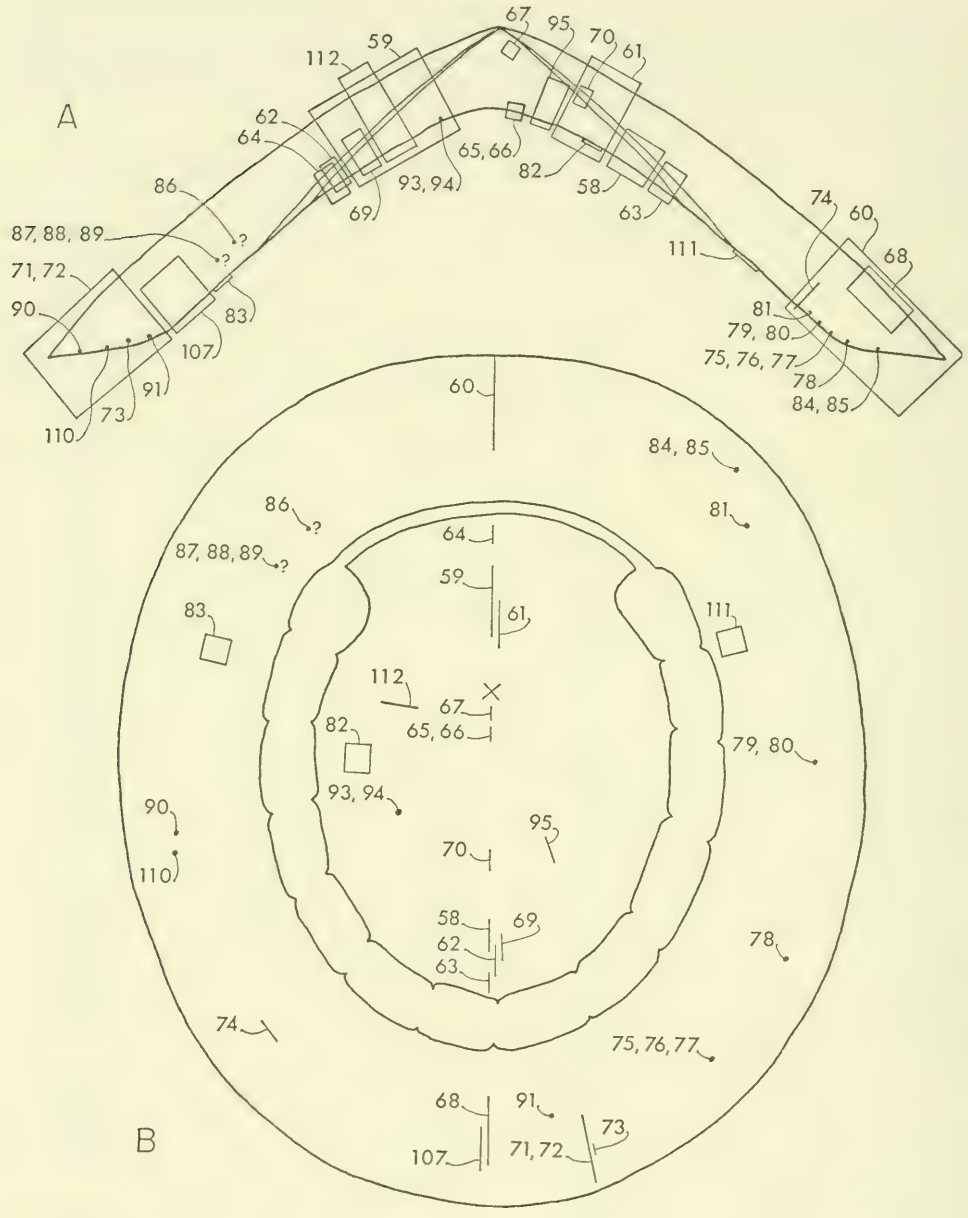
A
67
95
70
61
59
112
62
64
65, 66
82
58
63
74
60
68
111
86
?
87, 88, 89
?
71, 72
90
83
107
91
73
110
69
93, 94
81
79, 80
75, 76, 77
78
84, 85
B
60
84, 85
86
?
87, 88, 89
?
81
64
59
61
83
111
112
67
65, 66
82
79, 80
93, 94
90
110
95
70
58
62
63
69
78
74
75, 76, 77
68
91
73
107
71, 72

Text-fig. 4.

Text-fig. 4.—Location of patelloid figures on plates 1-26 and 32. Location numbers (58-112 on Text-fig. 4) given on the cross-sectional and ventral views are cross referenced with the plate-figure numbers in the conversion table below. The location numbers are the numbers of the original photographic negatives. A, generalized cross sections indicating vertical, radial sections anywhere in shell. B, ventral view.

Plate	Figure	Location no.
1	1	7
	2	14
	3	107
	4	12
	5	16
	6	8
	7	13
2	1	87
	2	88
	3	86
	4	9
3	1	29
	2	30
	3	22
	4	89
4	1	6
	2	5
	3	17
5	1	18
	2	15
	3	19
6	1	10
	2	11
7	1	26
	2	27
	3	28
8	1	25
	2	24
	3	20
	4	21
9	1	53
	2	55
	3	54
10	1	52
	2	111
11	1	59
	2	58
	3	90
	4	91
	5	91
12	1	60
	2	61
	3	62
13	1	41
	2	51
	3	57
	4	56
14	1	71
	2	72
	3	73
	4	110
15	1	70
	2	74
16	1	68
	2	69
17	1	83
	2	82
18	1	42
	2	43
19	1	44
	2	45
	3	63
	4	64
20	1	85
	2	84
21	1	79
	2	80
	3	81
	4	67
	5	93
	6	94
	7	76
	8	77
	9	75
	10	78
22	1	65
	2	66
	3	95
23	1	36
	2	37
	3	34
	4	33
24	1	2
	2	4
	3	35
25	1	38
	2	39
	3	40
26	1	1
	2	3
	3	23
32		112

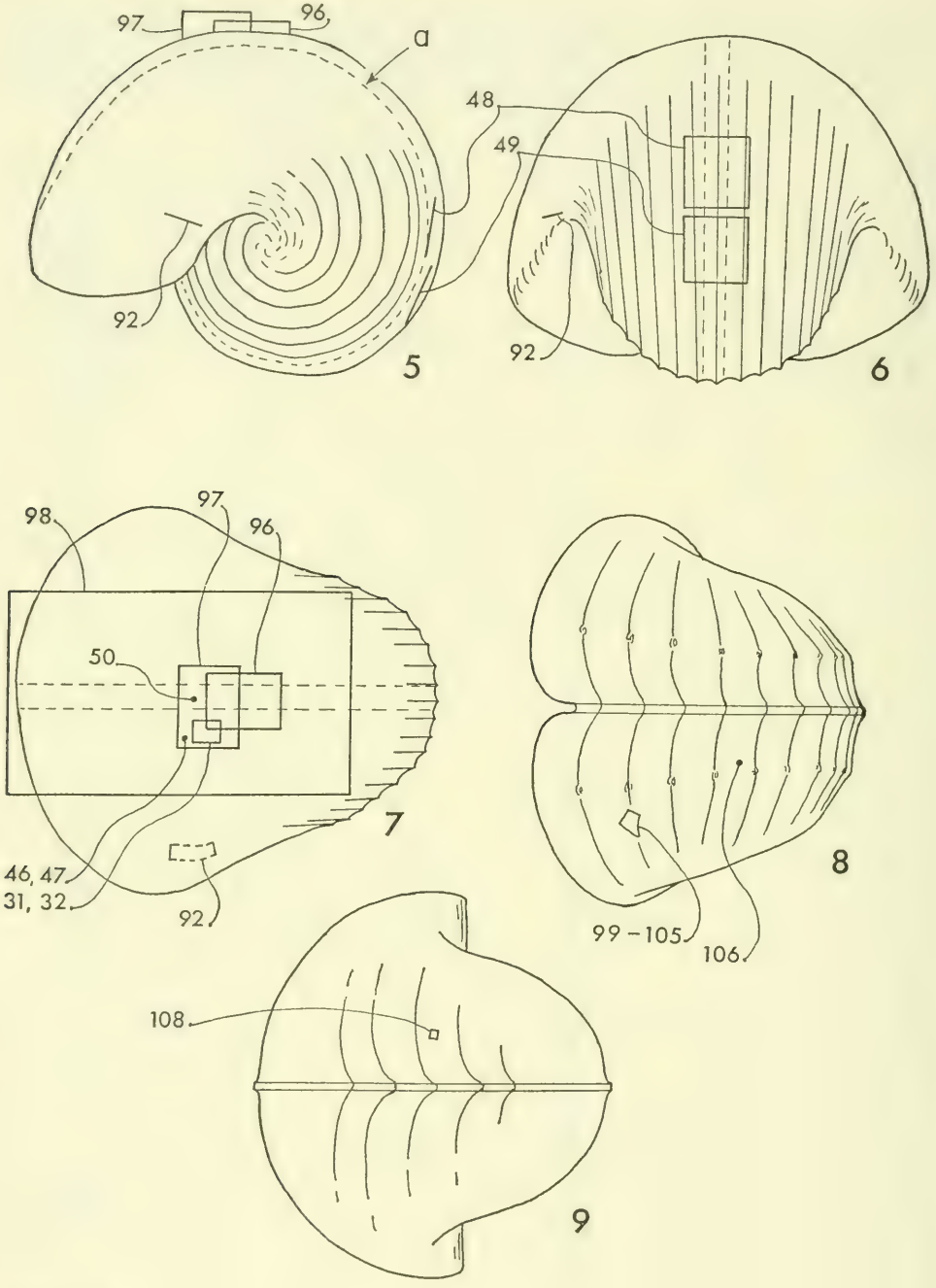

Text-figs. 5-9.

listed specimen other than those on which the taxon was originally based. Each individual animal is given a specimen number, and each slide or isolated fragment from that specimen receives a letter (eg., hypotype, UCMP no. 30112-a). If a single slide is all that remains of the specimen, it does not receive a letter after the number. See Table 5 for additional information on numbering system. A glossary of terms is given near the end of this report.

In its unrevised form this report was submitted in June, 1964, as a dissertation for the degree of Doctor of Philosophy at the University of California (Berkeley).

Following Knight *et al.* (1960) the suprageneric classification of the groups examined is given below. The superfamily ending (-oidea) used here is recommended by the International Commission on Zoological Nomenclature (Stoll, 1961).

Class **GASTROPODA** Cuvier
- Subclass PROSOBRANCHIA Milne Edwards
  - Order ARCHAEOGASTROPODA Thiele
    - Suborder BELLEROPHONTINA Ulrich and Scofield
      - Superfamily BELLEROPHONTOIDEA M'Coy
        - Family SINUITIDAE Dall
          - Subfamily EUPHEMITINAE Knight
        - Family BELLEROPHONTIDAE M'Coy
          - Subfamily BELLEROPHONTINAE M'Coy
    - Suborder PATELLINA von Ihering
      - Superfamily PATELLOIDEA Rafinesque
        - Family ACMAEIDAE Carpenter
        - Family PATELLIDAE Rafinesque
          - Subfamily PATELLINAE Rafinesque
          - Subfamily NACELLINAE Thiele
        - Family LEPETIDAE Dall

Text-figs. 5-9.—Location of all bellerophontoid plate-figures. The location numbers (the numbers of the original photographic negatives) are cross referenced with the plate-figure numbers in the conversion table below. 5-7, side, back and top views of *Euphemites vittatus;* dashed line (a) in figure 5 shows inner surface of shell along median plane. 8, top view of *Bellerophon percarinatus.* 9, back view of *Bellerophon* sp.

Plate	Figure	Location no.	Plate	Figure	Location no.
27	1	31	29	3	92
	2	32	30	1	99
	3	50		2	102
	4	46		3	101
	5	47		4	105
28	1	98		5	103
	2	96		6	104
	3	97	31	1	100
29	1	49		2	106
	2	48		4	108

Acknowledgments

To Dr. J. Wyatt Durham, Department of Paleontology, University of California, appreciation is here expressed for suggesting the thesis topic, discussing problems related to the research, and for his critical reading of the manuscript. Acknowledgment is made to Dr. Leo G. Hertlein, Department of Geology, California Academy of Sciences, Dr. Ralph I. Smith, Department of Zoology, University of California, and to Dr. Paul MacClintock, Department of Geology, Princeton University, for critically reading the manuscript. I wish to thank Mr. Allyn G. Smith, Department of Invertebrate Zoology, California Academy of Sciences, and Dr. Hertlein, for checking identifications of west American gastropods and for making available the Hemphill collection of Recent mollusks at that institution. Thanks are also due to Dr. G. Arthur Cooper, Department of Geology, United States National Museum, for his loan of Pennsylvanian bellerophontids; to Dr. Bernard C. Cotton, Curator of Molluscs, The South Australian Museum, for sending to the Univ. of California, in exchange, rare Australian patelloids; to Mr. Emery P. Chase, Curator of Conchology, San Diego Natural History Museum for permission to use the Museum's collection of Recent mollusks; and to my wife, Dorcas, for initially typing and helpfully criticizing the manuscript. Text-figures 26, 39, 43, 47, 62, 63 and 84 were drafted by Miss Martha Dimock. Mr. David M. Keith drafted minor changes on most of the other text-figures.

The Gastropod Shell

Most adult cap-shaped archaeogastropod shells are nearly bilaterally symmetrical. The shell is composed of several conical shell layers which crop out concentrically on the inner surface of the shell. In any one shell all sections through the apex and normal to the aperture ideally show the same sequence of shell layers. The problem of obtaining oriented sections in cap-shaped shells is therefore relatively simple compared to the problem of making oriented sections in conispiral shells. All shell layers are exposed on the ventral surface of the shell where they can be readily studied under the binocular microscope without breaking the shell as would have to be done in conispiral shells if the outcrop area of all the layers were to be exposed. With only a few thin sections, therefore, a relatively complete comparative study can be carried out on the patelloids.

In the attempt to illustrate each of the shell structures in as much detail as possible, it is difficult, even in the patelloids, to describe the exact location and orientation of those parts of sections or fragments from which plate-figures and text-figures are made. Those text-figures requiring a location description are shown in text-figure 1. The locations of all patelloid plate-figures are given in text-figures 2-4. All bellerophontoid plate-figures are located in text-figures 5-9. Where necessary, more detailed information is given in the figure explanations.

The muscle scar is the most important morphological feature on the ventral surface of patelloid shells. *Myostracum* (Text-fig. 1) is a term proposed by Oberling (1955, p. 128) for deposits "secreted over the muscle-attachment areas." The muscle scar, therefore, is that part of the inner surface of the shell where the myostracum crops out.

SHELL STRUCTURES

The following discussion is largely restricted to shell structures found in patelloids and bellerophontoids. Other structures are described only for comparative purposes. Except for the nacreous structure all of the major molluscan structures are present in patelloid shells. Bøggild (1930) described most shell structures in detail, and where his descriptions are adequate the structures are here only briefly redefined. Modifications are introduced only where his discussion is lacking in critical details or where new information indicates the need for changed or additional descriptions. Where new structures are described, an attempt is made to relate them to Bøggild's terminology and concepts. Recent developments in the biochemical aspects of deposition of molluscan shell material have been summarized by Wilbur (1960, 1964).

For the groups studied, *prismatic, foliated, crossed,* and *complex crossed* structures are the four major types of shell structure here recognized. The structures are usually developed in different layers of the shell. Shell layers having a prismatic structure are made up of major and/or minor prismatic elements which are usually oriented at an angle of more than 10° to growth surfaces. Layers with a foliated structure are composed of thin sheets which intersect growth surfaces at an angle of less than 10°. Layers having a crossed structure are composed of major elements each of which contains minor elements oriented at an angle to growth surfaces. In side view, looking through two or more major elements, the minor elements form a cross pattern. Layers having complex crossed structures are composed of major prisms each of which is a series of cones stacked one inside the other. Under each major shell-structure type, several sub-types can be recognized. There is a nearly complete structural gradation not only between the sub-types but between each of the major types.

In all patelloid shells, except in the outermost shell layers of some acmaeids, the shortest dimension of all minor structural elements is less than two μ. The intermediate dimension ranges from two to about 50μ and the longest dimension may be as much as three mm. Thus in the average adult limpet shell there are many millions of individual crystals. Differences in crystal arrangement, both within the layers and from layer to layer, provide for a very strong shell.

Appearing on thin sections are several kinds of lines not all of which are necessarily related to the original shell structure. They are growth lines, contacts between major and minor structural elements, lines indicating cleavage and twinning planes of calcite, scratches, and cracks not paralleling any of the above-mentioned lines. In very thin sections, under crossed nicols, scratches appear as distinct lines having a lower order interference color than the surrounding, slightly thicker, part of the section. None of the other lines, at least in thin sections not etched with acid, cause an abnormal break in the interference colors. Lines produced by cleavage and twinning planes are usually present only on sections of recrystallized shells. While the section is being examined, great care must be taken in the proper interpretation of each kind of line. Any of the above-mentioned lines may also appear on broken (Text-fig. 10) or polished sections.

Prismatic Structures

SIMPLE-PRISMATIC STRUCTURE

Layers having this structure are built up of large blade-shaped single-crystal prisms. The structure was observed only in the outermost layer of the shells of some acmaeid species. The prisms are elongate in the radial direction with their

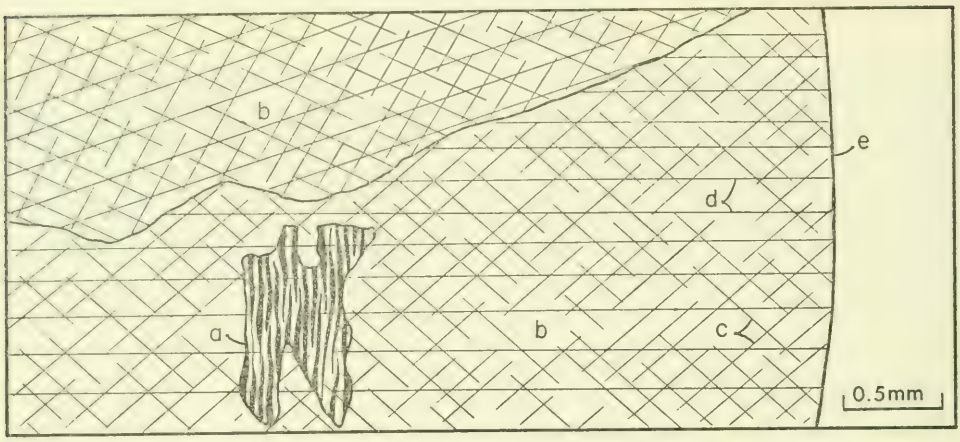

Text-fig. 10.—*Acmaea martinezensis;* area, parallel with growth surface in shell-layer m + 1, exhibiting primary and secondary structural features. Explanation of symbols: a, small area showing concentric crossed-lamellar structure; b, two calcite crystals (products of recrystallization); c, cleavage; d, twinning; e, posterior edge of shell. Based on holotype, UCMP no. 11742.

intermediate axes normal to the shell surface. In nearly tangential section most prisms (Pl. 1, fig. 6) extend from the ventral to the dorsal surface of the layer. In this orientation the prisms are between 200 and 300μ long and between five and 100μ wide. In one vertical, radial section (Pl. 1, fig. 1) a prism 800 $\times$ 70μ was observed. The minor dimension in this instance represents the thickness of the shell layer.

FIBRILLAR STRUCTURE

Layers with this structure (Pl. 1, figs. 1-5) are composed of thin fibril-like crystals with individually constant diameters. The diameter ranges from one to two μ in different crystals. Although the longest isolated fibril is 220μ long, each fibril probably extends from the ventral to the dorsal surface of its layer. At the margin of the shell of *Lottia gigantea,* the largest acmaeid, the reclined fibrils, if continuous through the layer, would be as much as three mm long. In sections normal to the fibrils (Pl. 1, fig. 5) each fibril has a roughly polygonal outline.

Layers composed entirely of fibrils are called fibrillar layers only where all the fibrils, as seen in vertical, radial section, are parallel to each other and have the same orientation with respect to growth lines. In fibrillar layers (Table 1) all fibrils are reclined at an angle ranging from 48°-53° with growth surfaces. This angle can be measured only in vertical, radial sections. If the fibrillar layer of Recent shells is crushed, the axes of the elongate fragments are parallel to the fibrils. If these fragments are mounted on a slide (Pl. 1, fig. 7), the true angle of reclination can be measured only in those fragments which have their vertical, radial plane parallel to the slide. In all other elongate fragments only the apparent reclination angle can be measured. This angle is always larger than the true reclination angle. Therefore, the elongate fragments having the lowest angle between fibrils and growth lines are the ones most nearly showing the true angle of reclination.

In fossil shells where the fibrils are bound together or where partial recrystallization has occurred, the fibrillar structure is harder to identify. In such shells isolated fragments (Pl. 1, figs. 3,4) broken in the vertical, radial direction may

show a "fibrous" texture. If the "fibers" (Table 1) of the "fibrous" texture form an angle of between 48° and 54° with growth lines, it is probable that the fibrillar structure characteristic of acmaeid shells is present.

In shell layers where fibrils tend to be arranged in prisms, the fibrillar structure grades into the complex-prismatic structure.

TABLE 1: Reclination angle (in degrees) between fibrils and growth surfaces in the fibrillar layer of acmaeid shells.

Species	Reclination angle	Shell-structure group
Acmaea instabilis	53°	1
A. limatula	50°	1
*A. saccharina**	51°	2
*A. geometrica***	49°	2
Patella mexicana B. & S.:		
Durham**	53°	1
Scurria scurra	51°	3
Lottia gigantea	48°	1

* fibrils occur in small distinct bundles
** fossils

COMPLEX-PRISMATIC STRUCTURE

The concept of this structure is modified from Bøggild's to include regularly or irregularly shaped first-order prisms which, in turn, contain parallel or fan-shaped aggregates of fibrils or second-order prisms (Pl. 25, fig. 1). Laterally in the layer the fibril aggregates usually have a nearly alternating or alternating orientation (Pl. 23, figs. 1-3) where every other prism may have the same extinction angle. This structure grades into the fibrillar structure.

DEPENDENTLY PRISMATIC STRUCTURE

Layers having this structure are made up of prisms or bundles of prisms which have their optical and structural orientation controlled by the orientation of the structural elements in the overlying shell layer. This is true because the former is deposited on the latter and not *vice versa*.

Foliated Structures

FOLIATED STRUCTURE

Layers having this structure are composed of uniformly thin (about one μ) sheets or folia. The sheets are flat and of equal thickness. In radial section (Pl. 19, fig. 1) the contacts between these sheets resemble uniformly spaced parallel striations. Intersecting the ventral surface of the shell at an angle between 4° and 7°, each sheet crops out (Pl. 17, figs. 1, 2; Text-fig. 17) in a band between eight and 20μ wide. Individual sheets are made up of blades (Pl. 20, figs. 1, 2) which are oriented normal to the outcrop pattern. Bøggild (1930, p. 307) described the structure as "prismatic or foliated, with flat prisms placed horizontally in the concentrical direction." The blades are concentrically arranged, however, only in layers where the outcrop pattern of folia is radial. In layers where the outcrop pattern of folia is concentric the blades are radially arranged. Each blade has

straight, nearly parallel sides. Adjacent blades are easy to see in isolated sheets under crossed nicols (Pl. 21, figs. 7, 8) because there is a difference in extinction angle ranging from 10°-40°. Blades are also visible (Pl. 19, fig. 2; Pl. 24, fig. 2) in sections normal to their long axes. With recent electron-microscopic studies (Watabe and others, 1958; Watabe and Wilbur, 1961) of the foliated inner layer of *Ostrea* shells, much detailed knowledge of this structure is now available.

Observed blades range from 1-40μ wide. Because the sides of the blade are nearly parallel, each blade is probably 50 or more times as long as it is wide, but no complete blade has been observed. The longest fragment of an isolated blade observed (Pl. 21, fig. 10) measures 220 $\times$ 23μ. This specimen has a blade from an adjacent sheet attached to it in natural growth position. Both blades have the same extinction angles. At 45° to the extinction angle, at points where light passes through a single blade only, the interference color is gray. Where the blades overlap, the interference color is white because of the greater thickness. If one blade did not project beyond the area of overlap, it might appear that there were two adjacent blades in a single sheet. The higher interference color in the area of double-blade thickness indicates the presence of two adjacent sheets. In adjacent blades (Pl. 21, figs. 7, 8) of a single sheet the interference color is the same in alternate, nonextinction positions.

Within each folium there are lines normal to the blades. Occasionally additional blades (Pl. 21, fig. 9) abut against these lines. Presumably they are new blades, introduced into each folium just after the depositional change that produced each line.

Bøggild (1930) described the foliated structure as being similar to nacreous structure in that layers having them are made of thin (about one μ), parallel sheets of calcium carbonate. These sheets he described as parallel to the surface of the shell in both structures. Differences, according to Bøggild, are that in nacreous layers the mineral is aragonite, with the acute bisectrix (crystallographic c-axis of aragonite) normal to the sheets, whereas in the foliated layers of patelloids the mineral is calcite, with the optic axis (crystallographic c-axis of calcite) parallel to the sheets. Several other differences exist. The unit carbonate particle (Grégoire, 1962) in a sheet of nacre is a polygonal tile-like crystal (Text-figs. 13, 14) of aragonite; the unit particle in the folium is an elongate blade (Text-fig. 18) of calcite. Different kinds of depositional surfaces may in part account for the difference in shape of the unit particles. In nacreous layers (Text-figs. 11, 12) each sheet is parallel to the depositional surface. On this surface aragonite "seeds" are deposited in a growth spiral (Wada, 1961) and eventually coalesce to form a single sheet of polygonal crystals. Basically, sheets of nacre are parallel to depositional surfaces. In the foliated layer (Text-fig. 15), contrary to Bøggild's (1930) description, the folia always intersect the depositional surface at an angle. Therefore, during growth of the animal, all folia are growing simultaneously by additive deposition of calcium carbonate along their exposed edges. On the part of each folium exposed at the inner surface of the shell, growth probably takes place only at the margin (Text-fig. 15, surfaces at a). That folia intersect the shell surface at an angle is not apparent in sections (Text-fig. 16) normal to the folia and parallel to the outcrop pattern. The maximum angle of intersection is apparent only in sections normal to the outcrop pattern of the folia.

Unfortunately the term "nacreous" has been used in the literature in several different senses. To some it implies the inner layer or inner surface of the shell, regardless of the structure. To others it implies shell structure only. Some work-

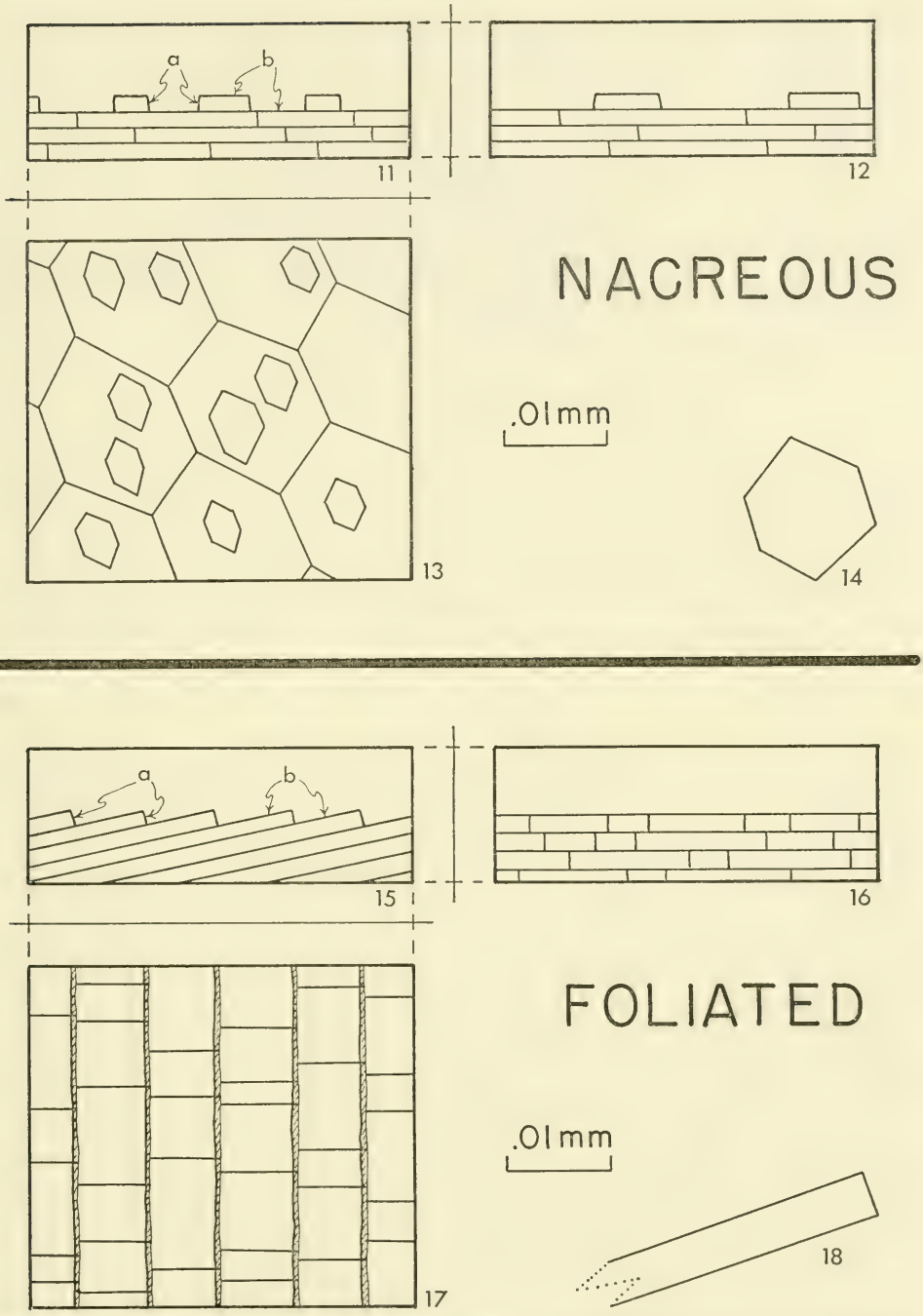

Text-figs. 11-18.—Diagrammatic sketches showing differences between nacreous and foliated structures. Inner surface of shell formed by combination of surfaces a and b. **11-14,** nacreous structure modified from Grégoire (1962). **11, 12,** vertical sections at right angles to each other at inner surface of shell. **13,** inner shell surface showing polygonal pattern. **14,** isolated polygon. **15-18,** foliated structure. **15, 16,** vertical sections at inner surface of shell. **15,** at right angles to outcrop pattern. **16,** parallel with outcrop pattern. **17,** inner shell surface showing outcrop pattern of folia and orientation of blades at right angles to that pattern. **18,** part of an isolated blade.

ers include the foliated structure within their concept of the "nacreous" structure. As used here in its restricted sense, however, "nacreous" describes a structural arrangement of polygonal aragonite crystals in thin sheets parallel to growth surfaces. A nacreous layer, therefore, is simply any shell layer, regardless of sequential position in the shell, having nacreous structure.

The regularly foliated structure grades into irregularly foliated structure (Pl. 17, fig. 2), recognized by Bøggild (1930), in which folia crop out on the ventral shell surface in irregular areas. In each area the strike of the folia is different from the strike in all adjacent areas. Cross-sections show that the folia of the different areas intersect the surface at various angles up to 10°. Different extinction angles reflect different blade orientation in each area. The irregularly foliated structure grades into crossed-foliated structure.

IRREGULARLY TABULATE FOLIATED STRUCTURE

In the shells of one species of *Cellana* there is a structure similar to the common foliated structure except for the shape of the unit crystals making up the folia. Instead of being composed of long parallel-sided blades, each folium (Pl 21, fig. 3) is built up of irregularly shaped tabulae. Roughly, the diameter of the tabulae ranges from 3-30μ. As in alternate sets of blades in each folium of the common foliated structure, the irregular tabulae are arranged in two sets (Pl. 21, figs. 1, 2), each having a slightly different extinction angle. The difference in extinction angle ranges from 4°-8°.

Crossed Structures

The crossed structures (Text-figs. 19, 30) include the aragonitic and calcitic crossed-lamellar structures of Bøggild (1930). They are aggregates of tiny crystals (third-order lamellae) arranged, parallel to each other, in one-μ thick sheets (second-order lamellae) which are in turn organized into larger units called first-order lamellae. In each first-order lamella the second-order lamellae are parallel to each other resembling an *en echelon* arrangement of cards in a stack. These second-order lamellae are oriented at an angle to growth surfaces and, in adjacent first-order lamellae, dip at equal angles to growth surfaces but in opposite directions, forming the characteristic cross pattern (Cox, 1960, fig. 77).

For purposes of orientation (Text-fig. 19) each first-order lamella is assigned three axes (length, width and height) at right angles to each other. The length axis lies in a plane parallel to growth surfaces and is parallel to the structural trend of the first-order lamella on the inner surface of the shell. The width axis is parallel to growth surfaces and normal to the length axis. The height axis is normal to growth surfaces. The length and height axes are the median bisectors of the supplementary angles formed by the intersection of second-order lamellae in adjacent first-order lamellae. The width axis is normal to the plane formed by the length and height axes, and is parallel to second-order lamellae. If projected laterally the width axis remains parallel to the second-order lamellae of adjacent first-order lamellae. It should be emphasized that these axes are used only to indicate orientation within the structure, and no necessary correlation with the actual length of axes is intended. Generally, within an idealized first-order lamella, the length axis is longest. Where the first-order lamellae are short, however, either the height or in some instances the width axis may be longer than the length axis.

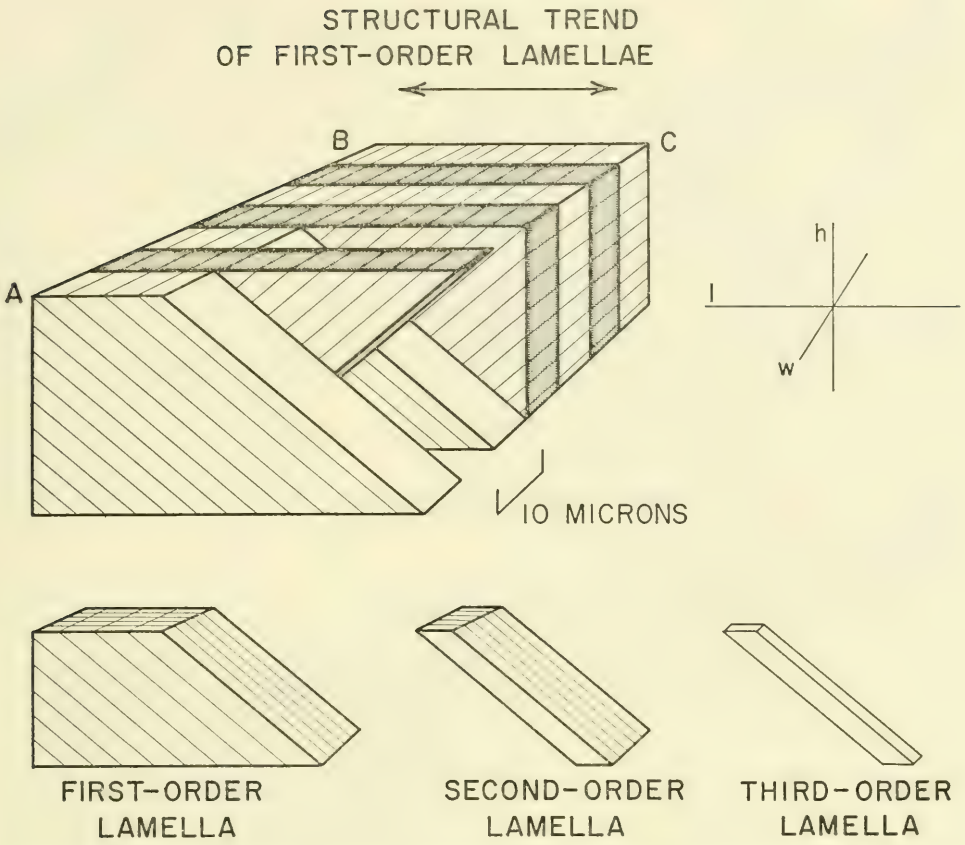

Text-fig. 19.—Crossed-lamellar structure. Surface ABC is parallel to growth surfaces. Scale indicates width of first-order lamellae; second- and third-order lamellae not to scale. Explanation of symbols for three-dimensional axes of first-order lamellae: h, height axis; l, length axis; w, width axis.

CROSSED-LAMELLAR STRUCTURE

In this structure second-order lamellae form an angle (Text-fig. 31) ranging from 16°-44° with the ventral surface of the shell, and the average width of first-order lamellae (Table 2) is about 15μ. Isolated second-order lamellae (Pl. 2, fig. 1) are so thin (1-1.5μ) that when one is viewed normal to its flat surface it can only be seen in plane light. Under crossed nicols (Pl. 2, fig. 2) even with the lamella oriented at 45° to the extinction position, the lamella is invisible because the interference color produced is so low as to appear black. The thickness (Text-fig. 22) of the isolated, flat-lying second-order lamellae is measured by determining the focal difference of two lamellae one of which lies across the other. The thicknesses obtained for three such sets of overlapping second-order lamellae are 1.0, 1.6, and 1.3μ. These figures agree with thicknesses of second-order lamellae as determined in thin sections normal to the width axes of first-order lamellae. That the isolated blades (Pl. 2, fig. 1) described above are second-order lamellae is supported by the fact that the width of the parallel-sided blades falls within the width range of first-order lamellae from which the blade came.

Within each crossed-lamellar layer second-order lamellae have a greater dip angle near the dorsal surface of the layer than they do at its ventral surface. The

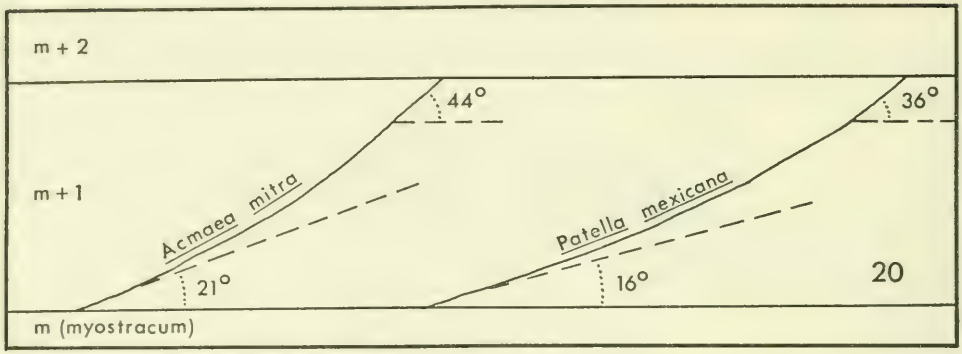

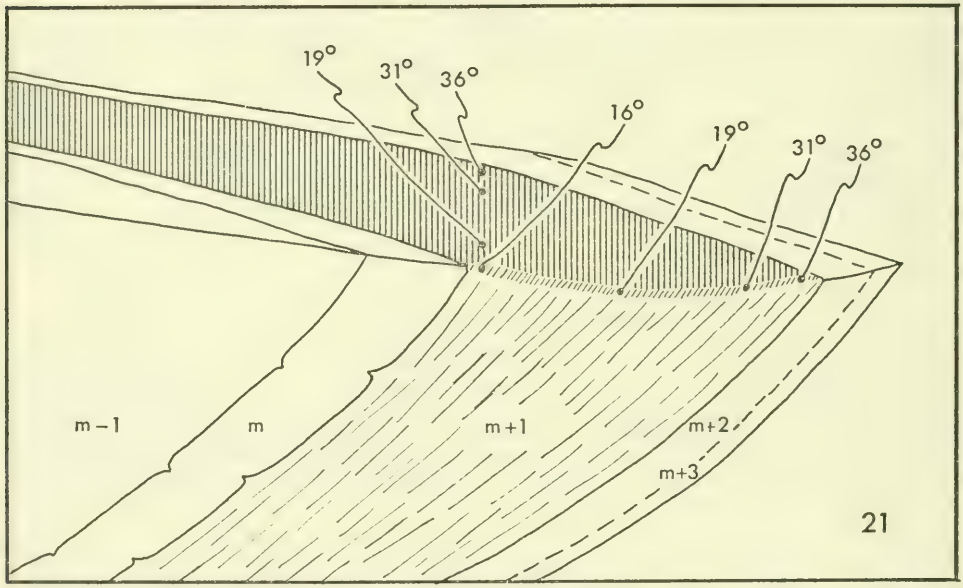

Text-figs. 20, 21.—Changing dip angle of second-order lamellae in crossed-lamellar layer m + 1 (see Text-fig. 42, and Table 2). **20,** comparison of two species in section normal to width axis of first-order lamella. **21,** *Patella mexicana,* oblique view of inner surface of radially sectioned shell. At the ventral surface of concentric crossed-lamellar layer m + 1, the dip angle of second-order lamellae decreases adapically from 36°-16°. The same dip-angle decrease is expressed in a single first-order lamella at the thickest part of the shell layer. Based on hypotype, UCMP no. 36487.

angular difference (Text-figs. 20, 21) can be measured in two ways. In a part of the shell where the crossed-lamellar layer is thickest, the minimum and maximum dip angles can be measured at one place in the layer, either in a vertical thin section (Pl. 11, fig. 2; Pl. 15, fig. 2) parallel to length axes of first-order lamellae, or in a section broken normal to the length axes of first-order lamellae. The dip-angle change can also be measured on the ventral surface of the shell. Here the maximum dip angle is at the abapical margin of the shell layer. Adapically, the dip angle decreases and is smallest where the shell layer is thickest.

Second-order lamellae appear to be made up of tiny elongate crystals, called third-order lamellae by Kobayashi (1964a). Evidence obtained here for the ex-

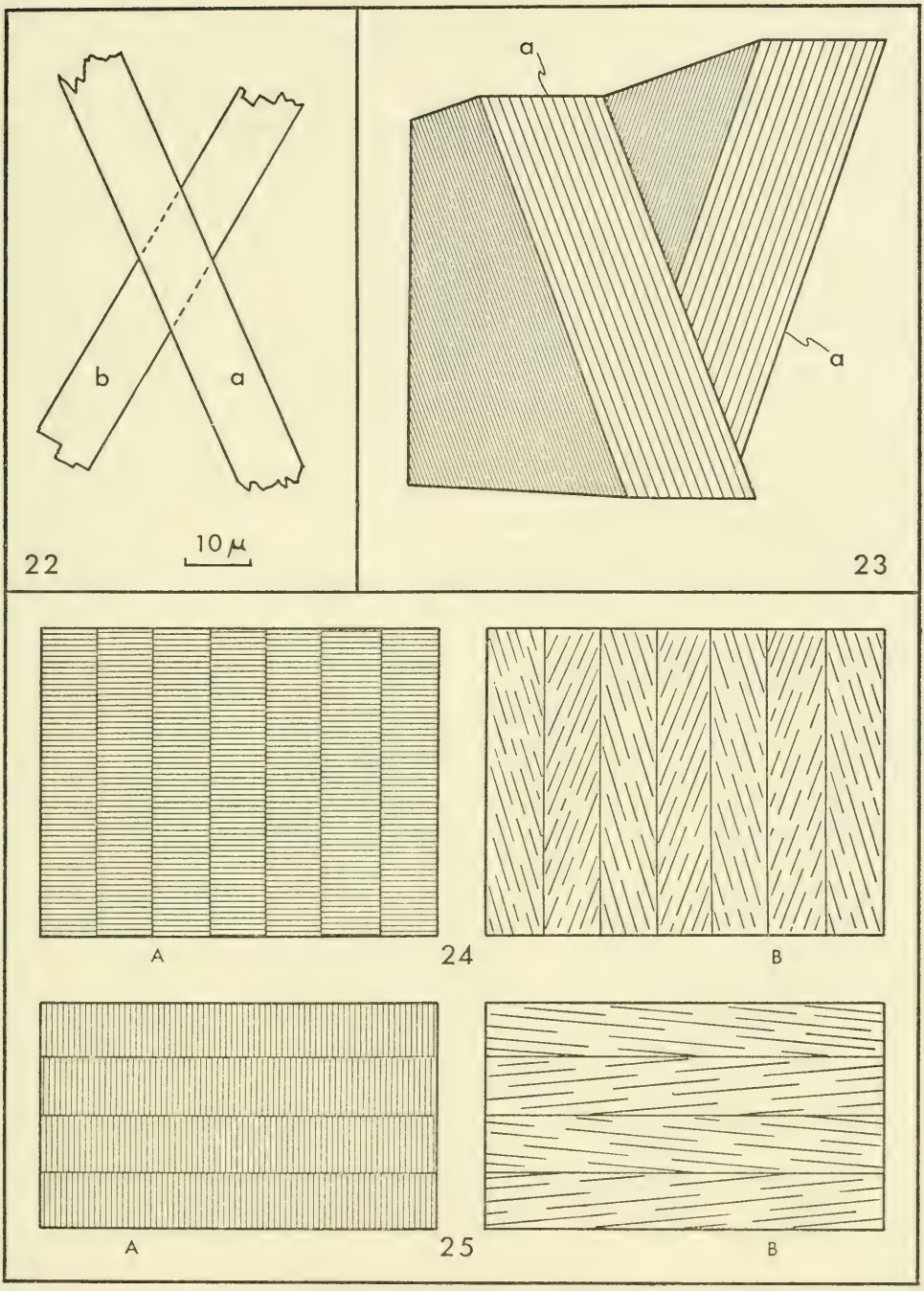

Text-figs. 22-25.—Third-order lamellae. **22**, diagram of two isolated second-order lamellae one of which (a) lies across the other (b). Based on hypotype, UCMP no. 30793-c. **23**, hypothetical diagram of two first-order lamellae of crossed-lamellar structure, showing many third-order lamellae exposed at the surfaces (a) of two second-order lamellae. **24, 25**, idealized diagrams showing second-order lamellae (A) and traces of third-order lamellae (B) in two sections. **24**, section almost normal to length axes of seven first-order lamellae (see Pl. 3, figs. 1, 2). **25**, section almost normal to height axes of four first-order lamellae (see Pl. 3, fig. 3).

istence of third-order lamellae is as follows. In thin sections normal to length axes of first-order lamellae (Pl. 3, fig. 1; Text-fig. 24A), second-order lamellae are visible in the parts of sections where the thicknesses are such as to produce interference colors between second-order green and second-order red under crossed nicols. In thicker areas of thin sections, where the colors are higher, and in thinner areas, where the colors are lower, the second-order lamellae are not visible in both sets of first-order lamellae. If the microscope stage is rotated 11° (Pl. 3, fig. 2; Text-fig. 24B), the traces of second-order lamellae disappear and within each first-order lamella there appears an *en echelon* arrangement of what seem to be small (about 0.5μ wide) elongate crystals oriented at an angle of about 10° to the sides of first-order lamellae. In any two adjacent first-order lamellae this angle is generally equal but opposite, producing the chevron pattern described by Thiem (1917b). In these sections none of the individual crystals can be traced from one side of a first-order lamella to the other. In thin sections (Pl. 3, fig. 3; Text-fig. 25B) normal to the height axes of first-order lamellae, a similar chevron pattern can be seen. The observed angle between the traces of the tiny crystals and the sides of first-order lamellae is about 4°. Although no second-order lamellae were seen in sections with this orientation, they should ideally have the pattern shown in text-figure 25A.

No evidence of third-order lamellae could be seen in isolated second-order lamellae for reasons already given. However, looking down through two or more articulated second-order lamellae (Pl. 3, fig. 4), one can see small third-order lamellae paralleling the flanks of the second-order lamellae. In an idealized reconstruction (Text-fig. 23) third-order lamellae are shown paralleling the length axes of second-order lamellae. The chevron pattern exhibited in adjacent first-order lamellae (Pl. 3, figs. 2, 3) probably results from thin sections which are not quite normal to the length axes and height axes of first-order lamellae. Presumably, in sections exactly normal to the length axes and height axes, the traces of third-order lamellae would parallel the flanks of first-order lamellae.

Clear resolution of both second- and third-order lamellae in the same series of first-order lamellae is the exception rather than the rule. Generally what one sees in thin sections (under crossed nicols) oriented parallel to width axes of first-order lamellae (Pl. 2, fig. 4; Pl. 13, fig. 1, m + 1) is an alternating series of light and dark bands. At high magnifications the alternating light-dark bands (Pl. 9, fig. 2; Pl. 15, fig. 1, m + 1) exhibit patterns which show alternating or mixed influence of second- and third-order lamellae. Representative figures showing these relationships are given by Rose (1859, Pl. 2, figs. 8, 9), Nathusius-Königsborn (1877, Pl. 4, fig. 22C), Biedermann (1902, Pl. 4, figs. 25-27), Thiem (1917b, Text-figs. 35, 36, 38), Schmidt (1924, Text-fig. 85), Kessel (1936, Text-figs. 8a, 11) and Barker (1964, Text-fig. 4). Past interpretations of the crossed-lamellar structure have varied according to the micro-structural elements observed. The interpretations given by Nathusius-Königsborn (1877, Pl. 4, fig. 23, *fide* Biedermann, 1902, p. 93; 1914, Text-fig. 183), Biedermann (1902), Flössner (1914, Text-fig. 3), Kessel (1936) and Kobayashi (1964a, Text-fig. 4) are all in agreement with the present interpretation in that tiny fibrils, rods or third-order lamellae less than one μ in diameter are given as the smallest structural elements of the crossed-lamellar structure. The diagram given by Nathusius-Königsborn is reproduced here in plate 26, figure 4. In an electron microphotograph of the outer crossed-lamellar layer of a *Glycymeris* shell, Kobayashi (1964b, Pl. 1, fig. 5) has presented strong evidence for the existence of third-order lamellae as the fundamental crystalline elements of first-order lamellae. In the interpretations of

Rose (1859, Pl. 3, fig. 1) and Bøggild (1930, Text-fig. 2), second-order lamellae are given as the fundamental building blocks of the crossed-lamellar structure.

Two interpretations which are entirely different from the generally accepted concept of the crossed-lamellar structure are given by Thiem (1917b) and Barker (1964). Thiem was able to see only the chevron pattern in thin sections cut parallel to width axes of first-order lamellae. Accordingly, in his reconstructions of the structure, Thiem (1917b, Text-figs. 41, 42) conceived of the first-order lamellae as being composed of very thin lamellae (*Blättchen* or *Lamellen*) which, corresponding to the chevron pattern seen in thin sections, were themselves arranged in a chevron pattern. These *"Blättchen"* he considered the ultimate crystalline particles. There are internal inconsistencies within both of Thiem's reconstructions, and his interpretation is here considered erroneous. In his block diagram (Thiem, 1917b, Text-fig. 41-I) he showed a side view of only one first-order lamella in a sequence of four adjacent first-order lamellae. In an expansion of Thiem's block diagram (Text-fig. 26), a side view of all four first-order lamellae is given. The striations on all four are parallel, thus contradicting the basic crossed pattern of this structure, even as given by Thiem (1917b, Text-fig. 34). In his other interpretive sketch of the crossed-lamellar structure, Thiem (1917b, Text-fig. 42) shows a small transparent box representing segments of two first-order lamellae. Through this box four idealized *"Blättchen"* are inserted in such a way as to show the characteristic "crossed" pattern of the structure. Unfortunately, in each first-order lamella (Pl. 26, fig. 5) the two

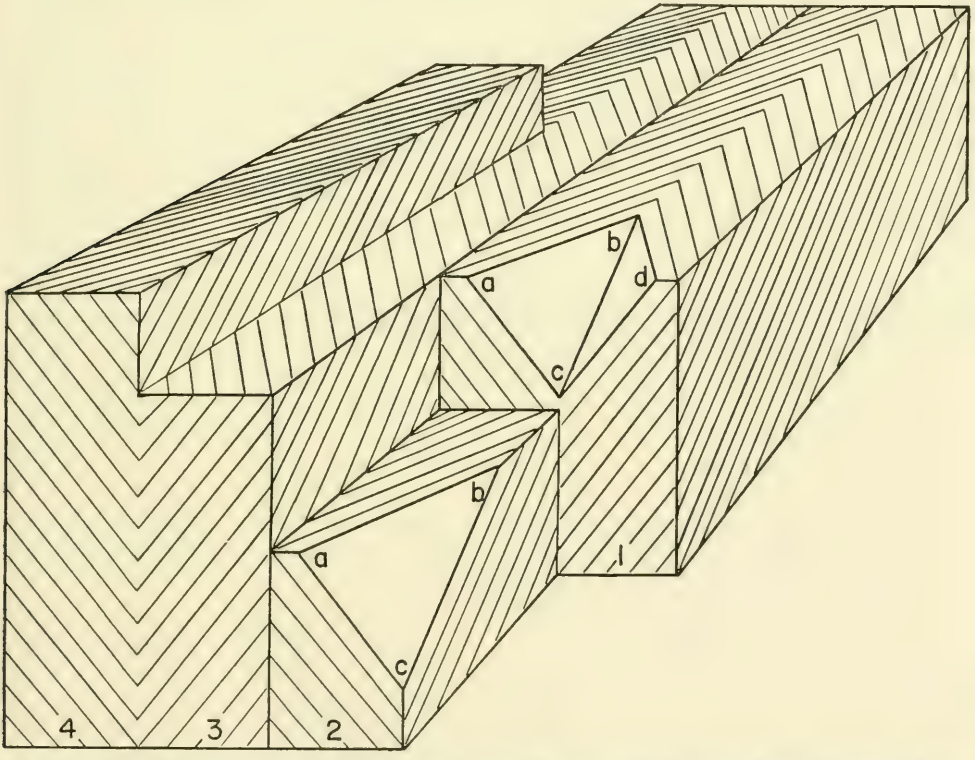

Text-fig. 26.—Thiem's concept of the crossed-lamellar structure showing four *"Platten"* [first-order lamellae] made up of tiny *"Blättchen"* (e.g. abc, bcd). Expanded from Thiem (1917b, Text-fig. 41-I).

"Blättchen" are at nearly right angles to each other. This illustration, therefore, is in direct contradiction to the one shown in text-figure 26, which shows the *"Blättchen"* within each first-order lamella as a sequence of oblique but parallel lamellae.

In an unusual interpretation of the crossed-lamellar structure in several pelecypod species, Barker (1964, p. 76) recognized two optically different sets of blocks [first-order lamellae] as seen in thin sections parallel to width axes of first-order lamellae. Based on observed differences in extinction properties, Barker considered that each block of one set is "not crystallographically continuous," whereas each block of the other set is a "single crystal." With properly oriented sections (Pl. 3, figs. 1, 2), however, it can be demonstrated that under crossed nicols both sets of first-order lamellae have identical extinction properties. This observation lends support to the well-established idea that, except for their oppositely dipping second-order lamellae, first-order lamellae are identical in every way. Continuing his description, Barker described Bøggild's second-order lamellae as "impurity layers" within the single-crystal first-order lamellae. Resolving the problem of the unit crystal in the crossed-lamellar structure will require obtaining combined information using the techniques of electron microscopy and X-ray microdiffraction analysis. Wainwright (1964) has successfully used these techniques in determining the size of the ultimate aragonite crystal in scleractinian corals. Carriker *et al.* (1963, Text-figs. 13, 29) gave electron microphotographs of the inner surface of a crossed-lamellar layer in the gastropod *Murex fulvescens*. These photographs show what appears to be an interleaving relationship between third-order lamellae and thin films of organic matrix.

In Recent shells the crossed-lamellar structure (Pl. 7, figs. 1, 2) is easily recognized in thin sections normal to the width axes of first-order lamellae. In thin sections (Pl. 7, fig. 3) normal to the length axes of first-order lamellae, the structure can be confused with prismatic structure. For example, Mackay (1952) described the shell structure of several species of *Conus*. Although recognizing that the shells had three crossed-lamellar layers, he preferred to describe the structure, in sections normal to the length axes of first-order lamellae, as prismatic. Presumably he did this because he could not recognize crossed-lamellar structure in sections normal to the length axes of first-order lamellae. In fact, however, crossed-lamellar structure can be identified in sections with that orientation using the following technique. In adjacent first-order lamellae (Pl. 3, fig. 1; Text-fig. 27) second-order lamellae dip in opposite directions. The second-order lamellae in every other first-order lamella dip south (compass directions are used to simplify the discussion) while those of the alternate set dip north. When the plane of focus is lowered through the section, the east-west pattern of south-dipping second-order lamellae shifts toward the south while the pattern of north-dipping second-order lamellae shifts northward. When the focus is raised, the direction of shift is reversed. Recognition of the shifting pattern is facilitated if the focus is raised and lowered rapidly.

Crossed-lamellar structure can also be identified in sections normal to the height axes of first-order lamellae. In these sections the same shift of pattern, caused by second-order lamellae, can be seen. The actual traces of second-order lamellae, however, were not seen in these sections. Also in these sections (Pl. 2, fig. 4), as well as on the ventral surface of the shell, the characteristic intertonguing relationship of the first-order lamellae is observable. In these sections, and in sections normal to the length axes of first-order lamellae, alternate first-order lamellae have different extinction or near-extinction angles. As observed

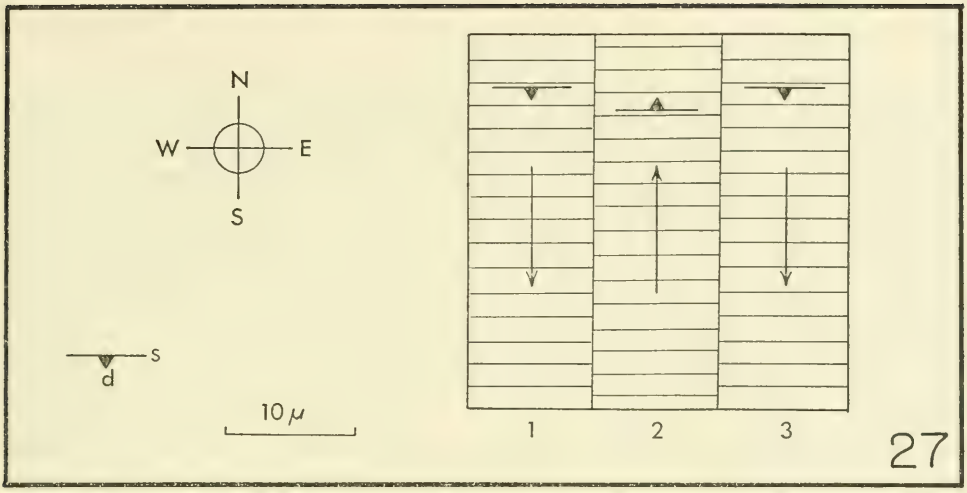

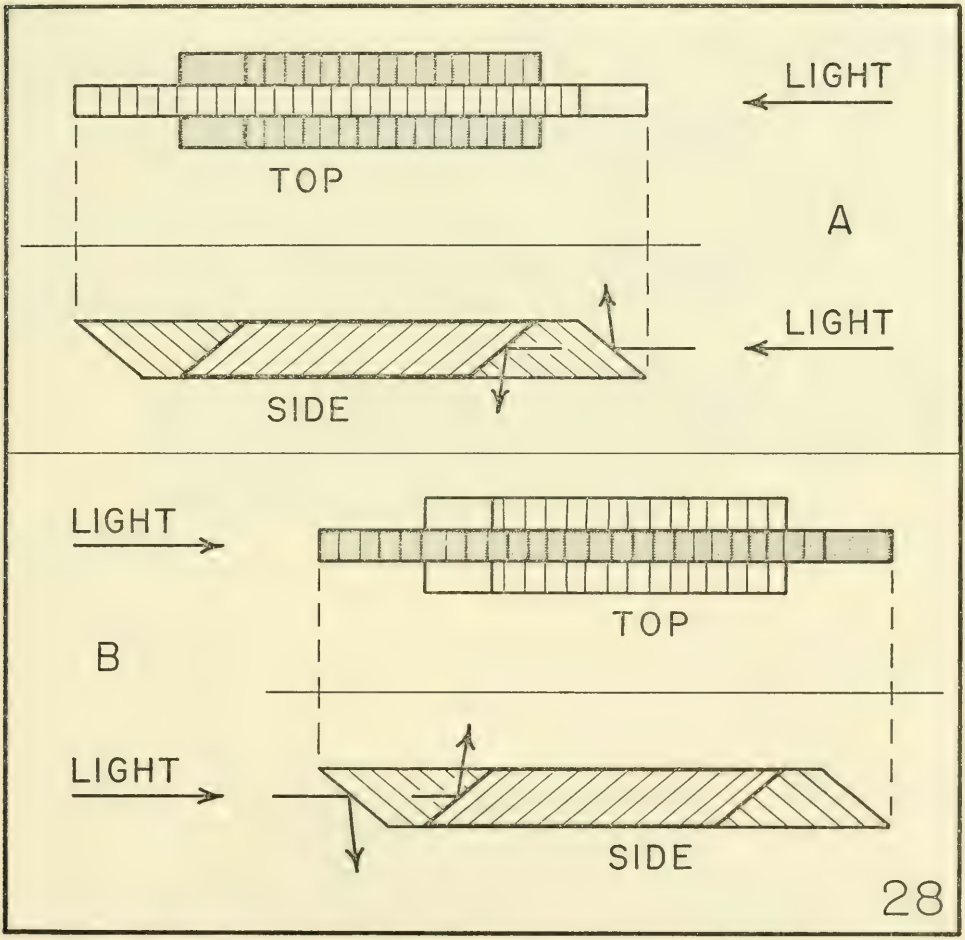

Text-figs. 27, 28.—Two criteria for recognition of crossed-lamellar structure. **27,** transmitted light; diagram of thin section normal to length axes of three first-order lamellae; note compass directions; arrows indicate direction in which the patterns shift while microscope tube is being lowered. Note strike (s) and dip (d) symbol used to indicate dip direction of second-order lamellae. **28,** low-angle incident light; alternation of light-dark pattern on three adjacent first-order lamellae with change in light-source direction. A, light from the right. B, light from the left.

by Bøggild (1930), in outer shell layers first-order lamellae are long and regularly shaped whereas in inner layers they are short and irregularly shaped.

In Recent shells, and in fossil shells where partial to nearly total recrystallization has rendered thin-section study useless, the following criteria can be used for recognition of crossed-lamellar structure. In fossil shells, where the structure is apparently well preserved (Pl. 27, fig. 1) when seen under reflected light, the structure (Pl. 27, fig. 2) may appear completely obliterated by recrystallization when seen under crossed nicols. In this case the shell is only partially recrystallized and second-order lamellae retain the ability to reflect light. With light (Text-fig. 28) directed at a low angle to the surface of a fragment having crossed-lamellar or crossed-foliated structure, second-order lamellae dipping toward the light source reflect light upward making one set of first-order lamellae appear bright (Pl. 11, fig. 4; Pl. 27, fig. 4). In the alternate set of first-order lamellae, second-order lamellae dip away from the light source and reflect light downward. These first-order lamellae appear dark. If either the fragment or the light source (Text-fig. 28; Pl. 11, fig. 5; Pl. 27, fig. 5) is rotated 180°, the light-dark pattern of first-order lamellae alternates.

Small fragments (Text-fig. 29; Pl. 2, fig. 3) from crushed crossed-lamellar

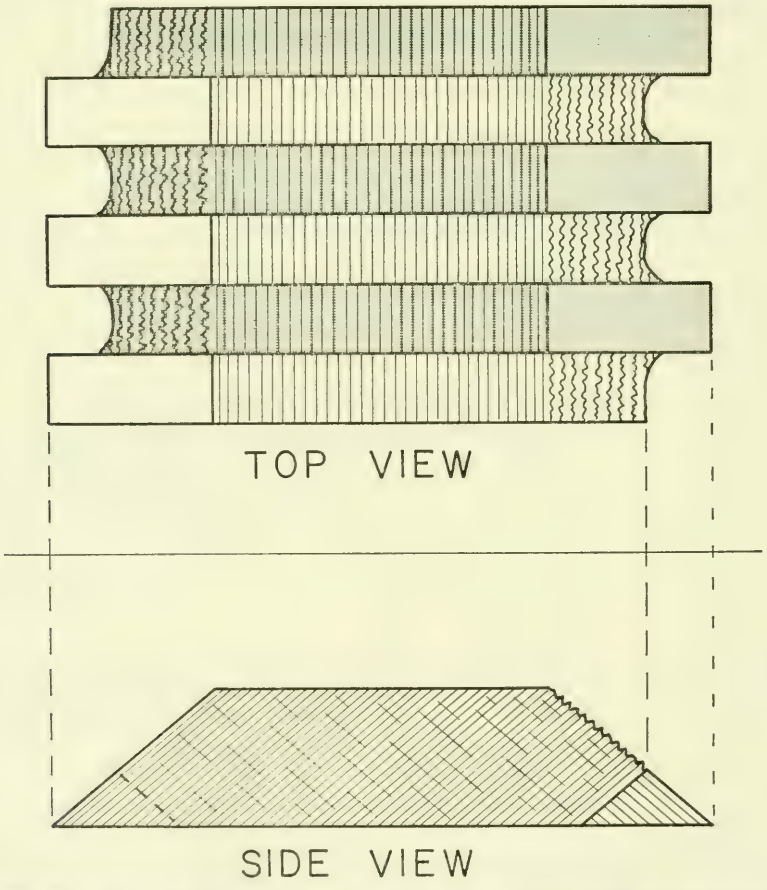

Text-fig. 29.—Rectangular fretwork pattern at broken ends of first-order lamellae in shell chip having crossed-lamellar structure. In top view the chip is illuminated by low-angle incident light from the left.

layers often display a rectangular fretwork pattern at the broken ends of first-order lamellae. This pattern reflects the beveled mortise and tenon relationship in alternate first-order lamellae, produced by the opposite dip directions of second-order lamellae. Although the shell may be partially recrystallized (Pl. 27, fig. 3), if zones of weakness remain between second-order lamellae, layers having crossed-lamellar structure will occasionally break into small fragments exhibiting the fretwork pattern.

In crossed-lamellar layers of Recent shells, exposed surfaces broken normal to the width axes of first-order lamellae often show the cross pattern of second-order lamellae. Depending on the degree of recrystallization, fossil shells may or may not break normal to first-order lamellae and show the cross pattern. In shells that do not, weathered surfaces (Text-fig. 118; Pl. 29, fig. 3) occasionally show the cross pattern of second-order lamellae even though recrystallization prevents breakage along first- or second-order lamellae.

CROSSED-FOLIATED STRUCTURE

This term is here proposed for the structure Bøggild (1930, p. 251) referred to as the "calcitic crossed-lamellar structure." He described this structure as the calcitic counterpart of the common aragonitic crossed-lamellar structure. Besides the mineralogic difference he also described the dip angle of second-order lamellae as being low (13°) in the calcitic crossed-lamellar layers and high (41°) in aragonitic crossed-lamellar layers. Within the calcitic layers (Table 3) of *Patella fluctuosa, P. plicate* and *P. vulgata,* Bøggild (1930, p. 306) recognized the gradational transition from foliated to irregularly foliated to calcitic crossed-lamellar structure. He recognized no gradational structures leading to the aragonitic crossed-lamellar structure.

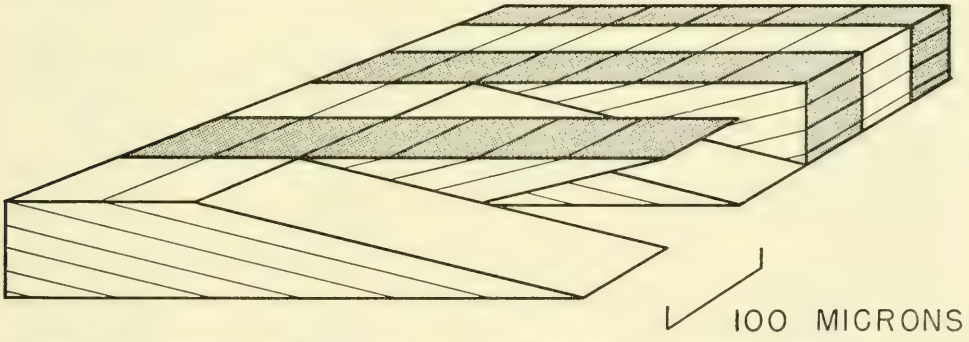

Text-fig. 30.—Crossed-foliated structure. Third-order lamellae omitted from diagram.

Based on differences described by Bøggild and on other differences discussed below, Bøggild's calcitic crossed-lamellar structure, here called crossed-foliated structure (Text-fig. 30), is recognized as a structure distinct from the aragonitic crossed-lamellar structure. No attempt was made here to determine the mineral composition of the shell layers. Until further work is done on their mineralogy, it will not be possible to state for certain that all layers (Table 2) here called crossed-foliated are calcitic and that all layers called crossed-lamellar are aragonitic. As yet, therefore, there is no assurance that all of Bøggild's calcitic crossed-lamellar layers are equal to the crossed-foliated layers described here.

In order to differentiate between crossed-foliated and crossed-lamellar layers in fossil shells completely altered to calcite, it is necessary to be able to differenti-

TABLE 2: Dip angle of second-order lamellae and width of first-order lamellae column gives ratio of width of first-order lamellae in crossed-foliated text-figure 42 for explanation

Species, layer, and dip-angle measurements (degrees)	Crossed-foliated			Crossed-lamellar			Width ratio
	min.-max. (degrees)	average (degrees)	width (μ)	min.-max. (degrees)	average (degrees)	width (μ)	
Acmaea mitra							
m + 1: 21, 41 (Text-fig. 20)				21–41	31	16	
m − 1: 33, 40, 44				33–44	39	13	
Acmaea instabilis							
m + 1: 21, 30, 31				21–31	27	8	
m − 1: 30, 35, 37, 39, 39				30–39	36	8	
Lottia gigantea							
m + 1: 22, 22, 24				22–24	23	16	
m − 1: 32, 33, 33				32–33	33	16	
Patella vulgata							
m + 2: 12, 12, 13	12–13	12	74				4.6
m + 1: 26				26–26	26	16	5.1
m − 2: 8, 10	8–10	9	82				
Patella lusitanica							
m + 2: 11, 12, 12	11–12	12	32				4.0
m + 1: 23, 24, 25				23–25	24	8	
Patella argenvillei							
m + 2: 7, 8, 9	7–9	8	90				9.0
m + 1: 17, 23, 26, 29, 29				17–29	25	10	6.9
m − 1: 21, 23, 25				21–25	23	13	
Patella granularis							
m + 2: 12, 13, 14	12–14	13	136				6.5
m + 1: 25, 25				25–25	25	21	10.1
m − 1: 40, 41				40–41	41	12	
Patella longicosta							
m + 2: 14, 18	14–18	16	131				10.0
m + 1: 21				21–21	21	13	

in crossed-foliated and crossed-lamellar layers of patelloid shells. Width-ratio layers to width of first-order lamellae in crossed-lamellar layers. See of shell-layer notation system.

Species, layer, and dip-angle measurements (degrees)	Crossed-foliated			Crossed-lamellar			Width ratio
	min.-max. (degrees)	average (degrees)	width (μ)	min.-max. (degrees)	average (degrees)	width (μ)	
Patella mexicana							
m + 2: 13, 14, 15, 17, 19, 27	13–27	18	980				31.0*
m + 2: 16, 17, 20, 21, 25	16–25	20	500				31.0*
m + 1: 16, 19, 31, 34 (Text-fig. 20)				16–34	25	16	25.0*
m + 1: 23, 23, 32, 36				23–36	29	16	
m − 1: 35				35–35	35	20	
Patella compressa							
m + 2: 10, 10, 10	10–10	10	61				6.1
m + 1: 22, 22, 24				22–24	23	10	5.1
m − 1: 30, 33, 34				30–34	32	12	
Patella granatina							
m + 2: 11, 12	11–12	12	94				4.5
m + 1: 26				26–26	26	21	5.9
m − 1: 35				35–35	35	16	3.3
m − 2: 7	7–7	7	69				4.3
Patella ocula							
m + 2: 12, 12	12–12	12	53				4.1
m + 1: 26, 27				26–27	27	13	4.1
m − 1: 37, 38, 42				37–42	39	13	
Helcion pellucida							
m + 2: 3, 3, 4	3–4	3	94				
Cellana argentata							
m + 1: 24, 25				24–25	25	23	
m − 1: 32, 32				32–32	32	41	
min.-max. (Text-figs. 31, 32)	3–27	3–20		16–44	21–41		
average (Text-figs. 33, 34)	10.5–13.3	11.7		26.6–31.4	28.8		
average width			184.0			15.5	
average width**			83.3			15.2	
average width ratio**							5.9

* only the lowest ratios are recorded here
** excluding *Patella mexicana*

ate between the two structures on physical criteria alone. A comparison was made (Table 2) between crossed-foliated layers and crossed-lamellar layers of adult shells of 14 Recent patelloid species. Assignment of structure type for each of the layers studied is based on two criteria: (1) width of first-order lamellae in one layer relative to width of first-order lamellae in other layers of the same shell, and (2) dip angle of second-order lamellae.

The width of first-order lamellae was measured normal to the length axes of first-order lamellae on the inner surface of the shell. The recorded width, in microns, for each layer is the average width for ten or more adjacent first-order lamellae. *Patella mexicana* (Pl. 14, fig. 2) has extraordinarily wide first-order lamellae in its crossed-foliated layer (m + 2), and measurements made on the width of first-order lamellae in all layers of *P. mexicana* are therefore excluded from the present discussion. The average width of first-order lamellae in 11 crossed-foliated layers is 83.3μ, whereas the average width of first-order lamellae in 21 crossed-lamellar layers is 15.2μ. Of more significance, however, are measurements made on equal-sized shells of a species which has both crossed-foliated and crossed-lamellar layers (Pl. 10, fig. 2; Pl. 13, fig. 1) in its shell. The results of these measurements can be expressed as the ratio of the width of first-order lamellae in crossed-foliated layers to the width of first-order lamellae in crossed-lamellar layers. This ratio was obtained in eight species. The lowest ratio (3.3:1) was obtained in *Patella granatina* and the highest ratio (10.1:1) in *P. granularis*. The average of 16 width ratios shows that, in general, first-order lamellae of crossed-foliated layers are about six times as wide as first-order lamellae of crossed-lamellar layers.

Analysis and averaging of measurements of the dip angle of second-order lamellae (Table 2; Text-figs. 31-34) demonstrate that, in spite of the overlap of dip angles, the usual dip angle of second-order lamellae in layers here considered to have crossed-foliated structure appears to be significantly smaller than the usual dip angle of second-order lamellae in layers here considered to have crossed-lamellar structure. The separation of Bøggild's crossed-lamellar structure into crossed-foliated and crossed-lamellar types seems to be justified because the two structures can be differentiated when combinations of the two characteristics described above are used.

In layers having crossed-foliated structure, each second-order lamella (Pl. 11, fig. 3; Pl. 13, figs. 3, 4) is made up of third-order lamellae parallel to the long axis of the second-order lamella. Adjacent third-order lamellae have slightly different extinction angles. Although analagous to the third-order lamellae of the crossed-lamellar structure, third-order lamellae of the crossed-foliated structure are homologous to the blades which make up the folia of the foliated structure. A complete gradational sequence between the foliated and crossed-foliated structures can be demonstrated in the following morphologic series: foliated structure (Pl. 17, fig. 1; Pl. 19, figs. 1, 2; Text-fig. 77, m + 1), irregularly foliated structure (Pl. 17, fig. 2; Text-fig. 77, m — 1), and crossed-foliated structure (Pl. 11, figs. 3-5; Pl. 13, figs. 3, 4; Text-fig. 30). The crossed-foliated structure can be derived from the irregularly foliated structure by lateral "compression" of patches of folia in such a way that the blades assume the role of third-order lamellae, and the folia become second-order lamellae which alternate dip directions in adjacent first-order lamellae. No phylogenetic direction is intended in the description just given. The process could just as well go the other way.

In the shell of *Patella mexicana* a distinctive structural variation (Text-fig. 35) exists in the concentric crossed-foliated layer (m + 2). Second-order lamel-

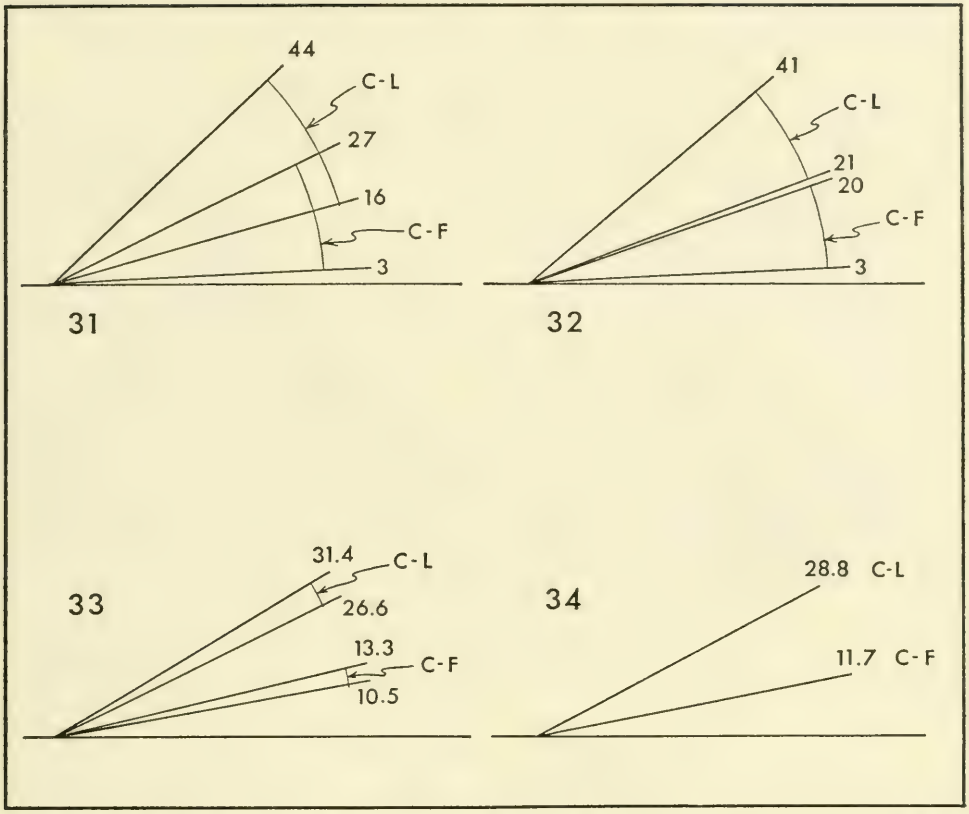

Text-figs. 31-34.—Differences in dip angle (in degrees) of second-order lamellae (Table 2) in crossed-foliated (C-F) and crossed-lamellar (C-L) layers. **31,** total minimum to maximum range of dip angles. **32,** range of average dip angles. **33,** average minimum to average maximum range of dip angles. **34,** average of the average dip angles.

lae (Pl. 14, figs. 1-4) exhibit a wavy structural pattern. Each second-order lamella is corrugated, with the crests of the waves oriented in the down-dip direction of the second-order lamellae. The wave length of the corrugations is about 20μ and the flanks of each wave intersect the dip plane of second-order lamellae at an angle of about 12°. At the ventral surface of the shell, where the corrugated second-order lamellae crop out, a light-dark pattern caused by the two alternate reflection surfaces can be seen under the binocular microscope if the shell is properly oriented. By rotation of the length axis of the first-order lamella, the shell can be brought into such a position that the light-dark pattern alternates. The axis of rotation necessary to produce the alternating light-dark pattern on the corrugated surfaces of second-order lamellae is thus at right angles to the axis of rotation necessary to produce the alternating light-dark pattern on adjacent first-order lamellae.

The wavy structural pattern (Pl. 14, fig. 1) tends to mask the boundaries of first-order lamellae when thin sections are seen under crossed nicols. However, the first-order lamellae (Pl. 14, fig. 2) stand out clearly when the same thin sections are seen in reflected light.

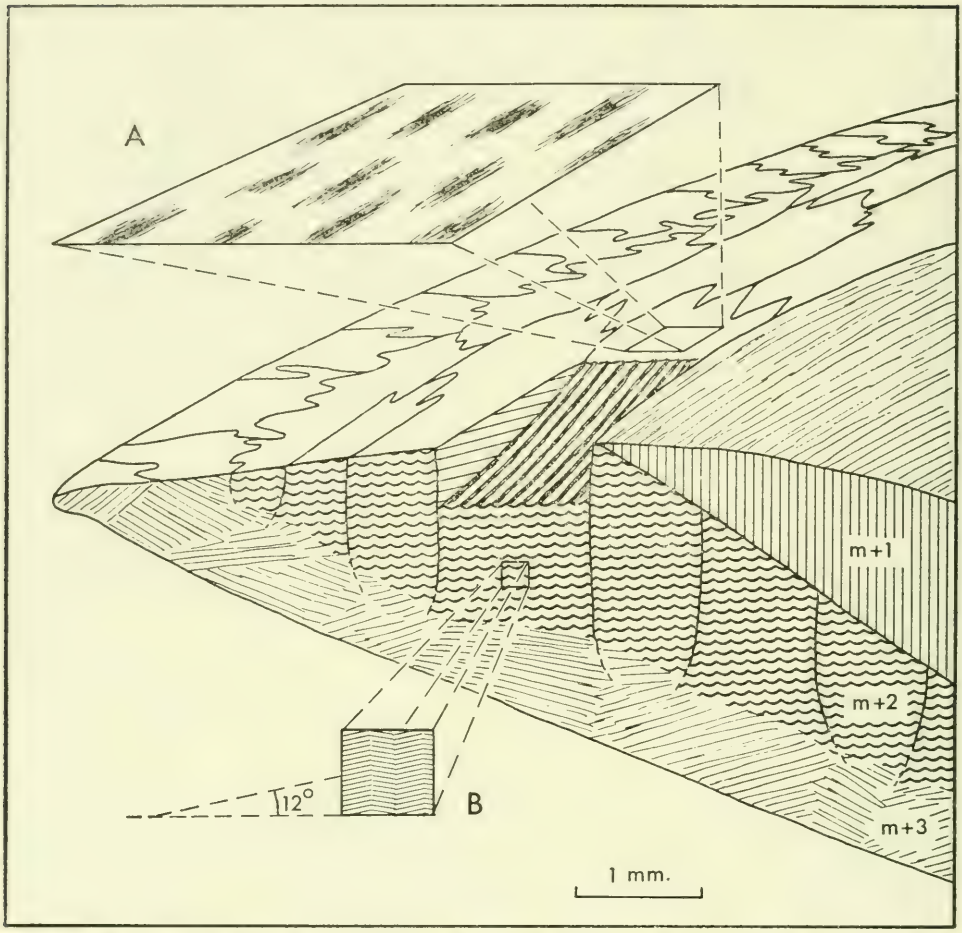

Text-fig. 35.—Oblique view of inner surface of radially sectioned shell of *Patella mexicana* showing wavy structure of second-order lamellae in concentric crossed-foliated layer (m + 2). A, enlargement of part of ventral surface of shell showing light-dark pattern caused by two different reflection-angle sets in the wavy structure. B, enlargement (see Pl. 14, fig. 3) showing angle of wave-flank intersection with dip plane of second-order lamellae. Based on hypotype, UCMP no. 36487.

Complex Crossed Structures

These structures include the complex crossed-lamellar structure of Bøggild (1930) and the complex crossed-foliated structure, a term proposed here for what Wada (1963a, 1963b) described as a spiral growth phenomenon in the calcitic foliated layers of some pelecypods. The complex crossed structures can be described most simply as a cone-in-cone (see glossary) arrangement of crystal

Text-figs. 36-38.—Idealized diagrams of elements of a major prism of the complex crossed-lamellar structure. Explanation of symbols: a, cone apex; ad, apparent dip angle; b, median bisecting plane of major prism; c, central axis of major prism; g, growth line; m, cone margin; r, rhomboidal prismatic segment of third-order lamella; s, conical second-order lamella; t, third-order lamella; td, true dip angle of conical second-order lamellae; ts, thin section. **36,** single conical second-order lamella. **37,** section along central axis of major prism showing chevron pattern of second-order lamellae. **38,** section on flank of major prism parallel to central axis; A, enlarged rhomboidal prism representing the part of a third-order lamella in thin section (ts).

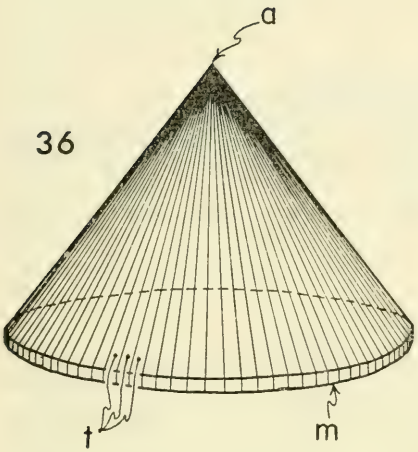

36

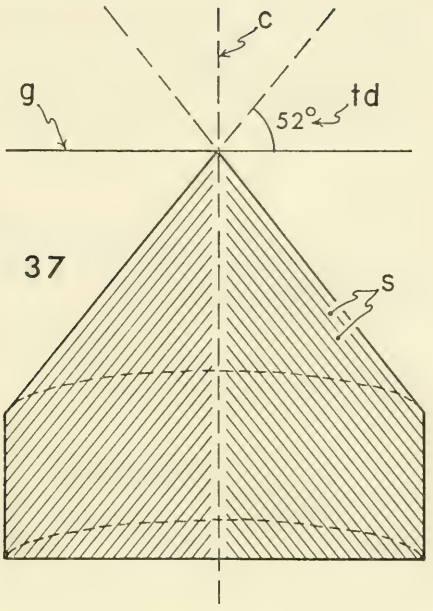

37

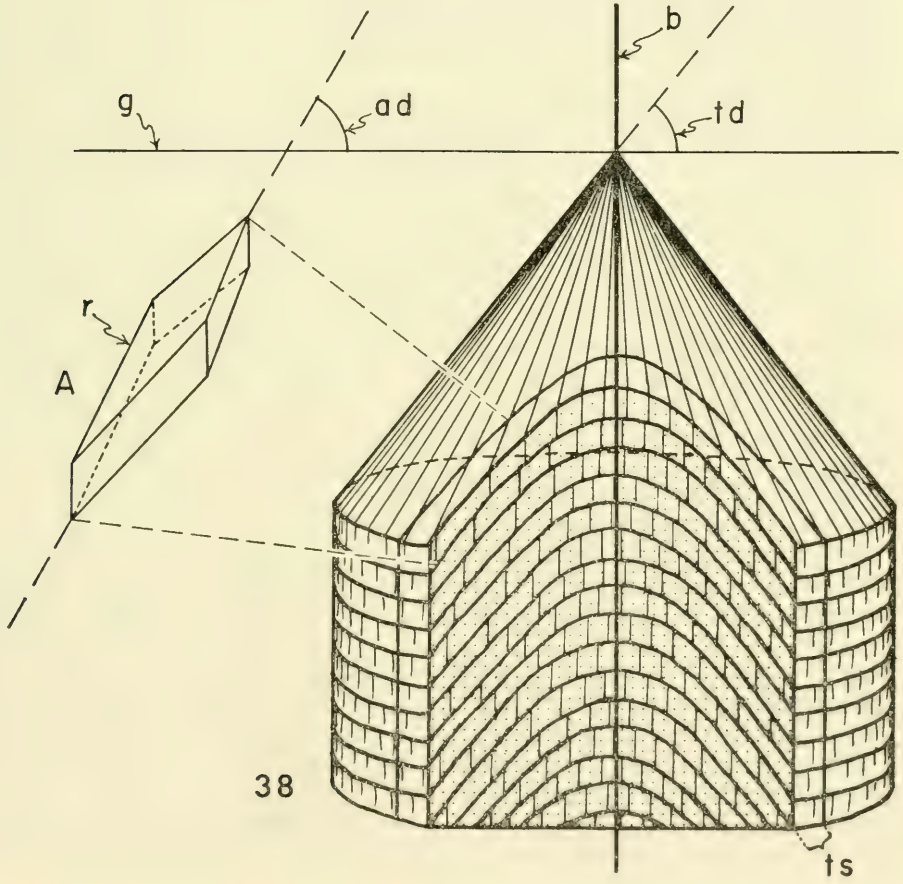

38

aggregates. Roughly cylindrical major prisms (Text-fig. 38) are here interpreted as being composed of a series of one-μ thick cones (Text-figs. 36, 39) stacked one inside the other, with the apex of the stack pointing into the shell away from the depositional surface. Individual cones are here termed conical second-order lamellae. Third-order lamellae radiate from the apex of each conical second-order lamella.

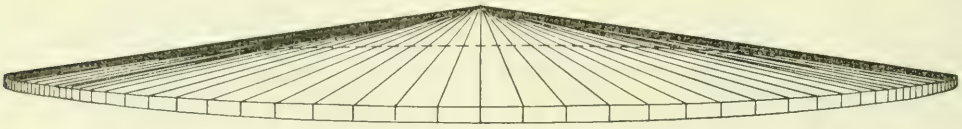

Text-fig. 39.—Generalized side view of isolated conical second-order lamella of the complex crossed-foliated structure.

COMPLEX CROSSED-LAMELLAR STRUCTURE

This structure was described by Bøggild (1930) as consisting of prisms, each apparently composed of first-order lamellae which radiate, like the septae of a coral, from the central axis of the prism. The prisms are oriented with the central axes normal to growth surfaces. Bøggild, recognizing a close structural relationship between the crossed-lamellar and complex crossed-lamellar structures, described each hypothetical first-order lamella as being composed of second-order lamellae which dip away from the central axis of the prism at an angle of 41° to growth surfaces.

Knowledge of the existence of third-order lamellae in the crossed-lamellar structure permits a more meaningful description of the complex crossed-lamellar structure than was given by Bøggild. As recognized by Kobayashi (1964a, Pl. 3, figs. 1, 2), each conical second-order lamella (Text-fig. 36) is composed of small crystals (0.5μ diameter) which radiate from the apex of the cone. These small crystals are here homologized with third-order lamellae of the crossed-lamellar structure, and the conical second-order lamellae are homologized with the second-order lamellae of that structure. Major prisms of this structure are homologous with one or perhaps two first-order lamellae of the crossed-lamellar structure.

In vertical sections (Text-fig. 37) along the central axis of a major prism, the true dip angle (52° in this case) can be measured. Ideally in these sections, only two third-order lamellae per cone are intersected. From the central axis to the margin of the prism the dip angle remains constant. In vertical sections (Text-fig. 38) through the flank of a prism, the long axes of all third-order lamellae are intersected at an angle. Therefore, many third-order lamellae per cone are exposed. In thin section each third-order lamella is represented in the section by a small rhomboidal prism. With reference to a median bisecting plane normal to the plane of section and containing the central axis, the rhomboidal prisms adjacent to this plane have an apparent dip angle of 90° and are parallel to the plane. Progressively farther from the median bisecting plane, the apparent dip angle (measured diagonally across each rhomboidal prism) decreases. At no place, however, is the apparent dip angle as small as the true dip angle. Only in vertical sections near the central axis does the apparent dip angle of third-order lamellae approach the true dip angle.

Vertically oriented thin sections of complex crossed-lamellar layers form the basis for the preceding interpretation. In section (Pl. 21, fig. 4) along the central

axis of a major prism, unit crystals, which are here considered third-order lamellae, have a dip angle of about 52°. The extinction exhibited by all third-order lamellae in central-axis sections is total, not wavy, and occurs where the central axis of the major prism is at an angle of about 45° to the horizontal cross hair of the microscope.

The farther from the central axis the section is taken the greater is the area exhibiting a wavy extinction. In vertical section (Pl. 11, figs. 1, 2) through the flank of a major prism, two structural trends can be seen. One structural trend is the attitude of what are here interpreted as rhomboidal prismatic segments of third-order lamellae. The other structural trend is a series of arches formed by conical second-order lamellae where they intersect the plane of section. At the median bisecting plane (Text-fig. 38) the cones are normal to that plane. Progressively farther from the median plane the angle between the cone sections (projected to the median plane) and the median plane decreases. Farthest from the median plane the trend of the cone sections merges with the trend of the third-order lamellae. The wave of extinction seen in off-central-axis sections of major prisms is caused by the orientation of the rhomboidal prismatic units of third-order lamellae. Along the median bisecting plane (Pl. 21, fig. 4) extinction is parallel to the central axis of the major prism. Laterally from the median bisecting plane the extinction angle becomes progressively greater. Near the margin (Pl. 22, fig. 1) of the major prism the rhomboidal prismatic units of third-order lamellae, the cone surfaces, and the extinction position are all parallel. Bøggild's (1930, fig. 3) diagram of the complex crossed-lamellar structure shows the wave of extinction seen in sections cutting the flanks of major prisms and parallel to their central axes.

For simplicity (Text-fig. 38) the prisms may be considered cylindrical. Actually, in complex crossed-lamellar layers major prisms have an irregularly polygonal outline in section normal to the central axes. In vertical section at the contact (Pl. 21, fig. 4) between prisms there is always an angular relationship between the conical second-order lamellae of adjacent prisms. This relationship holds even where vertical sections (Pl. 22, figs. 1, 2) do not include the central axes of prisms. As can be seen in the three figures just mentioned, the boundaries between major prisms can be very irregular. Generally, within this structure, the high degree of lateral interpenetration of major prisms makes interpretation of the complex crossed-lamellar structure extremely difficult. In any one vertical section through a layer having this structure, only a few major prisms are intersected along their central axes. Thin sections usually show an irregular patchwork with the patches exhibiting correspondingly irregular wavy extinctions. The visible fine structure within each patch results from the combined influence of conical second-order lamellae and third-order lamellae. Under the control of these two structural elements, the resultant micro-trends can appear oriented in any direction. Unless this possibility is appreciated, it would be possible to misinterpret the structure as being composed of a completely irregular arrangement of major and minor structural elements.

The major prisms of the complex crossed-lamellar structure result from a basically simple, spherulitic growth of unit crystals. Similar patterns have been observed in the growth of non-organic minerals (Bryan, 1941, Text-fig. 6b) and in the growth of coral trabeculae (Bryan and Hill, 1941). Kato (1963, Text-fig. 2) gives three longitudinal sections through a single idealized coral trabecula showing patterns similar to those of the traces of conical second-order lamellae and third-order lamellae shown in text-figures 37 and 38 of this paper.

Bøggild (1930, p. 255) states that the major prisms of the complex crossed-lamellar structure strongly resemble first-order prisms of the complex-prismatic structure in the similarity of the wave of extinction visible in sections parallel to the long axis of both kinds of prisms. As demonstrated here, however, the prisms of the complex crossed-lamellar structure can be recognized by the arrangement of conical second-order lamellae in a cone-in-cone structure. The complex crossed-lamellar structure can also be distinguished by the fact that, in many cases the structure grades laterally and vertically into the common crossed-lamellar structure. The exact relationship between the structural elements through the transition zone was not determined.

Along the central axes of major prisms of the complex crossed-lamellar structure (Pl. 21, fig. 4), growth lines are periodically accentuated by dark brown accumulations resembling the rungs of a ladder.

In Recent shells, and in fossil shells where partial recrystallization of the shell has rendered thin-section study useless, several criteria can be used for recognition of complex crossed-lamellar structure. In the following discussion the three criteria used may be observed only in shell layers which, where fractured, break along original zones of weakness between major and minor structural elements. The first criterion is the occurrence of exposed conical surfaces on the ends of major prisms. The conical surfaces point toward the outer surface of the shell. These isolated conical surfaces can be seen in Recent (Pl. 21, figs. 5, 6) and fossil (Pl. 30, figs. 2, 3; Pl. 31, fig. 1) shells. The second criterion is the chevron pattern revealed in vertical broken sections through the cones of major prisms. The chevron patterns indicate the presence of second-order lamellae of the complex crossed-lamellar structure only if the chevrons are seen in two vertical sections at right angles to each other. The chevron patterns can be seen in Recent (Pl. 22, fig. 3) and fossil (Pl. 30, figs. 4-6) shells. The third criterion is the rapid expansion of major prisms toward the inner surface of the shell. This feature can be seen in vertical breaks through Recent shells. Expansion of the prisms in fossil shells (Pl. 31, figs. 1, 2) can be determined by measuring the width of the polygons in the polygonal patterns seen on growth surfaces. The polygons near the inner surface of the layer are relatively larger than the polygons on surfaces near the outer part of the shell layer.

COMPLEX CROSSED-FOLIATED STRUCTURE

This term is here proposed for a variation of the calcitic foliated structure described in detail by Wada (1963a, 1963b). On the inner surface of the shells of two pelecypods (*Anomia* and *Ostrea*) he described a spiral or concentric outcrop pattern of folia with the blades oriented radially. This complex crossed-foliated structure bears the same morphologic relationship to the crossed-foliated structure that the complex crossed-lamellar structure has to the crossed-lamellar structure. However, the conical second-order lamellae (Text-fig. 39) of this structure differ from the cones in the complex crossed-lamellar structure in having a very low dip angle (about 5°) to growth surfaces and in having wider (2-4μ) third-order lamellae. This structure is poorly developed in only one patelloid species (*Patella granularis,* hypotype, YPM no. 13380), and is mentioned here mainly because of its close relationship to the other described structures. In pelecypod shells (e. g. *Hinnites multirugosus,* hypotype, YPM no. 13371) the structure can occur as coalesced major prisms or even as perfectly circular major prisms isolated in shell material having a regularly foliated structure.

STRATIFICATION OF SHELL MATERIAL

In its broadest sense, *shell structure* includes not only the architectural arrangement of crystals and crystal aggregates but also the different kinds of stratification units within the shell, and the interrelationships among them. In its restricted sense, *shell structure* refers only to the architectural arrangement of the crystals or crystal aggregates. A sharp distinction is made here between shell structure, in the restricted sense, and shell stratification, which reflects expansion of the shell and results from different kinds of layering during growth. This layering is expressed either by changes in shell structures or, within material of uniform structure, by compositional or textural changes such as trace-element content, organic content, and color.

Deposition of shell material by the mantle on the inner surface of the shell results in two major kinds of layering within the mollusk shell. These layers have their simplest and most idealized form in the patelloid shell (Text-fig. 40). The most obvious of them is the *shell layer,* a stratal unit which thickens continuously during growth of the animal. All shell layers are deposited simultaneously in concentric bands on the inner surface of the shell (Text-fig. 71), and ideally the contacts between all shell layers are conical surfaces which have a common apex at the apex of the shell. In the sequence of shell-layer contacts, from dorsal to ventral through the shell, the angles between a horizontal plane (Text-fig. 40) and the conical surfaces become greater. The other major kind of stratification is the *growth layer,* which is the shell material bounded by any two of an essentially unlimited number of former depositional surfaces, here called growth surfaces. Because, at any particular instant during the growth of the animal, the whole ventral surface of the shell is the depositional surface, each growth layer is made up of concentric bands of all shell layers present. The contacts between shell layers and growth layers always intersect at an angle. Usually growth layers are delimited by changes other than structural. In some instances, however, a growth layer may have a structure different from that of the surrounding shell material. Where this kind of growth layer is restricted to one shell layer, it is here called a *shell sublayer* (Text-fig. 61).

Perhaps the relationships among the three kinds of layering described above can be presented more clearly by a direct comparison with the deposition of sedimentary rocks through geologic time. Caster (1934) gave a diagram (Text-fig. 43) in which he showed magnafacies (sedimentary rock units each having a characteristic lithology) transgressing time-stratigraphic units, which are bounded by planes of contemporaneity. The planes of contemporaneity are analogous to growth surfaces in the mollusk shell, and the time-stratigraphic units are analogous to growth layers. Continuing the analogies, the magnafacies are the equivalents of molluscan shell layers, and the parvafacies are delimited by boundaries analogous to those of the shell sublayer in the mollusk.

Shell Layers

Each shell layer of a sequence is characterized by either a structure different from that of the adjacent shell layers or, where the structure is the same, by corresponding major structural elements oriented at right angles to each other. Some shell layers (Text-fig. 61) are characterized by an alternating sequence of shell sublayers.

Ideally, all patelloid shell layers thicken with growth of the animal, and the contacts between shell layers intersect growth surfaces at an angle. Each shell

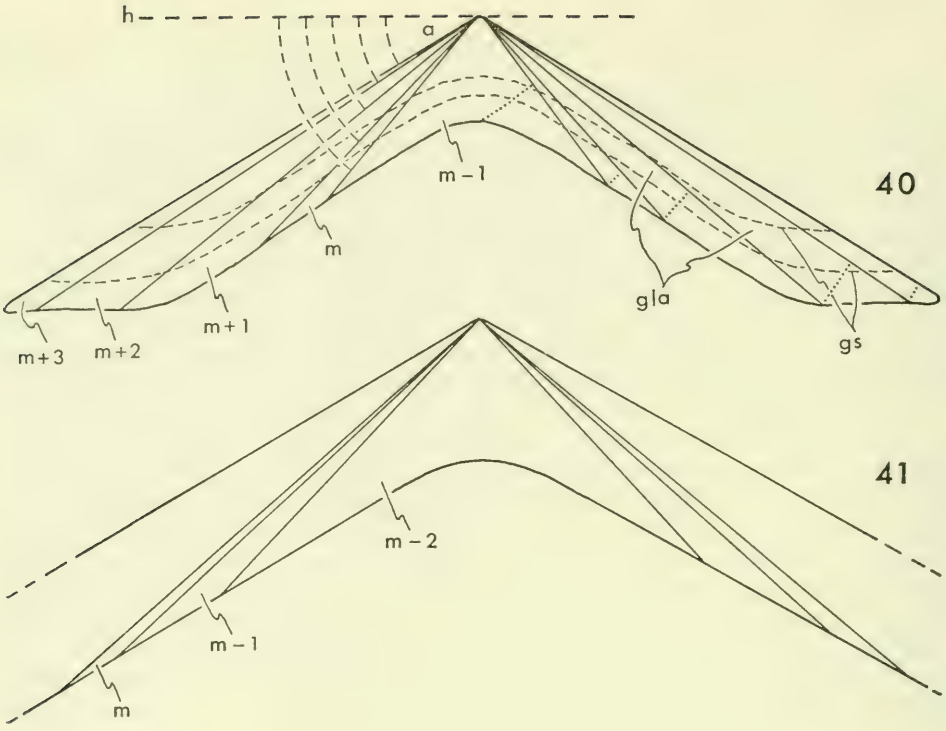

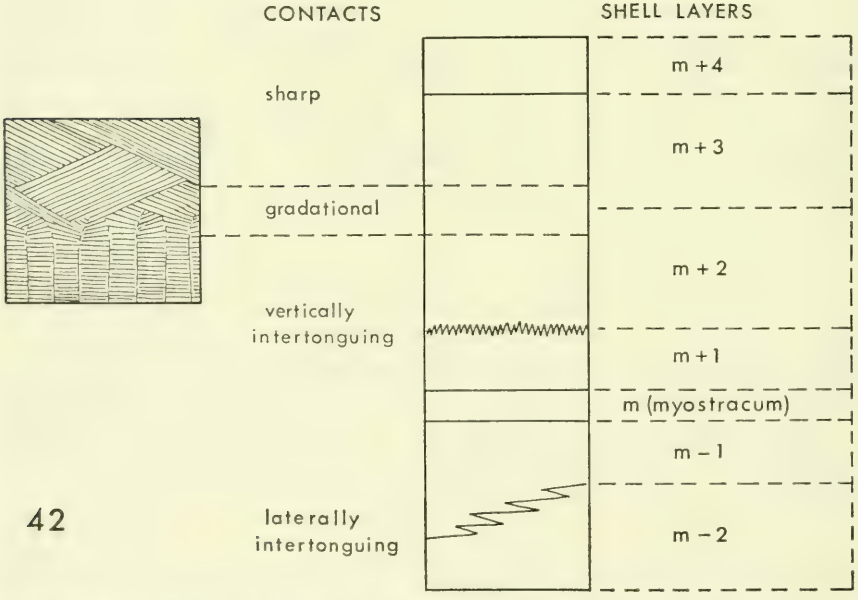

Text-figs. 40-42.—System of shell-layer notation in patelloid gastropods. Explanation of symbols: a, angle between horizontal and shell-layer contacts; m, myostracum; m + 1 etc., shell layers dorsal to myostracum; m — 1 etc., shell layers ventral to myostracum; gla, single growth layer; gs, growth surfaces; h, horizontal. **40,** transverse section showing relationship of shell layers to growth layers; dotted lines show place of maximum shell-layer thickness. **41,** transverse section with two shell layers ventral to myostracum. **42,** columnar section showing kinds of shell-layer contacts; the gradational contact is illustrated by a 90° twist of first-order lamellae of the crossed-foliated structure.

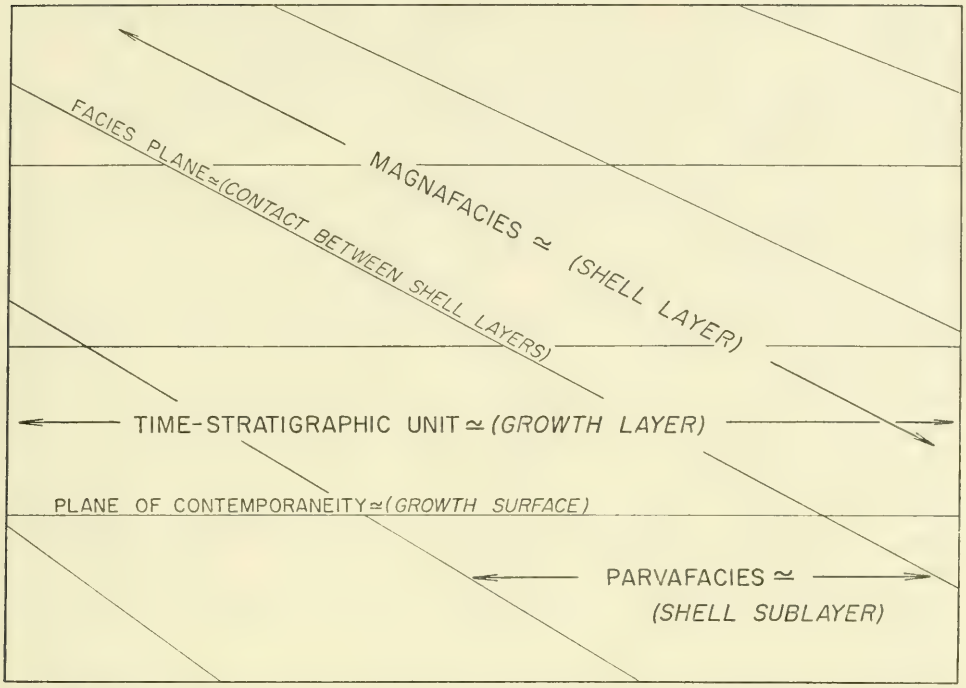

Text-fig. 43.—Comparison between stratigraphic relationships in the geologic sedimentary record and stratification relationships in the patelloid shell as seen in vertical, radial section. Shell-stratification terminology in italics. Diagram and geologic terminology, in Roman capitals, modified from Caster (1934, Text-fig. 2).

layer (Text-fig. 40) is thickest where its ventral surface (contact with underlying shell layer) intersects the ventral surface of the shell. Each layer then thins to a feather edge where its dorsal surface intersects the ventral surface of the shell. With the exception of the innermost layer, all shell layers thin adapically. The innermost shell layer (Text-fig. 40, m — 1) has its point of maximum thickness near the apex of the shell. Because of its unique position among the shell layers, there is no adapical thinning of the ventralmost layer. The continual thickening of this layer in the apical region compensates for the adapical thinning of all the other shell layers. At any one stage during its growth, therefore, the shell is equally thick at all points except along the margin, where the shell becomes thinner. In shells (Text-fig. 41) where there are two or more shell layers ventral to the myostracum (muscle-scar shell layer), only the innermost layer thickens adapically.

Depending on the species, differing degrees of mantle reflection occur during growth. As a result, the outermost shell layer (Text-fig. 62) does not thin to a feather edge. In shells of some species (Pl. 26, fig. 19) only the outermost part of the outermost layer is affected by the reflected mantle. In other species (Pl. 12, fig. 1) the whole outermost layer is affected by the reflected mantle.

In the patelloid shell (Text-figs. 1, 40) the pedal-retractor myostracum is continuous with and at the same horizon as the anterior mantle-attachment myostracum. In the system of shell-layer notation (Text-figs. 40, 42) used here for patelloids, therefore, the myostracum is used as a datum. Regardless of their thickness, shell layers dorsal to the myostracum are referred to respectively as

layers m + 1, m + 2, m + 3, etc. Layers ventral to the myostracum are referred to respectively as layers m — 1, m — 2, etc. The notation designates only the position of each shell layer with respect to the myostracum and in no way refers to the shell structure of these layers. For example (Pl. 32), layer m + 1 has concentric crossed-lamellar structure in group 1, radial crossed-lamellar structure in group 6, and foliated structure in group 11.

The contact (Text-fig. 42) between two shell layers may be *sharp* (Pl. 5, fig. 2) and consistently at one horizon, *gradational* (Pl. 13, fig. 20) involving a 90° twist, through a measurable zone, of the main structural elements, or *intertonguing* (Pl. 13, fig. 2) involving a lateral interdigitation of two shell layers. At high magnifications (Pl. 12, fig. 3) a contact which appears sharp at low magnifications may actually involve a vertical intertonguing relationship between the structural elements of the two adjacent layers. In shells having two ventral layers there may be either an intertonguing relationship (Pl. 13, fig. 2) or no intertonguing relationship (Pl. 11, fig. 1) between layers m — 1 and m — 2. An intertonguing relationship between two shell layers ventral to the myostracum does not necessarily mean that intertonguing relationships exist between layers dorsal to the myostracum. In an analogous situation for pelecypod shells, Oberling (1964, p. 42) applied the terms *heterochronous secretion* to "secretion such that the periods of fast-growth and slow-growth do not correspond on the apical and marginal sides of the pallial line" and *homochronous secretion* to "secretion such that the periods of fast-growth and slow-growth correspond on both sides of the pallial line.'

Dorsal to the myostracum, in each layer showing crossed-lamellar structure, the relationship of the first-order lamellae to the overall symmetry of the shell is relatively simple. They are either radially arranged or concentrically arranged. Ventral to the myostracum, however, if the ventralmost layer has crossed-lamellar structure, the relationship of the first-order lamellae to the overall symmetry of the shell is complex. In an idealized ventral view (Text-fig. 44) of the layer ventral to the myostracum, in the shell of an acmaeid, several trends of first-order lamellae can be seen. In this view there is an overlap relationship in both the posterior and anterior part of the shell layer. Text-figure 45 is a diagram showing the surface trend of first-order lamellae at three different growth stages of the shell.

On the inner surface of the shell (Text-fig. 44) near the margin of the ventral layer the first-order lamellae are generally arranged radially. Unless all first-order lamellae converge on a point directly under the apex, there must of necessity be an overlap of first-order lamellae within the shell layer. In ventral view of the most common overlap relationship (Text-fig. 44) first-order lamellae with a left to right orientation overlap first-order lamellae having an anteroposterior orientation. Along the median sagittal plane (Pl. 4, fig. 2; Pl. 6, figs. 1, 2) the angle of overlap is 90°. Point "A" (Text-fig. 44) is where the anteroposteriorly oriented first-order lamellae are initially overlapped by the lamellae with a left to right orientation. A transverse section (Pl. 5, fig. 2) between the posterior part of the pedal-retractor scar and point "A" of text-figure 44 shows anteroposteriorly oriented first-order lamellae. A transverse section (Text-fig. 48; Pl. 5, fig. 1) between point "A" of text-figure 44 and the apex of the shell shows, at the median plane, first-order lamellae at right angles to each other. Laterally the angle of overlap decreases gradually to the point where no overlap angle exists. At all points of overlap the first-order lamellae are involved in a twist rather than a sharp break in the continuity of the structural elements. Several first-order

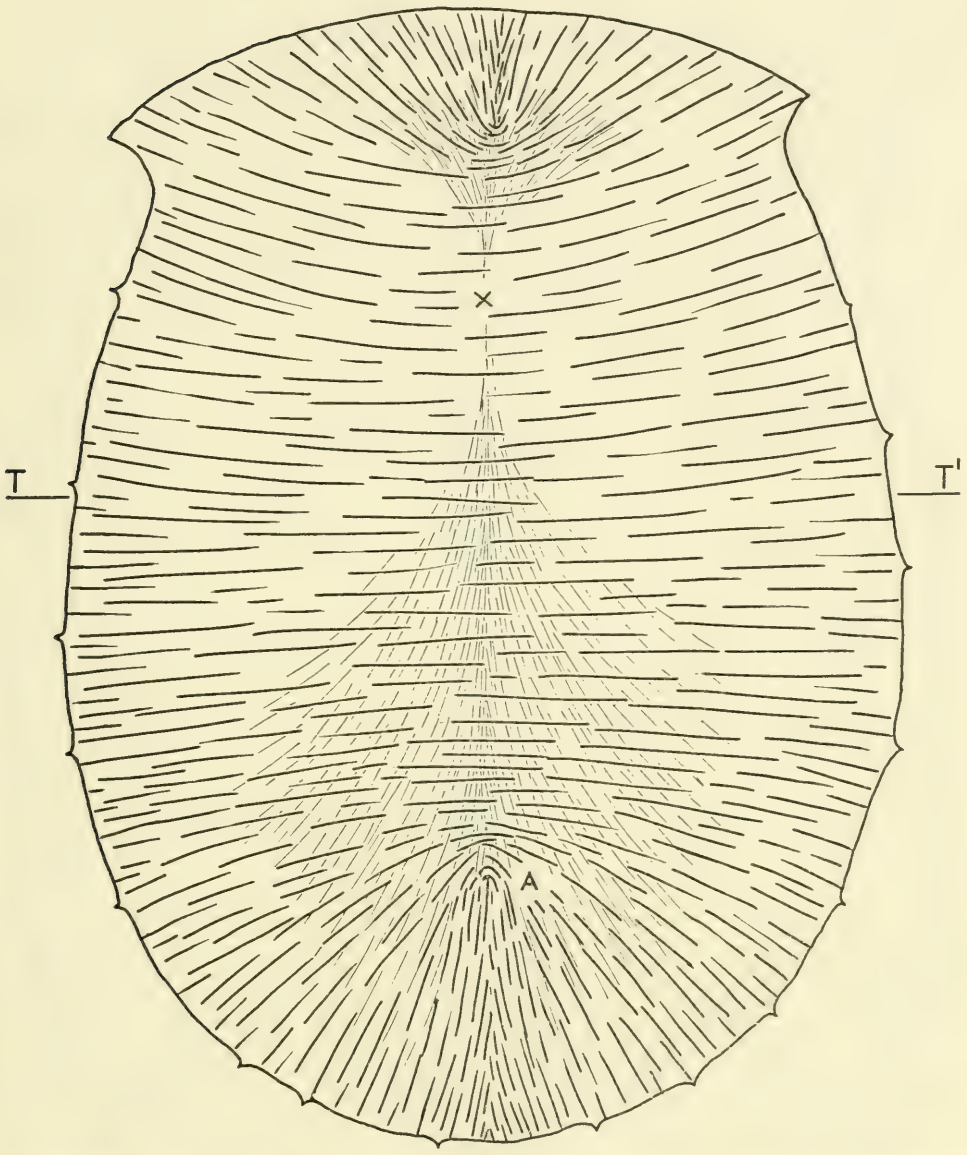

Text-figs. 44-47.—Ventral views inside patelloid muscle scar showing idealized surface and subsurface structural trend of first-order lamellae in radial crossed-lamellar layer m — 1. × marks position of apex of shell. **44**, overlap of first-order lamellae at anterior and posterior ends (see Text-fig. 53); the wide broken lines indicate ventral-surface trend; the fine broken lines show subsurface trend, which is often visible if shell layer is transparent; section at TT′ is given in text-figure 48. **45, 46**, structural overlap of first-order lamellae at posterior end only. **45**, surface (unbroken lines) and subsurface (broken lines) trends at three stages of growth. **46**, the trend of first-order lamellae at inner surface of shell and subsurface only in zone of median sagittal plane. **47**, the trend of first-order lamellae at ventral (solid lines) and dorsal (dashed lines) surface of shell layer; section at SS′ shown in Pl. 5, fig. 1; note that the pattern is truly radial at the dorsal surface of the layer.

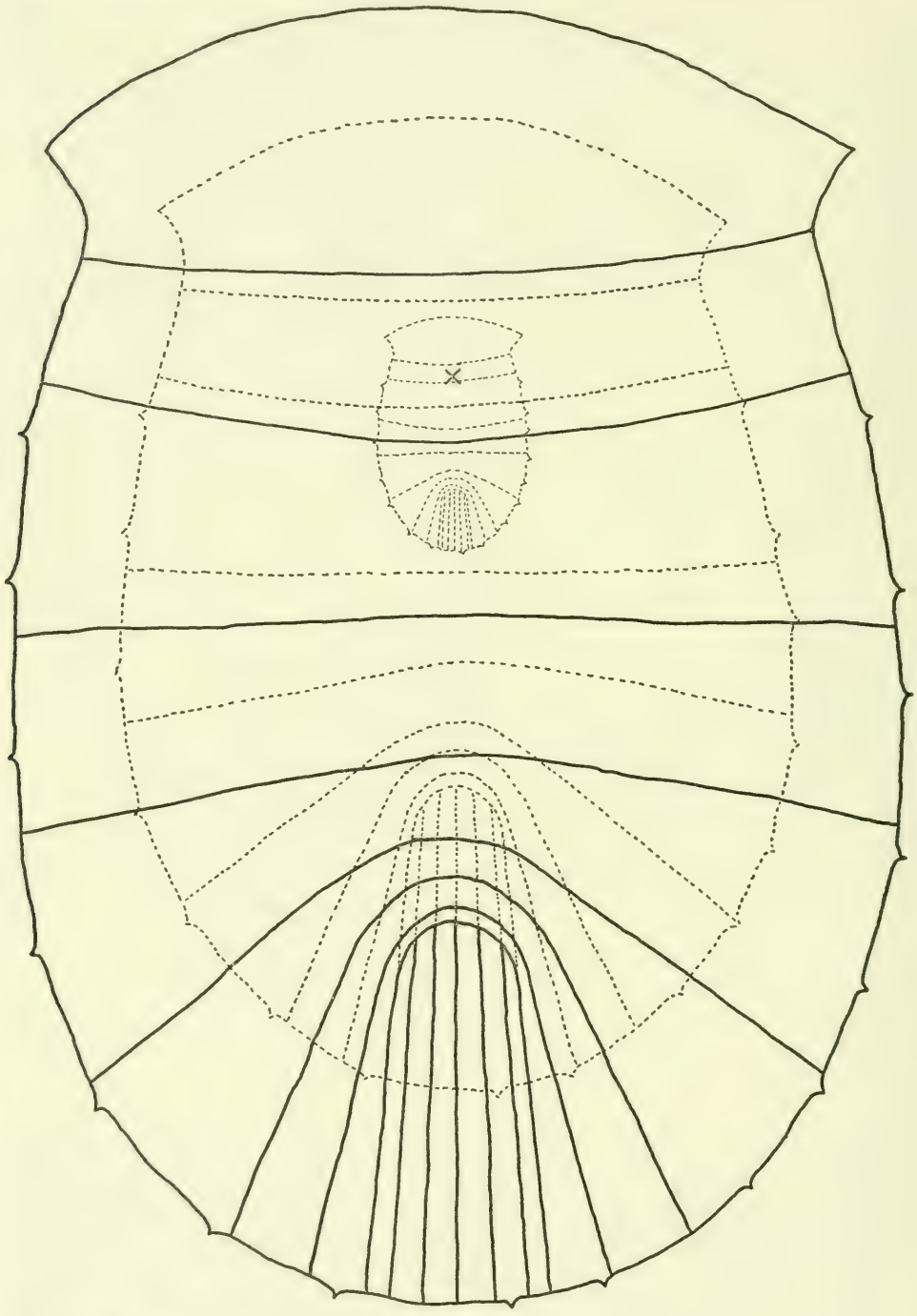

Text-fig. 45.—See explanation under text-figure 44.

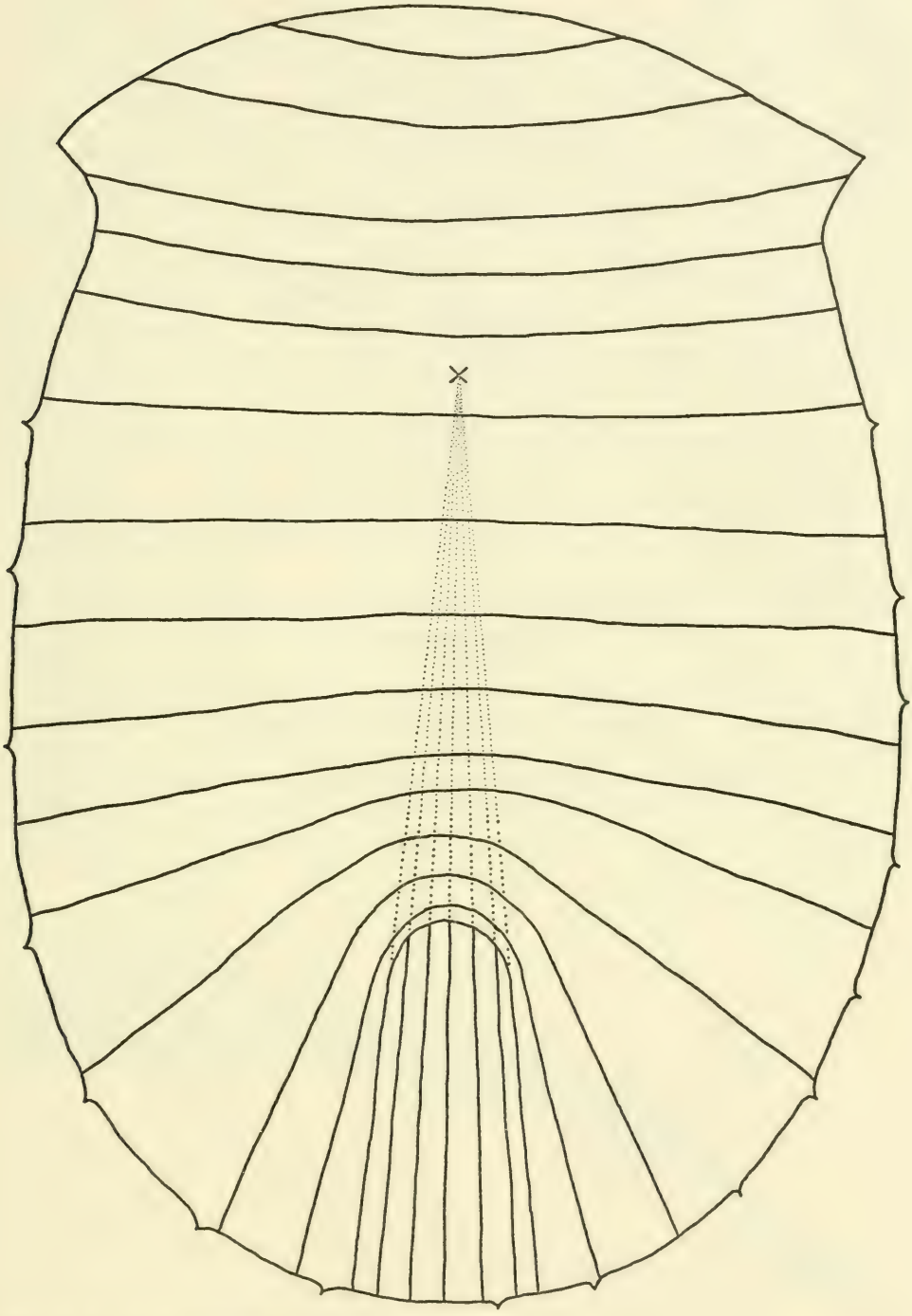

Text-fig. 46.—See explanation under text-figure 44.

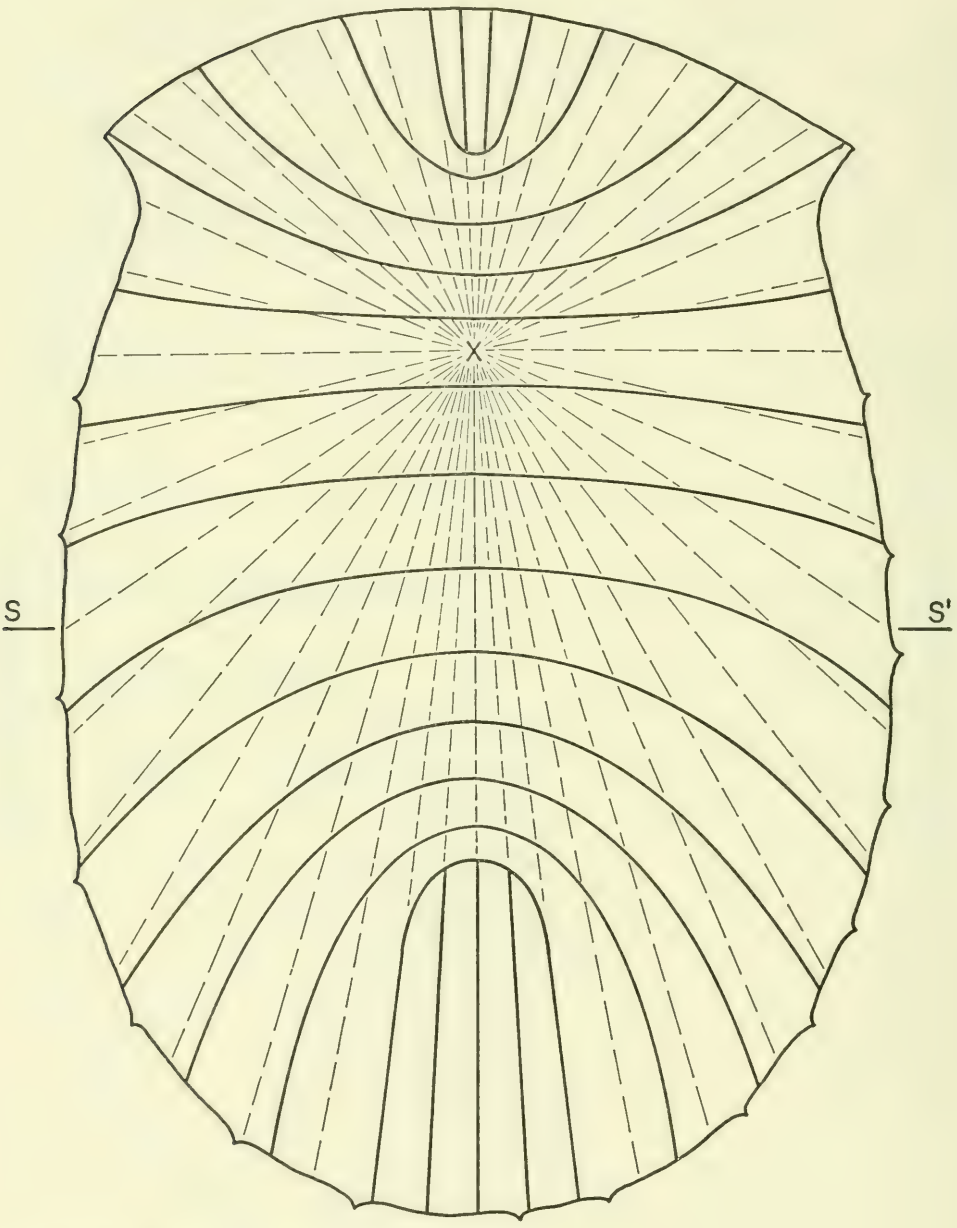

Text-fig. 47.—See explanation under text-figure 44.

lamellae (Pl. 4, fig. 3) can be traced across the twist zone. Dorsally the first-order lamellae, oriented at a high angle to the plane of section, appear narrow, with the second-order lamellae apparently having a low angle to growth surfaces. Ventrally, through the twist zone, the first-order lamellae appear to become wider and the apparent angle of the second-order lamellae to the inner surface of the shell becomes greater. Ventral to the twist zone the first-order lamellae are oriented at a low angle to the plane of section and they appear wide, with the second-order lamellae having a higher angle to growth surfaces. In transverse section (Pl. 5, fig. 3) near the apex of the shell first-order lamellae trend from left to right.

In median sagittal section (Pl. 4, fig. 2) of the layer shown in text-figures 44 and 46 one gets the false impression that there are two distinct shell layers ventral to the myostracum, an upper radial crossed-lamellar layer and a lower concentric crossed-lamellar layer. After studying the three-dimensional relationships, however, the conclusion is reached that these two *pseudolayers* actually belong to one shell layer.

In the ideal arrangement of first-order lamellae in a crossed-lamellar ventral shell layer (Text-fig. 47), the first-order lamellae are truly radial at the dorsal surface of that shell layer. The structural trends of first-order lamellae at the dorsal and ventral surfaces of the layer merge and are parallel to each other only at the abapical margin of the shell layer. Because of the radial arrangement of first-order lamellae at the dorsal surface of this "ideal layer," all crossed-lamellar ventralmost shell layers are here defined as radial crossed-lamellar in spite of the apparent inconsistencies mentioned below. The same relationship holds true for all ventralmost crossed-foliated shell layers.

Of those patelloids having a ventral crossed-lamellar layer, the pattern shown in text-figures 49-51 is the most common arrangement of first-order lamellae on the ventral surface of the shell. The overlap relationship is in the posterior half of the layer. Patterns not conforming to the common arrangement of first-order lamellae are shown in text-figures 52-56. In some shells (Text-fig. 52) the

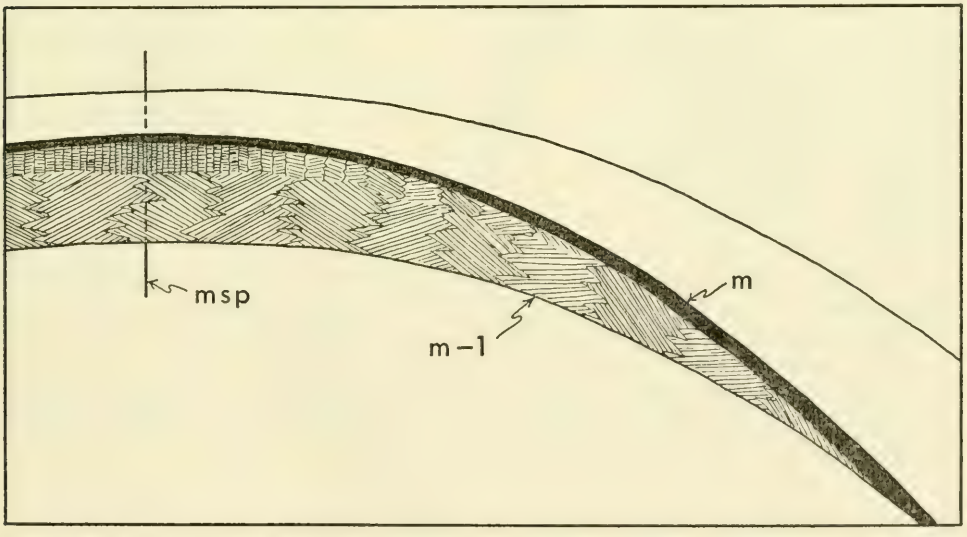

Text-fig. 48.—Transverse section of patelloid shell showing overlap relationship of first-order lamellae in crossed-lamellar layer m — 1 at and laterally from median sagittal plane (msp). See text-figure 44 for location of section.

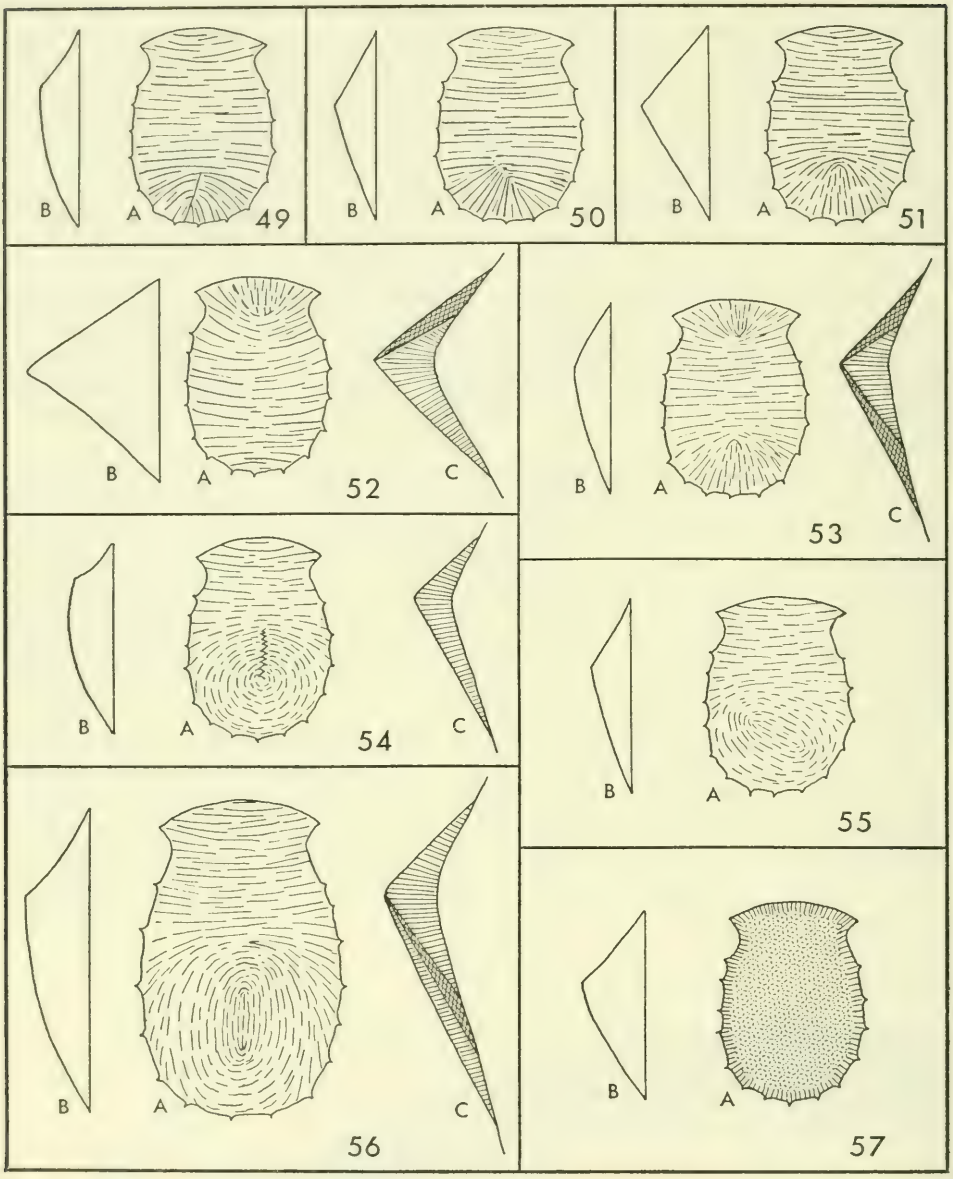

Text-figs. 49-57.—Arrangement of structural elements in shell layer(s) ventral to the myostracum of some patelloids. A, ventral view of layer(s) inside the muscle scar. B, side view of entire shell. C, median sagittal section showing structure of shell-layer m — 1 only: note the relationship between ventral and cross-sectional views of this shell layer; pseudolayers are shown in figures 52, 53 and 56. 49-56, pattern of first-order lamellae of radially crossed-lamellar layer m — 1. 57, adapical change in pattern from radial crossed-lamellar to complex crossed-lamellar.

overlap relationship is restricted to the anterior half of the layer. Only rarely (Text-figs. 44, 53) does the overlap relationship exist at both ends of the layer. If a median sagittal section were made through the shell (Text-figs. 54, 55) having first-order lamellae arranged concentrically about a point near the posterior part of the shell layer, and if only this one section were considered, one could be misled into describing the ventral layer as concentrically crossed-lamellar. Text-figure 56 shows, near the posterior margin of the layer, a pattern in which elliptically arranged first-order lamellae surround longitudinally arranged first-order lamellae. In longitudinal cross-section of this layer the vertical sequence of structure patterns gives the impression that, in the posterior half of the layer, there are three separate shell layers. In the ventral layer each different pattern will yield a different structural configuration in median sagittal section. However, careful examination of the three-dimensional relationships will indicate that, basically, all the shell layers described above are radially crossed-lamellar.

No attempt was made to determine if there is any relationship between taxonomic categories and the pattern on the surface of the ventral crossed-lamellar layer. Several tendencies, however, were noted. The anterior overlap relationship occurs most often in high conical shells, such as those of *Acmaea mitra* and *Scurria scurra*. The posterior overlap relationship occurs most often in conical shells of intermediate height, such as those of *A. limatula*. The pattern in which first-order lamellae are arranged concentrically within the posterior part of the layer occurs most often in low shells having the apex near the anterior margin.

The system of overlapping first-order lamellae is one arrangement which solves the spatial relation problem of getting radially arranged first-order lamellae into the ventralmost conical shell layer without having all first-order lamellae converge at the apical part of the layer. The other arrangement (Text-fig. 57) involved in solving the same problem is an adapical change in structure from radial crossed-lamellar near the inner margin of the muscle scar to complex crossed-lamellar. In some shells the radially arranged first-order lamellae are not present and the major prisms of the complex crossed-lamellar structure are in direct contact with the myostracum.

Bøggild (1930, p. 305-308, Pl. 10, figs. 2-5) described the shell structure of 15 patelloid species. He then stated (p. 307), "The species investigated, though rather a random selection, will be sufficient to show that the structures . . . are so variable that the picture of the whole is one of great confusion." Based on results of the present work, Bøggild's confusion is understandable. Of the 17 shell-structure groups recognized herein, eight (Table 3) appear to be represented within the group of 15 species he described. This in itself, however, is not the major cause for confusion. Bøggild's description of the shell structure of individual shell layers is excellent but his discussion of layer sequences within each shell and the correlation of these sequences from species to species is weak for several reasons. Perhaps because of the lack of extra-thin sections, Bøggild failed to recognize the presence of a muscle-scar shell layer, which, as is now known, exists in all patelloid shells. In one case Bøggild (1930, Pl. 10, figs. 4, 5) described a prismatic layer ventral to a crossed-lamellar layer, but he did not recognize it as the prismatic muscle-scar shell layer. This prismatic shell layer described by Bøggild must be the myostracum because, based on the present study, the myostracum is the only prismatic shell layer that has been found ventral to any of the crossed-lamellar layers. Bøggild also failed to give in detail the exact location and orientation of each of the sections he described and figured. He described the sections as being either vertical, concentrical (that is, tangential to

TABLE 3: Patelloid species described by Bøggild (1930, p. 305–308).

Bøggild's nomenclature	Present nomenclature	Present shell-structure group
Acmaea (Tectura) virginea	*Acmaea (Tectura) virginea*	1
Acmaea persona	*Acmaea persona*	1
Acmaea cubensis	*Acmaea cubensis*	1
Scurria sp.	*Scurria* sp.	3
Scurria zebrina	*Scurria zebrina*	3
Patella vulgata	*Patella (Patella) vulgata*	8
Patella plicata	*Patella (Scutellastra) barbara*	9
Patella Bavia [= P. badia]	*Patella (Patellona) ocula*	6
Patella rustica	*?*	—
Helcion pellucidum	*Helcion (Ansates) pellucida*	7
Patella (Helcioniscus) radians	*Cellana radians*	12
Tectura testudinaria	*Cellana testudinaria*	13
Helcioniscus ardosiaeus	*Cellana ardosiaea*	12
Patella fluctuosa	*Cellana flexuosa*	—
Scutellina fulva	*Iothia fulva*	—

concentrically arranged structural elements) or vertical, radial. Bøggild did not, however, state whether his vertical, concentrical sections were taken inside or outside the muscle scar or whether they were parallel or normal to the longitudinal axis of the shell. In vertical, radial sections he gave the abapical direction but he did not state whether the descriptions of the sections were based on layer sequences adapical or abapical from the muscle scar, nor did he give the orientation of the radial sections with respect to the longitudinal axis of the shell.

As an example of the necessity of knowing the exact location of sections before attempting correlation of shell-layer sequences from species to species, the following quotation from Bøggild (1930, p. 307) is given. He is describing only shell layers under the outermost calcitic layer.

> In *Scurria* . . . the upper layer is prismatic, the lower one concentrically crossed lamellar, and the same combination is found in *Acmaea virginea* (pl. X, fig. 3), while, in *A. persona,* there is, under the two above mentioned layers, a third consisting of radial crossed lamellae.

Based on present observations, all three species described by Bøggild have an inner radial crossed-lamellar shell layer. Apparently, the reason for lack of correlation between the three species in Bøggild's description is that the first two shell-layer sequences, in *Scurria* and *Acmaea virginea,* were based on sections abapical from the muscle scar, whereas the sequence in *A. persona* was based on a section or sections adapical from the muscle scar.

A problem which may or may not have affected Bøggild's work is the partial loss of outer shell layers by erosion. If the shell has been strongly eroded during the life of the animal, shell layers may be exposed in concentric bands on the dorsal surface of the shell. The outermost layer (Text-fig. 58) may exist only as a narrow ring at the margin of the shell. Adapically, layers progressively lower in the shell-layer sequence are exposed until, near and at the apex, the layer ventral to the myostracum is exposed on the dorsal surface of the shell. Vertical, radial sections must, therefore, include the shell margin if the complete shell-layer sequence is to be obtained.

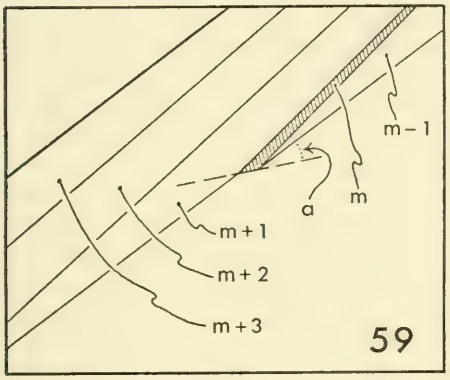

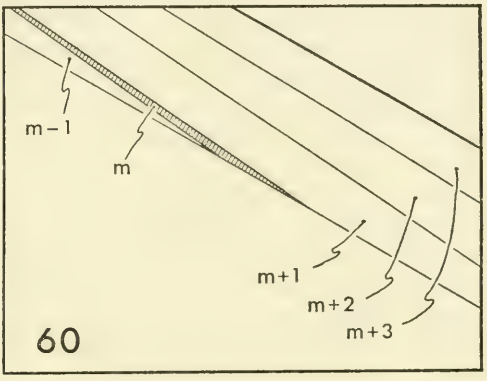

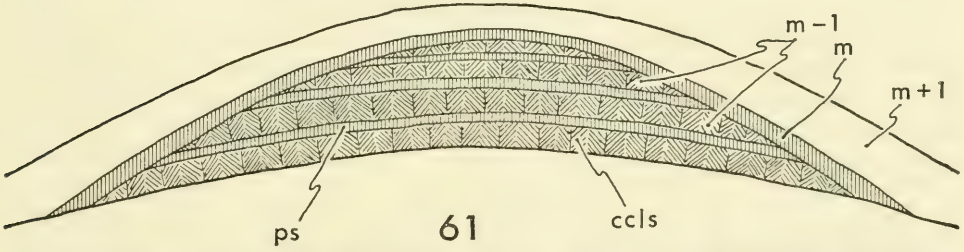

Text-figs. 58-61.—Transverse sections through patelloid shell. Explanation of symbols: a, angle between the general inner shell surface and the shell surface where the anterior mantle-attachment muscle is attached; ccls, complex crossed-lamellar sublayer; m, myostracum; m + 1, m — 1, other shell layers; ps, prismatic sublayer. **58,** all shell layers exposed on strongly eroded dorsal surface. **59, 60,** relationship between angle of depositional surface and thickness of myostracum. **59,** anterior mantle-attachment myostracum. **60,** posterior part of pedal-retractor myostracum. **61,** two kinds of shell sublayers in shell-layer m — 1.

Further complications resulting from the lack of perfectly oriented sections in Bøggild's work can probably be traced to the already-discussed problem of the geometric relationship of first-order lamellae in the layer ventral to the myostracum.

Some of the problems associated with interpreting shell-layer sequences also affected the work of Thiem (1917b), who used shell structures in his systematic descriptions of 12 acmaeid species. Thiem applied the term "ostracum" [*Ostrakum*] to the outer shell layers and "hypostracum" [*Hypostrakum*] to the inner

shell layers. From his discussion, it appears that Thiem (1917b, p. 462-474, text-fig. 30) preferred to restrict the "hypostracum" to "crossed-lamellar layers" [*Blätterschichten*]. In his one exception to this rule, Thiem (1917b, p. 475, text-fig. 31) described the outer "ostracum" of *Acmaea cubensis* as having the same [crossed-lamellar] structure as that of the "hypostracum." There are several reasons for Thiem's confusion. Although he described and figured a 90° twist of first-order lamellae within the "hypostracum," he did not recognize the fact that this twist occurred wholly within a single shell layer. In thin sections of four of the 12 species examined, Thiem (fig. 30) recognized a thin "intermediate shell layer" [*Zwischenschicht*] within the "hypostracum." In a polished section of *Scurria coffea*, Thiem (fig. 40) recognized the relationship between the muscle scar and a colorless zone within the shell indicating the advance of the shell muscle with growth. He did not, however, describe any relationship between the *Zwischenschicht* and the colorless zone, and hence did not recognize the *Zwischenschicht* as a muscle-scar shell layer which, as is now known, is present in all patelloids. Consequently the layer labeled *Ostrakum* in Thiem's figure 31 is here considered homologous with the layer labeled *Gestreift Hypostrakum* in Thiem's figure 30.

In his table comparing the shell-layer sequence of the 12 acmaeid species, Thiem (1917b, p. 481) presented the structure as seen in vertical, radial sections through the shell. He used the symbol "III" for crossed-lamellar layers cut normal to length axes of first-order lamellae and the symbol "X" for crossed-lamellar layers cut normal to width axes of first-order lamellae. The upper and lower "hypostracum" are always represented by "X" or "III." He also represented all but one of the "ostracum" layers (in *Acmaea cubensis*) by the symbol "X." Unfortunately, in these "ostracum" layers, the "X" was intended to show the crossed relationship between the shell-layer prisms and the growth lines. Using the structure of *A. cubensis* as an example, it is impossible to tell from the symbols alone the structure of the upper and lower "ostracum" of the remaining species. As presently interpreted, growth surfaces, although they may be parallel to structural elements, are not themselves structural elements in the sense of crystals or crystal aggregates.

Myostracum

Myostracum is the term proposed by Oberling (1955, p. 128) for all shell material deposited in areas of muscle attachment in pelecypods. As here defined a myostracum is a molluscan shell layer or partial shell layer deposited adjacent to mantle epithelial cells in the areas of muscle insertion on the shell. As mentioned before, the combined pedal-retractor and anterior mantle-attachment myostracum in patelloids forms a complete shell layer (Text-fig. 1). In other mollusks, such as the oyster, large isolated scars leave only a partial myostracal shell layer. For each isolated accessory scar in the mollusk shell, there is a lath-shaped blade of shell material starting at the apex of the shell and gradually expanding to the outcrop area on the inner surface of the shell. Each of these myostracal blades is completely surrounded by the shell material of the enclosing shell layer, and each blade maintains a constant position within the layer with respect to the outer and inner surface of that layer. Each isolated myostracum has one important attribute characteristic of all shell layers—that is, it cuts across growth surfaces.

To avoid confusion in descriptions of patelloid shell-layer sequences, it is

extremely important that the combined pedal- and mantle-attachment myostracum be located in the section. This is essential in clearly separating shell layers which may have identically oriented structural elements above and below the myostracum.

The following description of the shell structure of myostracal deposits is based only on the study of thin sections of patelloid shells. Basically the structure is complex-prismatic. The elongate first-order prisms (Pl. 7, figs. 1-3) are normal to growth surfaces. In section normal to the long axes, first-order prisms (Pl. 8, fig. 4) have an irregularly polygonal outline. Within each first-order prism (Pl. 8, fig. 1) second-order prisms are arranged nearly parallel to each other, but not quite normal to growth surfaces, and at a slight angle to the second-order prisms of adjacent first-order prisms. These relationships are emphasized by the extinction angles of the various structural elements. Thin sections in a large shell (8 cm long) of *Lottia gigantea*, where the maximum thickness of the myostracum is 1.5 mm, show these relationships best. In a section (Pl. 8, fig. 4) through the myostracum parallel to growth surfaces, gross differences in extinction angle reveal the polygonal outline of first-order prisms. These prisms, near the ventral surface of the layer are large, ranging from 7-80μ in diameter. At this place in the myostracum the smaller, second-order prisms (Pl. 8, fig. 3) range from 2-15μ in diameter. The irregularly polygonal outline of the second-order prism is difficult to detect because the extinction angles of all second-order prisms within any one first-order prism are nearly the same. Toward the dorsal surface of the myostracum (Pl. 8, fig. 4) the first-order prisms become smaller and more numerous. Near the dorsal surface of the myostracum, immediately under the contact with the overlying concentric crossed-lamellar shell layer, the first-order prisms cannot be distinguished from the second-order prisms. Here the diameter of the prisms is very small (1-2μ). The prismatic crystals (Pl. 8, fig. 2) thin to a point at the contact with the overlying shell layer. In the ventral part of the myostracum, as seen in vertical sections, each first-order prism exhibits a wavy extinction which is the result of a slightly fan-shaped arrangement of second-order prisms.

The myostracum, in shells where it is overlain by a layer having crossed-lamellar structure, exhibits a dependently prismatic structure. The dependence of the complex-prismatic structure in the myostracum is seen best in vertical sections oriented at right angles to the length axes of first-order lamellae of the overlying crossed-lamellar layer. In such sections (Pl. 15, fig. 1) all crystals directly under a first-order lamella have an optic orientation which is slightly different from that of the crystals directly under the adjacent first-order lamellae. In vertical sections (Pl. 7, figs. 1, 2) normal to the width axes of first-order lamellae, the dependently prismatic structure is difficult to recognize. The optical dependence can be seen in sections (Pl. 3, fig. 3) normal to the height axes of first-order lamellae.

The thickness of a myostracum is not necessarily proportional to the width of the muscle scar generating it. For example, in some patelloid shells (Pl. 19, figs. 3, 4) the myostracum generated by the narrow anterior mantle-attachment scar is as much as five times the thickness of the myostracum generated by the wide pedal-retractor scar. This inverse relationship is related to the angle of the shell surface on which the myostracum is deposited. If the myostracum is deposited at a surface which is at an angle to the surrounding shell surface (Text-fig. 59), the resulting myostracum will be thicker than the myostracum deposited in the same shell (Text-fig. 60), at the same time, on a surface parallel with the surrounding shell surface. The anterior mantle-attachment myostracum will also

be thicker in shells where the anterior slope angle of the shell is much steeper than the posterior slope angle.

Growth Layers

Growth layers are layers of contemporaneity; that is, they are bounded by surfaces of equal time (growth surfaces). A line formed by the intersection of a growth surface and any other surface is a growth line. The most familiar expression of growth lines is on the outside of the shell, where growth surfaces intersect the outer surface of the shell. In shell layers where elongate crystals are oriented at a high angle to growth surfaces (Pl. 1, fig. 1; Pl. 8, fig. 1), growth layers stand out clearly. In shell layers were elongate crystals are oriented at a very low angle to growth surfaces (foliated layers of Pl. 16, figs. 1, 2), growth layers may be entirely masked by the structural units of the shell layer.

The differences between growth layers and shell layers cannot be emphasized too strongly. In addition to the angular relationship between the two kinds of layers, another important difference is in the number of layers. Once past the larval-shell stage, the number of shell layers per shell remains fixed. The number of growth layers, however, increases continuously during growth of the shell. A growth layer may be the material deposited during a day, or a year, or it may be the whole shell itself.

Shell Sublayers

A shell sublayer (Text-fig. 61) is that part of a single shell layer which is bounded dorsally and ventrally by growth surfaces and which exhibits a shell structure different from that of the overlying and underlying material. Not all shell layers have sublayers, but those that do usually have a sequence of alternating sublayers with each set having a distinct structure. Shell sublayers differ from shell layers in several ways. Sublayers are parallel to the growth surfaces bounding them above and below, whereas shell layers are intersected at an angle by growth surfaces. Only the ventralmost sublayer in a sequence is exposed on the ventral surface of the shell, whereas a shell layer is continually exposed on the ventral surface of the shell during growth of the animal. Each sublayer generally has a uniform thickness except near its margin where it is truncated by the overlying or underlying shell layer. Shell layers (Text-fig. 40) have a characteristic system of thickening and thinning as described in the section on Shell Layers.

In his discussion of shell structures, Bøggild (1930) defined a structure which he called the complex structure. This structure he described as an alternating sequence of complex crossed-lamellar sublayers and prismatic sublayers. The prismatic sublayers, however, may alternate with sublayers having a structure other than complex crossed-lamellar. In layer m — 1 (Pl. 9, fig. 1) of *Acmaea (Collisellina) saccharina* the prismatic sublayers alternate with radial crossed-lamellar sublayers. In the figure illustrating this alternation, one prismatic sublayer can be traced laterally through the two pseudolayers of shell-layer m — 1. In the ventral pseudolayer (Pl. 9, fig. 2) the prismatic sublayer intersects first-order lamellae which are normal to the plane of section. Laterally, the same prismatic sublayer intersects the dorsal pseudolayer (Pl. 9, fig. 3) in which the first-order lamellae are parallel to the plane of section. Farther laterally the same prismatic sublayer is truncated by the prismatic myostracum. As seen in the last plate-figure mentioned, prismatic sublayers may be as thick as or thicker than the similarly appearing prismatic myostracum. At the present state of knowl-

edge, the only way to distinguish between a prismatic sublayer and a thin prismatic myostracum is to determine the relationship between the layer in question and the growth surfaces.

The transition from the crossed-lamellar or complex crossed-lamellar sublayers to the prismatic sublayers involves an approximately 45° structural "bend" of third-order lamellae into a position normal to growth surfaces. While "bending" structurally, the optical continuity (Pl. 9, fig. 3) remains the same in the change from third-order lamellae to the tiny prisms.

Measurement of Stratification Units

In measuring the thicknesses of stratification units in the mollusk shell it is important to identify clearly the kind of layer being measured and the exact line or lines along which measurements are made. Lines of measurement must be chosen so that the results for each kind of layer will be comparable within any one shell and from species to species not only of patelloid but hopefully of all molluscan shells. Three different lines of measurement (Text-fig. 62) are here

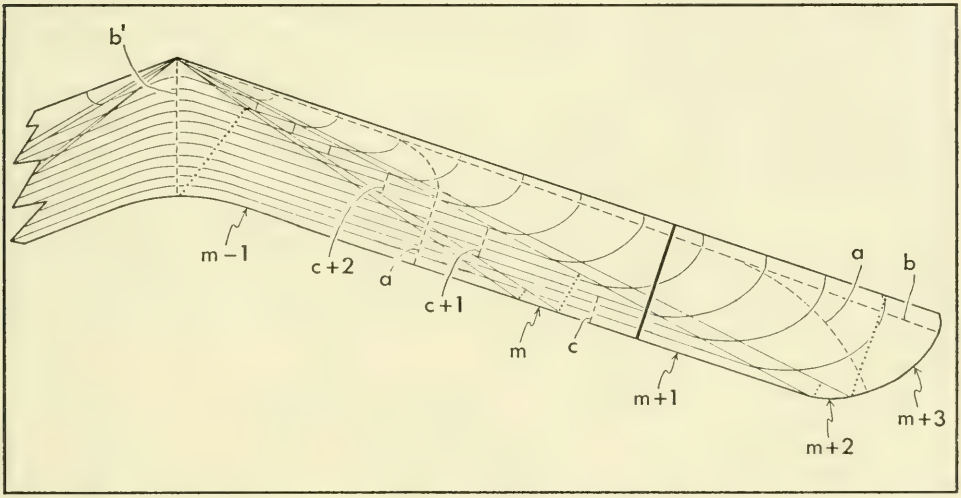

Text-fig. 62.—Radial section of patelloid shell showing the system used to measure shell-layer thicknesses (dotted lines), shell thickness (thick line), and growth layer thicknesses (dashed lines). Explanation of symbols: a, lines of non-proportional growth-layer thicknesses; b, b', lines of proportional growth-layer thicknesses; c, c + 1, c + 2, offset lines of proportional growth-layer thicknesses; m, m — 1, etc., shell layers.

used for (1) shell layers, including myostracal deposits, (2) overall shell thickness, and (3) growth layers and shell sublayers.

For comparable results in all shell layers, the thickness of each shell layer (Text-fig. 62) must be measured along a line which is normal to the contact with the overlying shell layer and which intersects the ventral or inner surface of the shell at the point of contact with the underlying shell layer. In the outermost shell layer this measurement is made normal to the dorsal or outer surface of the shell. In the ventralmost shell layer, which has no underlying shell layer, the measurement is made from a point on the ventral surface of the shell directly below the apex of the shell. Thickness plays no role in the concept of the shell layer. As can be seen in patelloids (Table 4), shell-layer thicknesses may range from a few microns to a thickness greater than the overall thickness of the shell.

Precise measurements are often impossible because of both vertical and lateral intertonguing relationships which may exist between shell layers. A twist relationship between layers also hinders exact measurements.

The overall thickness of the shell (Text-fig. 62) is measured normal to the dorsal surface of the shell in the thickest part of the shell other than at the apical region. It should be noted (Table 4) that in this system the thickness of the ventralmost shell layer of patelloids is generally greater than the thickness of the shell.

Growth layers (Text-fig. 62) and shell sublayers are measured normal to the growth surfaces bounding them. In any study involving detailed measurements of complete growth-layer sequences, it is essential to use a wholly consistent system. In a shell having a recurved outer shell layer, there are only two places in the shell (Text-fig. 62-b, b′) where the complete growth-layer sequence can be consistently measured along a single straight line. One place is directly under the apex and the other is from the outermost margin of the shell adapically in a line nearly parallel to the outer surface of the shell. In all other places measurements must be offset (Text-fig. 62-c, c + 1, c + 2, etc.) to produce consistently proportional results in a complete growth-layer sequence. If measurements are made along continuous lines (e. g. Text-fig. 62-a) other than those at b and b′ the results will be distorted because, with a change in curvature of growth surfaces, the thickness of growth layers changes. The greater the angle of growth surfaces to the dorsal surface of the shell, the greater the thickness of the growth layers. Each line of measurement in an offset series, therefore, must not be continued beyond the point where the angle between the growth surfaces and the dorsal surface of the shell changes. The thickest part of each growth layer occurs along a line (Text-fig. 62-b) where the growth surfaces are at 90° to the dorsal surface of the shell. This means that the fastest rate of shell deposition takes place at this point along the margin of the shell.

SUPERFAMILY PATELLOIDEA

Of all the molluscan groups of comparable taxonomic size, the patelloids have the most complex and diverse shell structure. Based on examination of the shell structure of 121 fossil and Recent species (Table 5), the superfamily Patelloidea is here divided into 17 taxonomically informal groups (Pl. 32), some containing many species and others containing only one. Starting with the dorsal layer, the structure of all shell layers for each group is described. The several species or groups of species which are in need of reclassification on the basis of shell structures, are discussed under their respective shell-structure groups. A key to the 17 patelloid shell-structure groups is given at the end of this section.

In patelloids (Pl. 32) several generalities can be made concerning the relationship between shell-layer sequences and structure. With the exception of the myostracum, shell layers having a prismatic structure are restricted to the outermost layers of the shell. As in the shells of group 1, there may be two different prismatic layers, but in these instances the outermost simple-prismatic layer, for example, is directly underlain by the fibrillar layer. Inner shell layers may exhibit prismatic structures, but only in thin shell sublayers.

Layers with distinctly foliated structure were observed both above and below the myostracum but never, with the possible exception of shells of group 16, at the dorsal surface of the shell. In all shells where there is a distinct foliated layer dorsal to the myostracum, the structure of the outermost layer is complex-prismatic.

A few consistent generalities can be made about the occurrence of crossed and complex crossed structures. Crossed-lamellar layers are always either in direct contact with the myostracum or separated from it by another crossed-lamellar layer. They may occur either on the ventral or dorsal side of the myostracum. The crossed-lamellar structure is never present in the dorsalmost shell layer. Complex crossed-lamellar structure is generally restricted to layers ventral to the myostracum. The observed exceptions are in shells of groups 7 and 8, where occasionally there is a very thin complex crossed-lamellar layer resting on the dorsal surface of the myostracum. The crossed-foliated structure, wherever present, is restricted to the outermost and innermost shell layers and only very rarely comes in contact with the myostracum. In all shells having outer crossed-foliated layers, no outermost prismatic layer was observed. Instead there is a radial crossed-foliated layer.

Among pelecypods the foliated and crossed-foliated structures are present in shells of many higher taxa. Among Recent gastropods, however, the foliated and crossed-foliated structures appear to be restricted to the Patelloidea.

Tubules have been observed in the shells of many pelecypods (Oberling, 1955, 1964; Ōmori, Kobayashi and Shibata, 1962; Ōmori and Kobayashi, 1963; Kobayashi, 1964a). Schmidt (1959) has also seen them in the nacreous inner layer of the monoplacophoran *Neopilina galatheae*. These molluscan tubules range in diameter from 1-24μ and extend outward from the inner surface of the shell. In some instances they penetrate to the outer surface of the shell. As yet no definitive statement of their function has been given. No tubules were seen in any of the patelloid shells studied.

Detailed measurements of shell-layer thicknesses (Table 4) were made on thin sections of 17 shells representing 12 shell-structure groups. The maximum thickness of each of these shells was also measured. The cumulative total of shell-layer thicknesses is always greater than the thickness of the shell. Although no firm generalizations can be drawn from such a small sample, the average ratio of cumulative shell-layer thicknesses to thickness of shell is 2.86 : 1. The extremes of

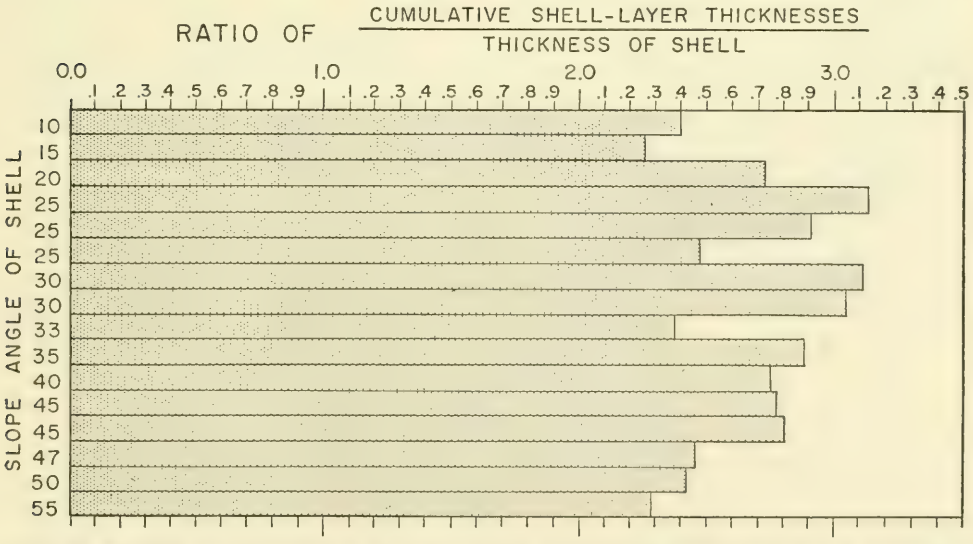

Text-fig. 63.—Bar graph suggesting a relationship in patelloids, between the ratio of cumulative shell-layer thicknesses to thickness of shell *and* the slope angle of shell (Text-fig. 40) where the thicknesses were measured. For detailed information on specimens and measurements see Table 4.

TABLE 4: Comparison of adult patelloid shell-layer thicknesses with thickness of shell. All measurements from thin sections. For method of measuring shell-layer thicknesses see text-figures 40 and 62.

Shell-structure group	Species	Hypotype no. (UCMP unless otherwise stated)	Thickness of shell layers in μ							Thickness of shell in μ	Ratio of cumulative shell-layer thicknesses to thickness of shell	Slope angle of shell where thicknesses were measured
			m + 4	m + 3	m + 2	m + 1	m	m − 1	m − 2			
1	*Acmaea limatula*	30111	—	84	570	258	6	960	—	600	3.13 : 1	25°
1	*A. limatula*	30792	—	120	528	474	48	1140	—	840	2.75 : 1	40°
2	*A. saccharina*	36480	—	—	720	540	12	1140	—	840	2.89 : 1	35°
2	*A. alticostata*	CAS 12740	—	—	480	930	6	1590	—	1260	2.38 : 1	33°
3	*Scurria scurra*	30795	—	930	72	336	12	1350	—	1188	2.29 : 1	55°
6	*Patella compressa*	36482	—	360	840	30	6	900	420	840	3.04 : 1	30°
7	*Helcion pellucida*	36483	—	90	600	3	4.5	12	1080	660	2.72 : 1	20°
8	*Patella vulgata*	30794	—	750	900	60	12	570	960	1350	2.45 : 1	47°
8	*P. lusitanica*	36481	—	360	720	198	9	420	1260 ±	1080	2.77 : 1 ±	45°
9	*P. mexicana*	36487	—	1500	2130	2340	456	2160 +	—	3480	2.47 : 1 +	25°
11	*Nacella aenea*	36486	—	—	660	948	9	1320	—	1050	2.80 : 1	45°
12	*Cellana argentata*	36484	—	540	870	60	27	1620	—	1380	2.26 : 1	15°
13	*C. testudinaria*	36485	930	1200	6	36	24	2250	—	2130	2.91 : 1	25°
15	*Acmaea mitra*	30796	—	600	660	132	18	1500	—	1200	2.42 : 1	50°
15	*Lepeta concentrica*	30798	—	180	120	150	6	480	—	300	3.12 : 1	30°
17	*Proscutum elongatum*	34717	—	51	75	51	1.7	134	—	130	2.40 : 1	10°
											average 2.68 : 1	
											extremes 2.26 : 1 to 3.13 : 1	

this ratio are 2.26 : 1 and 3.14 : 1. A bar graph (Text-fig. 63) shows that there may be some relationship between these thickness ratios and the slope angle of the shell on the side where the thicknesses were measured. It appears that the ratio increases from about 2.3:1 to about 3.1:1 with an increase in slope angle from 10°-30°. With further increase in the slope angle from 30°-55°, however, the ratio decreases back to about 2.4:1. For confirmation of this relationship, measurements must be made on many more specimens.

Shell-structure Groups

group 1

(Pl. 1-8: *Acmaea; Lottia; Nomaeopelta*)

M + 3. Simple-prismatic.—The prisms in this thin outer shell layer (Text-fig. 71) are narrow elongate blades oriented radially. This shell layer is prominent only in shells having a thin sharp edge.

M + 2. Fibrillar.—This is the one structure (Pl. 1, figs. 1-5, 7) which characterizes nearly all species currently referred to the family Acmaeidae. This structure has not been observed in shells of non-acmaeid species and consequently is very useful in identifying fossil acmaeid shells. The layer having this structure is about as thick as the underlying layer (m + 1).

M + 1. Concentric crossed-lamellar

Myostracum

M — 1. Radial crossed-lamellar

Discussion. In animals with shells having rounded margins, the outer layers of the shell were deposited by a wholly or partially reflected mantle. Two tendencies, both leading to other shell-structure groups, were observed in the structure of the outer shell layers. One tendency is apparently toward reduction and loss of layer m + 3 with resultant modification of the fibrillar layer (cf. group 2). The other tendency is apparently toward extreme thinning of the fibrillar shell layer accompanied by modification of the outer simple-prismatic layer (cf. group 3).

Durham (1950, p. 134) described a single patelloid specimen from the Pleistocene of the Gulf of California as possibly being referable to *Patella mexicana* Broderip and Sowerby. Examination of the shell structure (Pl. 1, fig. 3) of this specimen shows clearly that it is in no way related to the living *Patella mexicana* (cf. group 9). Dorsal to the myostracum there are at least two shell layers; a concentric crossed-lamellar layer overlain by a fibrillar layer. Recrystallization of the shell has not affected the capacity of the shell to fracture along the boundaries between structural units. The angle of reclination of fibrils in this specimen (Table 1) corresponds well with the angle of reclination in other acmaeid shells. It is therefore concluded that this specimen should be referred to group 1. Because extreme wear has removed the original margin and all of the details of the surface sculpture necessary for trivial identification, the specimen should probably be referred to *Acmaea* sp.

group 2

(Pl. 1, 9: *Acmaea; Patella,* fossil)

M + 2. Complex-prismatic.—The structure of this layer (Pl. 9, fig. 1) is very close to the fibrillar structure of group 1, layer m + 2. Here, however, small bundles of fibrils are arranged in slender prisms each having an extinction angle slightly different from that of adjacent prisms. Probably the lack of a completely parallel arrangement of fibrils results from the fact that in this group this essen-

TABLE 5: Shell-structure groups of patelloid gastropods. All numbers, unless designated otherwise, are UCMP locality numbers. Examples of type-specimen indications are as follows. Hypotype, YPM no. 13380. Hypotype, UCMP no. 104/30794, which means specimen 30794 from locality 104. Hypotype, SDNHM nos. 35586/705, 706, which means specimens 705 and 706 both from locality 35586. Open parentheses indicate subgeneric assignment not known by me. Explanation of symbols: *, type species of genus; **, type species of subgenus; 1, western N. America; 2, western S. America; 3, southern S. America; 4, Hawaii; 5, western Pacific; 6, southern Pacific; 7, southern Australia; 8, western Australia; 9, Indian Ocean; 10, eastern Africa; 11, southern Africa; 12, western Africa; 13, Mediterranean Sea; 14, Europe; 15, northeastern N. America; 16, Caribbean Sea. See text-figure 83 for geographic distribution by shell-structure group.

Shell-structure group, and species	Specimen and locality nos. of material examined	No. of shells examined	Fossil or Recent	Geographic distribution	Remarks
GROUP 1					
Acmaea (*Acmaea*) *depicta* Hinds	2390, B-829, 2388, 2395, 3117	10+	R	1	
A. (*Actinoleuca*) *polyactina* Verco	1760	1	R	8	m + 3 eroded off
A. (*Collisella*) *asmi* Middendorff	2439, 2412, 2395, 2403, B-911, 2416, 2419, 2782	10+	R	1	
A. (*C.*) *cona* Test	2434, 2390, 2392, 2395, 2777, 2782	10+	R	1	
A. (*C.*) *digitalis* Eschscholtz	hypotype, UCMP no. 2392/11070: 2392, 2395, 2393, 2403, 2411, 2770, 3117, 2419	10+	R	1	
A. (*C.*) *instabilis* (Gould)	hypotype, UCMP no. 30113: B-361, 3117, 7162, 2438, 7210	10+	R	1	
A. (*C.*) *limatula* Carpenter	hypotype, UCMP nos. 2392/30111, 30112, 30116, 30791, 30792: A-4198, B-835, 1188	10+	R	1	
A. (*C.*) *pelta* Eschscholtz**	2392, 2888, 2890, 2892, 3117, 3122, 3124, 7153, 1676, 23	10+	R	1, 5	
A. (*Collisellina*) *marmorata* Tenison Wood	CAS loc. no. 13539	?	R	7	
A. (*Patelloida*) *fenestrata* (Reeve)	2439, 2393, 2395, 3094, 2411, 2436, A-4216	10+	R	1	

A. (*P.*) *paleacea* Gould	B-1288, 2388, 2390, 2403, 2770, B-1268	10+	R	1	
A. (*P.*) *persona* Eschscholtz	2400, 2438, 2414, 2411, 2432, 2779, 2773, 2439, 2785	10+	R	1	
A. (*P.*) *scutum* Eschscholtz	B-539, 2395, 2402, 2410, 2411, 2888, 2412, 2414, 2770, 7152	10+	R	1	
A. (*Radiacmea*) *cingulata* (Hutton)	SDNHM loc. no. 35736	?	R	6	
A. (*R.*) *inconspicua* (Gray)	SDNHM loc. no. ?	?	R	?	
A. (*Subacmea*) *scopulina* (Oliver)**	1535	2	R	6	m + 3 (? present)
A. (*Tectura*) *virginea* (Müller)**	CAS loc. no. 3694	10+	R	14	
A. ( ) *atrata* Carpenter	A-3638, 2404, 6112, CAS loc. no. 24070	7	R	1	
A. ( ) *candeana* (d'Orbigny)	S-4 (19837) (19000), 269, 430, 3416	10+	R	16	
A. ( ) *conoidalis* (Pease)	CAS loc. no. 13536	?	R	6	
A. ( ) *cubensis* (Reeve)	269, 173, 6113	10+	R	16	m + 2 (? present)
A. ( ) *fascicularis* (Menke)	2404, 3407	10+	R	1	
A. ( ) *pallida* (Gould)	94	1	R	5	
A. ( ) *patina* Eschscholtz	B-539, 1677, 1689, 1687, 2439, B-829	10+	R	1	
A. ( ) *pedicula* (Philippi)	5098	3	R	1	
A. ( ) *pustulata* (Helbling)	6113	2	R	16	worn outer surface
A. (?) *rosacea* Carpenter	3089, A-3639, 2390, 2392, 2395, 2404	10+	R	1	
A. ( ) *stipulata* (Reeve)	3123	1	R	1	m + 3 (? present)
A. ( ) *striata* (Quoy and Gaimard)	1578, A-5100, 33, A-5102, A-5101, A-5108, A-4981	10+	R	5	
A. ( ) *subrotundata* Carpenter	479	3	R	1	m + 3 thin
A. ( ) *testudinalis* (Müller)	hypotype, YPM no. 13377: 61, B-1300, 161, 186, 410, B-6009, 194	10+	R	15	
A. ( ) *vespertina* (Reeve)	2404	3	R	1	
Lottia gigantea G. B. Sowerby*	hypotype, UCMP no. 30793: 2395, 3117, 2419, 5035, 3413, 2411, 2395	10+	R	1	
Nomaeopelta dalliana (Pilsbry)*	no num.	4	R	1	
N. mesoleuca (Menke)	6119, B-6008, 1662, 2404, 3092, A-8529	10+	R	1	
N. stanfordiana (Berry)	2404	2	R	1	
Patella mexicana B. & S.: Durham, 1950	hypotype, UCMP no. A-3508/32723	1	F	1	Pleistocene, Baja Calif.

TABLE 5: Continued

Shell-structure group, and species	Specimen and locality nos. of material examined	No. of shells examined	Fossil or Recent	Geographic distribution	Remarks
GROUP 2					
Acmaea (*Acmaea*) *sybaritica* Dall	CAS loc. no. 24053	3	R	1	
A. (*Collisellina*) *saccharina* Linnaeus**	hypotype, UCMP no. 50/36480; YPM no. 13378: 10, 77, no loc. num. (CAS)	10+	R	5	
A. (*Patelloida*) *alticostata* (Angas)	hypotype, CAS no. 32577/12740: 85, 301, 1760, B-6010, 132, 68	10+	R	7	
A. (*P.*) *nigrosulcata* (Reeve)	B-8721	1	R	7	commensal on *P. laticostata*
A. (*P.*) *profunda mauritiana* (Pilsbry)	314	3	R	10	
A. ( ) *martinezensis* Dickerson	holotype, UCMP no. 790/11742	1	F	1	Paleocene, Martinez fm.
A. ( ) *oakvillensis* VanWinkle	hypotype, UCMP no. A-1802/35249	1	F	1	Oligocene, Quimper fm.
Patella geometrica Merriam	holotype, UCMP no. 11933	1	F	1	Oligocene, Sooke fm.
P. raincourti Deshayes	B-5357, B-5370, B-5369	10+	F	14	Eocene, France
P. traskii Gabb	Cal. Geol. Surv. holotype 70/31393, paratype 70/14751 (both at UCMP)	2	F	1	Cretaceous, Calif.
GROUP 3					
Acmaea (*Patelloida*) *incessa* (Hinds)	hypotype, UCMP nos. 2395/36591, 36593: 2395, 2411, A-3659, B-876, 2776, 2403, 2390	10+	R	1	very thin m + 2
A. ( ) *ceciliana* (d'Orbigny)	3102, 3096	10+	R	3	thick m + 2
A. ( ) *viridula* (Lamarck)	3102, 3096, A-4004	10+	R	2, 3	medium m + 2
Scurria parisitica (d'Orbigny)	3102	5	R	2, 3	thick m + 2

S. scurra (Lesson)*	hypotype, UCMP nos. 3096/30795, 36594: 1763, 6007, 3102, 1764, 1762, 3104	10+	R	2, 3	thin m + 2
S. zebrina (Lesson)	hypotype, YPM no. 13379: 3102, 3104	10+	R	2, 3	thick m + 2
GROUP 4					
Acmaea (*Atalacmea*) *fragilis* (Sowerby)**	hypotype, YPM no. 13373: 1536, no loc. num.	4	R	6	
A. (*Notoacmea*) *pileopsis* (Quoy & Gaimard)**	hypotype, YPM no. 13375: A-4208	10	R	6	m + 3 (? complex-prismatic)
GROUP 5					
Acmaea (*Conacmea*) *parviconoidea* Suter**	1555	3	R	6	
A. (*C.*) *subundulata* Angas	B-8722	1	R	7	
A. (*Notoacmea*) *septiformis* Quoy & Gaimard	B-8722	1	R	7	
GROUP 6					
Patella (*Cymbula*) *compressa* Linnaeus**	hypotype, UCMP no. 1654/36482: 1654	10+	R	11	
P. (*C.*) *miniata* Born	hypotype, YPM no. 13381: 1654, 231	2	R	11	
P. (*C.*) *sanguinans* Reeve	hypotype, SDNHM nos. 6551/704; 35586/705, 706	3	R	11	
P. (*Patellona*) *granatina* Linnaeus**	1640, 1654, 231	10+	R	11	m — 2 extensive, and radial crossed-fol.
P. (*P.?*) *ocula* (Born)	hypotype, YPM no. 13374: 231	3	R	11	m — 1 radial crossed-lamellar; no m — 2
P. ( ) *variabilis* Krauss	SDNHM loc. no. 35643	?	R	11	
Helcion (*Helcion*) *pectinatus* (Born)*	hypotype, UCMP no. 1640/36598: 1640, 1654	6	R	11	m — 1 radial crossed-lamellar; no m — 2
H. (*Patinastra*) *pruinosus* (Krauss)**	hypotype, UCMP no. 429/36599: 429, B-8034	3	R	11	m — 1 radial crossed-lamellar; no m — 2
GROUP 7					
Helcion (*Ansates*) *pellucida* (Linnaeus)**	hypotype, UCMP no. 65/36483; YPM no. 6429/13383: 65, 363	5	R	14	

TABLE 5: Continued

Shell-structure group, and species	Specimen and locality nos. of material examined	No. of shells examined	Fossil or Recent	Geographic distribution	Remarks
GROUP 8					
Patella (*Patella*) *caerulea* Linnaeus	90, B-7332, 400, 130, B-2375, 470, B-8033	10+	R	13	
P. (*P.*) *vulgata* Linnaeus*	hypotype, UCMP no. 140/30794; YPM no. 13382: 140, 65, 98, 144, 363	10+	R	14	
P. (*Patellastra*) *lusitanica* Gmelin**	hypotype, UCMP no. B-8033/36481: B-8033, 343	8	R	13, 14	
P. (*Patellidea*) *granularis* Linnaeus**	hypotype, YPM no. 13380: 1654, 469, 240, 1640	10+	R	11	
P. ( ) *argenvillei* Krauss	1654	9	R	11	
GROUP 9					
Patella (*Ancistromesus*) *mexicana* Broderip & Sowerby**	hypotype, UCMP no. 7188/36487; YPM no. 13384: 7188, 7108, B-4232, B-4236, 2404	10+	R	1	
P. (*Patellona*) *longicosta* Lamarck	1640, 429, 301	5	R	11	
P. (*Penepatella*) *optima* Pilsbry	no loc. num.	2	R	6	
P. (*P.*) *pentagona* Born	88, 7133	4	R	6	
P. (*P.*) *pica* Reeve	A-5098, A-5097, A-5099, 113, A-5112	10+	R	5, 9	
P. (*P.*) *stellaeformis* Reeve	1578, A-7664, A-4905	6	R	5	
P. (*Scutellastra*) *barbara* Linnaeus**	hypotype, YPM no. 13385: 1640, 1654, 231	10	R	11	
P. (*S.*) *squamifer* Reeve	no loc. num. (CAS)	?	R	7	
P. (*S.*) *laticostata* Blainville	1760, B-8721	2	R	8	
P. ( ) *tabularis* Krauss	CAS loc. no. 33342	?	R	11	

GROUP 10				
Patella (*Olana*) *cochlear* Born**	hypotype, UCMP no. 1640/36592; YPM no. 13390: 231, 1654	10	R	
GROUP 11				
Nacella (*Nacella*) *mytilina* (Helbling)*	hypotype, UCMP no. 7119/36596: 7119	7	R	3
N. (*Patinigera*) *aenea* (Martyn)	hypotype, UCMP nos. 1767/36486; 3091/36488: 7119, 1767, 3091, 7150	10+	R	3
N. (*P.*) *clypeater* (Lesson)	hypotype, YPM no. 3686/13386: 3102, 7150	8	R	3
N. (*P.*) *magellanica* (Gmelin)**	7150, 3091, 1768, B-1819, 1772	10+	R	3
GROUP 12				
Cellana amussitata (Reeve)	10, 142, 110	8	R	5, 9
C. ardosiaea (Hombron & Jacquinot)	3102, 7151	2	R	3
C. argentata (Sowerby)	hypotype, UCMP no. 11/36484; YPM no. 13388: 11	10+	R	4
C. boninensis (Pilsbry)	240, 10	10	R	5
C. denticulata (Martyn)	A-4207	4	R	6
C. eucosmia (Pilsbry)	12, 10	10+	R	5, 10
C. exarata (Nutall)	11, 104	10+	R	4
C. illuminata (Gould)	148, 405, B-6374	5	R	6
C. nigrisquamata (Reeve)	3102	2	R	3
C. nigrolineata (Reeve)	10	4	R	5
C. ornata (Dillwyn)	A-4208, A-5099, 1539	9	R	5, 6
C. radians (Gmelin)	hypotype, UCMP no. 1524/36490: 97, A-4208, 110, 1521, 1524	10+	R	6
C. rota (Gmelin)	S-188, B-6016, S-190	10+	R	9, 10
C sagittata (Gould)	94, 137, 10	8	R	6
C. toreuma (Reeve)	A-5096, 142, 10	10+	R	5
C. tramoserica (Martyn)	B-6010, 97, 379, 68	10+	R	6, 7
Helcion (*Rhodopetala*) *rosea* (Dall)	hypotype, SDNHM nos. 11610/707, 708, 709, 710	4	R	1

TABLE 5: Continued

Shell-structure group, and species	Specimen and locality nos. of material examined	No. of shells examined	Fossil or Recent	Geographic distribution	Remarks
GROUP 13					
Cellana testudinaria (Linnaeus)	hypotype, UCMP no. 137/36485: 137, 50, 10, A-4191, 412, A-4045, 113	10+	R	5	
GROUP 14					
Cellana capensis (Gmelin)	411	3	R	11	
C. redimicula (Reeve)	hypotype, UCMP no. 36597; YPM no. 13376: 1539, no loc. num.	3	R	6	
GROUP 15					
Acmaea (*Acmaea*) *mitra* Eschscholtz*	hypotype, UCMP nos. 2440/30796, 30797; YPM no. 9997/13389: 2440, 2395, 2403, 2424, 3398, 2787	10+	R	1	
Lepeta (*Cryptobranchia*) *concentrica* (Middendorff)**	hypotype, UCMP nos. 2896/30798, 32462: 2896, 1519, 2788, 1584, 3343, 7016	10+	R	1	
GROUP 16					
Acmaea (*Collisella*) *scabra* (Gould)	hypotype, UCMP nos. 3117/36595; 2771/36600; YPM no. 13387: 2771, 3117, 2419, 2412, 2411, 2410, 2440, 2485	10+	R	1	
GROUP 17					
Patella centralis Deshayes	B-5373, B-5372	5	F	14	Eocene
P. glabra Deshayes	B-5356, B-5374, B-5373	10+	F	14	Eocene
Proscutum angustum (Deshayes)	hypotype, UCMP no. 34724: B-5362, B-5350	3	F	14	Eocene

P. canaliculum (Deshayes)	hypotype, UCMP no. 34725: B-5388	2	F	14	Eocene
P. compressum (Deshayes)*	hypotype, UCMP no. 34714: B-5366	3	F	14	Eocene
P. concavum (Deshayes)	hypotype, UCMP no. 34721: B-5357, B-5356	10+	F	14	Eocene
P. elongatum (Lamarck)	hypotype, UCMP nos. 34716, 34717: B-5365	10+	F	14	Eocene
P. radiolatum (Deshayes)	hypotype, UCMP no. 34723: B-5349, B-5359	4	F	14	Eocene
Proscutum? arenarium (Watelet)	hypotype, UCMP no. 34726: B-5360, B-5361	9	F	14	Eocene
P.? ovalinum (Deshayes)	hypotype, UCMP no. 34727: B-5358	3	F	14	Eocene
P.? pyramidale (Cossmann)	hypotype, UCMP no. 34722: B-5360, B-5355	10+	F	14	Eocene

tially fibrillar layer forms the outermost layer of the shell. Assuming the species in this group are most closely related to species in group 1, it is difficult to determine which of the two outer layers in group 1 is homologous with layer m + 2 of this group. Because the tiny bundles of fibrils (Table 1) are reclined at the same angle to growth surfaces as are the fibrils in layer m + 2 of group 1, the outer layer of this group is probably homologous with layer m + 2 of group 1.

M + 1. Concentric crossed-lamellar

MYOSTRACUM

M — 1. Radial crossed-lamellar and/or complex crossed-lamellar

DISCUSSION. Five fossil species, four from western North America and one from France, are referred to this shell-structure group. Of these five, only in the shell of *Patella geometrica* (Pl. 1, fig. 4) is structure visible in all shell layers. Based on the structure observed in layer m + 2, this species can confidently be referred to *Acmaea*. In shells of the other four species, layer m + 2 is recrystallized to the point where no original structure can be seen. These species, therefore, are only questionably referred to this shell-structure group. The whole shell of *Acmaea martinezensis* (Text-fig. 10) is recrystallized to the point where the only visible structure is restricted to small isolated areas within layer m + 1.

GROUP 3
(Pl. 10: *Acmaea; Scurria*)

M + 3. Complex-prismatic.—This layer (Pl. 10, fig. 1) forms ⅔ of the total thickness of the shell. It is made up of horizontally arranged, irregularly shaped first-order prisms. Each first-order prism appears to consist of many horizontally arranged very small second-order prisms. Each first-order prism exhibits a wave of extinction under crossed nicols.

M + 2. Fibrillar.—Although thin, this layer has all the structural characteristics of the fibrillar layer of group 1 (see Table 1). The outcrop pattern of this layer (Text-fig. 72) is very narrow. In shells of *Scurria scurra* (Pl. 10, fig. 1) the layer is only about 1/12 the thickness of the overlying layer. If the fibrillar layer were missing from shells of *S. scurra,* it would be very difficult to establish the homologies of the outermost layer. Even with only a very thin fibrillar layer present, however, it can safely be inferred that layer m + 3 is not homologous with layer m + 2 of group 1.

M + 1. Concentric crossed-lamellar

MYOSTRACUM

M — 1. Radial crossed-lamellar and complex crossed-lamellar

DISCUSSION. Two species which, based on shell structures, are closely related are *Scurria scurra* from western South America and *Acmaea incessa* from western North America. In shells of both species the fibrillar layer (m + 2) is very thin relative to the thick outer layer. Previously no special attention has been given to the other similarities present in the shells of the two species. Pilsbry (1891, p. 62) described the outer layer of the shell of *S. scurra* as having a "waxen translucency." The shell of *A. incessa* has this same appearance. Both species have shells with very fine external radial and concentric sculpture. Although the adult shell of both species (Text-figs. 64, 65) is conical with a nearly central apex, the protoconch in each is shaped like a miniature shell of *Lottia gigantea* with the apex protruding beyond the anterior margin of the protoconch. A further similarity between both protoconchs is the presence of a light-dark pattern. There are no light-dark patterns on the adult part of either shell.

As noted in the preceding paragraph, layer m + 2 is very thin and layer

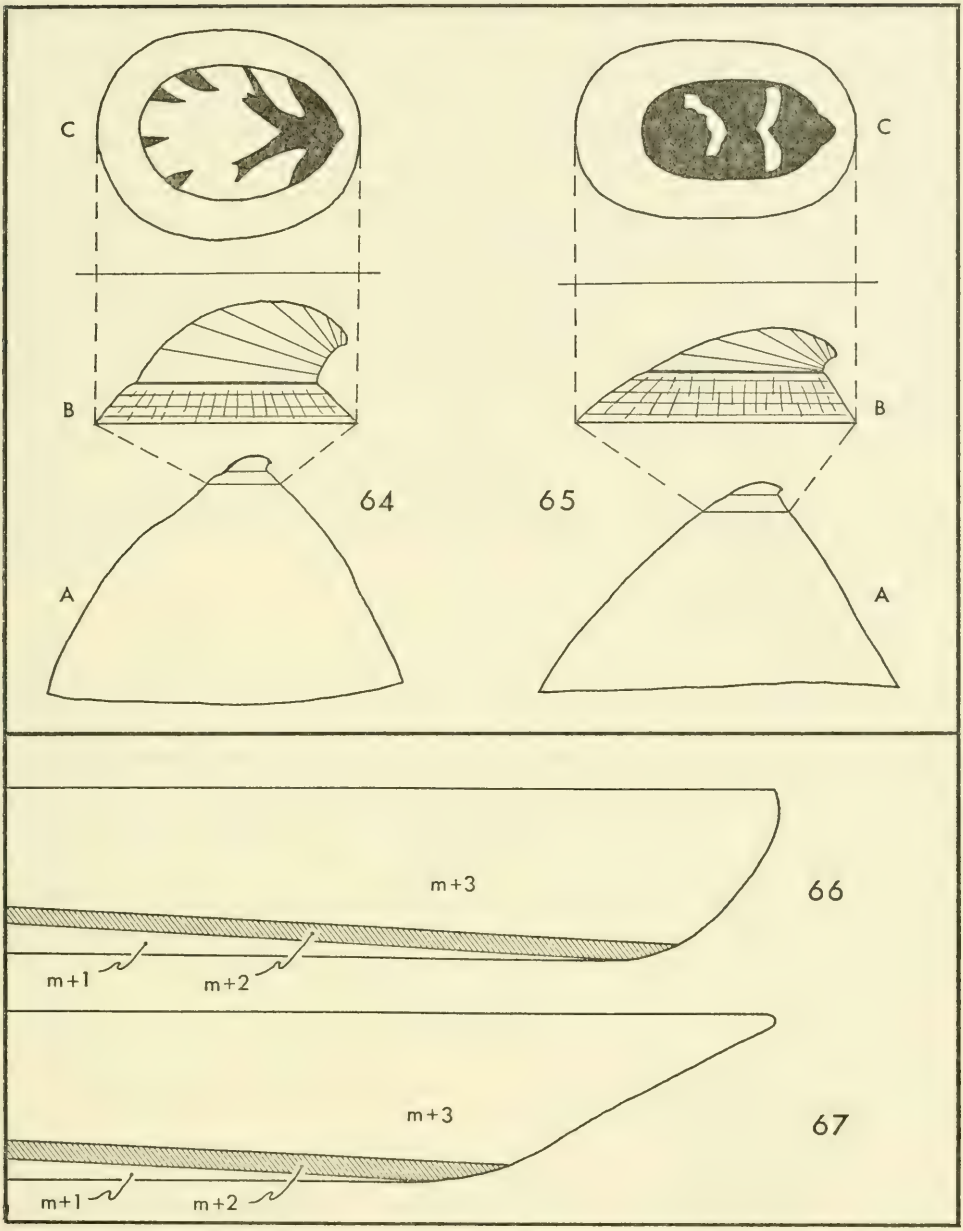

Text-figs. 64-67.—Comparison of two related species of group 3. **64, 65,** *Lottia*-shaped protoconch; note light-dark pattern. A, side view of shell, ×3. B and C, side and top view of protoconch. **64,** *Scurria scurra* (hypotype, UCMP no. 36594). **65,** *Acmaea incessa* (hypotype, UCMP no. 36593). **66, 67,** diagrammatic cross sections of shells having equally thick layers m + 3. **66,** *S. scurra* with rounded shell margin. **67,** *A. incessa* with sharp shell margin (hypotype, UCMP no. 36591).

m + 3 is very thick in both species. This is true despite the fact that in shells of *Scurria scurra* (Text-fig. 66) the entire thickness of layer m + 3 is involved in the production of the bluntly rounded margin, whereas in shells of *Acmaea incessa* (Text-fig. 67) only the dorsalmost parts of layer m + 3 are involved in the production of a sharp margin. This demonstrates conclusively that the thickness of the outer shell layer is not necessarily dependent on the degree of mantle reflection during growth of the shell. Perhaps the lack of relationship between layer thickness and margin shape also indicates that the shell structures reflect phylogenetic relationships and that the structures remain constant even though the two species probably occupy different ecologic niches. In this instance, however, a factor which must be considered is the major difference, between the two species, in the type of gill present. In *A. incessa* (Text-fig. 107) there is a ctenidium only, whereas in *S. scurra* (Text-fig. 109) there is a ctenidium as well as a complete ring of pallial gills.

GROUP 4

(*Acmaea fragilis; A. pileopsis*)

M + 4. Simple-prismatic?—Although not seen in thin section this thin layer probably has simple-prismatic structure similar to that of layer m + 3 in group 1.

M + 3. Fibrillar

M + 2. Concentric crossed-lamellar

M + 1. Radial crossed-lamellar

MYOSTRACUM

M — 1. Radial crossed-lamellar

DISCUSSION. The presence of radial crossed-lamellar structure in layer m + 1 (Text-fig. 73) distinguishes the two species of this group from all other acmaeids observed. This presents an interesting problem in relation to the systematic position of the Eocene patelloid *Proscutum* (cf. group 17). A radial crossed-lamellar structure is a feature common to layer m + 1 in shells of many species of the family Patellidae. Layer m + 1 in shells of *Proscutum* has radial crossed-lamellar structure and the genus has therefore been referred to the Patellidae (MacClintock, 1963). From observations on the structure of shells of group 4, however, the solution to the *Proscutum* problem may not be so simple.

GROUP 5

(*Acmaea*)

M + 4?. Because shells of this group were not examined in thin section, the presence of this shell layer is doubtful.

M + 3. Fibrillar

M + 2. Concentric crossed-lamellar

M + 1. Crossed-lamellar?—This layer is very thin, and no structure was seen in the narrow outcrop zone next to the muscle scar. Because the shells of this group are related to shells of group 4 in most other respects, it is inferred that the structure of this layer is probably crossed-lamellar. Thin sections will provide the answer.

MYOSTRACUM

M — 1. Radial crossed-lamellar

GROUP 6

(Pl. 10, 11: *Patella; Helcion*)

M + 3. Radial crossed-foliated?—In shells of some species (Pl. 11, fig. 1) the

structure of this layer is doubtful because there appears to be no development of first-order lamellae. However, in shells where this is true, the tiny radially arranged blades which make up the folia are visible. In shells of other species, *Patella granatina* and *P. ocula* for example, radial first-order lamellae are strongly developed. The transition from the radially arranged first-order lamellae of this layer to the concentrically arranged first-order lamellae of layer m + 2 involves a 90° twist of the structural elements.

M + 2. Concentric crossed-foliated.—Relative to the other two shell layers dorsal to the myostracum this layer (Text-fig. 74) is thickest and covers most of the inner surface of the shell outside the muscle scar.

M + 1. Radial crossed-lamellar.—The structure of this thin layer serves to differentiate this group from group 8. In two small areas (Text-fig. 74A) to the left and right of the muscle scar in shells of *Patella sanguinans* the first-order lamellae of this layer are concentrically arranged. Laterally from the areas of concentric crossed-lamellar structure the first-order lamellae curve into the radial position. Shells having both orientations in this layer might be thought of as morphologically transitional between shells having radially arranged first-order lamellae and shells having concentrically arranged first-order lamellae (cf. group 8).

MYOSTRACUM

M — 1. Radial crossed-lamellar with or without complex crossed-lamellar

M — 2. Radial crossed-foliated or irregularly foliated.—In shells of some species, *Patella granatina* for example, this layer covers almost the entire inner surface of the shell inside the muscle scar. In shells of other species (Table 5) this layer is greatly reduced or absent. In no shells observed was this layer present to the complete exclusion of the radial crossed-lamellar layer (m — 1).

GROUP 7
(Pl. 12: *Helcion pellucida*)

M + 3?. Radial crossed-foliated?—Because most of the shell material (Pl. 12, figs. 1, 2) dorsal to the myostracum was deposited by a strongly reflected mantle, the structure of the outermost layer, if this layer is present, is difficult to determine. Because there appears to be no structural break between layer m + 2 and the dorsal surface of the shell, the existence of layer m + 3 is very doubtful.

M + 2. Concentric crossed-foliated.—In one distinctive way the structure of this layer is different from all other patelloid shell layers having the crossed-foliated structure. In most layers having crossed-foliated structure, the first-order lamellae are normal to growth surfaces. In shells of this group, however, the first-order lamellae are reclined at an angle of about 30° to growth surfaces.

M + 1. Complex crossed-lamellar.—Because this thin layer (Pl. 12, fig. 3) has a maximum thickness of 10μ, it is difficult to determine the structure. A wave of extinction across what appear to be major prisms indicates that the structure is probably complex crossed-lamellar. If the layer were thicker, the structure would probably be crossed-lamellar. In all patelloid shells having a crossed-lamellar layer dorsal to the myostracum the dorsalmost elements of the layer have a complex crossed-lamellar structure. This observation is in agreement with those of Kessel (1936, 1950), who has demonstrated that the crossed-lamellar structure is merely a variation of an initially spheritic construction. In any crossed-lamellar layer, therefore, which is restricted to a thickness of only 10μ, the structure will appear complex crossed-lamellar.

MYOSTRACUM

M — 1. Complex crossed-lamellar.—As in layer m + 1 this layer is only a few μ thick.

M — 2. Radial crossed-foliated to irregularly foliated.—This layer covers almost the entire inner surface of the shell inside the muscle scar.

GROUP 8
(Pl. 13: *Patella*)

M + 3. Radial crossed-foliated

M + 2. Concentric crossed-foliated.—As in shells of group 6 this thick shell layer (Text-fig. 75) dominates the inner surface of the shell outside the muscle scar. The transition from this layer to the outer layer involves a 90° twist of first-order lamellae. Lhoste (1946) has used the outcrop pattern of first-order lamellae (*rubans*) of this layer to differentiate among shells of three species of *Patella* from France.

M + 1. Concentric crossed-lamellar.—In shells of most species examined, this layer is thin relative to layer m + 2. Where very thin this layer may have complex crossed-lamellar structure.

MYOSTRACUM

M — 1. Radial crossed-lamellar and/or complex crossed-lamellar

M — 2. Irregularly foliated to radial crossed-foliated.—From shell to shell this laver ranges from a thin layer present only in the apical region of the shell to a thick layer covering almost the entire shell surface inside the muscle scar. Unusually well developed in shells of this group is the intertonguing relationship (Pl. 13, fig. 2) between this layer and layer m — 1. In one shell of *Patella granularis* (hypotype, YPM no. 13380), the irregularly foliated structure grades into complex crossed-foliated structure. Although not as perfectly developed as in the shells of some pelecypods, this occurrence does represent the only appearance of this structure in the patelloids.

DISCUSSION. One of the differences between shells of this group and shells of group 9 is in the relative thickness of layer m + 1, which is concentric crossed-lamellar in both groups. In group 8 the layer (Text-fig. 75) is thin and restricted to a narrow zone just outside the muscle scar. In group 9 the same layer (Text-fig. 76) is thick and covers most of the inner surface of the shell outside the muscle scar. Based on this characteristic alone, the boundary between the two groups is arbitrary, because the thickness of this layer grades uniformly from one group to the other. The increase in thickness can be seen in shells of the following series of species: *Patella vulgata* (Pl. 13, fig. 2), *P. lusitanica* (Pl. 13, fig. 1), *P. argenvillei,* and *P. mexicana* (Pl. 14, fig. 1; Pl. 15, figs. 1, 2). The boundary between the two groups for the species just listed is between *P. argenvillei* and *P. mexicana*. The other characteristic used to define the two groups is the presence or absence of a foliated layer ventral to the myostracum. This layer is present in group 8 but absent in group 9.

Carpenter (1848, p. 112-114, Pl. 12, fig. 51) described the "middle and inner" shell layers of *Patella*. Presumably he was describing the complex crossed-lamellar structure of layer m — 1 and the radial crossed-foliated structure of layer m — 2 of *P. vulgata*, the common British limpet. The structure of the inner layer is inferred from the fact that, as indicated by the scale given with Carpenter's figure 51, the elongate prisms or first-order lamellae are about 50μ wide.

GROUP 9
(Pl. 14, 15: *Patella*)

M + 3. Radial cross-foliated

M + 2. Concentric crossed-foliated.—The relationship between these two outermost layers is the same as in group 8. Two features of this structure which set *Patella mexicana* apart from the other species of this group are (1) very wide first-order lamellae (Table 2; Pl. 14, figs. 1, 2) and (2) wrinkled second-order lamellae (Pl. 14, figs. 3, 4) described in the section on shell structures.

M + 1. Concentric crossed-lamellar.—As mentioned in the discussion of group 8, this layer is much thicker in shells of group 9. Furthermore, in shells of this group (Text-fig. 76) the layer covers most of the ventral surface of the shell outside the muscle scar.

MYOSTRACUM

M — 1. Complex crossed-lamellar and/or radial crossed-lamellar

DISCUSSION. In ventral view shells of this patellid group very much resemble the shells of most acmaeid groups. The critical structures for differentiating the two kinds of shell are restricted to the border areas. With the aid of a hand lens alone, however, the structures in the outer layers can be readily determined.

GROUP 10
(Pl. 26: *Patella cochlear*)

M + 2. Radial crossed-foliated

M + 1. Concentric crossed-lamellar

MYOSTRACUM

M — 1. Radial crossed-lamellar and complex crossed-lamellar

DISCUSSION. Shells of the single species in this group are distinguished from shells of group 9 by the presence of a radial crossed-foliated shell layer (m + 2) directly overlying the concentric crossed-lamellar shell layer (m + 1). Radial

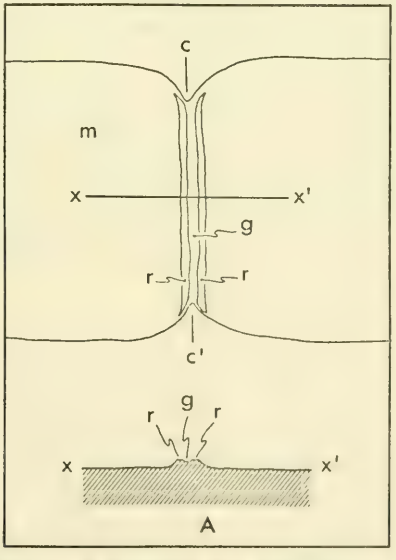

Text-fig. 68.—Generalized diagram of a part of the pedal-retractor muscle scar (m) of *Patella cochlear*. Bridging the gap at constriction (cc') is a ridge(r) along the crest of which is a distinct groove (g). A, vertical section along xx'. Based on hypotype, UCMP no. 36592.

ribs of the dorsal surface of the shell are expressed on the dorsal surface of shell-layer m + 1. The first-order lamellae of layer m + 2 are parallel to these ribs.

There is also a feature of the pedal-retractor muscle scar which distinguishes shells of this group from the shells of all other observed patelloids. In all patelloid shells constrictions (Text-fig. 1) divide the pedal scar into "segments." In the constricted areas of the scars of all shells other than those of this group, there is either a narrow sharp-crested ridge bridging the gap at each constriction or no sharp-crested ridge. Bridging the gap at each constriction in shells of group 10 is a flat-topped ridge (Text-fig. 68; Pl. 26, fig. 3) which has a distinct groove along its crest. This groove is probably the impression made by the efferent blood canal where it passes through the pedal muscle (Fisher, 1904).

GROUP 11

(Pl. 16, 17: *Nacella*)

M + 2. Complex-prismatic.—Both the large prisms (Pl. 16, fig. 1) and the small fibrils within them dip abapically at an angle of about 85° to growth surfaces.

M + 1. Foliated.—Over most of the exposed ventral surface of this shell layer, the folia (Pl. 17, fig. 1; Text-fig. 77) crop out in a concentric pattern and, when seen ventrally, dip abapically. Only near the contact with the overlying shell layer does the pattern bend into a radial position. At the contact all folia dip posteriorly. Along the anterior margin of the layer there is a point where the posteriorly dipping folia of the left side of the shell meet the posteriorly dipping folia of the right side of the shell. At this point the folia have an anticlinal relationship to each other. Along the posterior margin of the layer, the folia have a synclinal relationship to each other. The optical dependence of blades, discussed more fully under shell layer m + 3 of group 12, is expressed only at the contact (Pl. 16, fig. 1) of layers where the transition from complex-prismatic to foliated structure takes place. The lack of lateral expression of optic dependence along folia in this group probably results from the fact that blade orientation changes from concentric to radial within a very short interval in the dorsal part of the layer.

MYOSTRACUM

M — 1. Irregularly foliated.—This is the only shell layer ventral to the myostracum. From patch to patch over the ventral surface of this layer (Pl. 17, fig. 2; Text-fig. 77) folia strike in completely random directions.

DISCUSSION. The shells of all four species of *Nacella* can also be distinguished from all other patelloids examined by the relationship, in the muscle scar, between the terminal enlargements of the pedal-retractor scar and the anterior mantle-attachment scar (MacClintock, 1963).

GROUP 12

(Pl. 18, 19, 22: *Cellana; Helcion rosea*)

M + 3. Complex-prismatic.—Both the large prisms (Pl. 18, figs. 1, 2) and the small fibrils within them are oriented at roughly 90° to growth surfaces.

M + 2. Foliated.—Over nearly the whole exposed ventral surface of this shell layer (Text-fig. 78), folia crop out in a radial pattern and dip posteriorly. Where the posteriorly dipping folia meet in the anterior part of the shell, the folia are anticlinal. Where they meet in the posterior part of the shell, they are synclinal. In some places (Pl. 18, figs. 1, 2), near the contact with the overlying layer, the optic orientation of the blades making up the folia appears definitely

to be dependent on the optic orientation of the fibrils making up the prisms of the overlying complex-prismatic layer. The dorsalmost elements of this layer, therefore, might be called dependently foliated, in the same sense that the myostracum is dependently prismatic where it directly underlies a crossed-lamellar shell layer. From the base of the complex prisms, the optical dependence is expressed laterally along folia (cf. group 15, m + 2). The optical dependence of folia is expressed to a depth of no more than 1/8 the distance vertically from the dorsal to the ventral surface of the shell layer (cf. group 11, m + 1). The extent of penetration of visible optic dependence into the foliated layer is probably directly related to the orientation of blades. In any radial section of a member of this group, the blade orientation is constantly normal to the plane of section (cf. group 11, m + 1). Therefore, maximum penetration will be observed.

The uniformly radial outcrop pattern of folia is usually interrupted near the contact between this layer and layer m + 1. In this narrow zone the folia crop out in irregularly shaped patches. From patch to patch in this area, there is a random distribution of strike and dip of folia (cf. group 13, m + 2). In thin section the change of blade orientation (Pl. 19, figs. 1, 2) in the lower parts of layer m + 2 can be recognized. Where the blades are normal to the thin section, there is a rectangular pattern (Pl. 24, fig. 2). Where the blades are parallel to the thin section, there is no rectangular pattern and the folia resemble elongate threads.

M + 1. Radial crossed-lamellar.—Relative to the other two shell layers dorsal to the myostracum, this layer (Pl. 19, figs. 1, 2) is very thin and crops out on the inner surface of the shell only in a narrow zone adjacent to the muscle scar.

MYOSTRACUM

M — 1. Complex crossed-lamellar and/or radial crossed-lamellar.—In shells of several species (Pl. 22, fig. 3) the structure directly under the myostracum is radial crossed-lamellar, and in shells of a few species the whole layer is radial crossed-lamellar.

DISCUSSION. The most distinctive feature of the shells of this group is the thick foliated shell layer (m + 2) dorsal to the myostracum. Schuster (1913), in his discussion of the shell structure of *Cellana ardosiaea,* described the structure of this layer as blocky and gives a cross-sectional view of the shell showing a blocky network of lines. Thiem (1917a, p. 346) stated that the polygonal pattern seen by Schuster resulted from fracturing of the fibrous structure during preparation of the thin section. Neither of these two authors described this layer as being composed of very thin sheets nearly parallel to growth surfaces. The thin radial crossed-lamellar layer (m + 1), also characteristic of this shell-structure group and here observed in shells of *C. ardosiaea,* was not observed by Schuster or Thiem.

Recent gastropod species which are known only from small shells and whose soft parts are unknown, are often the cause of systematic and taxonomic chaos. *Helcion (Rhodopetala) rosea* (Dall, 1872) is a good example of such an animal. Originally Dall (1872, p. 270) referred the species questionably to the genus *Nacella* (cf. group 11), which, based on the present study, is characterized by having foliated layers cropping out over nearly the entire inner surface of the shell inside and outside of the muscle scar. Pilsbry (1891, p. 113) thought the shells more closely resembled shells of *Patina* [= in part, *Helcion*]. With regard to the inner shell surface he stated, "Nacre, especially when weathered, silvery." All other species of *Helcion* are now known to have shells with a thick crossed-foliated layer dorsal to the myostracum. Where this layer crops out on the inner

surface, the shell appears irridescent. Keen (1960) recognized four subgenera of *Helcion*, one of which, *H.* (*Rhodopetala*), is monotypic, with *H. rosea* being the type species.

Examination of four shells of *Helcion rosea* (Text-fig. 79), using a binocular microscope, shows that the structure of the shell is nearly identical with that of shells of those species of *Cellana* here referred to group 12. Because nothing is known of the soft-part anatomy of *H. rosea* it seems clearly proper that this species should be reclassified as *Cellana (Rhodopetala) rosea*. Retention of *Rhodopetala* as a subgenus of *Cellana* is justified because the morphology of the shell of *C. rosea* is different from the shell of all other established species of *Cellana*. The following characteristics can be used to set *Rhodopetala* apart from *Cellana* s.s.: adult shell less than ½ inch long; prismatic outer shell layer is uniformly bright red; apex of shell is at or anterior to the anterior margin of the shell and rests directly on, not above, the margin.

If the above systematic change is accepted, this will be the first record of *Cellana* on the west coast of North America. To date *C. rosea* is known only from subtidal waters of the Aleutian Islands.

GROUP 13
(Pl. 19-22: *Cellana testudinaria*)

M + 4. Complex-prismatic.—Same as m + 3 of group 12.

M + 3. Foliated.—On the whole exposed ventral surface of this shell layer (Text-fig. 80), folia crop out in a radial pattern and dip posteriorly. The anticlinal and synclinal relationships of folia are discussed under layer m + 2 of group 12. The blades near the contact with layer m + 4 (cf. group 12, m + 2) are optically dependent on the fibril orientation of layer m + 4.

M + 2. Irregularly tabulate foliated.—This structure was observed only in a thin shell layer of one species (*Cellana testudinaria*). Although, even in the larger specimens, this shell layer is never more than 100μ thick, it is consistently present and is here regarded as a feature distinctive enough to warrant placing this single species in a separate shell-structure group. Only the presence of this layer serves to differentiate this group from group 12, in which are placed most of the other species of *Cellana* examined. The irregularly tabulate foliated structure may represent an ultimate stage in the development of the irregularly foliated structure seen in the ventralmost parts of layer m + 2 in most members of group 12.

M + 1. Radial crossed-lamellar

MYOSTRACUM

M — 1. Complex crossed-lamellar and/or radial crossed-lamellar

GROUP 14
(*Cellana*)

M + 3. Complex-prismatic

M + 2. Foliated.—With radial outcrop pattern of folia.

M + 1. This shell layer is so thin that, with a binocular microscope, its structure is indeterminable. Probably the layer is radial crossed-lamellar, in which case the two members of this group should be referred to group 12.

MYOSTRACUM

M — 1. Complex crossed-lamellar and/or radial crossed-lamellar

GROUP 15

(Pl. 23-25: *Acmaea mitra*; *Lepeta concentrica*)

M + 3. Complex-prismatic.—In shells of *Lepeta concentrica* (Pl. 25, figs. 1-3) fibrils forming this layer are aggregated into discrete first-order prisms. In shells of *Acmaea mitra* the structure is a modification of the complex-prismatic structure. No distinct first-order prisms are present. Instead, two sets of fibrils (Pl. 23, figs. 1-3) make up the layer. The fibrils of each set are oriented at a constant angle to growth surfaces. One set dips abapically at about 75° to growth surfaces. The other set dips adapically at about 73° to growth surfaces. The uniformly oriented fibrils of one set can be traced laterally through the layer even though at first glance fibrils of the oppositely dipping set appear to break up the layer into discrete prisms. In sections (Pl. 23, figs. 1, 2) parallel to growth surfaces, the interpenetrating relationship of one set to the other is best shown.

M + 2. Foliated.—Although cropping out in only a narrow band (Text-fig. 81) near the margin of the shell, this shell layer (Pl. 23, fig. 4; Pl. 24, figs. 1-3) is one of the three major layers dorsal to the myostracum. This is undoubtedly the layer responsible for the "pellucid" zone, near the inner margin of the shell of *Acmaea mitra,* referred to by Pilsbry (1891, p. 24). The folia crop out in a radial pattern and dip posteriorly as in the foliated layer of group 12. In both members of group 15 the width of the outcrop zone on the ventral surface of the shell is very narrow relative to the width of the foliated layer in group 12. In the foliated layer of one member (*Lepeta concentrica*), the optical dependence of blades on the overlying fibrils is expressed vertically (Pl. 25, figs. 2, 3) through the whole layer rather than laterally along folia (cf. group 12, m + 2). As a result, if one were to regard only the gross optical patterns, he might get the erroneous impression that there was only one layer (prismatic) dorsal to shell-layer m + 1. No vertical optical dependence was observed in shells of *Acmaea mitra.*

M + 1. Concentric crossed-lamellar.—This shell layer (Text-fig. 81) covers most of the ventral surface of the shell outside the muscle scar. This is true even though the layer has nearly the same thickness as each of the two overlying layers.

MYOSTRACUM

M — 1. Radial crossed-lamellar

DISCUSSION. Two major problems result from consideration of the shell structure of the two species referred to this group. The first problem involves the systematic position of *Acmaea mitra,* designated as the type species of *Acmaea* by Dall (1871). As can be seen in a comparison of shell-structure groups (Pl. 32), the structure of shells of *A. mitra* more closely resembles the structure of shells of group 12 than any other group. The thick foliated layer provides the basis for the close comparison. The only major difference is that in group 12 shell-layer m + 1 is radial crossed-lamellar rather than concentric crossed-lamellar as in layer m + 1 of *A. mitra.* Group 12 is composed almost entirely of members of the genus *Cellana,* which is currently (Keen, 1960) referred to the patellid subfamily Nacellinae. No other patelloid currently classed in the family Acmaeidae is known to have a shell structure similar to that of *A. mitra.* With one possible exception (cf. group 16) no other acmaeid (cf. groups 1-5) has a foliated shell layer. In radula (Text-fig. 104) and gill (Text-fig. 107) morphology, however, *A. mitra* resembles most of the other species in the family. Based on the present state of knowledge, it appears that the most logical way to handle the problem is to retain *Acmaea (Acmaea) mitra* as the type of the family and to restrict the

generic name to this species. Unless a further regrouping of species formerly bearing the name *Acmaea* were undertaken, the oldest available generic or subgeneric name would have to be used in place of *Acmaea*.

The other problem results from the fact that, in the currently accepted classification of patelloids, *Lepeta concentrica*, along with three other genera, is placed in a separate family (Lepetidae). Based on the shell structure alone, *L. concentrica* is more closely related to *Acmaea mitra* than to any other patelloid. In radula (Text-fig. 105) and gill (Text-fig. 112) morphology, however, *L. concentrica* has little in common with *A. mitra* (Text-figs. 104, 107). If reexamination of the soft-part anatomy of *L. concentrica* reveals other "more basic" similarities with *A. mitra*, then the similarity of shell structure between the two species might suggest a closer relationship than previously suspected. If this were the case then there would be several solutions to the problem. (1) *L. concentrica* could be transferred to the family Acmaeidae, retaining *Lepeta* as a subgenus of *Acmaea*. (2) *A. mitra* could be transferred to the family Lepetidae. (3) *A. mitra* and *L. concentrica* could be placed together in a new subfamily or even a new family. Any of these alternatives would significantly change the major nomenclatorial hierarchy of the patelloid gastropods. If soft-part differences, such as blindness, a distinctive radula, and lack of gills in *Lepeta*, proved too great, then *A. mitra* and *Lepeta* would more properly be retained in separate groups. Before a formal decision can be reached, the shell structures of many more species, particularly of lepetids, must be studied.

GROUP 16
(*Acmaea scabra*)

M + 3?. The presence of a shell layer in this position is doubtful.

M + 2. Modified foliated or possibly modified fibrillar.—Although not seen in thin section, this structure appears to be different from all other patelloid structures. The layer (Text-fig. 82) is very thick, composing almost the entire shell dorsal to the myostracum. The structure has characteristics which relate it to both the fibrillar and foliated structures. In this layer tiny fibrils dip at an angle of between 5° and 10° to growth surfaces. Near the outer margin of the shell the fibrils dip adapically, and near layer m + 1 the fibrils dip posteriorly. The change from one dip direction to the other occurs gradually within the outer half of the shell layer.

No pattern similar to the outcrop pattern of folia in layers having foliated structure was seen on the ventral surface of the shell. However, in layers having crossed-foliated structure, there is no definite outcrop pattern of folia on first-order lamellae. Therefore the lack of distinct folia cropping out at the ventral surface of the shell does not necessarily eliminate the possibility that the structure is basically foliated. Nevertheless, layer m + 2 is made up of fibrils which are not arranged in thin sheets as the blades of folia normally are. Rather, the inner surface of the shell (Text-fig. 69) has a minutely polygonal pattern with each polygon being the outcrop area of a single fibril.

M + 1. Concentric crossed-lamellar.—This layer is very thin and crops out in only a narrow zone around the muscle scar. No other acmaeid shell studied has such a thin crossed-lamellar layer dorsal to the myostracum.

MYOSTRACUM

M − 1. Modified foliated or possibly modified fibrillar.—Structure similar to that of layer m + 2 except that the fibrils are arranged in irregularly shaped masses. These masses crop out in irregularly shaped, sharp-edged patches. The

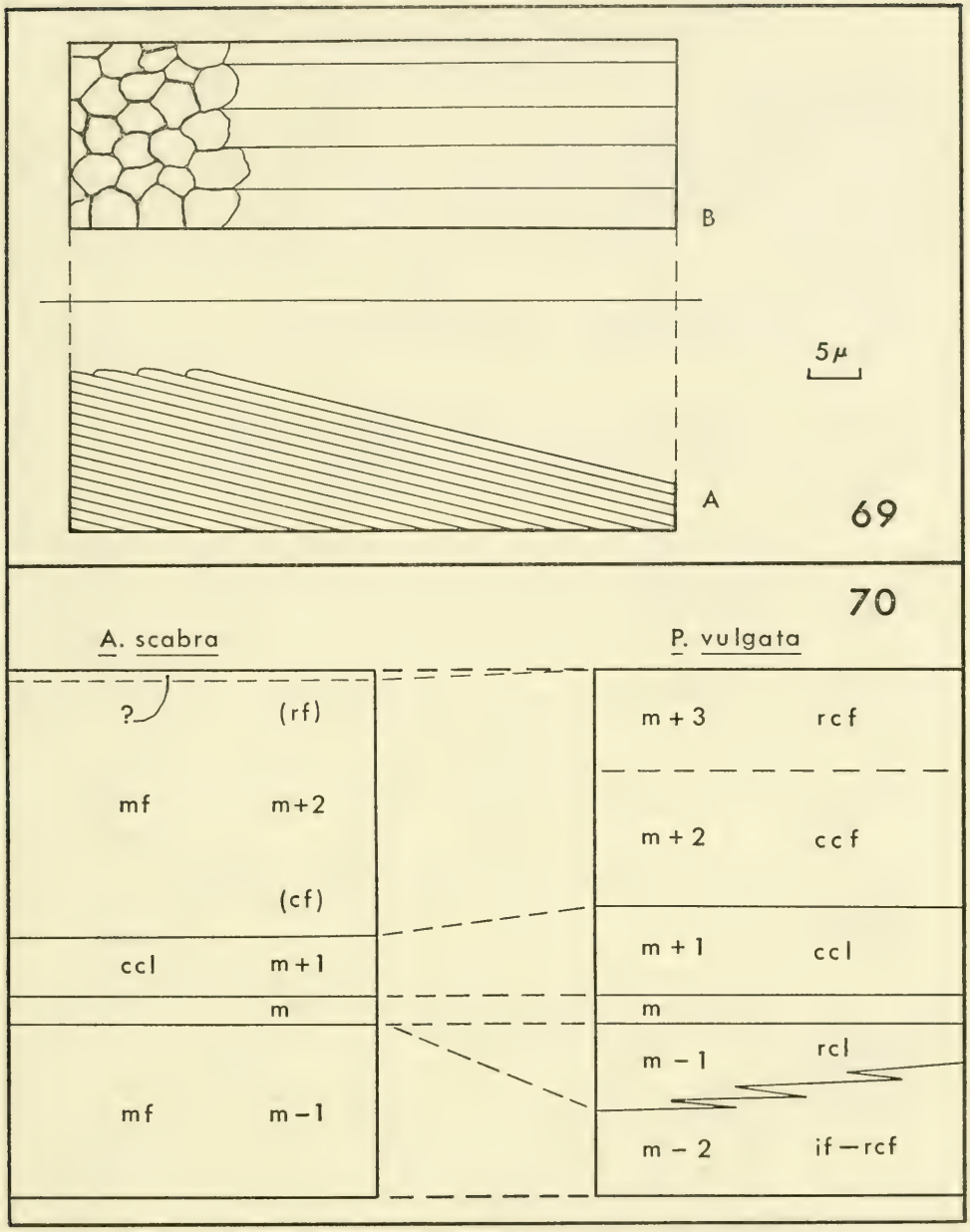

Text-figs. **69, 70.**—Shell structure of *Acmaea scabra* (hypotype, UCMP no. 36595). Explanation of symbols: ccf, concentric crossed-foliated; ccl, concentric crossed-lamellar; cf, concentric "fibrils"; if, irregularly foliated; m, myostracum; m + 1, m − 1, other shell layers; mf, modified foliated; rcf, radial crossed-foliated; rcl, radial crossed-lamellar; rf, radial "fibrils." **69,** diagrammatic sketches of "modified foliated" structure of layers m + 2 and m − 1. A, cross section. B, ventral view. **70,** comparison of the shell structure of *A. scabra* with *Patella vulgata* of group 8.

KEY: Key to patelloid shell-structure groups
(see Table 5; Text-figs. 71-82; Pl. 32)

1 Shell with a fibrillar (or complex-prismatic similar to fibrillar) layer between dorsal surface and myostracum; no foliated or crossed-foliated layers in shell (family Acmaeidae) 2
1 Shell with crossed-foliated layer(s) between dorsal surface and myostracum (family Patellidae, subfamily Patellinae) 4
1 Shell with foliated or modified foliated layer between dorsal surface and myostracum 8
1 Shell with radial crossed-lamellar, concentric crossed-lamellar and probably complex-prismatic (not similar to fibrillar) layers, respectively, dorsal to myostracum (*incertae sedis* in superfamily Patelloidea) .... *Group 17* (p. 82)

2 Layer m + 1 concentric crossed-lamellar, thick 3
2 Layer m + 1 radial crossed-lamellar; m + 2 concentric crossed-lamellar; m + 3 fibrillar; m + 4 probably simple-prismatic .. *Group 4* (p. 68)

2 Layer m + 1 very thin but probably radial crossed-lamellar; m + 2 concentric crossed-lamellar, thick; m + 3 fibrillar; m + 4 may or may not exist ..... *Group 5* (p. 68)

3 Layer m + 2 fibrillar; m + 3 simple-prismatic ..... *Group 1* (p. 57)

3 Layer m + 2 complex-prismatic (very similar to fibrillar) and is the dorsalmost layer of the shell ..... *Group 2* (p. 57)

3 Layer m + 2 fibrillar but much thinner than in shells of Group 1; layer m + 3 complex-prismatic (not similar to fibrillar) ..... *Group 3* (p. 66)

4 Layer m + 1 radial or concentric crossed-lamellar (occasionally the concentric crossed-lamellar grades into complex crossed-lamellar) 5
4 Layer m + 1 complex crossed-lamellar, very thin; m + 2 concentric crossed-foliated, thick ..... *Group 7* (p. 69)

5 Layer m + 1 concentric crossed-lamellar 6
5 Layer m + 1 radial crossed-lamellar, thin; m + 2 concentric crossed-foliated, thick ..... *Group 6* (p. 68)

6 Layers m + 2 and m + 3 concentric and radial crossed-foliated respectively 7
6 Layer m + 2 radial crossed-foliated and is the dorsalmost layer of the shell; m + 1 is thick ..... *Group 10* (p. 71)

7 Ventralmost layer (m — 2) irregularly foliated or radial crossed-foliated; layer m + 1 ranges in different species from very thin to nearly half the thickness of the combined outer layers .. *Group 8* (p. 70)

7 Ventralmost layer (m — 1) complex and/or radial crossed-lamellar; layer m + 1 very thick; m + 2 concentric crossed-foliated and although moderately thick, crops out only near margin of shell ..... *Group 9* (p. 71)

8 Layer m + 1 either radial crossed-lamellar and thin, probably radial crossed-lamellar and very thin, or foliated and thick (family Patellidae, subfamily Nacellinae) 9

8 Layer m + 1 concentric crossed-lamellar 12

9 Layer m + 1 foliated, thick; no crossed-lamellar or complex crossed-lamellar layers in shell; layer m — 1 irregularly foliated (*Nacella*) ..... *Group 11* (p. 72)

9 Layer m + 1 radial crossed-lamellar, or probably radial crossed-lamellar and very thin; thick foliated layer and thick complex-prismatic layer between layer m + 1 and dorsal surface of shell; layer m — 1 complex crossed-lamellar and/or radial crossed-lamellar (*Cellana*) 10

10 Layer m + 1 radial crossed-lamellar 11

10 Layer m + 1 probably radial crossed-lamellar ..... *Group 14* (p. 74)

11 Layer m + 2 foliated, thick ..... *Group 12* (p. 72)

11 Layer m + 2 irregularly tabulate foliated, very thin and is overlain by thick foliated layer ..... *Group 13* (p. 74)

12 Layer m + 1 concentric crossed-lamellar; m + 2 foliated with radial outcrop pattern of folia; m + 3 complex-prismatic; all three layers have nearly the same thickness (*Acmaea mitra, Lepeta concentrica*) ..... *Group 15* (p. 75)

12 Layer m + 1 concentric crossed-lamellar, very thin; layer m + 2 modified foliated or possibly modified fibrillar, very thick and probably occupies the entire thickness of the shell dorsal to layer m + 1; layer m — 1 modified foliated or possibly modified fibrillar (*Acmaea scabra*) ..... *Group 16* (p. 76)

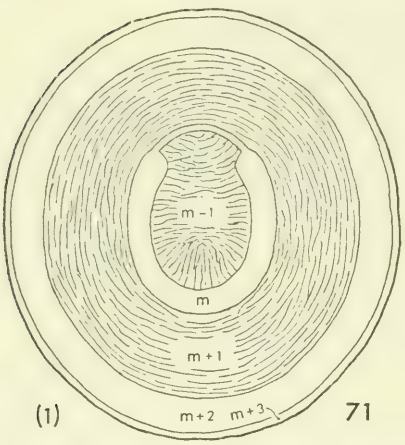

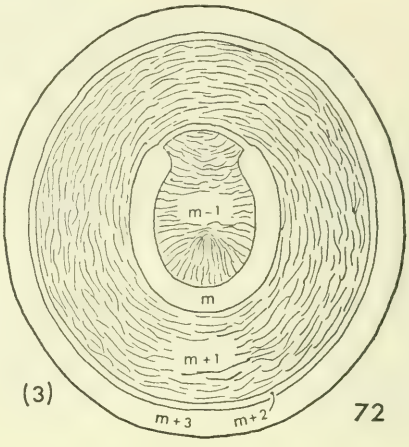

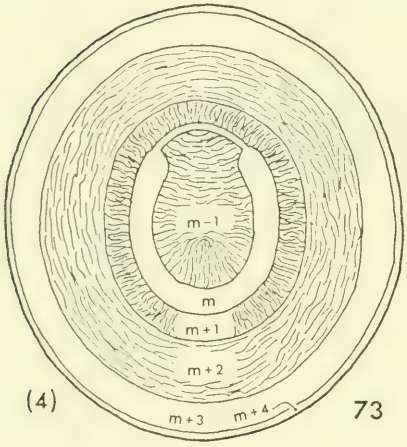

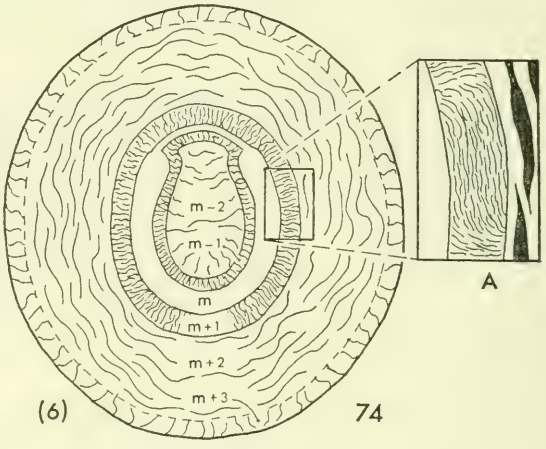

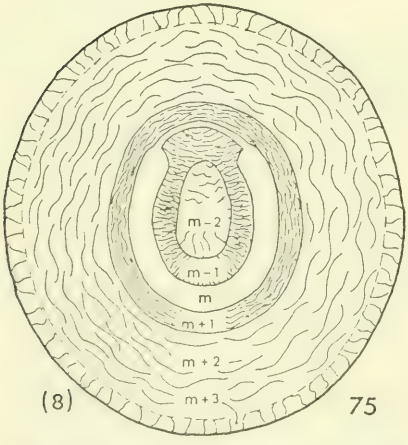

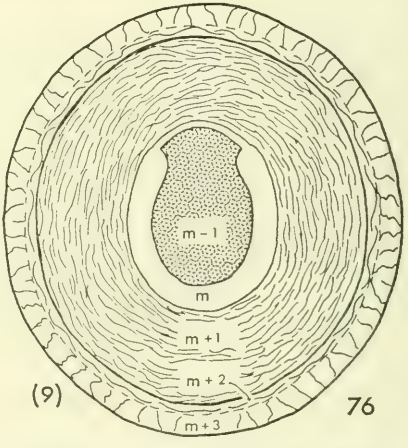

Text-figs. 71-82.—Idealized ventral views of patelloid shells showing relative outcrop widths of shell layers in eleven shell-structure groups (numbers in parentheses). Explanation of symbols: m, muscle scar; m + 1, m — 1, etc., outcrop of other shell layers. For detailed explanation of strike and dip symbols used in figures 77-81 refer to text under the proper shell-structure group. **71**, group 1. **72**, group 3. **73**, group 4. **74**, group 6, A, enlarged area showing small area

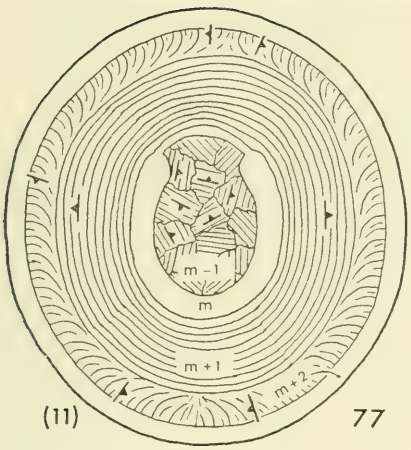

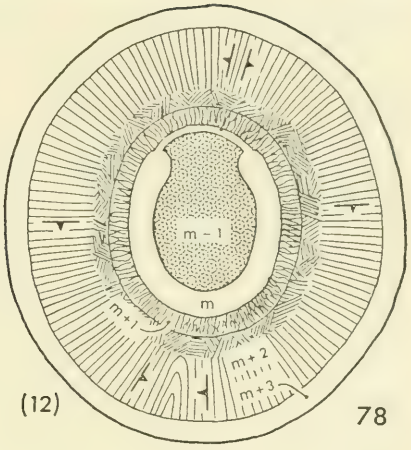

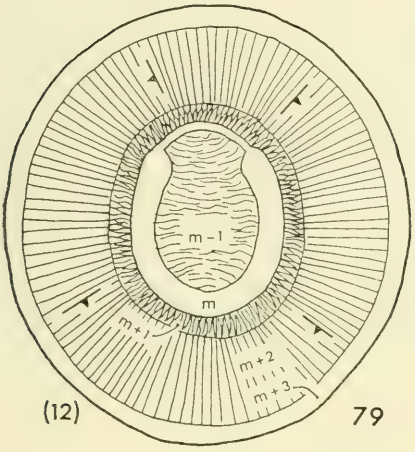

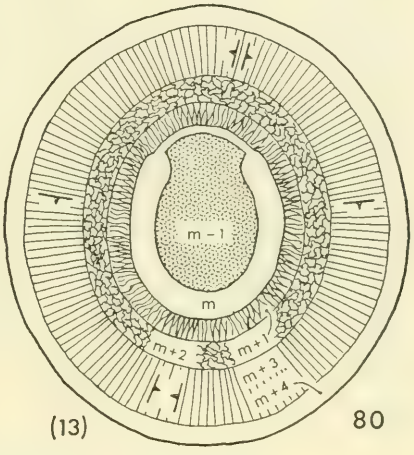

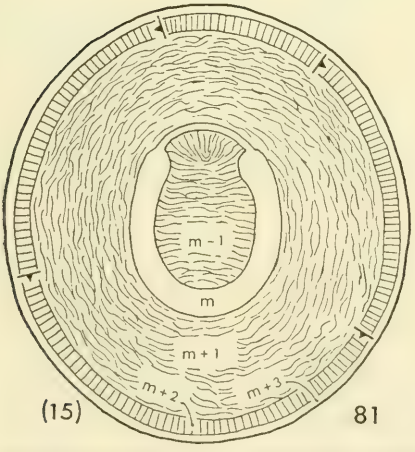

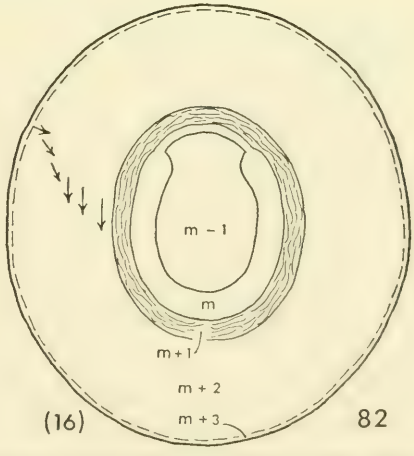

of concentric first-order lamellae in layer m + 1 (based on *Patella sanguinans,* hypotype, SDNHM nos. 704, 705, 706). **75,** group 8. **76,** group 9. **77,** group 11. **78,** group 12. **79,** group 12, *Helcion* (*Rhodopetala*) *rosea* (based on hypotype, SDNHM nos. 707, 708, 709, 710). **80,** group 13. **81,** group 15. **82,** group 16, arrows show the dip of "fibrils" (hypotype, UCMP no. 36595).

fibrils in each mass are parallel to each other, but from patch to patch over the ventral surface of this layer the fibrils dip in completely random directions. In this respect the structure resembles the irregularly foliated layer (m — 1) of group 11. The only difference is in the lack of discrete folia cropping out at the shell surface.

Discussion. Based on shell structures alone *Acmaea scabra,* the only species put in this group, is completely unrelated to all other species of the family Acmaeidae to which it is currently referred. There are three shell-structure groups (7-9) within the patellid subfamily Patellinae with which the structure of *A. scabra* may be reasonably compared. Of these three groups, group 8 is probably more similar in shell structure to *A. scabra* than the other two groups. In shells of group 8 (Text-fig. 70) the outer and inner layers are either crossed-foliated or irregularly foliated. These might correspond to the outer and inner layers of *A. scabra.* The concentric crossed-lamellar layer (m + 1) is common to both groups. The crossed-lamellar layer (m — 1) in shells of group 8 has no equivalent in shells of *A. scabra.*

The anatomy of the radula (Text-fig. 106) and the gill (Text-fig. 107) of *Acmaea scabra* suggests a close relationship with other acmaeids. If, however, the above comparison of shell structures is supported in any way by new observations of soft-part anatomy, it appears that *A. scabra* should be referred either to the patellid subfamily Patellinae or to a new acmaeid subfamily.

In her paper on speciation in closely related acmaeids, Test (1946, p. 12) stated, "the three species [*Acmaea scabra, A. digitalis* and *A. conus*] must have arisen by geographic segregation, since they occupy essentially the same microhabitat in three successive areas." Based on shell-structure relationships, the present interpretation would be that sometime in the past a phylogenetically unrelated species (*A. scabra*) established itself on the west coast of North America, where today it is in active competition for the microhabitats occupied by *A. digitalis* and *A. conus.*

GROUP 17

(Pl. 26: *Patella,* fossil; *Proscutum,* fossil)

M + 3. Complex-prismatic?—The observed major prismatic units (Pl. 26, figs. 18, 19) are reclined at an angle of 60°-70° to growth surfaces. Probably because of recrystallization, none of the finer crystalline details, if present originally, were observed.

M + 2. Concentric crossed-lamellar.—The first-order lamellae are from 7-8μ wide and the second-order lamellae have a dip angle ranging from 23°-30° (cf. Table 2; Text-figs. 31-34).

M + 1. Radial crossed-lamellar

Myostracum

M — 1. Radial crossed-lamellar.—The second-order lamellae have a dip angle ranging from 19°-25°.

Discussion. Nine species of *Proscutum* and two species of *Patella,* all from the Paris Basin Eocene, are included in this group. Based on muscle scars and shell structure, MacClintock (1963) transferred *Proscutum* from the fissurellid subfamily Emarginulinae to the patellid subfamily Patellinae. He referred *Proscutum* to the patelline shell-structure group 4 (here = group 6). However, because of the distinctive shell-layer sequence in shells of this group, the species involved are here referred to a separate shell-structure group and are included *incertae sedis* in the superfamily Patelloidea (Table 7). Shells of this group are

differentiated from shells of the subfamily Patellinae (Table 7) because they lack crossed-foliated outer layers.

Geographic Distribution

No attempt was made to determine accurately the geographic distribution of each patelloid shell-structure group. Most of the distributional patterns (Text-fig. 83) are based on locality information with specimens in the collections of the University of California. Accordingly this section on distribution is brief.

Several of the shell-structure groups are widely distributed; others have a very restricted range. Group 1 of the family Acmaeidae has the widest distribution, occurring on all major coasts except the east coast of South America and the coast of Africa. The next most widely distributed group is group 12 containing 17 species of *Cellana*. This group is found throughout the Indo-Pacific region. To the west it extends to the southern tip of Africa and to the northern tip of the Red Sea but not beyond the limits of the Indo-Pacific region. To the east, however, three species of the group are found outside the Indo-Pacific boundary. Two are from the southern coast of Chili and one from Alaska. The significance of the Alaskan member of the group is mentioned in the discussion of group 12.

Group 9, containing several species of *Patella,* is interesting in that its distribution is similar to that of group 12. It is found throughout much of the Indo-Pacific and, similar to the distribution of *Cellana,* it has a single representative (*Patella mexicana*) on the west coast of Central America.

Each of the remaining groups contains less than 10 species and most of these groups have restricted, southern-hemisphere ranges. The four southern-hemisphere coast lines (Table 6) of southern South America, southern Africa, southern Australia, and New Zealand have characteristic assemblages of shell-structure groups. For the most part these assemblages consist of the smaller shell-structure groups. Of the 11 groups represented on these southern coasts, two are

TABLE 6: Comparison of patelloid shell-structure groups of four southern-hemisphere coast lines.

Shell-structure groups	Geography			
	southern S. America	southern Africa	southern Australia	New Zealand
3	x	—	—	—
11	x	—	—	—
6	—	x	—	—
8	—	x	—	—
10	—	x	—	—
9	—	x	x	—
2	—	—	x	—
5	—	—	x	x
4	—	—	—	x
1	—	—	x	x
12	x	x*	x	x

* Represented by group 14 (one species which is very similar to those of group 12).

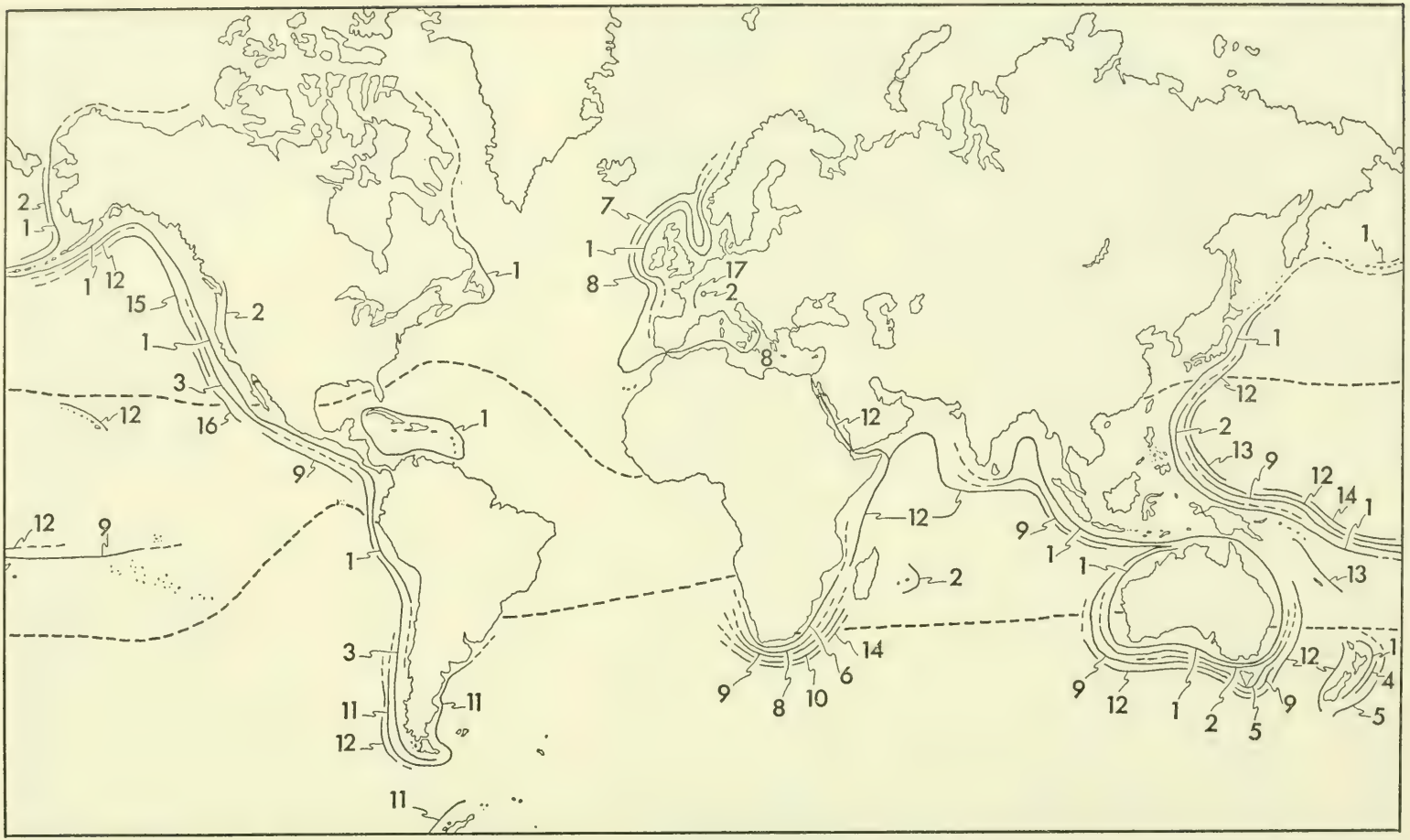

Text-fig. 83.—Geographic distribution of 17 patelloid shell-structure groups. Thick dashed line indicates limit of tropics (after Hedgpeth, 1957). Solid lines showing distribution indicate diagrammatically the coastal occurrences of the groups.

restricted to South America, three to Africa, one to Australia and one to New Zealand. Four groups common to Australia and New Zealand are not represented in Africa or South America. Only one group (12 and 14 combined) is common to all four southern coasts.

Among some of the larger shell-structure groups there appears to be no definite relationship between shell-structure group and latitudinal distribution. For example, group 1 (Acmaeidae) is represented from the tropics to the Arctic on both east and west coasts of North America. Among the patellids, however, one tendency should be noted. Within the shell-structure group sequence 9, 12, 11 there is an increase in the amount of shell material, per shell, having the foliated structure (foliated is here used to include both foliated and crossed-foliated structures). Group 9, which appears to be restricted to tropical and warm-temperate waters, has crossed-foliated layers which are restricted to the outer margin of the shells. Group 12 is dominantly tropical but also ranges latitudinally to boreal and antiboreal waters. Within shells of this group most of the shell material outside the muscle scar is foliated. Within shells of group 11, which is nearly restricted to antiboreal and antarctic waters, most of the shell inside and outside the muscle scar is made of foliated material. Assuming that all foliated structures are calcitic, there is a general increase (not supported here with quantitative measurements) in calcitic foliated material, relative to the amount of aragonitic shell material, with an increase in latitude. This conclusion agrees with that of Dodd (1964), who has firmly established a similar mineralogic relationship in shells of the pelecypod *Mytilus californianus*. In the *Mytilus* shells Dodd worked with, however, the calcitic layers have a prismatic structure and the aragonitic layers have a nacreous structure. Dodd also described a lateral intertonguing relationship between the two shell layers (inner prismatic and nacreous) inside the pallial myostracum of *Mytilus* shells. This relationship corresponds well with the lateral intertonguing of the calcitic foliated layer (m — 2) and the aragonitic complex crossed-lamellar layer (m — 1) in shells of *Patella vulgata* (Pl. 13, fig. 2). Dodd interpreted the intervals of maximum lateral extent of the inner prismatic layer of *Mytilus* as representing deposition during the winter. Although different structures are present, the same relations should hold true for the intertonguing inner layers of patelloid shells. As yet, however, within each patelloid shell-structure group, no definite conclusions can be drawn relative to shell structure and latitudinal distribution and seasonal growth.

Classification and Shell Structure

> Stoliczka . . . proposes to arrange the fossil limpets under *Helcion, Nacella, Tectura* and *Patella,* according to the external characters of the shell. As it is absolutely impossible to determine the true affinities of these remains, from the characters preserved in a fossil state, such a plan is doubtfully expedient, as it implies a knowledge which is not attainable. It would be preferable, perhaps, to refer all the fossil forms to *Patella,* with a query, rather than to give names implying the existence of characters which can never be determined. Paleontology, in great measure, does not admit the prosecution of the only satisfactory methods of zoological research, and hence must ever remain far behind them.
>
> —W. H. Dall, 1871

It is true that external features of the shell will probably never be useful in establishing relationships among major groups of patelloid gastropods. However, based on the results of the present study, relationships among recent species can

be determined from the shell alone by a systematic study of patelloid shell structure. In fossil patelloids, therefore, the presence of certain structures can be used in many instances to imply the presence of a definite radula or gill type. And thus it is possible to correlate soft-part morphology with hard-part morphology and arrive at a classification which is useful to both zoologists and paleontologists.

In general (Table 7; Text-fig. 84), for patelloid gastropods, there is a close relationship between the shell-structure groups established here and the cur-

TABLE 7: Relationship between shell-structure groups and currently accepted suprageneric classification (Keen, 1960) of superfamily Patelloidea.

Shell-structure group	No. of species	Genus	Subfamily	Family
1	38	*Acmaea*, *Nomeopelta*, *Scurria*, *Lottia*		Acmaeidae
2	10			
3	6			
4	2			
5	3			
6	8	*Patella*, *Helcion*	Patellinae	Patellidae
7	1			
8	5			
9	10			
10	1			
11	4	*Nacella*	Nacellinae	
12	17	*Cellana*, *Helcion* (*Rhodopetala*)		
13	1			
14	2			
15	2	*Acmaea mitra*, *Lepeta concentrica*		
16	1	*Acmaea scabra*		
17	11	*Proscutum*, *Patella*		

rently accepted classification based mainly on radula and gill morphology (Dall, 1871 and Pilsbry, 1891).

The radula formula, following the system of Dall (1871), is relatively simple in species referred to the family Acmaeidae. The formula ranges from $\frac{0}{(1\text{-}1.1\text{-}1)}$ to $\frac{0}{1(1\text{-}1\text{-}1.1\text{-}1\text{-}1)1}$. The radulas of 14 species (Text-figs. 85-89) referred to shell-structure groups 1-3 have simple formulas. Within the family Acmaeidae no significant correlations can be made between radula type and shell structure in the three groups represented. The question of the systematic position of *Acmaea mitra* (group 15) and *A. scabra* (group 16) is considered separately under the discussion of their respective shell-structure groups.

Relative to the acmaeid radula, the radula formula of species referred to the family Patellidae is complex. The formula ranges from $\frac{0}{3(1\text{-}1.1\text{-}1)3}$ to $\frac{1}{3(1\text{-}2.2\text{-}1)3}$. The radulas of 19 species referred to shell-structure groups 6-10 (all of the sub-

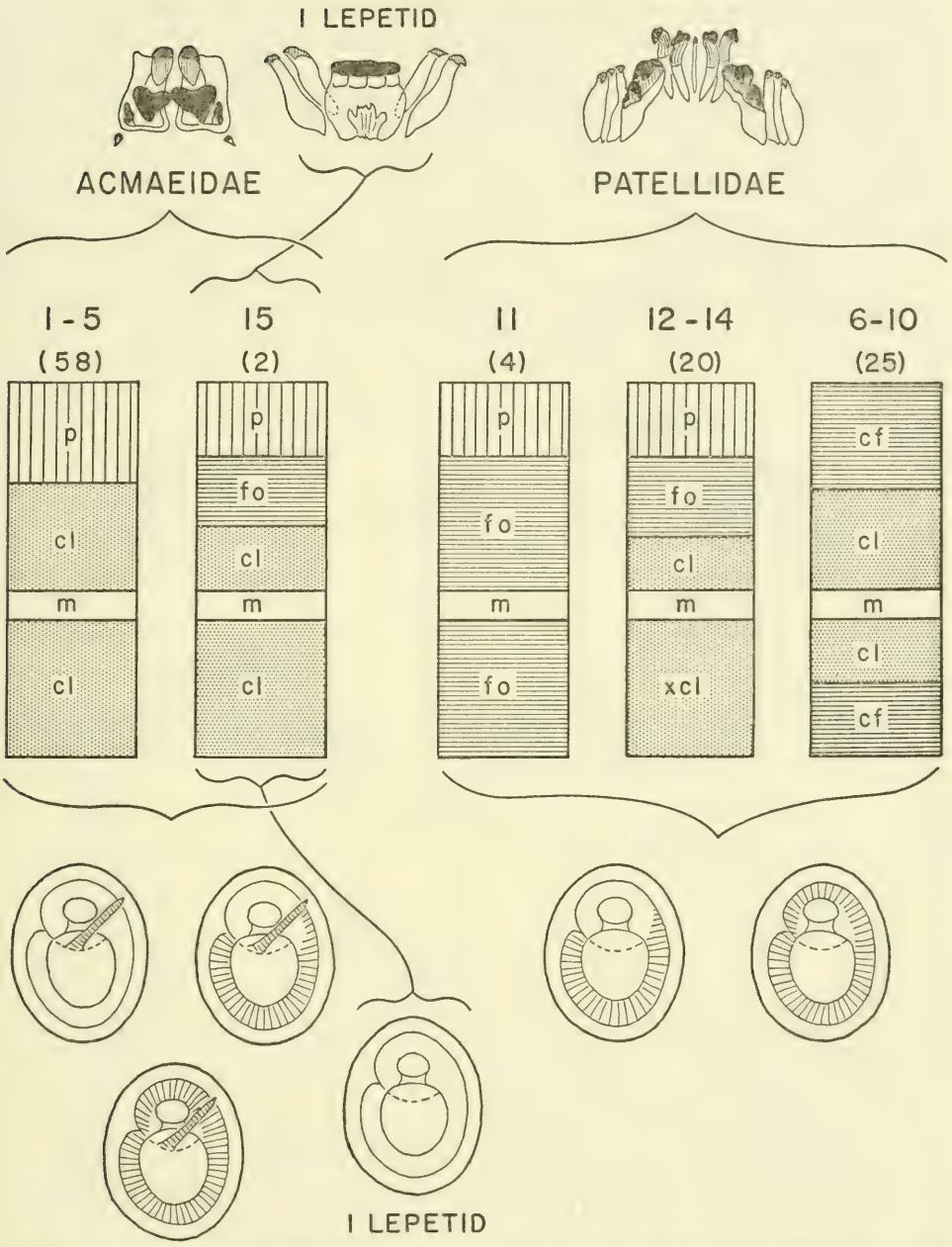

Text-fig. 84.—Generalized diagrams comparing radulas, gills, and shell structures of the three Recent patelloid families. Radula groups (above) generalized from text-figures 85-106. Shell-structure groups (middle) generalized and condensed from plate 32; at top of each structure section the large numbers refer to the shell-structure groups and the small numbers in parentheses give the number of species examined. Gill groups (below) generalized from text-figures 107-112. Explanation of structure symbols: cf, crossed-foliated; cl, crossed-lamellar; fo, foliated; m, myostracum; p, prismatic; xcl, complex crossed-lamellar. In the columnar sections, the crossed-lamellar and complex crossed-lamellar structures are indicated by one pattern, and the foliated and crossed-foliated structures are indicated by one pattern.

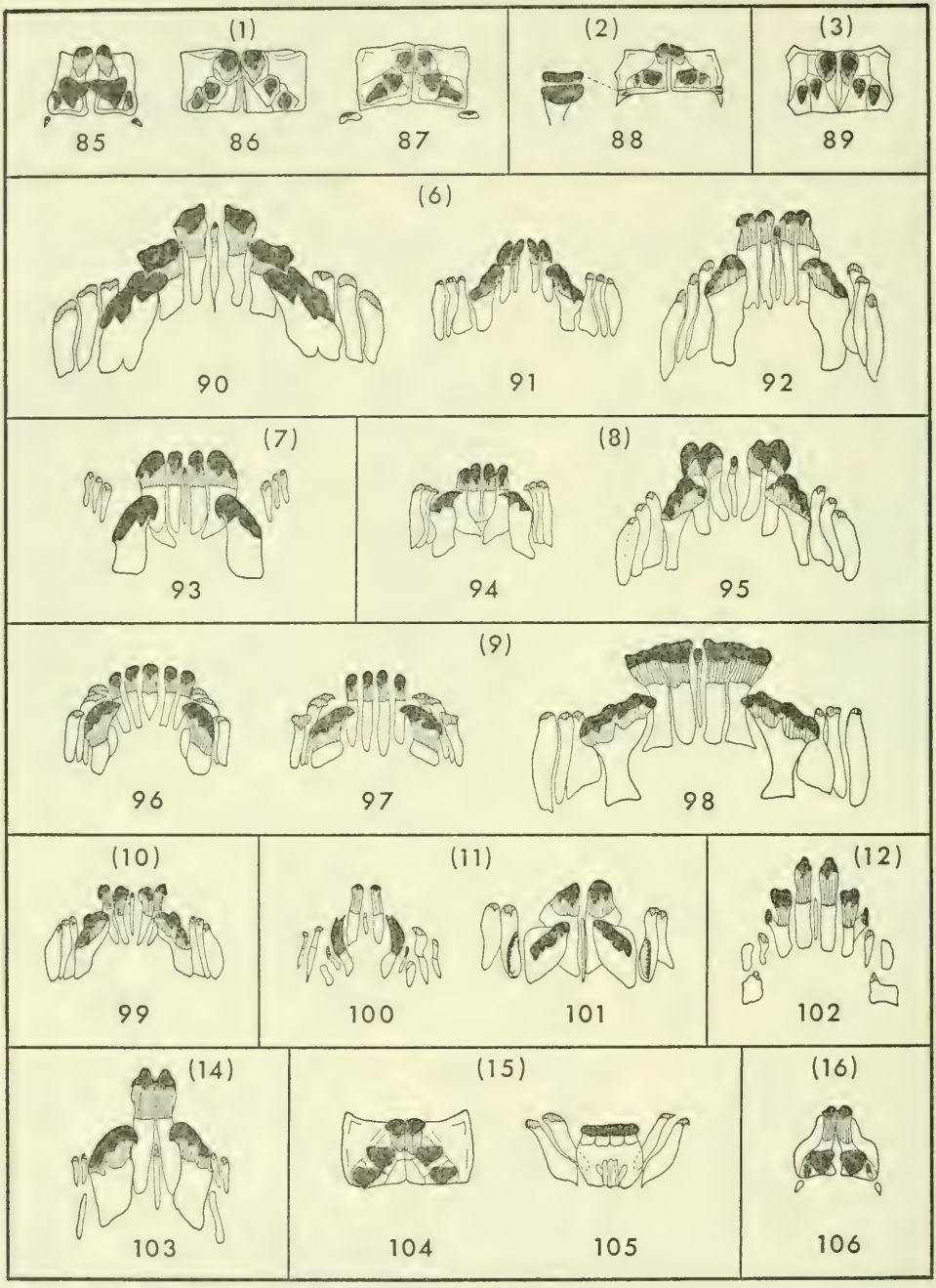

Text-figs. 85-106.

family Patellinae) are of two distinct types (Koch, 1949). In type one of Koch (Text-fig. 90) the six major teeth form a "V" which points anteriorly. In type two of Koch (e.g. Text-fig. 95) the middle four of the six major teeth lie in a straight line at right angles to the long axis of the radula band. Comparison of shell-structure groups 6-10 with these two radula groups (Table 8) shows a remarkable correlation. All five species of radula-group one belong to shell-structure group 6 (with layer m + 1 being radial crossed-lamellar). Ten of the 13 species of radula-group two belong to shell-structure groups 8, 9, and 10 (all with layer m + 1 being concentric crossed-lamellar). Three of these 13 species belong to shell-struc-

TABLE 8: Comparison of shell-structure groups with radula groups of the subfamily Patellinae. Radula groups expanded from Koch (1949, p. 493).

Radula-group **one** (Text-fig. 90)		Radula-group **two** (Text-figs. 91, 92, 94-99)	
shell-structure group	species	shell-structure group	species
6	*Patella granatina*	8	*Patella vulgata*
6	*P. compressa*	8	*P. granularis*
6	*P. miniata*	8	*P. argenvillei*
6	*P. ocula*	8	*P. lusitanica*
6	*P. sanguinans*	9	*P. tabularis*
		9	*P. barbara*
		9	*P. longicosta*
		9	*P. mexicana*
		9	*P. pentagona*
		10	*P. cochlear*
		6	*P. variabilis*
		6	*Helcion pruinosa*
		6	*H. pectinatus*

Text-figs. **85-106.**—Comparison of patelloid radula types with shell-structure groups 1-16. The radula illustrated in each figure is that of the species listed first after each figure number. All remaining species (not illustrated) per figure-number have radulas very similar to that of the first-listed species. Radulas not to scale. All radulas within a box belong to a single shell-structure group (indicated by the number in parenthesis). Explanation of symbols: D, Dall, 1871; P, Pilsbry, 1891; K, Koch, 1949. **85-87,** Group 1. **85,** *Lottia gigantea* (D, Pl. 15, f. 20), *Nomaeopelta mesoleuca* (D, Pl. 15, f. 19), *Acmaea pelta* (D, Pl. 14, f. 6), *A. patina* (D, Pl. 14, f. 4), *A. asmi* (D, Pl. 14, f. 7), *A. persona* (D, Pl. 14, f. 8), *A. fascicularis* (D, Pl. 14, f. 11), *A. testudinalis* (D, Pl. 14, f. 13), *A. atrata* (D, Pl. 14, f. 15). **86,** *A. virginea* (D, Pl. 14, f. 2). **87,** *A. pedicula* (D, Pl. 15, f. 16). **88,** Group 2, *A. saccharina* (D, Pl. 15, f. 18). **89,** Group 3, *A. incessa* (D, Pl. 14, f. 3). **90-92,** Group 6. **90,** *Patella granatina* (K, f. 10), *P. compressa* (K, f. 8), *P. miniata* (K, f. 16), *P. ocula* (K, f. 18), *P. sanguinans* (K, f. 16). **91,** *P. variabilis* (K, f. 22), *Helcion pruinosa* (P, Pl. 52, f. 3). **92,** *H. pectinatus* (P, Pl. 52, f. 4). **93,** Group 7, *H. pellucidum* (P, Pl. 52, f. 2). **94, 95,** Group 8. **94,** *Patella vulgata* (P, Pl. 52, f. 1). **95,** *P. granularis* (K, f. 12), *P. argenvillei* (K, f. 2), *P. lusitanica* (P, Pl. 52, f. 8). **96-98,** Group 9. **96,** *P. mexicana* (D, Pl. 15, f. 21). **97,** *P. pentagona* (D, Pl. 15, f. 22). **98,** *P. tabularis* (K, f. 20), *P. barbara* (K, f. 4), *P. longicosta* (K, f. 14). **99,** Group 10, *P. cochlear* (K, f. 6). **100, 101,** Group 11. **100,** *Nacella magellanica* (D, Pl. 15, f. 24). **101,** *N. mytilina* (P, Pl. 74, f. 4). **102,** Group 12, *Cellana rota* (D, Pl. 16, f. 28), *C. exarata* (D, Pl. 16, f. 29), *C. ardosiaea* (Schuster, 1913, f. 5). **103,** Group 14, *C. capensis* (P, Pl. 74, f. 6). **104, 105,** Group 15. **104,** *Acmaea mitra* (D, Pl. 14, f. 1). **105,** *Lepeta concentrica* (P, Pl. 40, f. 35). **106,** Group 16, *Acmaea scabra* (D, Pl. 14, f. 10).

ture group 6. Two of these, however, are referred to *Helcion,* whereas all remaining species of both radula groups are referred to *Patella.* None of the species having a concentric crossed-lamellar layer dorsal to the myostracum has a V-shaped radula.

In the currently accepted classification of patelloids, nine subgenera of *Patella* are recognized. Based on the above correlation between radula groups and shell-structure groups, however, it would perhaps be more meaningful to recognize no more than three subgenera.

The two genera, *Cellana* and *Nacella,* referred to the subfamily Nacellinae (Table 7) have similar radulas (Text-figs. 100-103). In shell structure, however, these two genera are quite distinct. The systematic position of *Helcion rosea* is considered at length in the discussion of group 12.

The systematic position of *Lepeta concentrica,* the one representative of the family Lepetidae in this study, is described in the discussion of group 15.

The second morphologic feature traditionally used in the classification of patelloids is the gills (used here in the broad sense to include both pallial gills and the single bipectinate ctenidium of some patelloids). Six basic types of patelloid gill arrangement (Text-figs. 107-112) are recognized. Acmaeids are characterized by the presence of a single bipectinate ctenidium with or without accompanying pallial gills, patellids are characterized by the presence of pallial gills only and lepetids have neither ctenidium nor pallial gills. At this classificatory level there is a close correlation (Table 7; Text-fig. 84) between gill-structure groups and shell-structure groups.

There are, however, several important exceptions to the above generalization. In at least one species (Willcox, 1898) of group 4, the animal has the characteristic acmaeid ctenidium. As indicated, however, by the radial crossed-lamellar structure of layer m + 1, animals of this group may be closely related to patellids. Although *Acmaea mitra* and *A. scabra,* both with a single ctenidium, are referred to different shell-structure groups (Table 7), shells of both species are characterized by the presence of foliated shell layers. As indicated before, the foliated structure, in most instances, is confined to shells of species referred to the family Patellidae. At the subfamilial and generic level there is very little correlation between the gill-structure groups and shell-structure groups.

Phylogenetic Implications

From the foregoing discussion it seems clear that in patelloids the gross structure of the shell reflects phylogenetic rather than ecologic relationships. The shell structure of patelloids is very diversified. In gastropod groups of taxonomically comparable or even larger size, the gross structure of the shell per group is relatively constant compared with the diverse shell structure of patelloids. This is true in spite of the fact that members of each of these other groups usually have a wider ecologic range than do patelloid species. Within the caenogastropods, for example, the shell (Bøggild, 1930) is generally composed of three crossed-lamellar layers although morphologically and ecologically the group is extremely diverse.

Because of the scarcity of patelloids in the fossil record, any phylogeny of the group must at this time be based mainly on Recent species. In most modern constructions of gastropod phylogenies, the presence of a cervical ctenidium is taken as indicating a primitive condition. Within the patelloids Yonge (1947) considered the acmaeids, with a single ctenidium, primitive, and the patellids, with "specialized" pallial gills only, advanced. He gives paleontologic support to

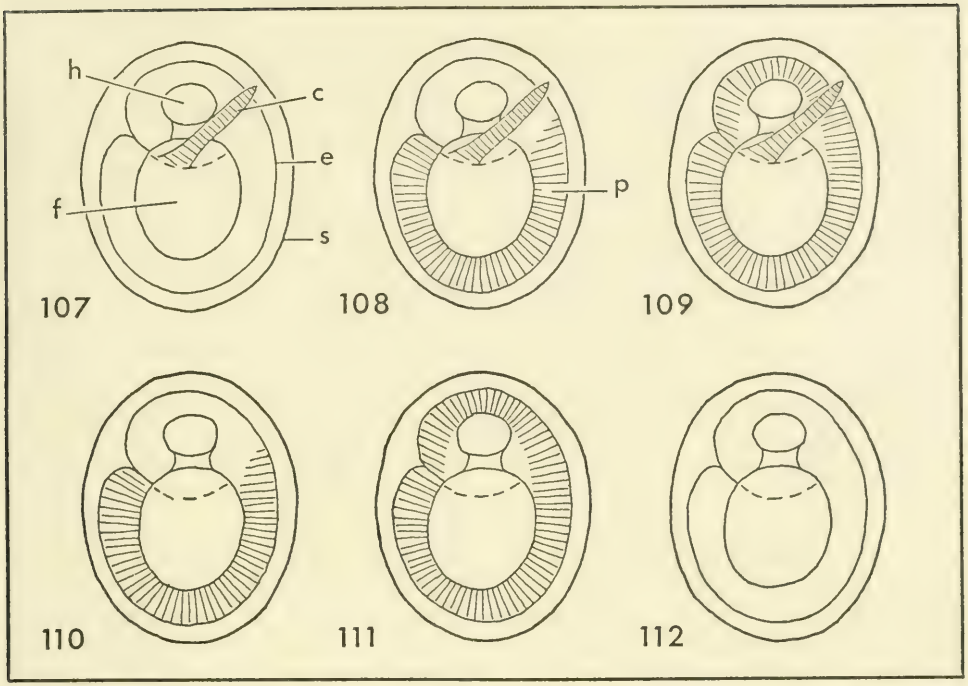

Text-figs. 107-112.—Comparison of patelloid gill types with shell-structure groups: dorsal view through transparent shell. Modified from Yonge (1947, 1960). Explanation of symbols: c, ctenidium; e, external pallial blood vessel; f, foot; h, head; p, pallial gills; s, shell margin.

Text-fig.	Classification		Shell-structure group
	family	genus	
107	Acmaeidae	*Acmaea, Nomaeopelta*	1, 2, 3, 4, 5, 15, 16
108	Acmaeidae	*Lottia*	1
109	Acmaeidae	*Scurria, Nomaeopelta*	3, 1
110	Patellidae	*Helcion, Cellana*	6, 7, 12, 13, 14
111	Patellidae	*Nacella, Patella*	6, 8, 9, 10, 11
112	Lepetidae	*Lepeta*	15

this argument by citing the time of origin, as given by Wenz (1938), of each patelloid family. Conveniently Wenz gave the acmaeids a Triassic origin and the patellids a Jurassic origin. These times of origin, however, even though perpetuated by Knight *et al.* (1960), may not be trusted, because recognition of familial characteristics using the shell alone is possible only after determining the presence of certain critical shell structures. It does not appear likely that the reported early occurrences of acmaeids and patellids are based on shell structures.

All archaeogastropods except the patelloids have a rhipidoglossan radula with about 10 central large teeth and an "infinite" number of tiny lateral teeth. Assuming the patelloids are monophyletic and were derived from archaeogastropods with a rhipidoglossan radula, then it follows that the patellids, with their more complex radular formula, are primitive and the acmaeids, with their simple radular formula, are advanced. In their most general forms, therefore, accepted

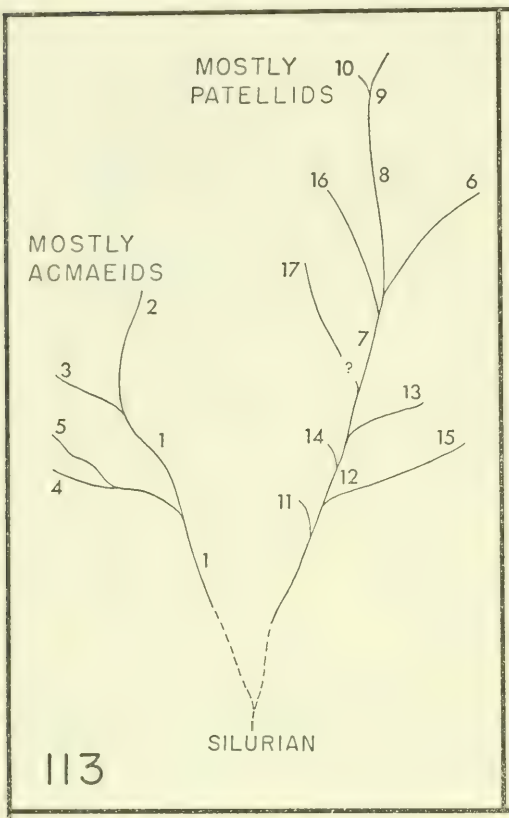
MOSTLY PATELLIDS
MOSTLY ACMAEIDS
SILURIAN
113

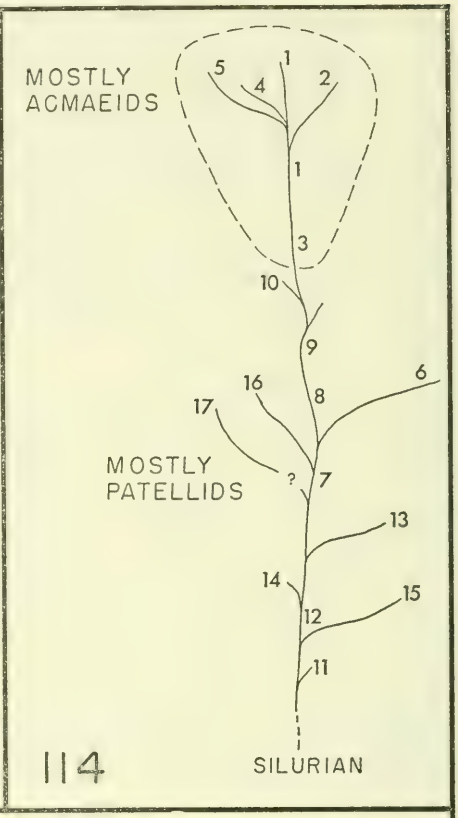
MOSTLY ACMAEIDS
MOSTLY PATELLIDS
SILURIAN
114

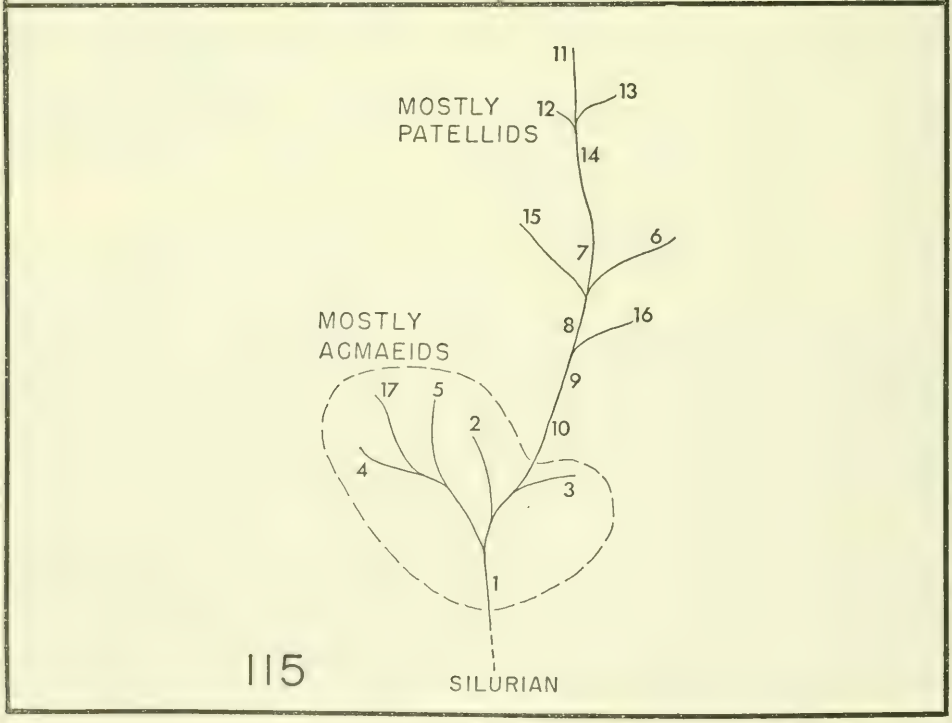
MOSTLY PATELLIDS
MOSTLY ACMAEIDS
SILURIAN
115

phylogenies based on gills are nearly the reverse of acceptable phylogenies based on radular changes.

Based on shell structure alone, several phylogenies (Text-figs. 113-115) can be constructed. Corresponding to the reversibility of phylogenies based on soft parts, phylogenies based on shell structure are also reversible. Among the 17 groups there is nearly a complete gradation of structural types. Based mainly on Recent species, therefore, three possible phylogenies should be considered. In the first (Text-fig. 113), acmaeids and patellids are derived from a common ancestor, with the separation of the two major taxa having taken place early. The shell structure of the "primitive" acmaeid group 1 is entirely different from the structure of the "primitive" patellid group 11. As depicted in this phylogeny the acmaeids primitively have shells with a thick fibrillar layer, whereas the patellids primitively have shells composed almost wholly of layers having a foliated structure. In this instance the foliated patellids are considered primitive merely because the shell structure is simpler than in the other patellid groups. Advancement in the acmaeids consists of a reduction of the fibrillar layer. Advancement in the patellids consists of reduction of the foliated layers either by change from foliated to crossed-foliated or by insertion of crossed-lamellar layers.

In the second possibility (Text-fig. 114) the patellids are considered primitive, with the structural transition from patellids to acmaeids taking place between group 10 and group 3. The only structural difference between these two groups is in the outermost shell layers. Shells of group 10 have a radial crossed-foliated outer layer (m + 2). Shells of group 3 have a complex-prismatic outer layer (m + 3) with horizontally arranged second-order prisms which may be homologous with the third-order lamellae of the crossed-foliated layer of group 10. The thin fibrillar layer (m + 2) of group 3 would be "inserted," phylogenetically, into the shells of acmaeids. This phylogeny, in which the patellids are considered primitive, is in opposition to Yonge's (1947) phylogeny based on gills. The phylogeny is, however, supported by the progression from a complex to a simple radula.

In the third possibility (Text-fig. 115) the phylogeny is reversed, with the acmaeids being considered primitive. The structural transition may still be regarded as taking place between group 10 and group 3. However, in this instance the acmaeid group 3 gives rise to the patellid group 10 by loss of the fibrillar layer and modification of the complex-prismatic to radial crossed-foliated structure. It should further be noted that within the Patellidae the phylogenetic sequence is reversed from the two preceding phylogenies. The tendency is for simplicity of shell structure with advancement, rather than increased complexity.

The advantage of the last-mentioned phylogeny is that it is supported almost in its entirety by the currently accepted patelloid phylogeny based mainly on gill structures. The gradational sequence of gill structures from *Acmaea* (Text-fig. 107) to *Lottia* (Text-fig. 108) to *Scurria* (Text-fig. 109) to *Patella* (Text-fig. 111) corresponds well with the gradational sequence of shell-structure groups from 1 to 3 to 10.

With the wide diversity of shell-structure groups within the patelloids, it is not unreasonable to assume a polyphyletic origin for the group. Before a meaningful

Text-figs. 113-115.—Dendritic diagrams showing morphologic and possibly phylogenetic relationships among the 17 patelloid shell-structure groups (Pl. 32). Other than a Silurian origin for superfamily, no attempt is made to show the geologic age relationships of the groups involved. 113, with acmaeids and patellids derived from a common ancestor. 114, with patellids primitive. 115, with acmaeids primitive.

phylogeny can be constructed, the fossil record, as well as all available neontological relationships, must be given full consideration. In the past it has been very difficult, if not impossible, to classify fossil patelloids because the only features available were general external shell morphology and internal muscle scars. To date, neither of these features has been useful in splitting the patelloids into smaller groups. Now, with the demonstrated usefulness of shell structures in the classification of Recent patelloids, there is a useful feature available which at least has a chance of being preserved in fossils. Unfortunately, fossil patelloids are not common, particularly in pre-Tertiary rocks. Nevertheless, even in rare Paleozoic patelloids, shell layers have been observed. For example, in the shell of *Calloconus humilis* (Perner) from the Devonian of Bohemia, Horný (1963, p. 60; Pl. 18, figs. 8, 9) described two distinct shell layers. Further investigations on this and other Paleozoic patelloids are essential before evolutionary sequences can be constructed.

No work on patelloid-shaped gastropods would be complete without some comparison with *Neopilina galatheae*, the living monoplacophoran described by Lemche and Wingstrand (1959). Schmidt (1959) gave a detailed account of the shell structure of *Neopilina*. Exclusive of the periostracum he recognized two shell layers; an inner very thin layer having a nacreous structure and an outer very thick layer composed of large columnar prisms oriented at right angles to growth surfaces. Each large prism he described as being composed of tiny fibrils which radiate from the point of origin of each major prism on the inner surface of the periostracum. Neither of these structures was observed in shells of patelloid gastropods. Based on the shell structure of *Neopilina* it may be concluded that there is very little relationship between living monoplacophorans and living patelloids.

SUPERFAMILY BELLEROPHONTOIDEA

It is generally believed that, in shells of Paleozoic mollusks, recrystallization of the original shell material would prevent the study of shell structures from being of significant value in the classification of a major group. Newell (1938, 1942), however, in his monographs on late Paleozoic pectinoid and mytiloid pelecypods, has demonstrated that (Newell, 1938, p. 24) "the preservation of original shell microstructure in Paleozoic mollusks is not a rare phenomenon—at least it is not rare in collections from the Pennsylvanian rocks." Not only did he recognize the shell structures but he demonstrated that in the pectinoids (Newell, 1938, p. 26) "easily recognizable and consistent differences in shell structure exist between tribes that are also separable on characters of form and ornamentation." Bathurst (1964) has recently summarized the literature on recrystallization in molluscan shells, and he gives criteria for recognition of shell material replaced by drusy calcite and shells which have undergone recrystallization *in situ*. Traces of the original structure are preserved only where the latter process was in effect.

The crossed-lamellar structure, which is here reported from two bellerophontoid species, is described in pectinoid shells by Newell (1938). His description and figures of crossed-lamellar layers in these Pennsylvanian pectinoids mark the earliest recorded occurrence of the crossed-lamellar structure in pelecypods.

Yochelson (1960, p. 230) reported, "There is no question but what further investigation into the structure and composition of the bellerophontacean shell would add significant details to a classification of the genera and might yield important new data on the position of the superfamily within the aspidobranch

gastropods." The following two sections on the shell structure of *Euphemites* and *Bellerophon* are first steps in the direction of a thorough study of the shell structure of bellerophontoid gastropods.

EUPHEMITES WARTHIN, 1930

Based on one longitudinal polished section, Weller (1930) described six shell layers in the shell of *Euphemites callosus* (Weller, 1930). According to Weller, layers one through three were deposited on the inner surface of the shell and are distinguished mainly on the basis of color differences. Layers four through six were deposited on the outer surface of the shell by parts of the mantle which folded back over the shell during the life of the animal. Weller mentioned shell structures (other than growth surfaces) only in connection with layers one and three. He described layer one (the innermost layer) as probably representing the inner nacreous shell layer. Layer three (deposited just within the apertural margin) Weller (1930, p. 19) described as being

> composed of a series of overlapping plate-like parts, lenticular in cross-section and inclosed in a brown matrix. The lenticular masses have a radial structure. They are slightly lighter colored than the surrounding portion of layer 3 and contain large numbers of short, parallel, but irregularly sized and spaced dark areas, as though the darker material of this layer had filled the spaces between the calcareous fibers or elongated crystals which make up these masses.

This was the first hint of prismatic structure in shells of *Euphemites*.

Moore (1941), using both longitudinal and transverse sections, redescribed the shell-layer sequence and shell structure of *Euphemites callosus*. He gave a detailed explanation of the relationship of the shell layers deposited on the inside of the shell to the layers deposited on the outside of the shell. Following Weller, Moore described the innermost layer (layer one) as probably representing the nacreous lining of the shell. Layers two and three of Weller he described and illustrated as having a prismatic structure. These two layers he could distinguish only on the basis of color. Where color differences were not present, he could find no basis for recognizing two distinct layers. Layers four (perinductura) and five (inductura) he likewise described as having a prismatic structure. No structure was reported for layer six (coinductura).

In longitudinal and transverse sections of shells of *Euphemites vittatus* (McChesney, 1860), Moore (1941) recognized five of the six shell layers described for *E. callosus*. The coinductura is the only layer not represented in *E. vittatus*. Layer three is the only layer described and figured (Moore, 1941, fig. 3a, b) as having a prismatic structure. Presumably Moore considered all but layer one of the remaining layers prismatic.

Through the combined efforts of Weller (1930) and Moore (1941) a wholly satisfactory explanation of the sequential relationship of the outer shell layers in shells of *Euphemites* has been presented. However, Moore's interpretation of the shell structure of layers deposited on the inside of the shell of *E. vittatus* is erroneous. His conclusion that the major inner layer (Weller's layers two and three combined) is prismatic is based on examination of longitudinal and transverse sections. If, as was done by Moore, the description of prismatic structure is based only on observation of longitudinal and transverse sections (Text-fig. 116), the conclusion is justified. However, what appear to be prisms in two dimensions (longitudinal and transverse sections) may, in three dimensions (Text-fig. 117), actually be truncated ends of first-order lamellae of a crossed-

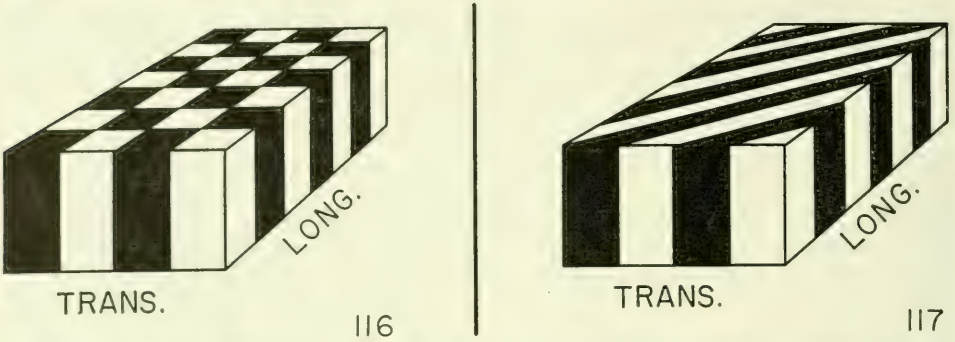

Text-figs. **116, 117.**—*Euphemites;* two different structural interpretations of "prisms" seen in transverse and longitudinal section. **116,** prismatic structure (Moore, 1941). **117,** crossed-lamellar structure (this paper).

lamellar shell layer. A three-dimensional examination of shells of two species of *Euphemites* has shown this to be the case.

Crossed-lamellar shell structure, previously unrecorded in the suborder Bellerophontina has been observed in *Euphemites vittatus* (20 specimens from the upper Pennsylvanian Wayland shale, 1.2 miles south of Gunsight, Texas, USNM loc. 510-A) and in *E. nodocarinatus* (Hall, 1858) (two specimens from middle Pennsylvanian rocks near Carbon Hill, Ohio, and one from the middle Pennsylvanian Boggy shale near Ada, Oklahoma). The specimens of *E. vittatus* examined by Moore also come from the Wayland shale of Texas. All the following detailed relationships of first-order lamellae were obtained from the shells of *E. vittatus.* Crossed-lamellar structure was observed in the inner shell layers of *E. nodocarinatus* (hypotype, UCMP no. 36489) but no details on the orientation of first-order lamellae were recorded.

In parts of several of the shells of *Euphemites vittatus,* the shell is preserved in punky, very light brown patches. In fragments having this kind of preservation the structure is best preserved. Although *in-situ* recrystallization (Pl. 27, fig. 2) has rendered thin-section study useless in transmitted light, the structural elements retain sufficient integrity to be readily seen in low-angle incident light (Pl. 27, fig. 1). In some cases (Pl. 27, fig. 3), the shell breaks along zones of original structural weakness.

TABLE 9: Dip angle (in degrees) of second-order lamellae in fragment of shell of *Euphemites vittatus.* Measurements from hypotype, USNM no. 144496-a (Pl. 29, fig. 3).

Location on fragment	Set one (dips right)	Set two (dips left)
1	30°	29°
2	32°	29°
3	26°	28°
4	27°	30°
5	35°	38°
average dip angle	30°	31°
average of average dip angles	30.5°	

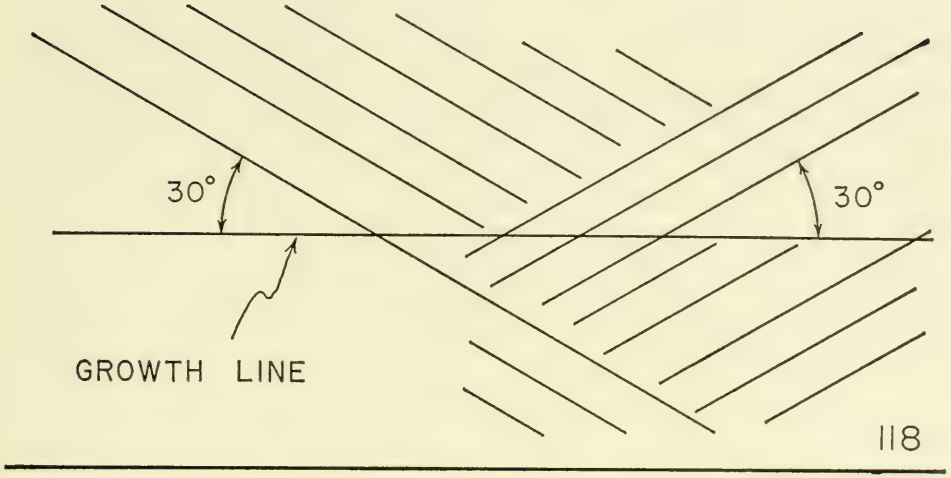

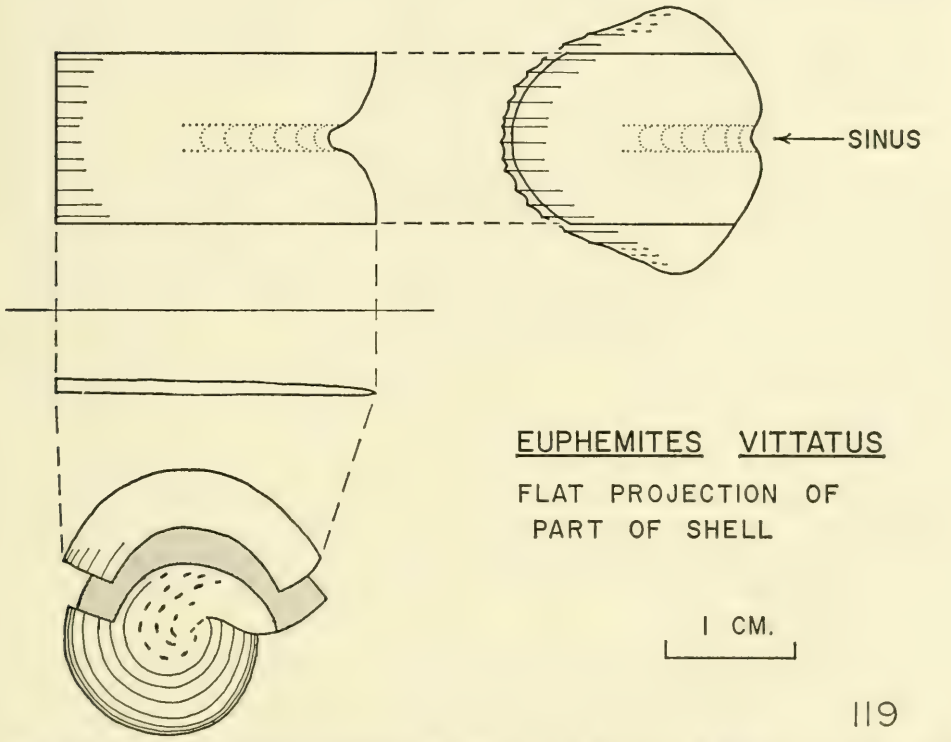

Text-figs. **118, 119.**—*Euphemites vittatus.* **118,** diagram of fragment of shell showing dip angles of second-order lamellae (Table 9; Pl. 29, fig. 3). **119,** flat projection of the part of the shell shown in text-figures 120-122.

Four criteria, already discussed in the section on Shell Structures, were used to identify crossed-lamellar structure in the shells of *Euphemites vittatus.* Briefly the criteria used are (1) the intertonguing relationship (Pl. 27, fig. 1) of first-order lamellae in fragments or sections viewed normal to growth surfaces, (2) the alternating light-dark pattern (Pl. 27, figs. 4, 5), in first-order lamellae, reflecting the presence of oppositely dipping second-order lamellae in alternate first-order lamellae, (3) the fretwork pattern (Pl. 27, fig. 3) at the broken edges of some chips, and (4) the cross pattern (Pl. 29, fig. 3) of two sets of topographic lineations on weathered surfaces normal to the width axes of first-order lamellae. The inference is here made that the lineations are produced by weathering parallel to second-order lamellae and thus reflect the true dip angle of second-order lamellae. The inference that the lineations (Text-fig. 118) reflect the orientation of second-order lamellae is based on the fact that lineations (Table 9) of one set intersect growth surfaces at nearly the same angle as the lineations of the other set. The average of the two average dip angles is 30.5°. This figure falls well within the limits (Text-fig. 31) established for crossed-lamellar structure. The average width (28μ) of first-order lamellae is nearer the average width (Table 2) established for first-order lamellae of crossed-lamellar structure than it is to the average width established for first-order lamellae of crossed-foliated structure.

In the three shells of *Euphemites nodocarinatus* recrystallization was more nearly complete than in shells of *E. vittatus.* Only criteria 1 and 2 were used to identify crossed-lamellar structure in these shells.

The inner nacreous layer (layer one), alluded to by both Weller and Moore as occurring in shells of *Euphemites vittatus* and *E. callosus,* does not exist in shells of *E. vittatus.* Shell material having crossed-lamellar structure is present at the inner surface of the shell of *E. vittatus* one volution back from the apertural margin. In the following discussion it is assumed that, except for the absence of a coinductura in *E. vittatus,* the shell-layer sequence and the shell structure of *E. vittatus* and *E. callosus* are identical. Shells of *E. callosus* were not available for study. Moore (1941, fig. 1B), in a median longitudinal section of the shell of *E. callosus,* illustrated layer one as being present at the inner surface of the shell one third of a volution back from the apertural margin. Although he did not describe it, Moore (1941, fig. 1D) illustrated a "prismatic" structure one volution back at the inner surface of the shell of *E. callosus.* This last-mentioned figure, therefore, is inconsistent with Moore's (1941, p. 133) statement that "an innermost very thin layer (designated no. 1 by Weller) seems to represent the nacreous lining of the shell interior." That figure, however, is consistent with the present observation of crossed-lamellar structure at the inner surface of shells of *E. vittatus.*

Observations on the orientation of first-order lamellae at several horizons within the shell material deposited on the inside of the shell indicate that only one shell layer was deposited on the inside of the shell under the perinductura. That layer is hereafter referred to as the inner crossed-lamellar shell layer. Within this inner crossed-lamellar shell layer along the median plane, at the apertural margin and adapically immediately below the perinductura (Pl. 28, figs. 1, 2), the first-order lamellae form a pattern concave adaperturally. On the inner surface of the shell, along the median plane, starting about one-third of a volution back and continuing adapically the first-order lamellae (Pl. 29, fig. 2) form a pattern strongly convex adaperturally. At levels within the shell layer, midway between the outer surface having a concave pattern and the inner surface having a convex pattern, the first-order lamellae (Pl. 28, fig. 3; Pl. 29, fig. 1) trend straight across the shell normal to the median plane. In a tangential

polished section (Pl. 29, fig. 2) intersecting inner and middle horizons of the inner crossed-lamellar shell layer, two of the structural trends mentioned above can be seen in a single section.

The structural trend (Text-fig. 120) of first-order lamellae on the inner surface of the shell of *E. vittatus* is reconstructed from the structure exhibited in

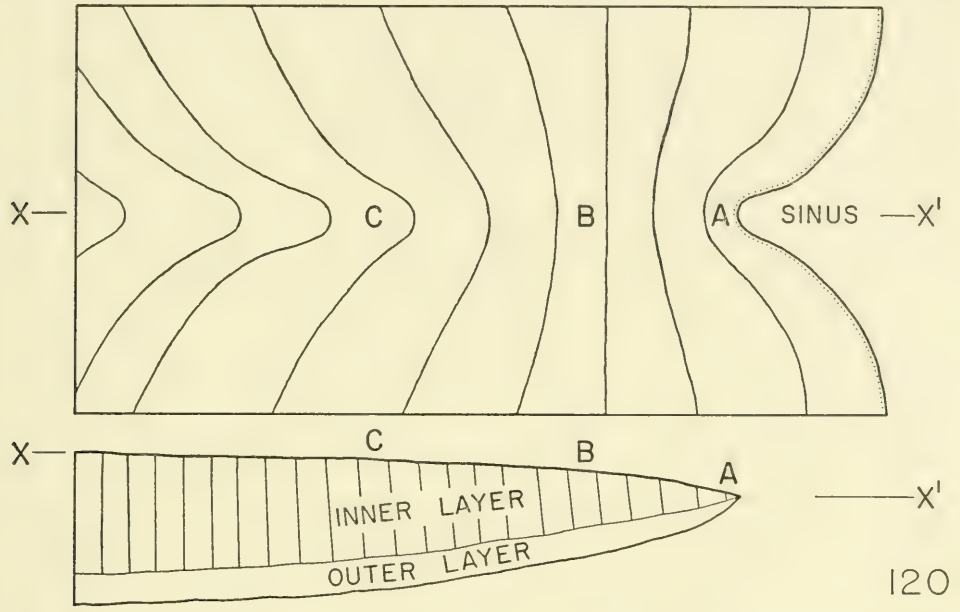

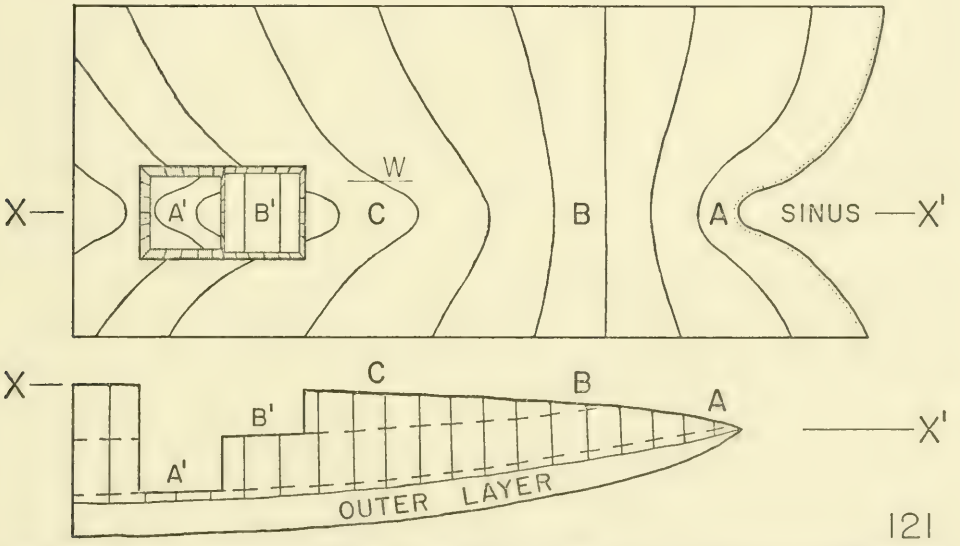

Text-figs. 120, 121.—*Euphemites vittatus;* view of the inner surface of the shell showing structural trends of first-order lamellae (e.g. at A, B, and C) of the inner shell layer, across the selenizone (see Text-fig. 119). Each surficial view is accompanied by a vertically exaggerated cross section along the median sagittal plane XX'; outer layer is perinductura of Moore (1941). **120,** trend only on inner surface. **121,** same but with two cut-away views (e.g. at A' and B'). Line at W shows position of section given in text-figure 124. Areas at B and C in both text-figures based in part on hypotype, USNM No. 156343-A.

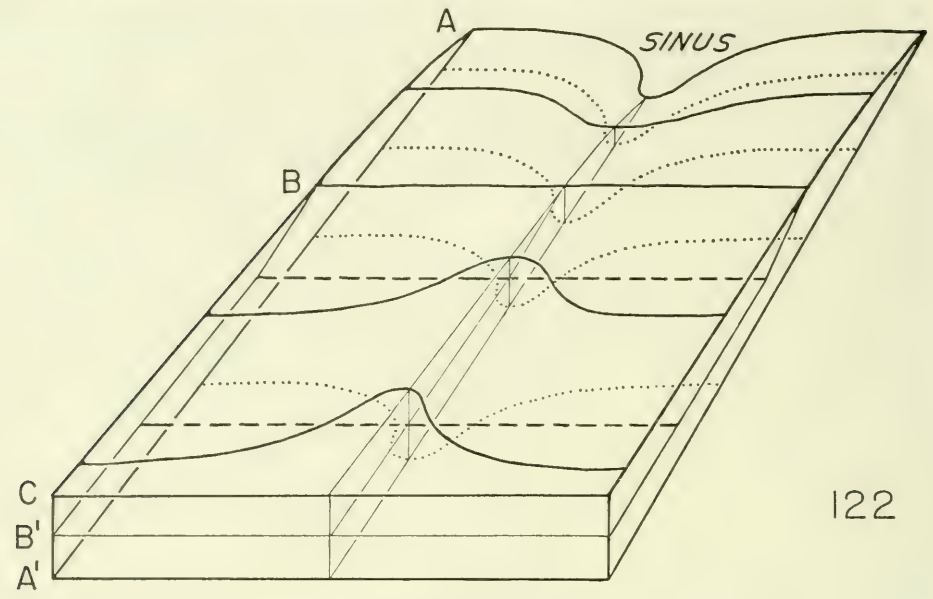

122

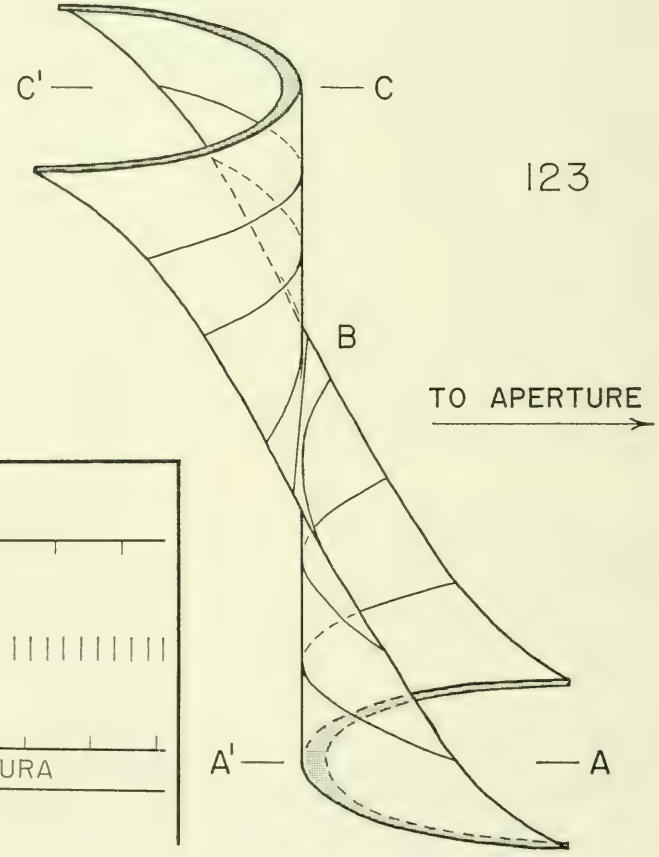

123

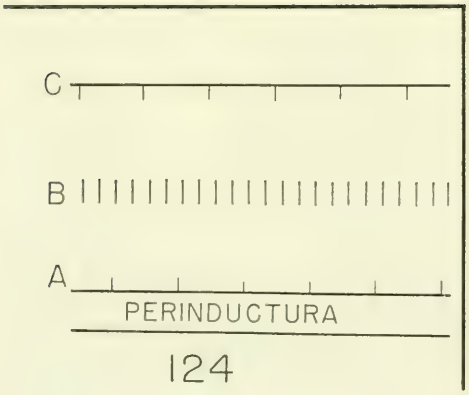

124

several specimens. Text-figure 120 is a view, distorted by flattening, of the inner surface of a part (Text-fig. 119) of the shell extending back from the aperture about half a volution. In spite of the distortion, the structural trend of first-order lamellae, as mentioned before, indicates that only one shell layer was deposited on the inside of the shell under the perinductura. Adjacent to the apertural margin (Text-fig. 120, point A) first-order lamellae are parallel to the margin and thus, along the median sagittal plane, form a pattern concave adaperturally. Adapically, along the median plane on the inner shell surface, the degree of concavity of first-order lamellae gradually diminishes to a point (point B), about one-quarter of a volution back from the aperture, where they trend straight across the shell. Adapically from point B the pattern formed by first-order lamellae is convex adaperturally, with the degree of convexity gradually increasing from point B to point C, about half a volution back, where the degree of convexity equals the degree of concavity of the pattern of first-order lamellae at the aperture. Laterally from the median plane all first-order lamellae curve into a position such that their length axes approach being normal to the median plane.

In cut-away views (Text-fig. 121, surface A′ and B′) the superposition of structural trends of first-order lamellae can be seen in the inner crossed-lamellar layer. As can be seen in the cross section (Text-fig. 121) the horizon at which first-order lamellae trend straight across the median plane is delimited by the surface BB′. The horizon at which first-order lamellae form a pattern concave adaperturally is delimited by the surface AA′. By looking only at the patterns at horizons A′, B′, and C one might get the impression that each pattern represented a distinct shell layer and that therefore three shell layers instead of one are present under the perinductura. Between the horizon AA′ and the inner surface at and adapically from C, however, there is a completely gradational sequence of patterns from concave adaperturally to convex adaperturally. This gradational sequence is more clearly demonstrated in a three-dimensional block diagram (Text-fig. 122) of the same part of the shell as shown in text-figures 120 and 121. A curved surface (Text-fig. 123) can also be used to demonstrate the changing pattern of the trend of first-order lamellae across the median plane. It should be emphasized that this is not a picture of a first-order lamella but simply a surface showing the *trend* of first-order lamellae at any given horizon. In other words, the intersection of any growth surface with the hypothetical curved surface is the pattern formed by first-order lamellae at that horizon. The gradational sequence of trends of first-order lamellae is sufficient evidence to demonstrate that one shell layer, not two or more, is present under the perinductura.

In the inner crossed-lamellar shell layer, the pattern exhibited by first-order lamellae in vertical, longitudinal section (through point W, Text-fig. 121) along the margin of the selenizone might, if considered without regard for the three-dimensional relationships, be misinterpreted as an indication of three distinct shell layers. In such sections (Text-fig. 124) the first-order lamellae at the outer surface (horizon A) and at the inner surface (horizon C) intersect the plane of section at a low angle and therefore have a wide outcrop pattern. In the middle

Text-figs. 122-124.—*Euphemites vittatus;* structural trends across selenizone of first-order lamellae of the inner shell layer. **122,** block diagram showing trends at horizons AA′, BB′ and ABC (see Text-fig. 121). **123,** hypothetical surface showing gradational change in structural trend from the outer surface AA′ to the inner surface CC′. **124,** sagittal section at margin of selenizone showing width of outcrop pattern of first-order lamellae at horizons A, B and C (see Text-fig. 121, line at W).

of the layer (horizon B) the first-order lamellae are normal to the plane of section and therefore have a narrow outcrop pattern. This alternation of wide and narrow outcrop patterns might be interpreted as an indication of the existence of three shell layers. Inward to the inner surface and outward to the outer surface from horizon B (Text-fig. 124), however, there is a gradational increase in the width of the outcrop pattern of first-order lamellae. In vertical, longitudinal sections within the selenizone along the median plane (Text-fig. 120, section XX′) and laterally, at a distance from the selenizone, the width of the outcrop pattern of first-order lamellae is constant, relative to widths measured at and near the margin of the selenizone. These relationships confirm the already-demonstrated existence of only one shell layer under the perinductura.

In adjacent crossed-lamellar layers of Recent shells, first-order lamellae may be oriented from 45°-90° to each other. This change of direction of first-order lamellae adds greatly to the strength of the shell. In the inner crossed-lamellar layer of *Euphemites* the changes of structural trend of first-order lamellae across the selenizone serves a similar strengthening function.

Although crossed-lamellar structure could be seen near the umbilical area on the outer surface of the shell of *Euphemites vittatus,* no shell structure was seen in the perinductural and inductural shell layers in the area of the selenizone.

The presence of crossed-lamellar structure in shells of the Pennsylvanian *Euphemites vittatus* and *E. nodocarinatus* marks the earliest recorded occurrences of crossed-lamellar structure in the gastropods. Previously the earliest record of crossed-lamellar structure in the gastropods was given as Permian by Waterhouse (1963, p. 109, figs. 35-37), who described one crossed-lamellar layer in the body whorl of the euomphaloid archaeogastropod *Coronopsis vagrans* from New Zealand.

BELLEROPHON Montfort, 1808

The observation of crossed-lamellar structure in shells of *Euphemites* is not to be construed as meaning that crossed-lamellar structure is to be expected in all remaining bellerophontoid shells. Bøggild (1930) described and figured a section of the shell of one species of *Bellerophon* from the Ordovician of Bornholm, Denmark. He (Bøggild, 1930, p. 299) stated, "the shell . . . consists throughout of a peculiar, foliated calcite possessing a characteristic micaceous lustre. . . . Without doubt we have here the original structure, and it is easily seen that this layer has constituted the whole shell." Bøggild mentioned that this shell, made up entirely of unaltered calcite, was an unusual occurrence. He stated that usually the bellerophontid shells consisted of irregularly grained calcite and that this indicated alteration from an originally aragonitic shell.

Stehli (1956), in a description of unaltered shells from the Pennsylvanian Buckhorn asphalt in Oklahoma and Kendrick shale in Kentucky, reported that several shells of an unidentified bellerophontid species had a very thin outer calcitic layer and a thick inner aragonitic layer. In other shells of the same species, however, no outer calcitic layer was observed by him. Stehli, in a general discussion of the Buckhorn asphalt and the Kendrick shale, stated that in shells of the fauna intricate microarchitectural details are preserved. He did not describe, however, the shell structure of the bellerophontids.

Shell structure is here reported from the shells of two species of *Bellerophon.* The complex crossed-lamellar structure is recognized in shells of *Bellerophon (Pharkidonotus) percarinatus* Conrad, 1842. Conclusions are based on a study of 20 shells from the same locality as the shells of *Euphemites vittatus.* All of the

critical features necessary for the recognition of the complex crossed-lamellar structure are preserved in only one specimen of *B. percarinatus*. In a small (3 × 3 mm) area of this shell (Pl. 30, fig. 1) partial recrystallization has left the shell material in such a state that, where broken, the shell came apart along zones of weakness which delimit the original structure. This is the same very light brown, punky type of preservation which best preserved the original structure in shells of *E. vittatus*.

A description of the criteria for recognition of the complex crossed-lamellar structure in partially recrystallized shells is given in the section on Shell Structures. The characteristics recognized in the single shell of *Bellerophon percarinatus* are briefly redescribed here. The topography (Pl. 30, figs. 2, 3; Pl. 31, fig. 1; Text-fig. 126) of the surface which was broken roughly parallel to growth surfaces consists of an arrangement of many small, adjoining cones. The horizon at which the cones are exposed is roughly one-third the distance from the inner shell surface to the outer surface of the shell layer. The apices of the cones point toward the outer surface of the shell. At their bases the diameters of the cones range from 50-145μ. Two microphotographs (Pl. 30, figs. 1, 2) show the shape of the cones as seen in the transverse and longitudinal directions. The dip angle (Table 10; Text-fig. 125) on the admedial flanks of six cones averages 33°. The dip angle on the adlateral flanks of the same six cones averages 39°. The discrepancy between these two angles is probably the result of the position of the structure on the curved flank of the shell.

At several places, in both transverse (Pl. 30, figs. 5, 6) and longitudinal (Pl. 30, fig. 4) vertically broken sections adjacent to the cone-studded surface, major prisms are exposed in cross section. The width of the major prisms equals the diameter of the cones exposed on the growth surface. All major prisms, which are almost normal to growth surfaces, are made up of chevron arrangements of striations. The chevrons point toward the outer surface of the shell. In any given chevron the angle between each of the two branches and growth surfaces is nearly the same. The angle between chevron branches and growth surfaces equals the angle between cone flanks (measured on the exposed growth surface) and growth surfaces. The chevrons are seen in both transverse (Pl. 30, figs. 5, 6) and longitudinal (Pl. 30, fig. 4) sections and are therefore interpreted as representing

TABLE 10: Dip angles (in degrees) of cone surfaces (see Text-fig. 125) in complex crossed-lamellar layer of *Bellerophon* (*Pharkidonotus*) *percarinatus*. Explanation of symbols: b, dip angle of adlateral flank of cone; c, dip angle of admedial flank of cone; d, dip angle of dominant lineations on surface of transverse break. Based on hypotype, USNM no. 144498.

Cone no.	Dip angles		
	c	b	d
1	24°	38°	39°
2	41°	42°	38°
3	32°	43°	44°
4	34°	43°	38°
5	34°	37°	—
6	33°	30°	—
average	33°	39°	40°

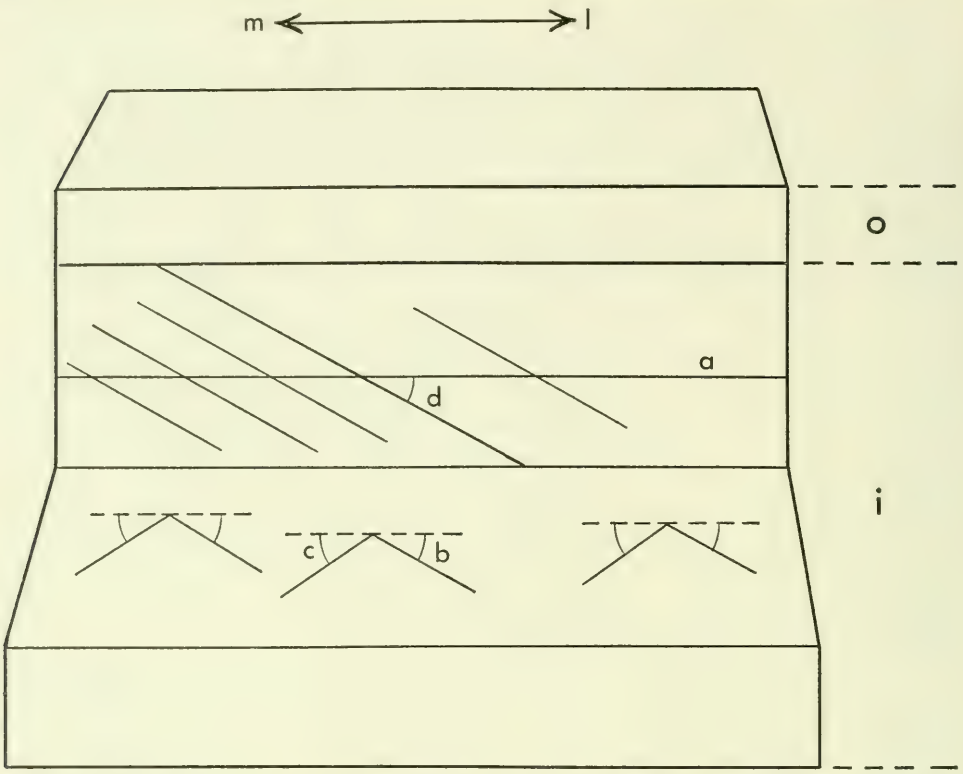

Text-fig. 125.—*Bellerophon percarinatus;* block diagram of complex crossed-lamellar inner layer showing location of dip angles given in Table 10. Explanation of symbols: a, growth line; b, dip angle of adlateral flank of cone; c, dip angle of admedial flank of cone; d, dip angle of dominant lineations on surface of transverse break; i, inner shell layer; l, adlateral; m, admedial; o, outer shell layer.

conical second-order lamellae as seen in cross-sectional views of major prisms of the complex crossed-lamellar structure. The diameter of the polygons (Pl. 31, fig. 2) on the surface of the shell layer, just under the outer shell layer of unknown structure, is smaller (40-70μ) than the diameter of the major prisms (Pl. 31, fig. 1) farther down in the layer toward the inner surface of the shell. It is concluded, therefore, that the structure of this inner layer is complex crossed-lamellar. All critical features which were used in reconstructing the structure are shown diagrammatically in text-figure 126.

Except for a few small areas, the exposed surface (Pl. 30, fig. 5; Text-fig. 126) of the transverse section is dominated by striations with only one orientation. The angle, however, between these striations and growth surfaces is equal to the angle between chevron branches and growth surfaces. It is here inferred, therefore, that the large areas having striations with only one orientation are the result of a structural dominance of second-order lamellae in the adlateral flanks of the major prisms. Where the shell was broken, therefore, only one structural trend, for the most part, was revealed.

The block diagram shown in text-figure 127 is a reconstruction, expanded from the information given in text-figure 126, showing the cone-in-cone structure of major prisms of the complex crossed-lamellar inner layer of *Bellerophon*

percarinatus. No structure was seen in the thin outer shell layer and the thick inductura at the inner lip. At the part of the shell where the cones are exposed, the inner shell layer is 1.0 mm thick and the outer layer is 0.4 mm thick.

Although the remaining 18 shells were more recrystallized than the two just described, several of them showed, on the surface immediately under the outer shell layer, an irregularly polygonal pattern reflecting the presence of major prisms.

It should be mentioned, as a general conclusion, that a polygonal or honeycomb pattern on the surface of a shell layer does not necessarily indicate that

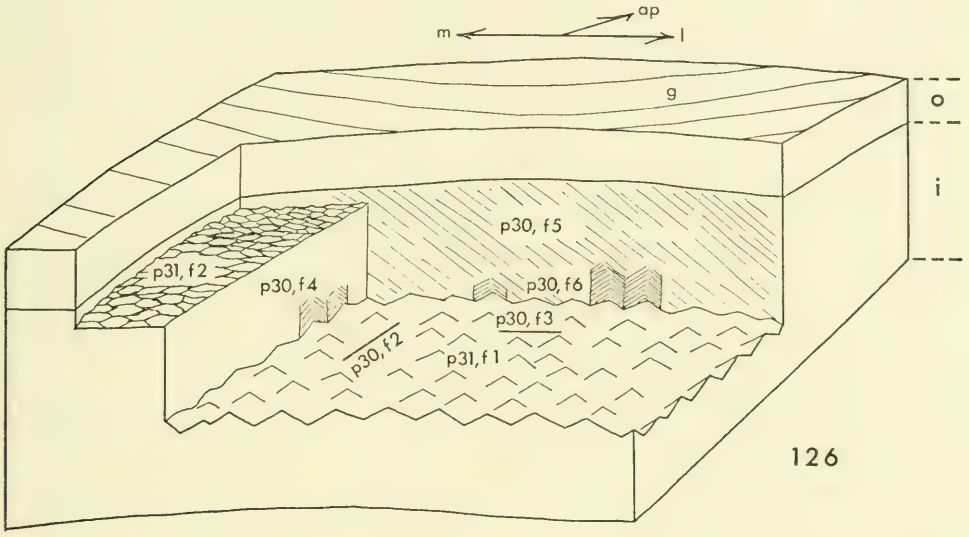

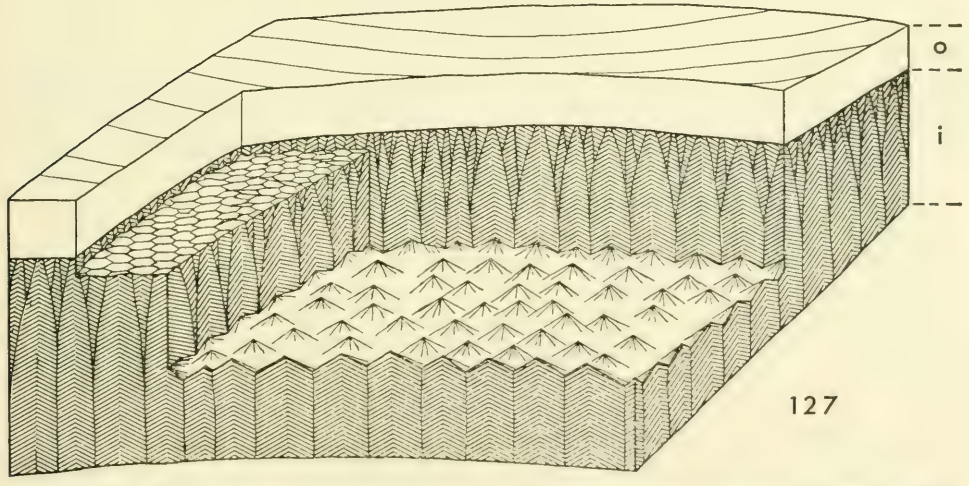

Text-figs. **126, 127.**—*Bellerophon percarinatus;* block diagrams showing complex crossed-lamellar structure of thick inner shell layer in area shown in Pl. 30, fig. 1. Explanation of symbols: ap, adapical; f, figure number; g, growth lines on outer surface of shell; i, inner shell layer; l, adlateral; m, admedial; o, outer shell layer; p, plate number. **126,** observed features only (Pl. 30, figs. 2-6; Pl. 31, figs. 1, 2). **127,** inferred structure of the inner shell layer.

large single-crystal prisms make up a prismatic shell layer. As has just been demonstrated, the polygonal pattern on the inner layer of shells of *Bellerophon percarinatus* reflects the presence of major prisms of the complex crossed-lamellar structure. In other words, when one recognizes a polygonal pattern on the surface of the shell layer of a fossil shell, he must first determine the microstructure of the individual prisms before making a definitive statetment as to the structure of the shell layer. In order to do this the shell must be either unaltered or only slightly recrystallized.

The following discussion of the shell structure seen in the shell of a single specimen of an unidentified species of *Bellerophon (Bellerophon)* will serve to illustrate the problem of recognition of prismatic structure in recrystallized shell material. In this shell from the Pennsylvanian Boggy shale in Ada, Oklahoma, two distinct shell layers were observerd. An outer, very thin, apparently homogeneous layer covers an inner, thick layer which, from the irregularly polygonal pattern (Pl. 31, fig. 4) on its outer surface immediately under the outer shell layer, appears to have a prismatic structure. The diameters of the individual polygons range from 25-70μ. Nearly complete recrystallization of the thick inner layer obliterated the original structure within that shell layer. Based on a comparison of the polygonal pattern on the surface of the inner shell layer of the fossil with the topographic expression (Pl. 31, fig. 3) of prisms on the inner growth surface of the prismatic layer of the Recent *Turbo (Lunatica) marmoratus* Linnaeus, it would seem logical to conclude that the inner shell layer in *Bellerophon* had an original prismatic structure. Knowing, however, that the corresponding inner layer of *B. (Pharkidonotus) percarinatus* (a species closely related morphologically to *B. (Bellerophon)* sp.) has a complex crossed-lamellar structure, it is more likely that the layer, called prismatic in the shell of *B. (B.)* sp., is actually complex crossed-lamellar. The pattern on the surface of the layer would, therefore, merely reflect the presence of major prisms of the complex crossed-lamellar structure. The only way this conclusion can be verified is to examine a shell of this species which is at least partially unrecrystallized.

Newell (1938, Pl. 20, fig. 13c) figured a regularly polygonal pattern near the weathered outer surface of the shell of a pectinoid pelecypod. Based on this view alone it would be difficult to determine whether this pattern reflected the presence of simple prisms of the prismatic structure or major prisms of the complex crossed-lamellar structure. The horizontal and vertical thin sections, which Newell (1938, Pl. 1) shows of the outer shell layer of fossil pectinoids, adequately demonstrate that the layer in question is truly prismatic. The main criterion used to recognize the prismatic structure is the extremely regular shape of the polygonal prisms seen in horizontal section.

This is the first recorded occurrence of the complex crossed-lamellar structure in the suborder Bellerophontina. It is also the earliest recorded occurrence of that structure in the gastropods. Previously, Bøggild (1930, p. 304) alluded to the existence of the complex crossed-lamellar structure in shells of early Tertiary neritids.

Systematic Position of *EUPHEMITES* and *BELLEROPHON*

In the currently accepted classification (Knight *et al.*, 1960) of the bellerophontoids, *Euphemites* and *Bellerophon* are referred to different families. The observed differences in shell structure between shells of the two genera support the assignment on these genera to different families.

The occurrence of crossed-lamellar and complex crossed-lamellar structures

in bellerophontoid shells militates against a close phylogenetic relationship between the superfamily Pleurotomarioidea and the suborder Bellerophontina. The general feeling expressed by Knight *et al.* (1960) is that the bellerophontins probably gave rise to the pleurotomarioids. In all pleurotomarioid shells, however, where the shell structure has been observed, an inner nacreous and an outer prismatic layer are present.

In the shells of the eleven genera and subgenera of the superfamily Fissurelloidea examined by MacClintock (1963), the shell structure, except for the outermost layer and myostracal deposits, is entirely crossed-lamellar. It would appear, therefore, that the bellerophontins are more closely related to the fissurelloids than they are to the pleurotomarioids, even though the muscle scars of fissurelloids (MacClintock, 1963, Text-figs. 21-31) differ from bellerophontid scars (Knight, 1947, Pl. 42, figs. 2-5). Perhaps, with further studies, shell structures will be useful in classification and evolutionary studies of bellerophontoid gastropods.

GLOSSARY

Abapertural: Spirally away from aperture, toward apex.

Abapical: Spirally away from apex, toward aperture.

Adapertural: Spirally toward aperture, away from apex.

Adapical: Spirally toward apex, away from aperture.

Adlateral: Toward the lateral area.

Admedial: Toward the median sagittal plane.

Anterior: Relatively near the head end.

Anticline: A geological term applied to strata [sheets of a shell layer] which dip in opposite directions from a common axis (Howell, 1957).

Anterior mantle-attachment scar: Narrow muscle scar, to which mantle is attached, connecting terminal enlargements of pedal-retractor scar (in patelloids). It generates a myostracum which is continuous with and in the same sequential position as the pedal-retractor myostracum.

Apparent dip angle: The angle between growth surfaces and second-order lamellae as exposed in any section not at right angles to the strike of the second-order lamellae.

Blade: See *foliated structure.*

Coinductura: Term proposed by Moore (1941, p. 140) for the shell layer, in shells of some species of *Euphemites,* deposited as a callus on the inner lip of the aperture. This layer overlies the inductura and is distinguished as a separate layer by its more steeply inclined growth surfaces. The coinductura does not extend as far adaperturally as the inductura.

Complex crossed-foliated structure: Similar to complex crossed-lamellar structure but having conical second-order lamellae with a very low dip angle to growth surfaces.

Complex crossed-lamellar layer: Shell layer having complex crossed-lamellar structure.

Complex crossed-lamellar structure: An arrangement of major prisms, resembling a cone-in-cone structure (see *cone-in-cone*), in which each prism is composed of conical second-order lamellae which in turn are made of radiating third-order lamellae.

Complex crossed structures: Term describing complex crossed-lamellar and complex crossed-foliated structures.

Complex-prismatic layer: Shell layer having complex-prismatic structure.

Complex-prismatic structure: An arrangement of regularly or irregularly shaped first-order prisms which contain aggregates of fibrils (second-order prisms).

Concentric: Oriented parallel to the shell margin (in patelloids).

Concentric crossed-lamellar (or crossed-foliated) layer: Crossed-lamellar layer in which first-order lamellae are arranged concentrically with respect to the margin of cap-shaped shells.

Conchioline: Organic (proteinaceous) matrix separating unit crystals of the molluscan shell.

Cone-in-cone structure: A geological term meaning a concretionary structure characterized by the development of a succession of cones one within another (Howell, 1957).

Conical second-order lamella: See *complex crossed-lamellar structure.*

Constriction: Narrowed parts of pedal-retractor scar (in patelloids) where paired projections (one on each side of the scar) constrict the scar into about 16 sausage-shaped segments.

Crossed-foliated layer: Shell layer having crossed-foliated structure.

Crossed-foliated structure: Like crossed-lamellar structure only with wider first-order lamellae and lower dip angle of second-order lamellae (3°-27°).

Crossed-lamellar layer: Shell layer having crossed-lamellar structure.

Crossed-lamellar structure: An arrangement of first-order lamellae (length and width axes parallel to, and height axes normal to, the shell surface) which are composed of second-order lamellae (intermediate axes parallel to the width axes of first-order lamellae) which, in alternate first-order lamellae, dip in opposite directions. Dip angle ranges from 16°-44°. Second-order lamellae are composed of third-order lamellae.

Crossed nicols: Two calcite prisms, of a petrographic microscope, placed so that their polarization planes are at right angles to each other. Anisotropic minerals inserted between the prisms show interference colors.

Crossed structures: Term describing crossed-lamellar and crossed-foliated structures.

Dependently prismatic structure: Prismatic shell layers having their minor and major structural elements structurally and/or optically dependent on the overlying shell layer.

Dip: In the geological sense, it is the angle between two intersecting planes one of which is horizontal. Here it is modified to mean the intersection angle between sheets of crystals, such as folia or second-order lamellae, and other surfaces (growth surfaces unless specified otherwise). Measured normal to strike. See *strike.*

Fibrillar layer: Shell layer having fibrillar structure.

Fibrillar structure: A parallel arrangement of thin (1-2μ) fibril-like crystals which have a reclination angle from 48°-53°.

First-order lamellae: See *crossed-lamellar* and *crossed-foliated structure.*

First-order prism: A prism-shaped element of the complex-prismatic structure made up of many smaller crystals (fibrils or second-order prisms).

Folia: See *foliated structure.*

Foilated layer: Shell layer having foliated structure.

Foliated structure: An arrangement of thin folia or sheets of calcite which intersect growth surfaces at a low angle (4°-7°). Each folium is composed of elongate blades normal to the outcrop pattern of folia.

Foliated structures: Term describing foliated and irregularly tabulate foliated structure.

Growth layer: Layer of shell material bounded by growth surfaces.

Growth line: A line formed by the intersection of a growth surface with another surface, such as a thin section or the outer surface of the shell.

Growth surface: Either the present depositional surface of a shell or a surface within the shell defining the position of an earlier depositional surface.

Height axis of first-order lamella: See *crossed-lamellar structure.*

Inclined: Intersecting a growth surface in such a way that the resultant acute angle dorsal to the growth surface opens abapically.

Inductura: Term proposed by Knight (1931, p. 180) for the shell layer, in gastropods, that covers the parietal wall in the region of the inner lip of the aperture. In bellerophontoids this layer extends adaperturally halfway around the outer surface of the shell from the inner lip of the aperture. Overlain by the coinductura and underlain by the perinductura in shells of *Euphemites.*

Inner layers: Shell layers (in patelloids) ventral to pedal-retractor myostracum.

Interference colors: Colors produced in an anisotropic crystal, between crossed nicols of a petrographic microscope, by the wavelength-dependent shifts in the polarization axis caused by paths of light going through that crystal with different velocities.

Irregularly foliated layer: Shell layer having irregularly foliated structure.

Irregularly foliated structure: Like foliated structure but with folia sequences occurring in irregularly arranged patches with different strike and dip of folia in adjacent patches.

Irregularly tabulate foliated layer: Shell layer having irregularly tabulate foliated structure.

Irregularly tabulate foliated structure: Like foliated structure but with unit crystals having the shape of irregularly margined tabulae.

Layer: See *shell layer.*

Left: See *right.*

Length axis of first-order lamella: See *crossed-lamellar structure.*

M: Myostracum

M + 1, m − 1, etc.: Notation system used to designate position of shell layer with respect to the myostracum (m) in patelloids. M + 1, for example, denotes the first layer dorsal to the myostracum.

Major prism: See *complex crossed-lamellar structure.*

Muscle scar: Area on the shell where muscle fibers are attached.

Myostracum: Shell layer, having complex-prismatic structure, deposited by the mantle where muscle fibers are attached to the shell.

Nacreous layer: Shell layer having nacreous structure. "Mother of pearl."

Nacreous structure: An arrangement of polygonal, aragonite crystals in thin (1μ) sheets parallel to growth surfaces.

Outer layers: Shell layers (in patelloids) dorsal to pedal-retractor myostracum.

Pedal-retractor scar: Muscle scar to which pedal-retractor muscles are attached. Generates pedal-retractor myostracum.

Perinductura: Term proposed by Moore (1941, p. 136) for the shell layer, in all shells of *Euphemites,* deposited on the outside of the shell by a part of the mantle folded back over the outer lip of the aperture. The layer is continuous adapically from outer apertural lip. One half a volution back it passes under the inductura.

Prismatic structures: Term describing fibrillar, simple-prismatic, complex-prismatic and dependently prismatic structures.

Pseudolayer: Part of the ventralmost crossed-lamellar shell layer (in some patelloids) in which first-order lamellae are so arranged that, in median sagittal section of the shell, they appear to form one of a distinct sequence of two or more shell layers. The contact between pseudolayers involves a twist of the structural elements.

Radial: Oriented normal to the shell margin (in patelloids).

Radial crossed-lamellar (or crossed-foliated) layer: Crossed-lamellar layer in which first-order lamellae are arranged radially with respect to the apex and margin in patelloid shells.

Reclined: Intersecting a growth surface in such a way that the resultant acute angle dorsal to the growth surface opens adapically.

Right: Right and left orientation, unless specified otherwise, is determined by viewing the shell dorsally.

Second-order lamellae: See *crossed-lamellar structure.*

Second-order prism: See *complex-prismatic structure.*

Selenizone: "Spiral band of concentric growth lines . . . generated by a narrow notch or [sinus in apertural margin]" (Cox, 1960, p. 133).

Shell layer: A bed of shell material, exhibiting a single shell structure or alternation of

structures (in alternating sublayers), which crops out on the ventral surface of the shell. Contacts between shell layers intersect growth surfaces at an angle.

Shell structure: The architectural arrangement of major and minor crystalline elements in the shell. In the broad sense, also includes the arrangement of layers within the shell.

Shell sublayer: One of an alternating sequence of shell-layer subdivisions. Each set of sublayers exhibits a shell structure different from the other set. Contacts between sublayers are parallel to growth surfaces. The dorsolateral margin of a sublayer, if it reaches the dorsal surface of the shell layer containing it, is truncated by the overlying shell layer.

Simple-prismatic layer: Shell layer having simple-prismatic structure.

Simple-prismatic structure: An arrangement of large blade-shaped prisms which have their long axes oriented radially and their intermediate axes normal to growth surfaces.

Sinus: Curved re-entrant (in bellerophontoids) of apertural margin along median sagittal plane. Generates a selenizone on outer surface of shell.

Slope angle: The angle, in patelloid shells, between the apertural plane and the shell wall.

Strike: In the geological sense, it is the line formed by the intersection of two planes one of which is horizontal. Here it is modified to mean the line formed by the intersection of any two planes: e.g. the line formed by intersection of a growth surface with any other surface, or the line formed by the intersection of second-order lamellae with a thin section. See *dip.*

Sublayer: See *shell sublayer.*

Syncline: A geological term meaning a fold in rocks in which the strata [sheets of a shell layer] dip inward from both sides toward a common axis (Howell, 1957).

Terminal enlargement of pedal-retractor scar: In patelloids, one of the pair of inflated areas in the anterior end of each branch of the horseshoe-shaped pedal-retractor scar. For insertion of neck and additional foot muscle.

Third-order lamellae: Tiny elongate crystals which make up second-order lamellae of the crossed-lamellar and crossed-foliated structures and the conical second-order lamellae of the complex crossed-lamellar and complex crossed-foliated structures.

True dip angle: See *dip.*

Tubules: Tiny, regularly arranged holes originating at the inner surface of the molluscan shell.

Twist zone: A zone forming the contact between two shell layers (or pseudolayers) in which the major and minor structural elements are apparently twisted from the orientation in the overlying layer to the orientation in the underlying layer.

Width axis of first-order lamella: See *crossed-lamellar structure.*

MATERIALS AND METHODS

The structure of the shell was studied by one or more of the following methods:

(1) Gross examination of the structure of all shells was made with a binocular microscope (9-150 power). The structure of some layers is visible on the inner surface of the shell where the shell layers crop out (Text-fig. 40). In other instances it was necessary to examine freshly broken or weathered surfaces.

(a) Freshly broken surfaces were occasionally obtained by a rapid alternation of heating the shell directly in the flame of a Bunsen burner and then plunging it into ice-cold water. The heat baked the conchioline matrix of the shell and induced fractures to form around structural elements. When the shell was broken, structural elements were easily recognized.

(b) A simple reflection goniometer (Text-fig. 128) was used to measure the dip angle (Table 1) of second-order lamellae in layers with crossed-foliated and

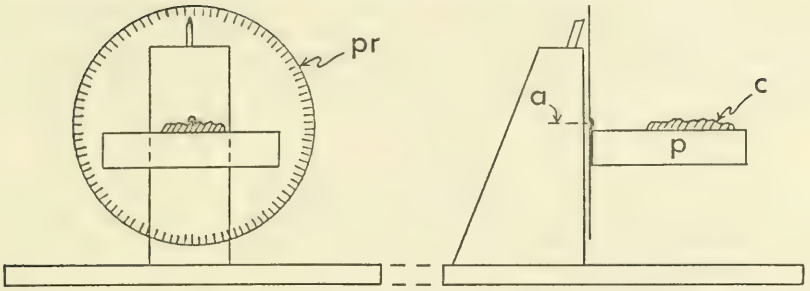

Text-fig. 128.—Reflection goniometer. Explanation of symbols: a, axis of rotation of platform; c, clay; p, platform; pr, protractor.

crossed-lamellar structure. To measure the dip angle the shell layer was either broken or lightly scratched normal to the length axes of first-order lamellae. This exposed the dip slopes of second-order lamellae. The shell was then rigidly mounted in clay on the platform of the reflection goniometer in such a way that the break or scratch was in the axis of rotation of the platform. The goniometer was then placed under a binocular microscope and the shell was illuminated with a strong, concentrated light. By rotating the platform three reflecting surfaces could be seen; the inner surface of the shell and the two sets of oppositely dipping second-order lamellae exposed in the break or scratch. The angular difference between the inner shell surface and each set of second-order lamellae is the dip angle of the second-order lamellae. The angle must be measured with reflections from second-order lamellae which are exposed to air. On the inner surface of unscratched shells reflections from second-order lamellae can be observed, but because of refraction the apparent dip angle so measured is about twice its real size.

(2) The structure of some shell layers was examined in isolated fragments.
   (a) Some fragments were crushed and mounted directly in HSR (Harleco Synthetic Resin) on a glass slide and covered with a cover glass.
   (b) Some fragments were soaked in a hot 5.25% solution of sodium hypochlorite (Clorox) to dissolve or weaken the conchioline matrix, crushed, and mounted in HSR. With the organic matrix weakened the individual carbonate crystals are often isolated after crushing.

(3) In fossil shells, where recrystallization has occasionally made thin-section study useless, polished sections were made by grinding the shell with 1000 grit corundum powder in water and then on a frosted glass plate in water without the grit. The sections were then mounted in HSR and protected with a cover glass. If recrystallization had not completely destroyed the structure these polished sections were studied using either a binocular or a petrographic microscope with concentrated light shining directly on and at a low angle to the polished surface.

(4) Thirty thin sections were made. Because of the difficulties encountered in preparing sections thin enough to see structural elements clearly, the following detailed outline of the procedure for preparing these sections is given.
   (a) Shells over 1.5 cm in diameter were cut on a four-inch diamond saw about three to five mm from the desired plane of section. Then the shells were ground to the plane of section using progressively finer grits (generally 320, 600 and 1000 grit corundum powder). If the shell was small or the structural elements split apart easily, the grinding started with 600 grit. The section was then polished in water on the 1000 grit plate without any grit. Shells under 1.5 cm in diameter were ground directly, not cut with the saw.
   (b) The shell was then soaked in hot Clorox 10-15 minutes to remove the organic

film from the polished surface and from the adjacent dorsal and ventral surfaces of the shell.

(c) The shell was washed, lightly etched in 0.5 per cent HCl for 10-15 seconds, washed again and allowed to dry.

(d) The glass slides, on which the shells were to be mounted, were frosted on the 1000 grit plate. Steps b, c, and d increased the adhesive power of the Lakeside cement to the shell and the glass.

(e) The four edges of the glass slide were beveled (45°) with 320 grit. This prevented small glass shards from chipping off during the final grinding stages when the edges of the glass slide were likely to come in contact with the grinding plate.

(f) The shell was put three inches from a desk lamp to drive off moisture and air and raise the temperature of the shell to reduce cracking which occurs during immersion of the shell in hot Lakeside cement.

(g) Lakeside cement, placed on a frosted slide, was heated on a hot-plate to 270°F. After the Lakeside melted, bubbles formed and quickly disappeared. The warmed shell was then placed in the Lakeside for about a minute, allowing the Lakeside to filter into pores and fractures in the shell. At the same time bubbles formed continuously between the polished surface of the shell and the glass slide. While these bubbles were still forming, the slide was quickly removed from the hot-plate and placed on a room-temperature desk surface. During the ten seconds while the Lakeside was cooling and beginning to solidify, constant vertical pressure was applied to the shell. At the same time the shell was moved back and forth on the slide thus squeezing out most of the bubbles. If bubbles still remained in areas of critical structural importance, the heating process was repeated.

(h) After the Lakeside cooled, the larger shells (about four cm) were sawed about five mm from the slide. For smaller shells the sawing process was omitted. The shells were then ground to between 30 and 50μ thick using 1000 grit powder in the final stages.

(i) To see the major structural elements clearly the section had to be between ten and 20μ. This thickness was obtained by grinding in water on the 600 grit plate with the grit removed.

(j) If the shell was not perfectly mounted on the slide, one end of the section was likely to be thicker than the other. In order to grind just the thick part of the section, a glass slide (frosted with 600 grit) was used for selective grinding.

(k) To see the minor structural elements (most of which are 1-2μ in their shortest dimension) the thickness of the section had to be between three and ten μ. Two methods were used to obtain this thickness. Either the frosted glass slide was used or 5 per cent HCl was applied to the section with a brush under a binocular microscope. Critical areas on the slide were made thinner either by selective grinding or selective application of acid. Some adjacent shell layers eroded differentially in acid. To properly expose the contact between two such layers more acid was applied to the more resistant layer than to the less resistant layer. By using a petrogaphic microscope the thickness of these very thin sections was measured by determining the interference color (Rogers and Kerr, 1942, plate facing p. 163) of the first- or second-order spectrum. The exact thickness of a section is often critical for seeing the structural elements clearly. For example, in the foliated layer (Pl. 24, figs. 1, 2), the brick-wall appearance of the component blades is exhibited in only those parts of the section where the thickness is such as to produce first-order orange. In both thicker and thinner parts of the section, the structure is not readily seen.

(l) The sections were then covered with HSR and a cover glass and studied under a petrographic microscope (40, 100, 400, and 970 power).

For each numbered slide, 104 in all, there was a similarly numbered index card on which was recorded the locality number, the specific name, one or more sketches showing

the exact orientation and location of the thin section, uncrushed fragment or polished section, or location of the crushed fragment. If there was more than one numbered slide per specimen, the cards for that specimen were cross-indexed and, if a fragment (or fragments) of the original specimen remained, it was given the number of the first-made slide.

LITERATURE CITED

Barker, R. M., 1964. Microtextural variation in pelecypod shells: Malacologia, v. 2, p. 69-86, 4 figs.

Bathurst, R. G. C., 1964. The replacement of aragonite by calcite in the molluscan shell wall: *in* John Imbrie and N. D. Newell, eds., Approaches to paleoecology, p. 357-376, 4 pls., 1 text-fig.

Biedermann, W., 1902. Untersuchungen über Bau und Entstehung der Molluskenschalen: Jenaische Zeitschr. Naturw., Bd. 36, p. 1-164, pl. 1-6.

———, 1914. Physiologie der Stütz- und Skelettsubstanze; pt. 6, Die Schalen und Gehäuse der Mollusken: *in* Hans Winterstein, ed., Handbuch der vergleichenden Physiologie, Bd. 3, Hälfte 1, Teil 1, p. 656-803, text-figs. 142-190.

Bøggild, O. B., 1930. The shell structure of the mollusks: D. Kgl. Danske Vidensk. Selsk. Skr., naturvidensk. og mathem., Afd., 9. Raekke, II, 2, p. 231-326, pl. 1-15.

Bryan, W. H., 1941. Spherulites and allied structures, pt. 1: Royal Soc. Queensland Proc., v. 52, no. 6, p. 41-53, pl. 3-5, 10 text-figs.

Bryan, W. H., and Hill, Dorothy, 1941. Spherulitic crystallization as a mechanism of skeletal growth in hexacorals: Royal Soc. Queensland Proc., v. 52, no. 9, p. 78-91, 2 text-figs.

Carpenter, William, 1848. Report on the microscopic structure of shells, pt. 2: British Assoc. Adv. Sci., Rept. 17th Mtg. [for 1847], p. 93-134, pl. 1-20.

Carriker, M. R., Scott, D. B., and Martin, G. N. Jr., 1963. Demineralization mechanism of boring gastropods: *in* R. F. Sognnaes, ed., Mechanisms of hard tissue destruction, Am. Assoc. Adv. Sci. Pub. 75, p. 55-89, 49 figs.

Caster, K. E., 1934. The stratigraphy and paleontology of northwestern Pennsylvania, pt. 1; stratigraphy: Am. Paleontology Bulls., v. 21, no. 71, 185 p., 12 text-figs.

Cox, L. R., 1960. General characteristics of Gastropoda: *in* R. C. Moore, ed., Treatise on invertebrate paleontology, pt. I, Mollusca 1, p. 84-169, (Geol. Soc. America and Univ. Kansas Press).

Dall, W. H., 1871. On the limpets; with special reference to the species of the west coast of America, and to a more natural classification of the group: Am. Jour. Conchology, v. 6, pt. 3, p. 227-282, pl. 14-17.

———, 1872. Descriptions of new species of mollusks from the northwest coast of America: California Acad. Sci. Proc., v. 4, p. 270-271, 1 pl.

Dodd, J. R., 1964. Environmentally controlled variation in the shell structure of a pelecypod species: Jour. Paleontology, v. 38, p. 1065-1071, pl. 160, 6 text-figs.

Durham, J. W., 1950. 1940 E. W. Scripps cruise to the Gulf of California; Part 2, Megascopic paleontology and marine stratigraphy: Geol. Soc. America Mem. 43, 216 p., 48 pls.

Fisher, W. K., 1904. The anatomy of *Lottia gigantea* Gray: Zool. Jahrb. Abt. Anat. und Ont. der Thiere, v. 20, p. 1-66

Flössner, W., 1914. Zur Kenntnis der Schalenstrucktur von *Helix pomatia:* Zool. Anz., Bd. 43, p. 463-468, 3 text-figs.

Grégoire, Charles, 1962. On the submicroscopic structure of the *Nautilus* shell: Koninkl. Belgisch Instit. voor Natuurwet., Meded., Deel 38, no. 49, Brussel, 71 p., 24 pls., 8 text-figs.

Hedgpeth, J. W., 1957. Marine biogeography: chap. 13 *of* Treatise on marine ecology and paleoecology: Geol. Soc. America Mem. 67, v. 1, p. 359-382, 1 pl., 16 text-figs.

Horný, Radvan, 1963. Lower Paleozoic Monoplacophora and patellid Gastropoda (Mol-

lusca) of Bohemia: Sborník Ústred. Ústavu Geologick., svazek 28, 1961, oddíl paleont., p. 7-83, 18 pls., 19 text-figs.

Howell, J. V., 1957. Glossary of geology and related sciences: Am. Geol. Inst. [Washington, D. C.], N.A.S.-N.R.C. pub. 501., 325 p.

Kato, Makoto, 1963. Fine skeletal structures in Rugosa: Hokkaido Univ., Fac. Sci. Jour., ser. 4, Geology and Mineralogy, v. 11, p. 571-630, 3 pls., 19 text-figs.

Keen, A. M., 1960. *In* J. B. Knight and others, Systematic descriptions [Archaeogastropoda]; *in* R. C. Moore, ed., Treatise on invertebrate paleontology, pt. I, Mollusca 1, p. 169-310 (Geol. Soc. America and Univ. Kansas Press).

Kessel, Erwin, 1936. Über Abwandlungen der typischen Gastropodenschalenstruktur (Beiträge zum Strukturproblem der Gastropodenschale II): Zeitschr. Morph. Ökol. Tiere, Bd. 30, p. 774-785, 11 text-figs.

———, 1950. Zum Strukturproblem der Molluskenschale: Zool. Anz., Bd. 145, Neue Erganzungeb. u. Probl. d. Zool. (Klatt-Festschrift), p. 373-379.

Knight, J. B., 1931. The gastropods of the St. Louis, Missouri, Pennsylvanian outlier; the Subulitidae: Jour. Paleontology, v. 5, p. 177-229, pl. 21-27.

———, 1947. Bellerophont muscle scars: Jour. Paleontology, v. 21, p. 264-267, pl. 42.

Knight, J. B., and others, 1960. Systematic descriptions [Archaeogastropoda], *in* R. C. Moore, ed., Treatise on invertebrate paleontology pt. I, Mollusca 1, p. 169-310 (Geol. Soc. America and Univ. Kansas Press).

Kobayashi, Iwao, 1964a. Microscopical observations on the shell structure of Bivalvia; pt. 1, *Barbatia obtusoides* (Nyst): Tokyo Kyoiku Daigaku, Sci. Repts., sec. C, Geology, Mineralogy and Geography, v. 8, no. 82, p. 295-301, 3 pls., 4 text-figs.

———, 1964b. Introduction to the shell structure of bivalvian molluscs: Earth Sci. v. 73, p. 1-12, 1 pl., 24 text-figs. [in Japanese with English abstract]

Koch, H. J., 1949. A review of the South African representatives of the genus *Patella* Linnaeus: Natal Mus. Ann., v. 11, pt. 3, p. 487-517, pl. 17-23, 22 text-figs.

Lemche, Henning, and Wingstrand, K. G., 1959. The anatomy of *Neopilina galathaea* Lemche, 1957, (Mollusca, Tryblidiacea): Galathea Rept., v. 3, p. 9-72, 56 pls., 1 text-fig.

Lhoste, L. J., 1946. Les microstructures des patelles: Jour. Conchyl., ser. 4, t. 41, v. 87, p. 28-29, 3 text-figs.

MacClintock, Copeland, 1963. Reclassification of gastropod *Proscutum* Fischer based on muscle scars and shell structure: Jour. Paleontology, v. 37, p. 141-156, pl. 20, 31 text-figs.

Mackay, I. H., 1952. The shell structure of the modern mollusks: Colorado School Mines Quart., v. 47, no. 2, p. 1-27

Moore, R. C., 1941. Upper Pennsylvanian gastropods from Kansas: Kansas State Geol. Survey Bull., v. 38, pt. 4, p. 121-164, 3 pls., 7 text-figs.

Nathusius-Königsborn, W. von, 1877. Untersuchungen über nicht-celluläre Organismen, namentlich Crustaceen-Panzer, Mollusken-Schalen und Eihüllen: Berlin, 144 p., 16 pls. [*fide* Zoological Record for 1877]

Newell, N. D., 1938. Late Paleozoic pelecypods; Pectinacea: Kansas Geol. Survey [Report], v. 10, pt. 1, 123 p., 20 pls., 42 text-figs.

———, 1942. Late Paleozoic pelecypods; Mytilacea: Kansas Geol. Survey [Report], v. 10, pt. 2, 80 p., 15 pls., 22 text-figs.

Oberling, J. J., 1955. Shell structure of West American Pelecypoda: Washington Acad. Sci. Jour., v. 45, no. 4, p. 128-130, 2 text-figs.

———, 1964. Observations on some structural features of the pelecypod shell: Mitteilungen der Naturforschenden Gesellschaft in Bern, Neue Folge, Bd. 20, p. 1-63, 6 pls., 3 text-figs.

Ōmori, Masae, and Kobayashi, Iwao, 1963. On the micro-canal structures found in the shell of *Arca navicularis* Bruguière and *Spondylus barbatus* Reeve: Venus, Japanese Jour. Malacology, v. 22, p. 274-280, pl. 19-20.

Ōmori, Masae, Kobayashi, Iwao, and Shibata, Matsutaro, 1962. Preliminary report on the shell structure of *Glycymeris vestita* (Dunker) with special reference to the newly

found structural patterns like to "punctum" in the shell of the Brachiopoda: Tokyo Kyoiku Daigaku, Sci. Repts., sec. C, Geology, Mineralogy and Geography, v. 8, no. 77, p. 197-202, 3 pls.

Pilsbry, H. A., 1891. Monographs of the Acmaeidae, Lepetidae, Patellidae and Titiscaniidae: v. 13 *of* Tryon, G. W. and Pilsbry, H. A., Manual of Conchology, ser. 1, 195 p., 74 pls.

Rogers, A. F., and Kerr, P. F., 1942. Optical mineralogy, 2nd ed.: New York and London, McGraw-Hill, 390 p.

Rose, Gustav, 1859. Über die heteromorphen Zustände der kohlensauren Kalkerde; II, Vorkommen des Aragonits und Kalkspaths in der organischen Natur: Physikalische Abhandlungen der Königlichen Akademie der Wissenschaften zu Berlin aus dem Jahre 1858 [Kgl. Akad. Wiss. zu Berlin, Phys. Abh. (1858)], p. 63-111, 3 pls.

Schmidt, W. J., 1924. Die Bausteine des Tierkörpers in polarisiertem Licht: Bonn, Friedrich Cohen, 528 p., 230 text-figs.

———, 1959. Bemerkungen zur Schalenstruktur von *Neopilina galatheae:* Galathea Rept., v. 3, p. 73-77, 2 pls.

Schuster, M. E., 1913. Anatomie von *Helcioniscus ardosiaeus* H. et J. sive *Patella clathratula* Reeve: Zool. Jahrb., suppl. 13 (Fauna Chilensis, Bd. 4), p. 281-384, pl. 19, 87 text-figs.

Stehli, F. G., 1956. Shell mineralogy in Paleozoic invertebrates: Science, v. 123, no. 3206, p. 1031-1032.

Stoll, N. R. (editorial chairman), 1961. International code of zoological nomenclature adopted by the XVth International Congress of Zoology: Internat. Trust for Zool. Nomencl., London, 176 p.

Test, A. R. (Grant), 1946. Speciation in limpets of the genus *Acmaea:* Univ. Michigan, Lab of Vertebrate Biology, Contr. no. 31, 24 p.

Thiem, Hugo, 1917a. Beiträge zur Anatomie und Phylogenie der Docoglossen; I, zur Anatomie von *Helcioniscus ardosiaeus* Hombron et Jacquinot unter Bezugnahme auf die Bearbeitung von Erich Schuster in den Zoolog. Jahrb., Supplement XIII, Bd. IV, 1913: Janaische Zeitschr. Naturw., Bd. 54, p. 333-404, pl. 23, 41 text-figs.

———, 1917b. Beiträge zur Anatomie und Phylogenie der Docoglossen; II, Die Anatomie und Phylogenie der Monobranchen (Akmäiden und Scurriiden nach der Sammlung Plates): Jenaische Zeitschr. Naturw., Bd. 54, p. 405-630, pl. 24-26, 128 text-figs.

Wada, Kōji, 1961. Crystal growth of molluscan shells: Natl. Pearl Research Lab. Bull., no. 7, p. 703-828, 149 plate-figs.

———, 1963a. On the spiral growth of the inner surface of the calcitic shell, *Anomia lischkei*—I: Japanese Soc. Sci. Fisheries Bull., v. 29, p. 320-324, 3 figs.

———, 1963b. On the spiral growth of the inner surface of the calcitic shell, *Ostrea gigas*—II: Japanese Soc. Sci. Fisheries Bull., v. 29, p. 447-451, 4 figs.

Wainwright, S. A., 1964. Studies of the mineral phase of coral skeleton: Experimental Cell Research, v. 34, p. 213-230, 13 text-figs.

Watabe, Norimitsu, Sharp, D. G., and Wilbur, K. M., 1958. Studies on shell formation, pt. 8, Electron microscopy of crystal growth of the nacreous layer of the oyster *Crassostrea virginica:* Jour. Biophys. and Biochem. Cytology, v. 4, p. 281-286, pl. 152-156.

Watabe, Norimitsu, and Wilbur, K. M., 1961. Studies on shell formation, pt. 9, An electron microscope study of crystal layer formation in the oyster: Jour. Biophys. and Biochem. Cytology, v. 9, p. 761-771, 18 figs.

Waterhouse, J. B., 1963. Permian gastropods of New Zealand; Part 1, Bellerophontacea and Euomphalacea: New Zealand Jour. Geology and Geophysics, v. 6, no. 1, p. 88-112, 37 figs.

Weller, J. M., 1930. A new species of *Euphemus:* Jour. Paleontology, v. 4, p. 14-21, pl. 2, 1 text-fig.

Wenz, Wilhelm, 1938. Gastropoda, Allgemeiner Teil und Prosobranchia: *in* O. H. Schindewolf, ed., Handbuch der Paläozoologie, Bd. 6, Teil 1, p. 1-240 (Berlin).

Wilbur, K. M., 1960. Shell structure and mineralization in molluscs: *in* R. F. Sognnaes,

ed., Calcification in biological systems, Am. Assoc. Adv. Sci. Pub. 64, p. 15-40, 12 figs.

———, 1964. Shell formation and regeneration: *in* K. M. Wilbur and C. M. Yonge, eds., Physiology of Mollusca, v. 1, chap. 8, p. 243-282, 14 figs.

Willcox, M. A., 1898. Zur Anatomie von *Acmaea fragilis* Chemnitz: Jenaische Zeitschr. Naturw., Bd. 32, p. 411-456.

Yochelson, E. L., 1960. Permian Gastropoda of the southwestern United States; Part 3, Bellerophontacea and Patellacea: Am. Mus. Nat. Hist. Bull., v. 119, art. 4, p. 211-293, pl. 46-57.

Yonge, C. M., 1947. The pallial organs in the aspidobranch Gastropoda and their evolution throughout the Mollusca: Royal Soc. London, Philos. Trans., ser. B, Biol. Sci., no. 591, v. 232, p. 443-518, 49 figs.

———, 1960. Mantle cavity, habits, and habitat in the blind limpet, *Lepeta concentrica* Middendorff: California Acad. Sci. Proc., ser. 4, v. 31, p. 103-110, 2 figs.

STRUCTURE DE LA COQUILLE DES GASTÉROPODES PATÉLLOÏDES ET BELLEROPHONTOÏDES (MOLLUSCA)

par COPELAND MACCLINTOCK

RÉSUMÉ

La classification supragénérique des archéogastéropodes patélloïdes récents, communément acceptée, est basée largement sur la morphologie de la radula et des branchies, tandis que la coquille est considérée peu importante. Étant donné que les variations de la forme conique des coquilles se répètent dans chacun des groupes taxonomiques principaux, une évaluation exacte et systématique des fossiles patélloïdes est extrêmement difficile. Les phylogénies existantes sont basées essentiellement sur les relations des parties molles parmi les formes vivantes. Cette étude contient des descriptions et des analyses détaillées des microstructures et des relations des couches de la coquille dans les gastéropodes récents et fossiles des superfamilles primitives Patelloïdea et Bellerophontoïdea.

Parmi tous les groupes de mollusques de dimensions taxonomiques comparables, les patélloïdes sont ceux qui possèdent les structures les plus diverses et complexes de la coquille, quoi que celle-ci soit la forme la plus simple (conique basse). L'on a examiné des coquilles de 121 espèces patélloïdes provenant de toutes les parties du monde. Dans ce travail nous avons identifié quatre types fondamentaux de structures des coquilles patélloïdes, soit: (1) *Prismatique* [prismatic]—cristaux majeurs et mineurs formant un angle plus grand que 10 degrés par rapport aux surfaces d'accroissement; (2) *Feuilleté* [foliated]—feuillets fins de carbonate de calcium intersectant les surfaces d'accroissement avec un angle inférieur à 10 degrés; (3) *Entrecroisé* [crossed]—structure lamellaire entrecroisée de Bøggild et entrecroisée-feuilletée, définie ici comme étant semblable à la structure lamellaire entrecroisée mais ayant les lamelles du second ordre avec un angle d'inclinaison plus bas et les lamelles du premier ordre plus larges; (4) *Entrecroisé complexe* [complex crossed]—structure lamellaire entrecroisée complexe de Bøggild et entrecroisée-feuilletée, ci-après définie comme étant semblable à la structure lamellaire entrecroisée complexe mais ayant un angle d'inclinaison des lamelles coniques du second ordre bien bas.

Chaque coquille patélloïde est composée de 4 à 6 couches, selon son espèce. Les couches de la coquille deviennent plus épaisses avec la croissance et intersèquent les couches d'accroissement. Chaque couche de la coquille est caractérisée soit par une structure différente des couches contigües, soit—lorsque cette structure est la même—par des majeurs éléments structuraux correspondants bâtis en angles droits les uns vis-à-vis des autres. Les variations de ces structures ainsi que les différentes combinaisons successives des couches par rapport au myostracum (couche des impréssions musculaires) sont à la base de l'identification, d'une façon non formelle du point de vue de la taxinomie, de 17 groupes de structures de coquilles. La plupart des groupes se conforment aux limites taxonomiques préalablement acceptées, bien que quelques uns ne s'y conforment pas. Généralement, les coquilles des deux majeures familles patélloïdes (Acmaeidae et Patellidae) peuvent se reconnaître par la présence de certaines structures diagnostiques de la coquille: les acmaeïdes ont une couche de structure fibrillaire (une variété de la structure prismatique) dans les couches successives entre le myostracum et la surface dorsale de la coquille; tandis que les patélloïdes ont des couches feuillitées ou entrecroisées-feuilletées dans le séquence dorsale jusqu'au myostracum. Puisque cette étude systématique de la structure de la coquille patélloïde a pourvu les informations nécessaires pour établir les relations existantes entre fossiles et formes récentes, il semble probable qu'une phylogénie plus exacte du groupe puisse être développée, étant donné les coquilles suffisamment bien préservées à travers toute l'histoire fossile des patélloïdes de la période post-Ordovicienne.

On a autrefois décrit plusieurs espèces de gastéropodes bellerophontoïdes du Paléozoïque comme ayant des coquilles à structure nacrée, feuilletée et prismatique. Dans cette étude, la structure lamellaire entrecroisée qui n'avait pas été mentionnée préalablement dans le subordre Bellerophontina a été observée dans la couche interne des coquilles *Bellerophon (Pharkidonotus)*. Ceux-ci sont les plus anciennes occurrences reportées (Pennsylvanian) des structures entrecroisées et entrecroisées complexes dans les Gastropoda. Prises séparément, les structures de ces deux bellerophontoïdes, au lointain degré de parenté, indiquent qu'elles sont bien plus proches des fissurelloïdes (avec couche interne à lamelles croisées, et externe du type prismatique) que des pleurotomarioïdes (avec couche interne nacrée et couche externe prismatique). Si on trouvait à

la suite d'une étude supplémentaire, que les structures des trois espèces examinées peuvent représenter le groupe en entier, il faudrait, à ce moment là, soumettre le subordre Bellerophontina à une reévaluation systématique.

DIE SCHALENSTRUKTUR VON PATELLOIDEN UND BELLEROPHONTOIDEN GASTROPODEN (Mollusca)

VON COPELAND MACCLINTOCK

ZUSAMMENFASSUNG

Die gegenwärtig gültige supragenerische Einteilung von rezenten patelloiden Archäo-gastropoden stützt sich hauptsächlich auf die Morphologie von Radula und Kiemen, wobei der Schale verhältnismässig wenig Beachtung geschenkt wird. Weil sich Variierungen der einfachen kegelförmigen Schale in jeder der taxonomischen Gruppen wiederholen, ist eine genaue, systematische Beurteilung von fossilen Patelloiden sehr schwierig. Bereits existierende phylogenische Beschreibungen haben sich vor allem auf die Weichteil-Beziehungen zwischen lebenden Formen gestützt. In der vorliegenden Arbeit werden ins einzelne gehende Beschreibungen und Analysen der Mikrostruktur- und Schalenschichten-Beziehungen zwischen rezenten und fossilen Gastropoden der primitiven Überfamilien Patelloidea und Bellerophontoidea gegeben.

Von allen Molluskengruppen von vergleichbarer taxonomischer Grösse haben die Patelloiden die komplexesten und mannigfaltigsten Schalenstrukturen und gleichzeitig die einfachste Schalenform (niederer Kegel). Die Schalen von 121 über die ganze Erde verteilten Spezies der Patelloiden wurden untersucht. Vier Grundtypen von patelloiden Schalenstrukturen wurden hier herausgearbeitet: (1) *prismatisch* [prismatic]—grössere und kleinere Kristalle, angeordnet in einem 10 Grad übersteigenden Winkel zur Wachstums-Oberflächen; (2) *blättrig* [foliated]—dünne Blättchen von Kalziumkarbonat, die die Waschstums-Oberflächen in einem Winkel von unter 10 Grad durchschneiden; (3) *überkreuzt* [crossed]—überkreuzt-lamelliert nach Bøggild [crossed-lamellar of Bøggild] und überkreuzt-blättrig [crossed-foliated], hier als überkreuzt-lamelliert ähnlich definiert, aber mit einem niedrigeren Kreuzungsgrad von Lamellen zweiten Grades und breiteren Lamellen ersten Grades; (4) *komplex überkreuzt* [complex crossed]—komplex überkreuzt-lamelliert nach Bøggild [complex crossed-lamellar of Bøggild] und komplex überkreuzt-blättrig [complex crossed-foliated], der wird hier definiert als komplex überkreuzt-lamelliert ähnlich, aber mit einem viel niedrigeren Neigungsgrad der kegelförmigen Lamellen zweiten Grades.

Die individuellen patelloiden Schalen sind aus zwischen vier bis sechs Schichten zusammengesetzt, wobei die Anzahl der Schichten von der Art abhängt. Die Schalenschichten werden dicker mit dem Wachstum und überschneiden die Wachtums-Schichten. Jede Schalenschicht ist charakterisiert durch entweder eine von den benachbarten Schichten differierende Struktur oder, bei gleichartiger Struktur, durch die rechtwinklige Orientierung der sich entsprechenden wichtigeren strukturellen Elemente. Variierungen dieser Strukturen und verschiedener aufeinanderfolgender Kombinationen von Schichten, mit Hinsicht auf das Myostracum (die Muskel-Eindruck-Schalenschicht), bilden die Grundlage für die Aufstellung von 17 nicht festen taxonomischen Schalenstrukturen-Gruppen. Die meisten dieser Gruppen stimmen überein mit bereits gültigen systematischen Grenzen; einige tun das nicht. Im allgemeinen können die Schalen von den beiden wichtigsten Patelloiden-Familien (Acmaeidae und Patellidae) an dem Vorhandensein gewisser unterscheidender Schalenstrukturen erkannt werden: Acmaeiden haben eine Fibrillenschicht (Variierung der prismatischen Schicht) in der Aufeinanderfolge von Schichten zwischen dem Myostracum und der Rücken-Oberfläche der Schale, wohingegen Patelliden blättrige oder überkreuzt-blättrige Schichten in der Aufeinanderfolge von Schichten rückwärts vom Myostracum haben. Weil die vorliegende systematische Untersuchung von patelloider Schalenstruktur die Information beibringt, die für die Feststellung der Beziehungen zwischen fossilen und rezenten Formen notwendig ist, scheint es nun wahrscheinlich, dass, das genügende Vorhandensein von gut erhaltenen Schalen durch die ganze nach-ordovizische Fossilgeschichte der Patelloiden hindurch vorausgesetzt, jetzt eine genauere phylogenische Beschreibung der Gruppe sich entwickeln kann.

Mehrere Arten von paleozoischen bellerophontoiden Gastropoden sind vorher als perlmuttrige, blättrige und prismatische Schalenstrukturen beschrieben worden. Die vorliegende Untersuchung bringt zum ersten Mal die Beobachtung von überkreuzt-lamelliert Struktur, bis jetzt

noch nie bei der Unterordnung Bellerophontina festgestellt, in den Schalen der *Euphemites*, und die Beobachtung von komplex überkreuzt-lamelliert Struktur in der inneren Schicht der Schalen der *Bellerophon (Pharkidonotus)*. Das sind die frühesten (Pennsylvanian) festgestellten Vorkommen von überkreuzten und komplex überkreuzten Strukturen in Gastropoden. Wenn man sie allein betrachtet, verweisen die Strukturen in diesen beiden entfernt verwandten Bellerophontoiden darauf, dass sie näher verwandt sind den Fissurelloiden (mit inneren überkreuzt-lamellierten und äusseren prismatischen Schichten) als den Pleurotomarioiden (mit inneren perlmuttrigen und äusseren prismatischen Schichten). Wenn bei einer weiteren Untersuchung die Strukturen der drei untersuchten Spezies als für die ganze Gruppe repräsentativ nachgewiesen werden können, dann sollte die Unterordnung Bellerophontina einer systematischen Neu-Beurteilung unterworfen werden.

СТРУКТУРА РАКОВИН У ПАТЕЛЛОИДНЫХ И БЕЛЛЕРОФОНТОИДНЫХ БРЮХОНОГИХ (MOLLUSCA)

Коуплэнд МэкКлинток

Абстракт

Обще-принятая надродовая классификация пателлоидных археобрюхоногих современной эпохи основана главным образом на морфологии радулы и жабр. Сравнительно мало внимания уделяется раковине. Так как вариации простой конусообразной формы раковины повторяются в каждой из главных таксономических групп, то точная систематическая оценка ископаемых пателлоидов очень затрудняется. Существующие филогении основаны главным образом на соотношении мягких частей в живущих видах. В предлагаемой работе приведены детальные описания и анализы микроструктуры раковин, и соотношения между раковинными слоями брюхоногих — как современных, так и ископаемых, принадлежащих к примитивным надсемействам Patelloidea и Bellerophontoidea.

Из всех групп моллюсков, имеющих примерно то же количество таксономических названий, пателлоидам характерно наиболее сложное и разнообразное строение раковины и в то же время наиболее простая форма раковины (низкая конусообразная). Были исследованы раковины 121-го вида пателлоидов со всех частей света. В данной статье выделены четыре основных типа структуры раковин пателлоидов: 1 — *Призматические структуры* [prismatic], в которых крупные и мелкие кристаллы направлены под углом, превышающим 10° по отношению к поверхностям нарастания; 2 — *Листоватые структуры* [foliated], состоящие из тонких листиков углекислого кальция пересекающих поверхности нарастания под углом менее 10-ти градусов; 3 — *Перекрещенные структуры* [crossed] — перекрещенно-пластинчатая структура Бёггильда [crossed-lamellar of Bøggild] и перекрещенно-листоватая структура [crossed-foliated], которая в данной статье определена как схожая с перекрещенно-пластинчатой структурой, но имеющая более низкий угол пересечения пластин второго порядка, и также более широкие пластины первого порядка; 4 — *Сложно-перекрещенные структуры* [complex-crossed] — сложная перекрещенно-пластинчатая структура Бёггильда [complex crossed-lamellar of Bøggild] и сложная перекрещенно-листоватая структура [complex crossed-foliated], причем последняя в данной статье определяется как схожая со сложно перекрещенно-пластинчатой, но со значительно меньшим углом наклона конусообразных пластин второго порядка.

Отдельные раковины пателлоидов состоят из от четырех до шести раковинных слоев, в зависимости от вида. Слои раковины становятся толще при росте и перерезают слои нарастания. Каждый слой раковины охарактеризован или строением, отличающимся от строения смежного слоя, или — в тех случаях когда строение одинаково — слой охарактеризован тем, что главные структуральные элементы направлены под прямым углом к тем же элементам смежного слоя. Вариации этих строений и разные последовательные сочетания слоев по отношению к миостракуму (раковинный слой мускульных отпечатков) легли в основу признания семнадцати таксономически неформальных групп по признаку строения раковины. Большинство из этих групп, но не все, укладываются в ранее признанные таксономические границы. Вообще, раковины двух главных семейств пателлоидов (Acmaeidae и Patellidae) могут быть опо-

знаны по наличию особого строения раковин: акмеиды [acmaeids] имеют волокнистый [fibrillar] (разновидность призматического) слой в последовательности слоев между миостракумом и дорсальной поверхностью раковины, в то время как пателлиды [patellids] имеют листоватые или перекрещенно-листоватые слои в последовательности слоев, дорсальных по отношению к миостракуму. Так как данное систематическое изучение строения раковин пателлоидов снабжает нам сведениями, необходимыми для установления соотношения между формами ископаемыми и современными формами, то представляется вероятным, что удастся составить более точную филогению всей группы, если достаточное количество хорошо сохранившихся раковин пост-ордовикского периода могут быть найдены.

Несколько ранее описанным видам палеозойских беллерофонтоидных брюхоногих приписывались перламутровые, листоватые и призматические структуры раковин. В данной работе в первый раз отмечена перекрещенно-пластинчатая структура в подотряде Bellerophontina (в раковине *Euphemites*) и сложно-перекрещенно-пластинчатая структура во внутреннем слое *Bellerophon* (*Pharkidonotus*). Эти два примера являются наиболее ранними (пенсильванского периода) отмеченными случаями наличия перекрещенной и сложно-перекрещенной структуры в раковинах брюхоногих. Взятые в отдельности, структуры в раковинах этих двух отдаленно родственных беллерофонтоидов показывают, что они стоят ближе к фиссюреллоидам [fissurelloids] (имеющим внутренние перекрещенно-пластинчатые слои и внешние призматические слои), чем к плевротомариойдам [pleurotomarioids] (имеющим внутренние перламутровые и внешние призматические слои). Если дальнейшее изучение покажет, что структуры в раковинах трех видов, подверженных исследованию, характерны для всей группы, то тогда подотряд Bellerophontina должен быть подвержен систематической переоценке.

INDEX

Numbers in *italic* type refer to detailed descriptions or definitions; numbers in **boldface** type refer to illustrations (plate numbers are preceded by **pl.**). In places the word "structure" is abbreviated str., and the word "structures" is abbreviated strs.

PLATES 1-32

Locations of figures in plates 1-32 are given in text-figures 2-9. All pictures are of thin sections unless otherwise designated. In all cross-sectional views dorsal is toward the top of the page unless specified otherwise. All pictures taken through polarizing microscope with transmitted light and crossed nicols unless stated otherwise. The magnification given in the plate-figure explanations is the *initial* magnification of the microscope lens system. This magnification determines resolution. The bar scale with each figure gives the *final* magnification in microns (μ) or millimeters (mm). Unless stated otherwise all photographs are unretouched. Where not stated specifically, the myostracum (m) is assumed to have a complex-prismatic structure.

As a result of the printing process, the marginal shell-layer contacts do not match the actual contacts on some of the figures. Necessary corrections are indicated on the appropriate plate explanations.

EXPLANATION OF PLATE 1

Group 1 (figs. 1-3, 5-7), group 2 (fig. 4). Structure of shell layers: m + 3, simple-prismatic; m + 2, fibrillar; m + 1, concentric crossed-lamellar; m — 1, radial crossed-lamellar.

Figs. **1, 5, 6**—*Acmaea limatula.* **1,** vertical, radial section showing the three outer shell layers; ×120; hypotype, UCMP no. 30111-a. **5,** section almost normal to fibrils of layer m + 2; small chip of thin-section rotated 45° from original position (see Pl. 5, fig. 2, a); ×900; hypotype, UCMP no. 30116-a. **6,** nearly tangential section showing simple-prismatic structure of layer m + 3; ×80; hypotype, UCMP no. 30112-a.

Figs. **2, 7**—*Acmaea instabilis;* hypotype, UCMP no. 30113-a. **2,** isolated fibril of layer m + 3; ×500. **7,** two isolated fragments having fibrillar structure; ×80. A, fragment oriented so that fibrils exhibit true angle of reclination. Note the two projecting fibrils. B, fragment oriented so that fibrils appear to intersect growth surfaces at 90°.

Fig. **3**—*Patella mexicana:* Durham; side view of fragment showing true reclination angle of fibrils in layer m + 2; incident light; ×150; hypotype, UCMP no. 32723-a.

Fig. **4**—*Patella geometrica;* side view of fragment showing true reclination angle between growth surfaces (g) and fibrils (f); ×200; holotype, UCMP no. 11933-a.

Figs. 1 and 3: contacts printed 1 mm too high.


1
m + 3
m + 2
m + 1
100 μ


2

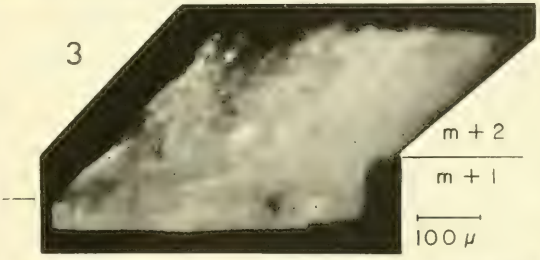
3
m + 2
m + 1
100 μ

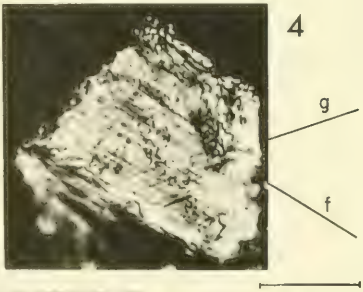
4
g
f
50 μ

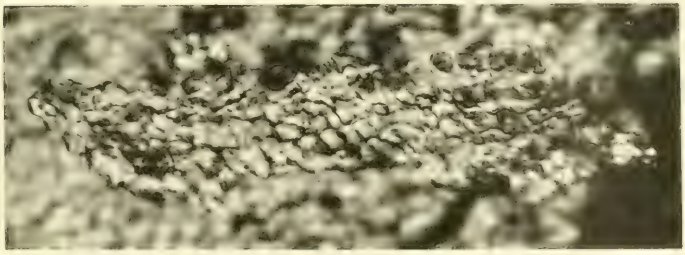
5
10 μ

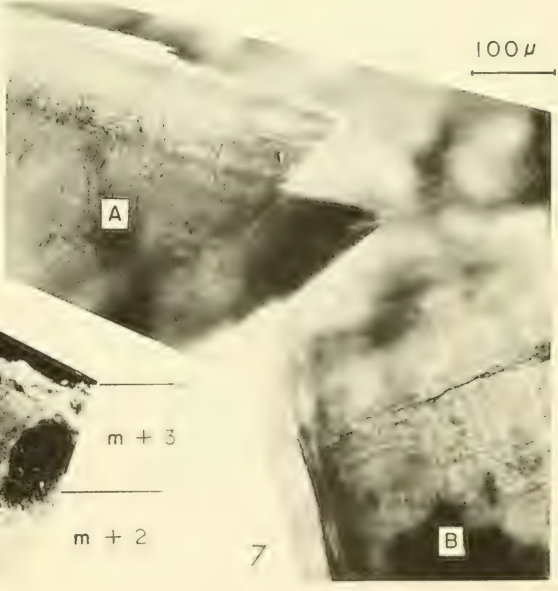
100 μ
A
B
7

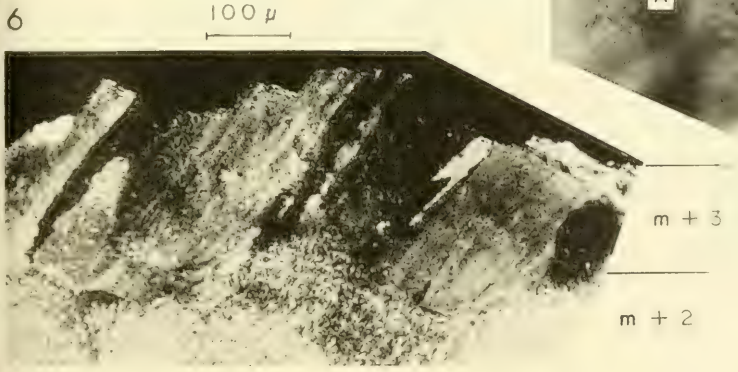
6
100 μ
m + 3
m + 2

1

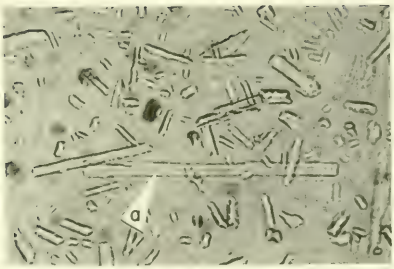

20 μ

2

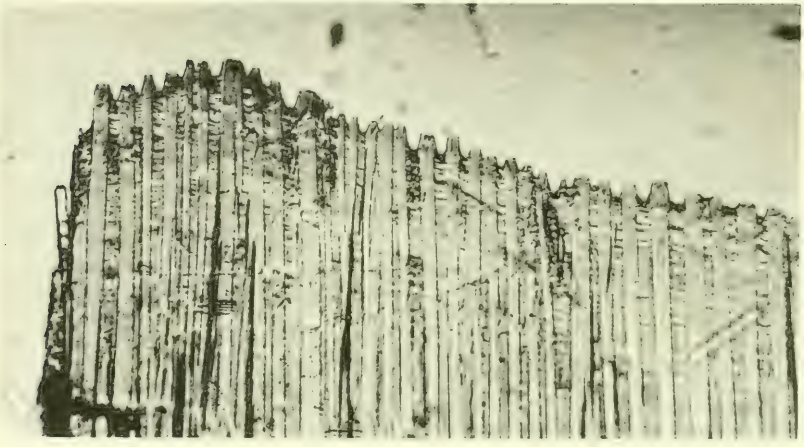

100 μ

3

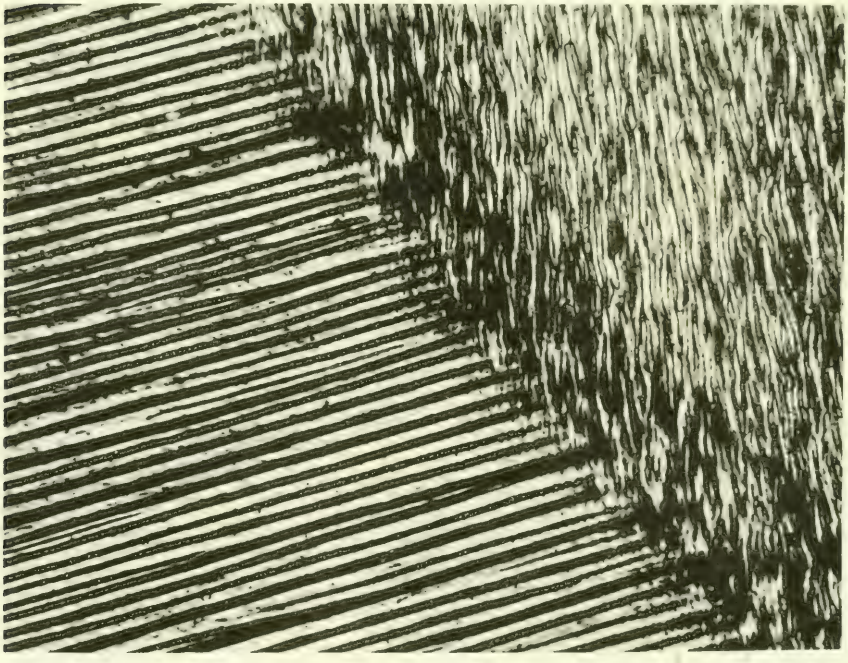

4

100 μ

m + 1 | n | m − 1

EXPLANATION OF PLATE 2

Group 1 (figs. 1-4)

Figs. 1-3—*Lottia gigantea;* crossed-lamellar layer m + 1. **1, 2,** isolated second-order lamella (a); ×500; hypotype, UCMP no. 30793-e. **1,** nicols uncrossed. **2,** same area as in figure 1 with the second-order lamella in the nonextinction position. Note that even in this position the lamella is invisible. The surrounding visible fragments are composed of two or more second-order lamellae. **3,** shell chip showing rectangular fretwork pattern at broken ends of first-order lamellae; on the first-order lamellae forming the indented part of the fretwork, note the traces of second-order lamellae; nicols uncrossed; ×200; hypotype, UCMP no. 30793-d.

Fig. 4—*Acmaea limatula;* nearly tangential section showing the regular, elongate first-order lamellae of layer m + 1 and the irregular, short first-order lamellae of layer m − 1; ×200; hypotype, UCMP no. 30112-a.

EXPLANATION OF PLATE 3

Group 1 (figs. 1-4)

Figs. 1-4—*Lottia gigantea.* **1, 2,** vertical, radial section nearly normal to length axes of first-order lamellae of concentric crossed-lamellar layer (m + 1); ×900; hypotype, UCMP no. 30793-c. **1,** sixteen first-order lamellae showing the horizontal traces of second-order lamellae; these traces are readily seen only in alternate first-order lamellae. **2,** exactly the same area as in figure 1 but with the microscope stage rotated 11° bringing to view chevron patterns which are the traces of third-order lamellae; the crack connecting points aa′ in figure 1 is the same faintly visible crack connecting points aa′ in this figure. **3,** section nearly normal to height axes of first-order lamellae showing the structure on either side of the contact between the concentric crossed-lamellar layer (m + 1) and the myostracum; in m + 1 note the traces of third-order lamellae nearly parallel with first-order lamellae; in the myostracum note the optical dependence of the prisms on the overlying structure; arrow points anteriorly; this is an enlargement from the same slide shown in Pl. 8, fig. 4; ×900; hypotype, UCMP no. 30793-a. **4,** isolated bundle of second-order lamellae with the plane formed by their height and length axes lying in the plane of the picture; note the traces of third-order lamellae; ×900; hypotype, UCMP no. 30793-e.

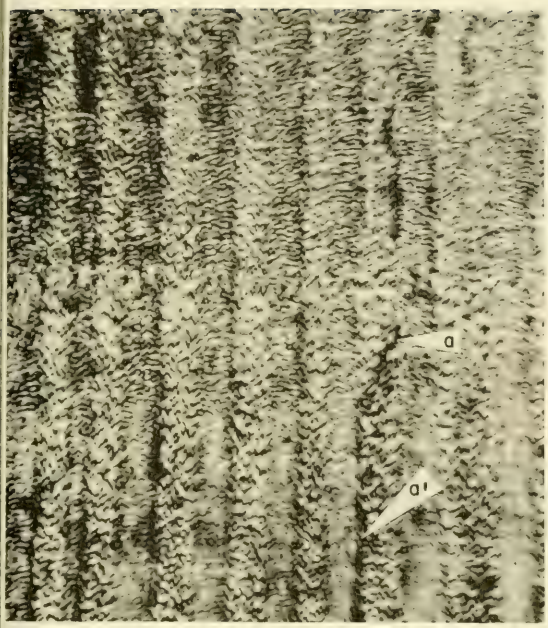

1

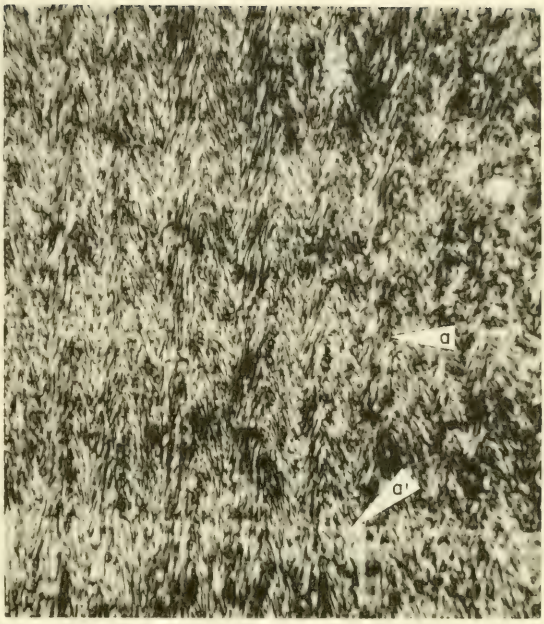

2

10 μ

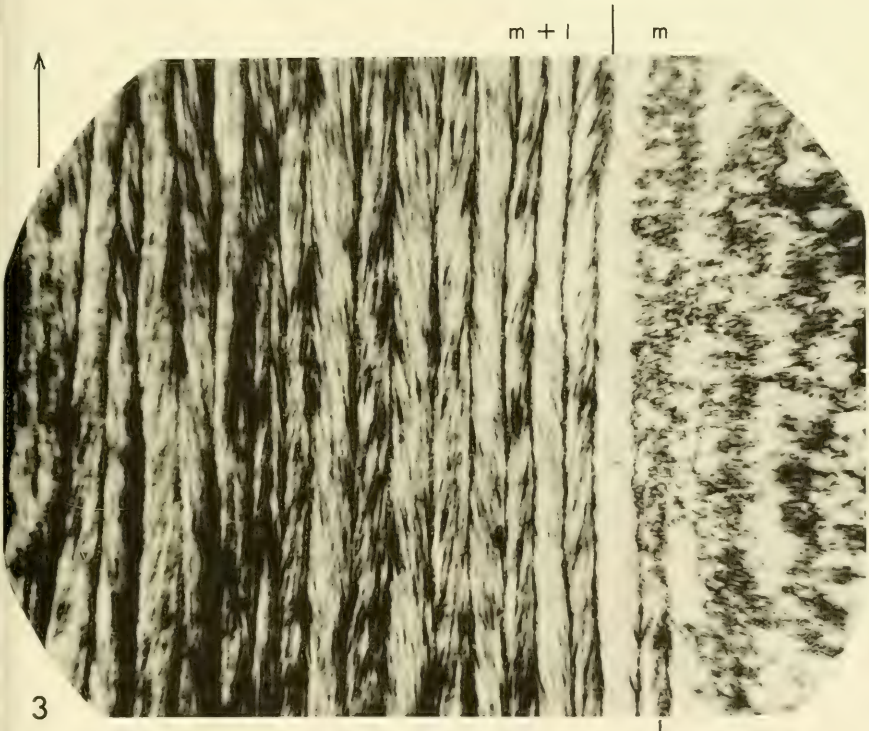

3

10 μ

10 μ

4

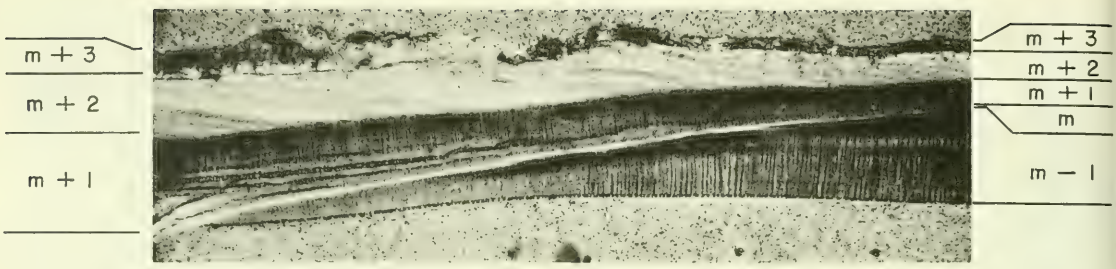

1

200 μ

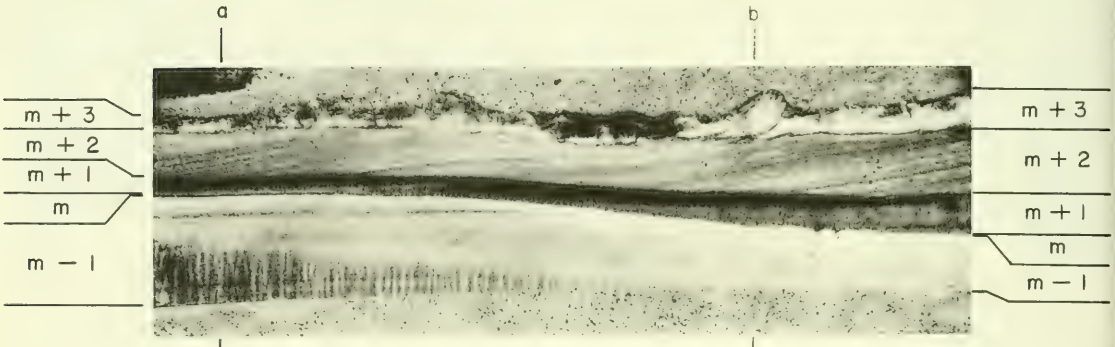

2

200 μ

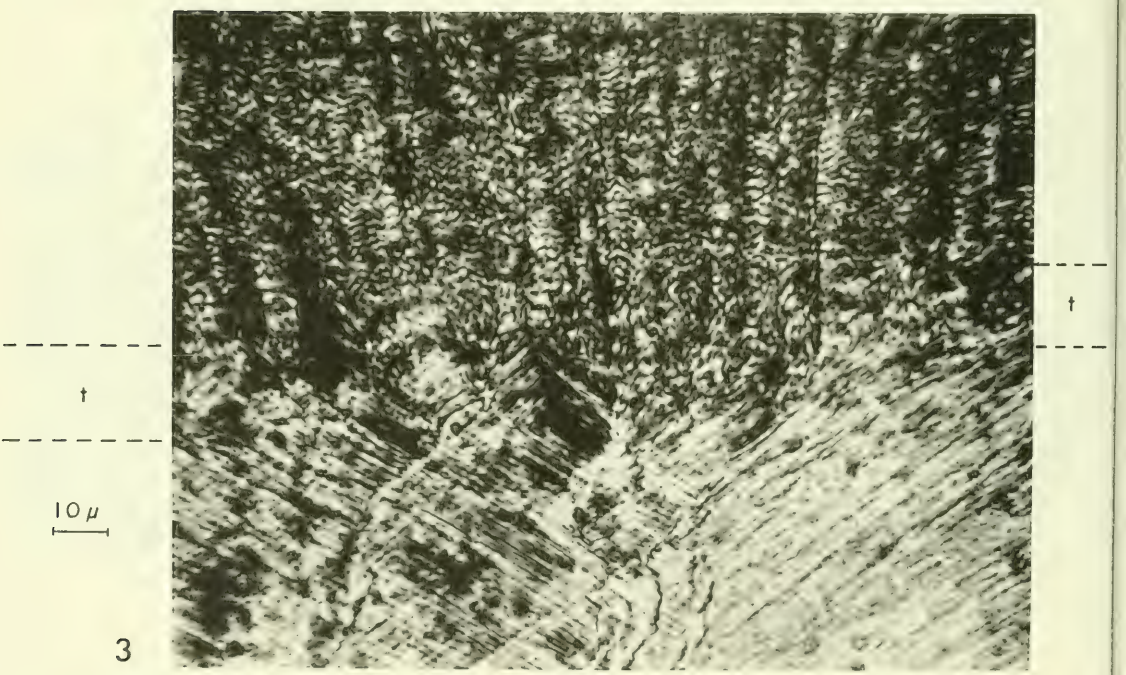

3

EXPLANATION OF PLATE 4

Group 1 (figs. 1-3)

Figs. 1-3—*Acmaea limatula*. Structure of shell layers: m + 3, simple-prismatic; m + 2, fibrillar; m + 1, concentric crossed-lamellar; m — 1, radial crossed-lamellar. **1, 2,** median sagittal sections showing shell-layer sequence; arrows point anteriorly; nicols partially crossed; ×25.5; hypotype, UCMP no. 30111-a. **1,** between anterior mantle-attachment scar and apex. **2,** between apex and posterior part of pedal-retractor scar; note the two pseudolayers in layer m — 1; aa′ is line of section shown in Pl. 5, fig. 1; bb′ is line of section shown in Pl. 5, fig. 2. **3,** transverse section across median sagittal plane showing the twist zone (t) between the two pseudolayers of layer m — 1; enlarged from slide shown in Pl. 5, fig. 1 and normal to the page surface at aa′ in Pl. 4, fig. 2; the cross pattern of second-order lamellae in two adjacent, transparent first-order lamellae can be seen in area below twist zone; ×900; hypotype, UCMP no. 30791-a.

Fig. 1, left margin: contacts printed 1 mm too high.
Fig. 2, left margin: contacts printed 0.5 mm too high.

EXPLANATION OF PLATE 5

Group 1 (figs. 1-3). Structure of shell layers: m + 3, simple-prismatic; m + 2, fibrillar; m + 1, concentric crossed-lamellar; m — 1, radial crossed-lamellar.

Figs. 1-3—*Acmaea limatula.* **1,** transverse section across median sagittal plane (aa′) showing lateral changes within layer m — 1; for location of section see Pl. 4, fig. 2, aa′ and text-figure 47; ×64; hypotype, UCMP no. 30791-a. **2,** transverse section across median sagittal plane (bb′); for location of section see Pl. 4, fig. 2, bb′; the chip at "a" is enlarged in Pl. 1, fig. 5; ×120; hypotype, UCMP no. 30116-a. **3,** transverse section near the apex and to the right of the median sagittal plane; ×200; hypotype, UCMP no. 30792-a.

Figs. 1, 2, 3: contacts printed 1 mm too low.

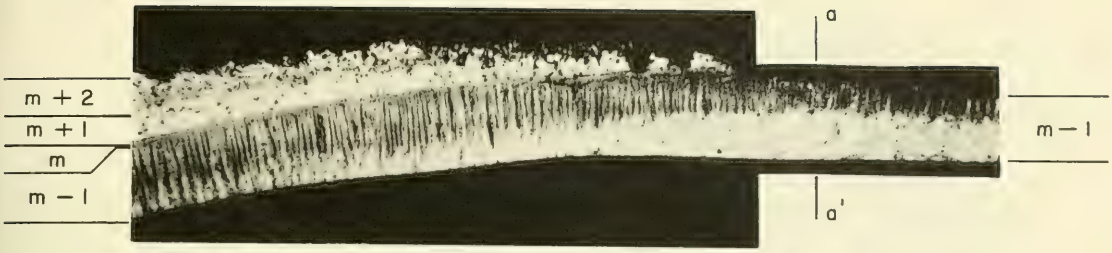

1

200 μ

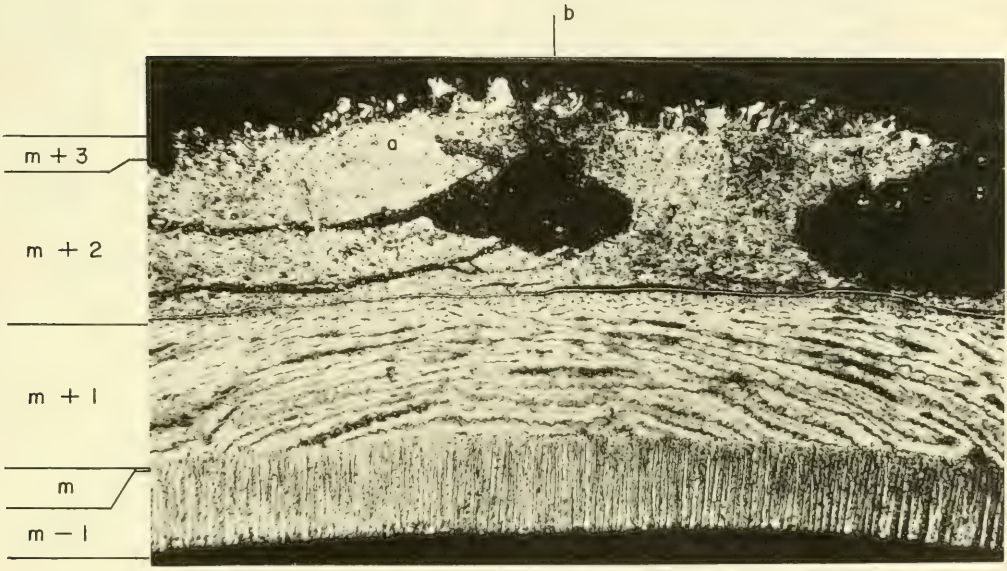

2

100 μ

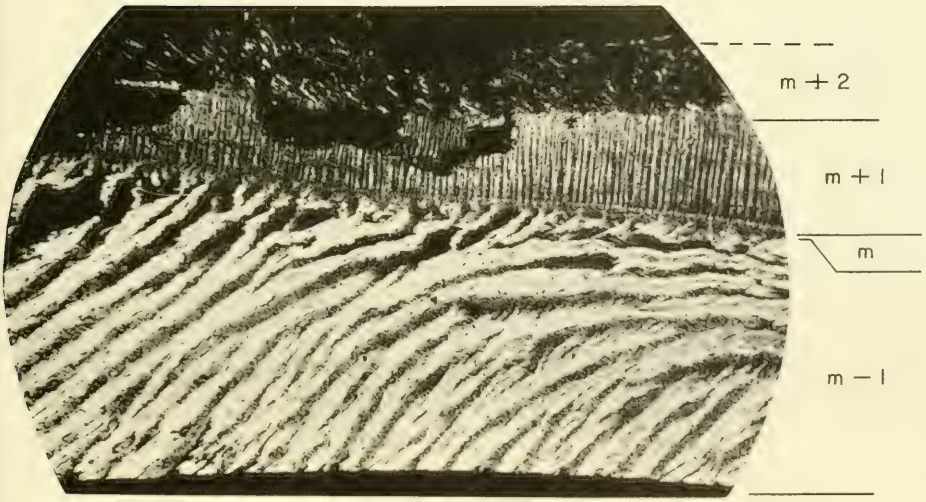

100 μ

3

1

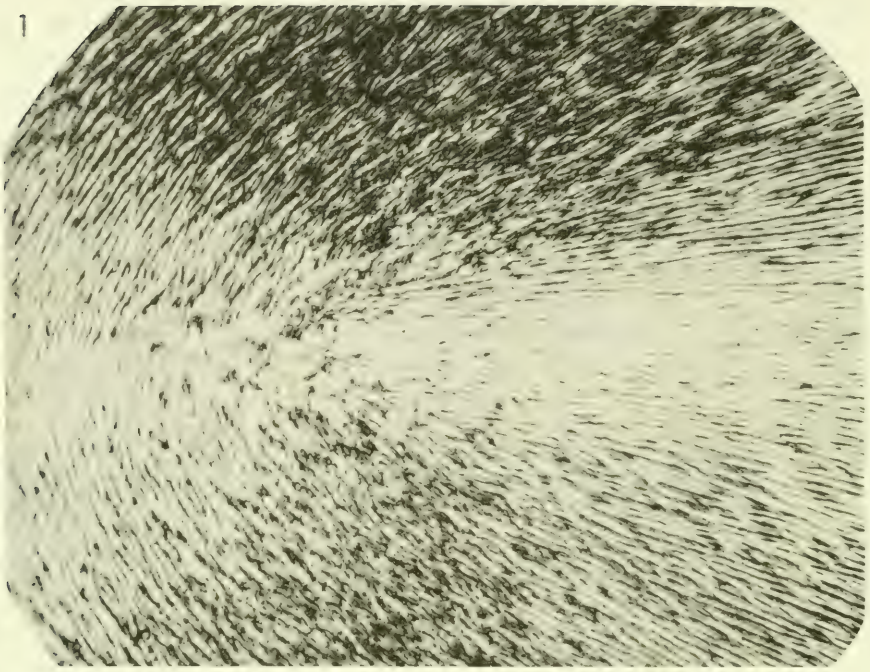

a a'

100 μ

2

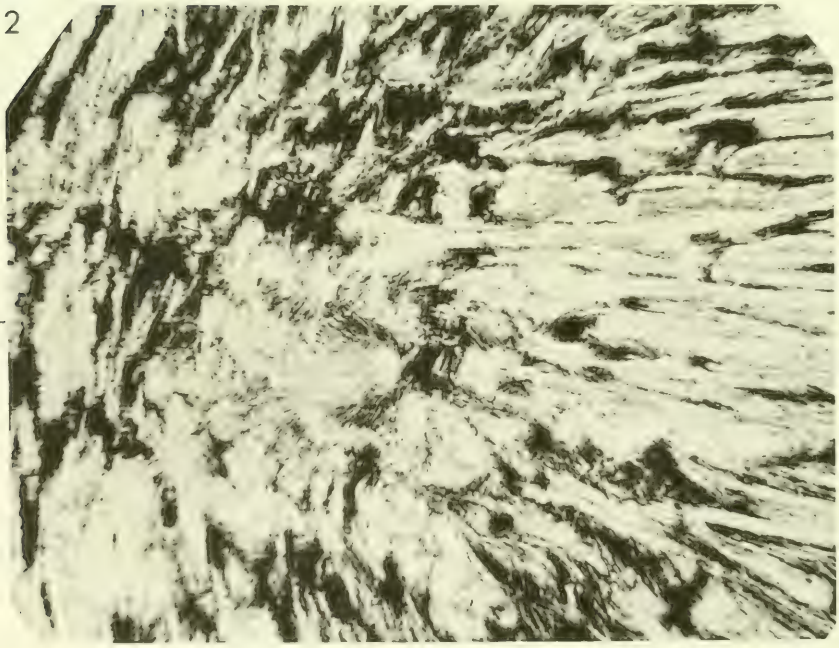

a a'

20 μ

EXPLANATION OF PLATE 6

Group 1 (figs. 1, 2)

Figs. 1, 2—*Acmaea limatula;* tangential section across median sagittal plane (aa′), almost at inner surface of shell, showing the overlap relationship within layer m — 1; arrows point anteriorly; hypotype UCMP no. 30112-a. 1, ×120. 2, enlargement of overlap area shown in the central part of figure 1; at point of overlap note radial cluster of third-order lamellae; ×500.

EXPLANATION OF PLATE 7

Group 1 (figs. 1-3)

Figs. 1-3—*Lottia gigantea;* vertical sections showing the upper part of the myostracum and the lower part of the concentric crossed-lamellar layer (m + 1); note that what appears to be a separate upper myostracal layer in figure 1 is actually (as seen in figure 3) part of the pedal-retractor myostracum which was formed at an earlier "extended period" during the growth of the animal. **1, 2,** sagittal section nearly parallel with first-order lamellae of layer m + 1 showing optical dependence of myostracal prisms on the overlying layer; note dip angle of second-order lamellae in layer m + 1; ×120; hypotype, UCMP no. 30793-b. **1,** one set of first-order lamellae, and the myostracal prisms adjoining them, at or near extinction. **2,** the alternate set of first-order lamellae, and the myostracal prisms adjoining them, at or near extinction; the angle between extinction positions is 11.5°. **3,** radial section of the same layers shown in figures 1 and 2 along the plane aa′; arrow points abapically; ×64; hypotype, UCMP no. 30793-c.

Fig. 1: contacts printed 1 mm too high.

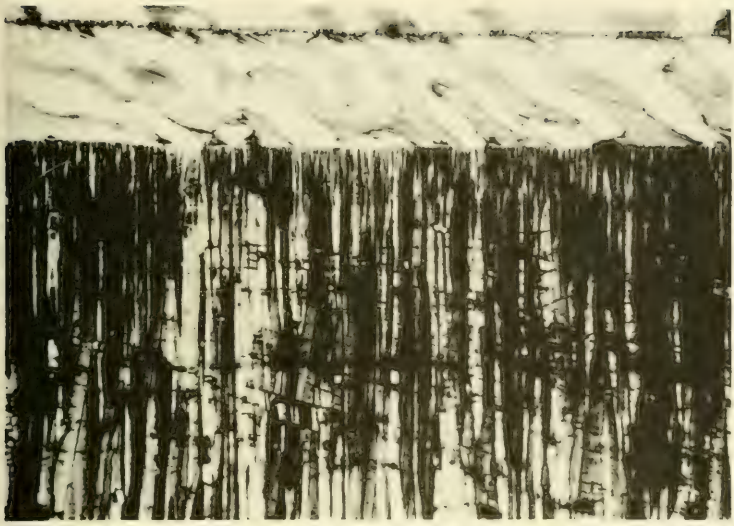

1

100 μ

2

3

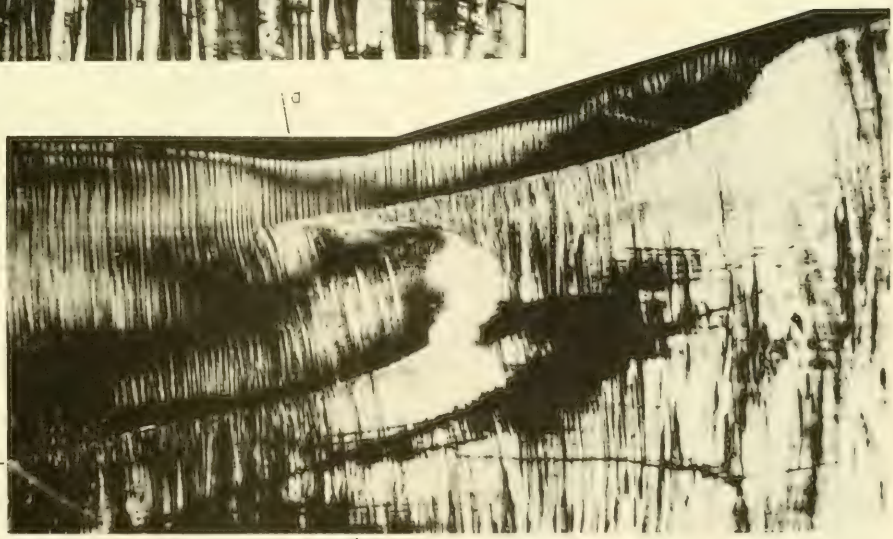

200 μ

m + 1

m

1

20 μ

m + 1

m

10 μ

2

3

10 μ

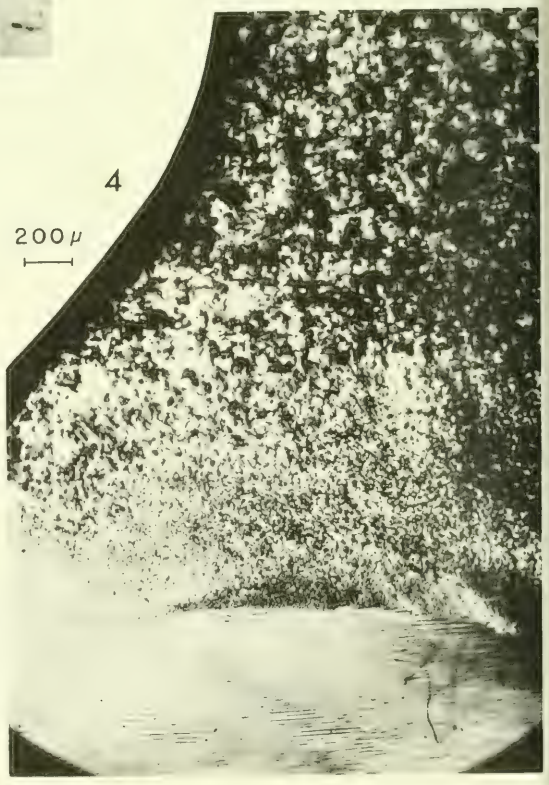

4

200 μ

m

m + 1

EXPLANATION OF PLATE 8

Group 1 (figs. 1-4)

Figs. 1-4—*Lottia gigantea;* structure of the myostracum. 1, 2, vertical, sagittal section; hypotype, UCMP no. 30793-b. 1, first-order prisms composed of second-order prisms; note also the finely spaced growth lines; ×500. 2, first-order prisms tapering to a point at the contact with the overlying crossed-lamellar layer; ×900. 3, 4, tangential section; hypotype, UCMP no. 30793-a. 3, a single first-order prism composed of many second-order prisms; ×900. 4, myostracum in contact with layer m + 1; note that first-order prisms become smaller as they approach the overlying layer; an enlargement of the contact between the two shell layers on this slide is shown in Pl. 3, fig. 3; ×25.5.

Figs. 2, 4: contacts printed 1 mm too low.

EXPLANATION OF PLATE 9

Group 2 (figs. 1-3)

Figs. 1-3—*Acmaea saccharina;* median sagittal section. Structure of shell layers: m + 2, complex-prismatic; m + 1, concentric crossed-lamellar; m — 1, radial crossed-lamellar; hypotype, UCMP no. 36480-a. **1,** three prismatic sublayers visible in layer m — 1; one sublayer (s) intersects the two pseudolayers of layer m — 1 at aa′ (see figure 2) and at bb′ (see figure 3); ×32. **2, 3,** enlargements of sublayer (s) seen in figure 1; ×900. **2,** at aa′ where length axes of first-order lamellae are normal to plane of the picture. **3,** at bb′ where width axes of first-order lamellae are normal to plane of the picture.

Fig. 1: contacts printed 0.5 mm too low.
Figs. 2, 3: contacts printed 1 mm too low.

1

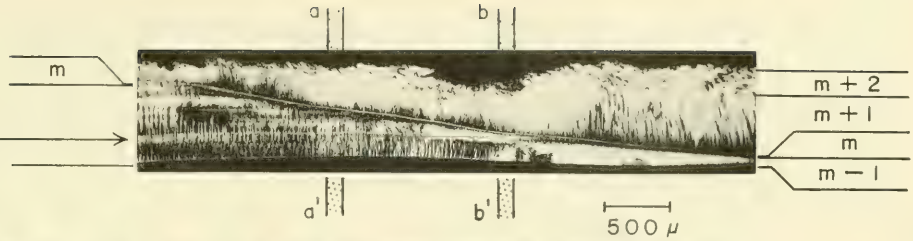

2

10 μ

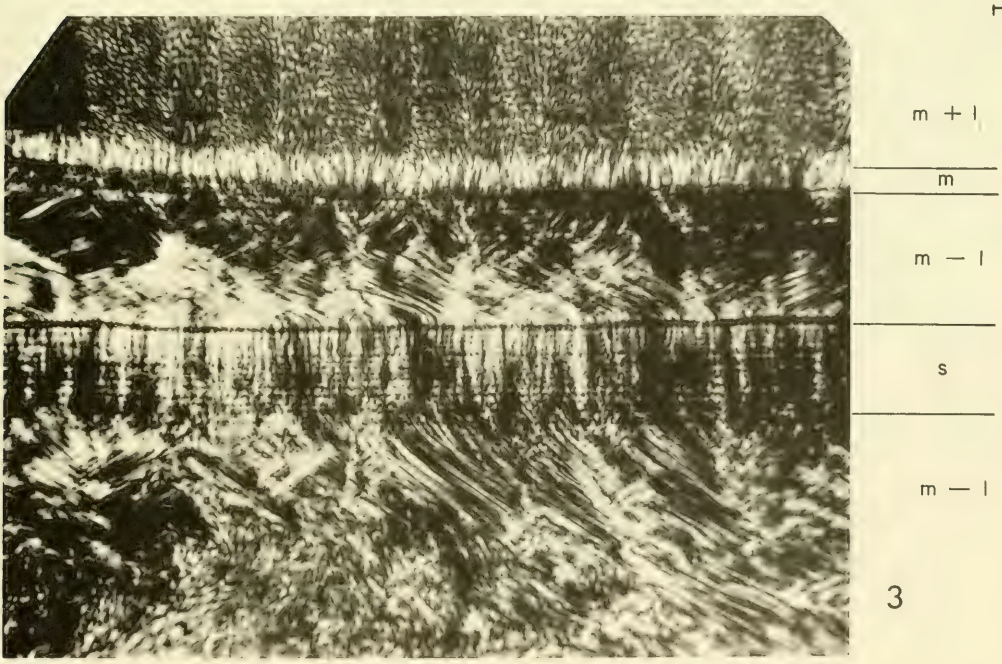

3

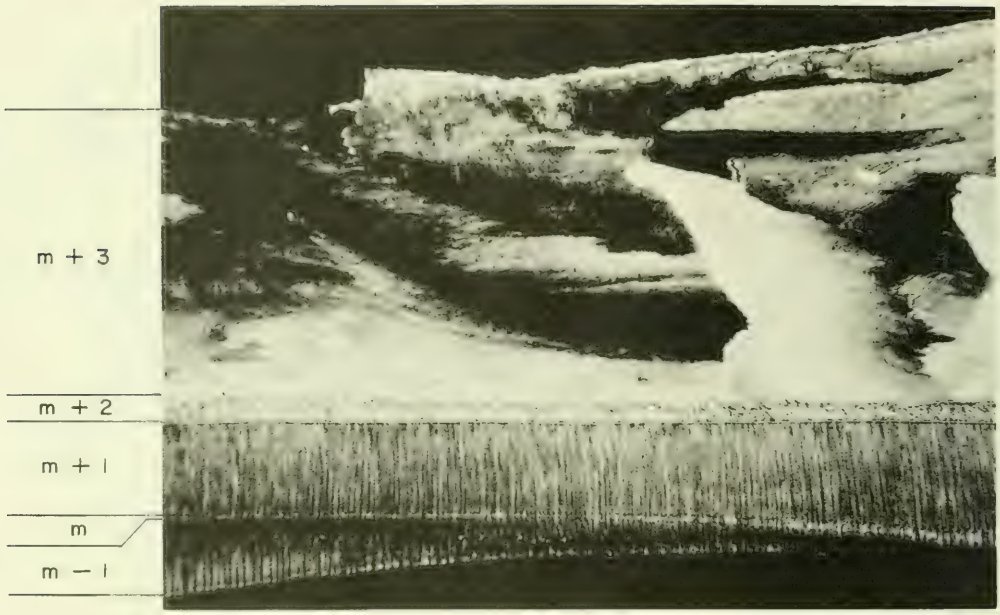

1

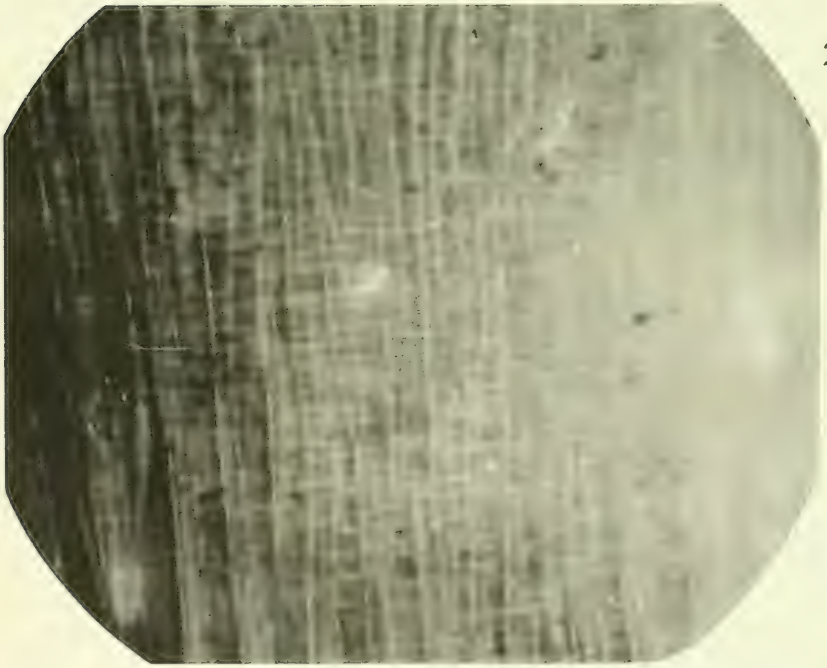

2

EXPLANATION OF PLATE 10

Group 3 (fig. 1), group 6 (fig. 2)

Fig. 1—*Scurria scurra;* median sagittal section. Structure of shell layers: m + 3, complex-prismatic; m + 2, fibrillar; m + 1, concentric crossed-lamellar; m − 1, radial crossed-lamellar; arrow points anteriorly; ×120; hypotype, UCMP no. 30795-a.

Fig. 2—*Patella ocula;* view of inner surface of shell looking down through the narrow first-order lamellae of the crossed-lamellar layer (m + 1) to the wide first-order lamellae of the overlying crossed-foliated layer (m + 2); the first-order lamellae of the two layers are at right angles to each other; arrow points to animal's left; low-angle incident light; × 150; hypotype, YPM no. 13374.

EXPLANATION OF PLATE 11

Group 6 (figs. 1-5)

Figs. 1-5—*Patella compressa*. **1, 2,** median sagittal section. Structure of shell layers: m + 3, radial crossed-foliated; m + 2, concentric crossed-foliated; m + 1, radial crossed-lamellar; m — 1, radial crossed-lamellar; m — 2, radial crossed-foliated; arrow points anteriorly; hypotype, UCMP no. 36482-a. **1,** section between apex of shell and anterior mantle-attachment scar; ×120. **2,** section between apex and posterior part of pedal-retractor scar; note the decrease in dip angle of second-order lamellae from the myostracum to the ventral surface of the shell; ×500. **3,** small chip of crossed-foliated layer m + 2 (viewed normal to flat faces of second-order lamellae of upper first-order lamella) with three first-order lamellae showing traces of third-order lamellae; note also the traces of second-order lamellae in bottom first-order lamella; ×500; hypotype, UCMP no. 36482-b. **4, 5,** chip from crossed-foliated layer m + 2 (viewed normal to growth surfaces) showing alternation of light-dark pattern of first-order lamellae with 180° change in light-source direction (arrow); low-angle incident light; ×112.5; hypotype, UCMP no. 36482-c. **4,** light from one direction. **5,** light from the other direction.

Fig. 1: contacts on right printed 0.5 mm too high.

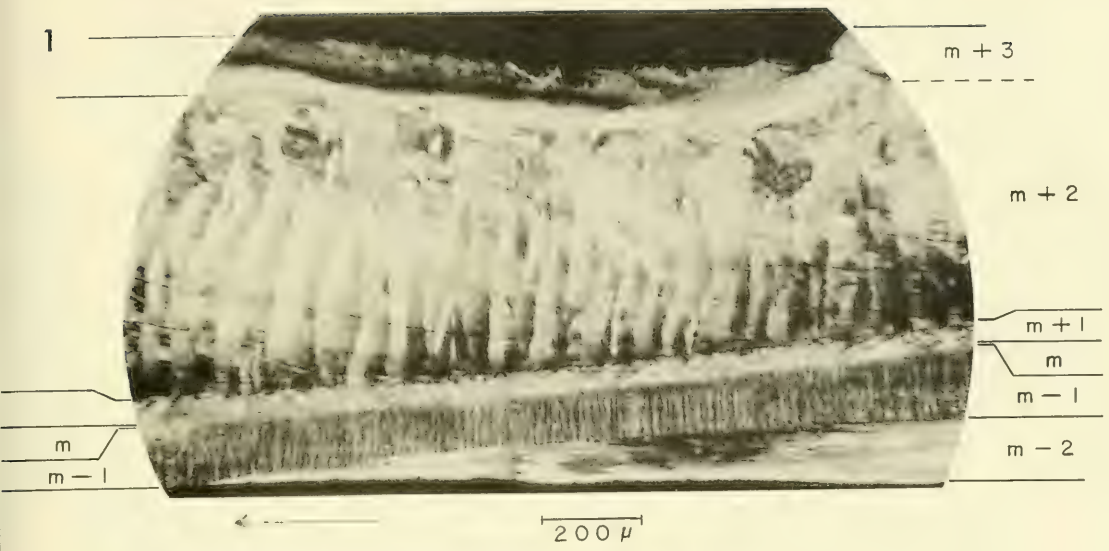
1
m + 3
m + 2
m + 1
m
m − 1
m − 2
m
m − 1
200 μ

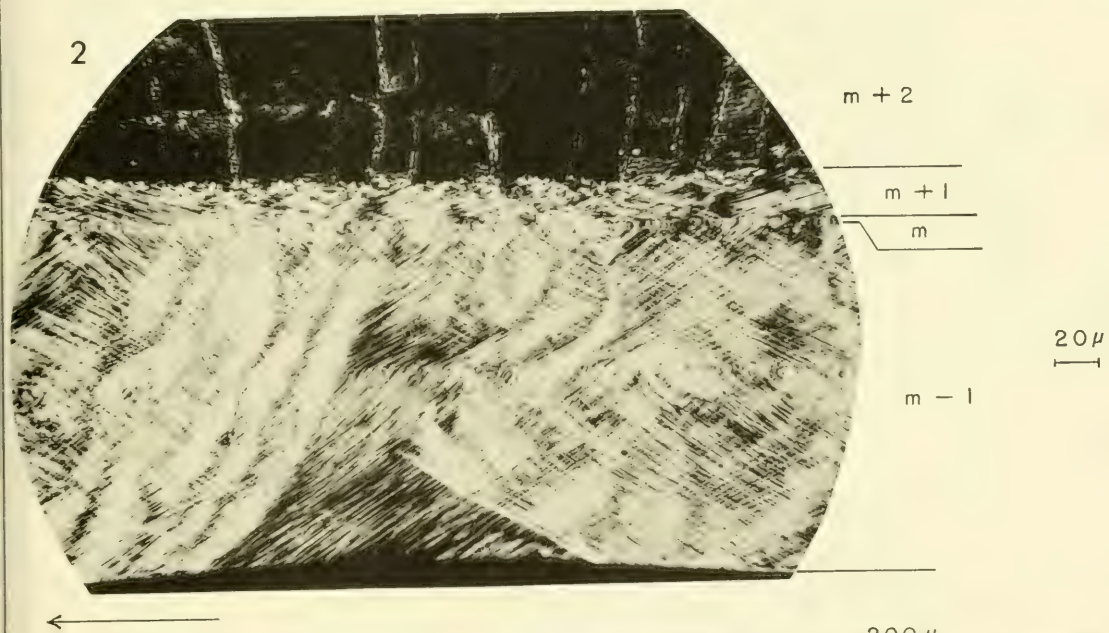
2
m + 2
m + 1
m
20 μ
m − 1

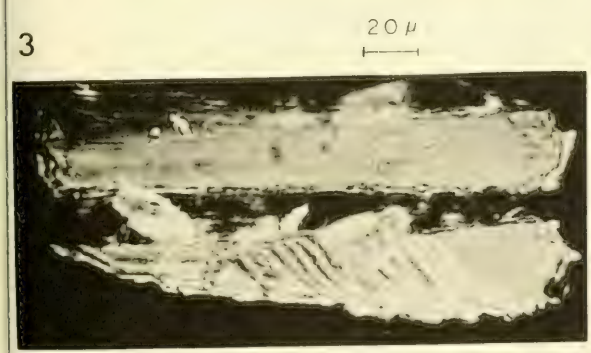
3
20 μ

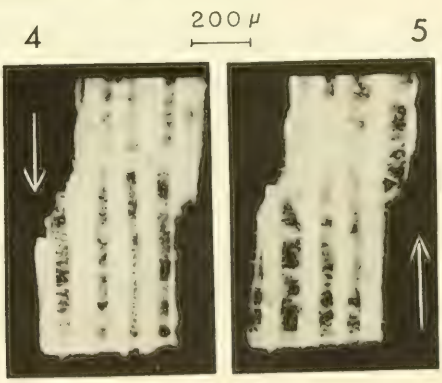
4
200 μ
5

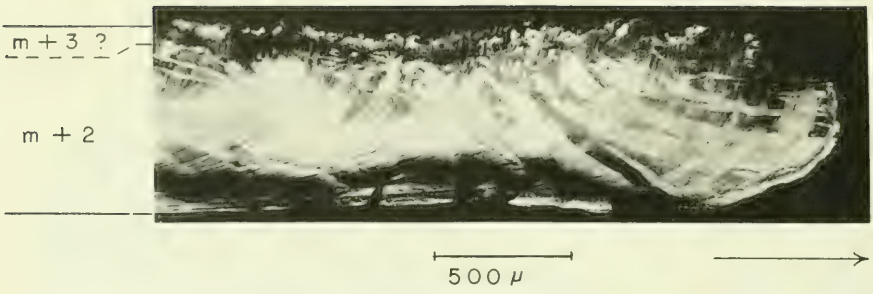

1

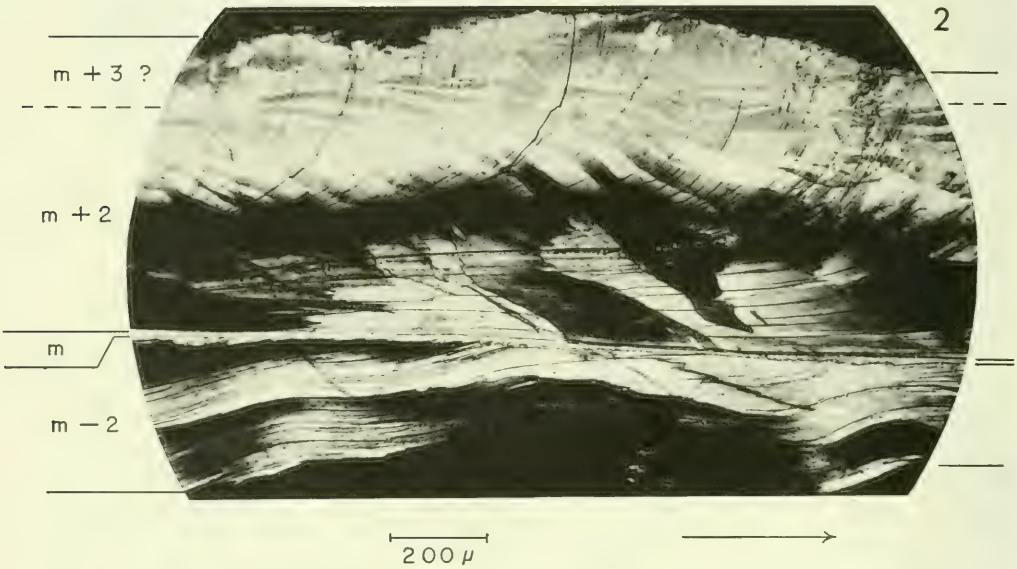

2

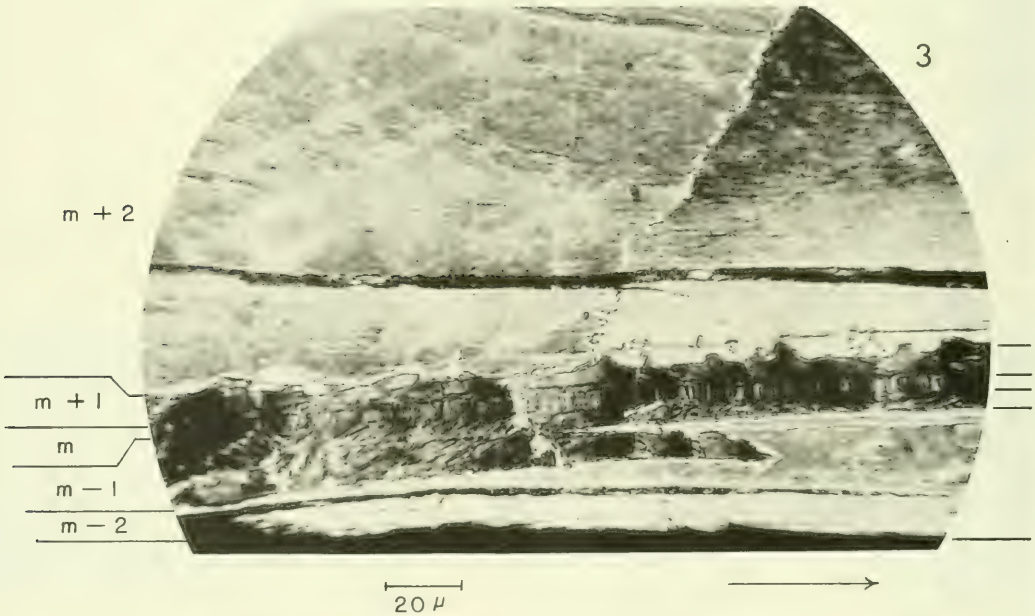

3

EXPLANATION OF PLATE 12

Group 7 (figs. 1-3)

Figs. 1-3—*Helcion pellucida;* median sagittal section. Structure of shell layers: m + 3?, radial crossed-foliated?; m + 2, concentric crossed-foliated; m + 1, complex crossed-lamellar; m − 1, complex crossed-lamellar; m − 2, radial crossed-foliated; arrows point anteriorly; hypotype, UCMP no. 36483-a. **1,** anterior margin of shell showing recumbent first-order lamellae of layer m + 2; ×64. **2,** between apex of shell and anterior mantle-attachment scar; note absence of shell layers m + 1 and m − 1; ×120. **3,** between apex and posterior part of pedal-retractor scar; ×900.

EXPLANATION OF PLATE 13

Group 8 (figs. 1-4); median sagittal sections. Structure of shell layers: m + 3, radial crossed-foliated; m + 2, concentric crossed-foliated; m + 1, concentric crossed-lamellar; m — 1, complex crossed-lamellar; m — 2, irregularly foliated; arrows point anteriorly.

Figs. 1, 3, 4—*Patella lusitanica;* hypotype, UCMP no. 36481-a. 1, section at pedal-retractor muscle scar; ×120. 3, 4, section between pedal-retractor scar and margin of shell showing the structure of a first-order lamella (a) of the crossed-foliated layer m + 2 (cf. Pl. 19, figs. 1, 2); ×900. 3, horizontal traces of second-order lamellae. 4, same area as in figure 3 but with stage rotated 9° to a position where the traces of third-order lamellae can be seen intersecting the traces of second-order lamellae at a high angle.

Fig. 2—*Patella vulgata;* section between apex of shell and the posterior part of the pedal-retractor scar; note the lateral intertonguing relationship between layers m — 1 and m — 2; ×64; hypotype, UCMP no. 30794-a.

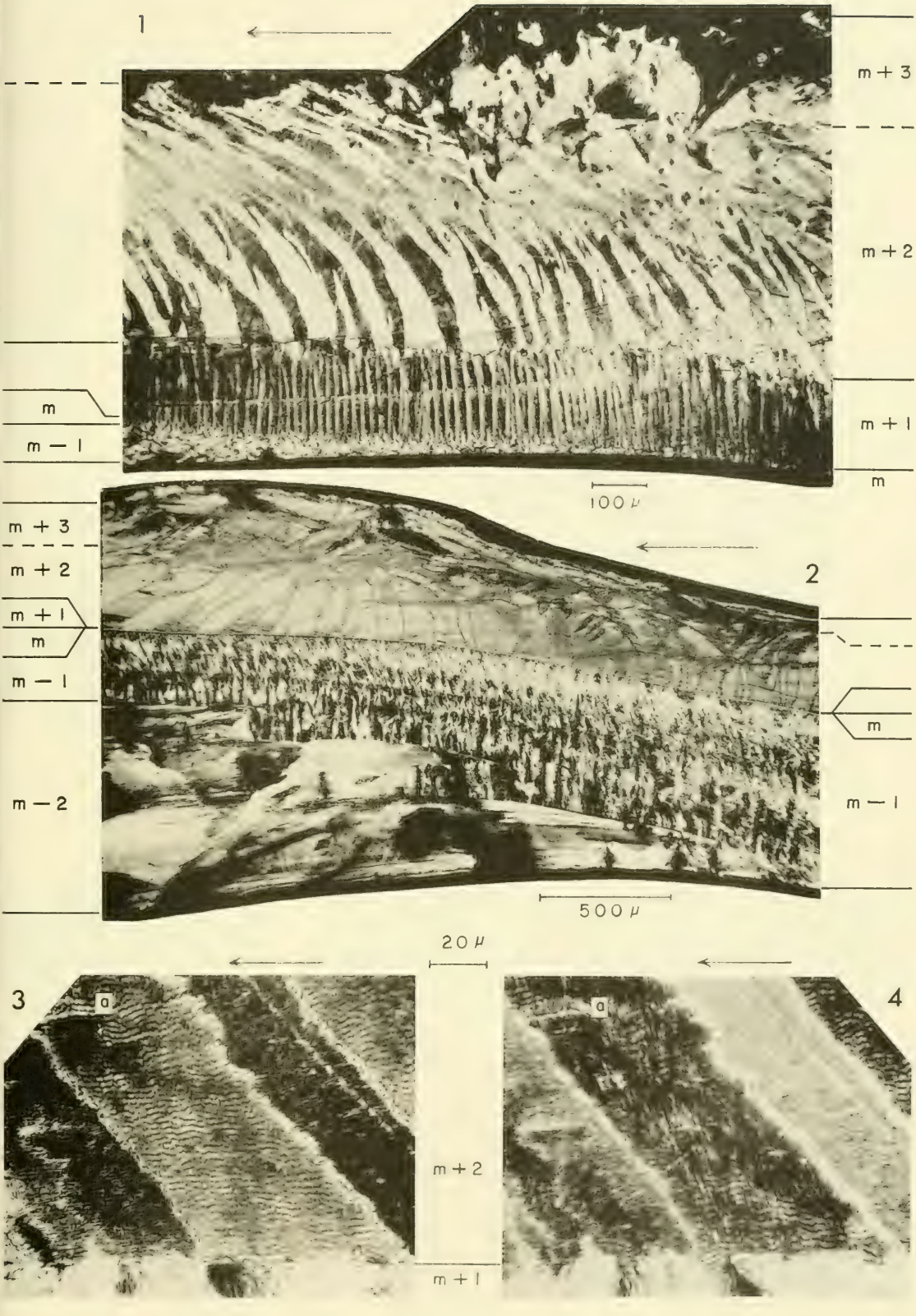
1
m + 3
m + 2
m
m − 1
m + 1
m
100 μ
m + 3
m + 2
m + 1
m
m − 1
m − 2
2
m
m − 1
500 μ
20 μ
3
a
m + 2
m + 1
4
a

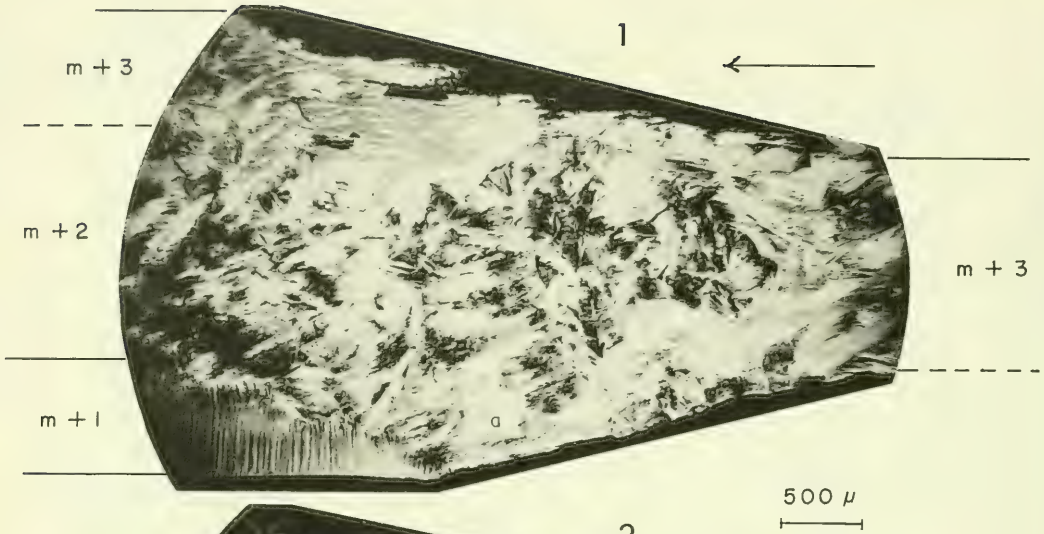
1
m + 3
m + 2
m + 1
a
m + 3
500 μ

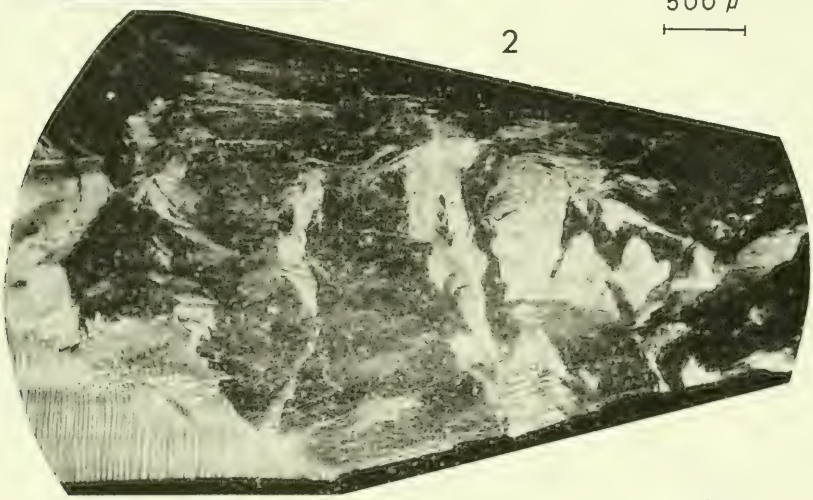
2

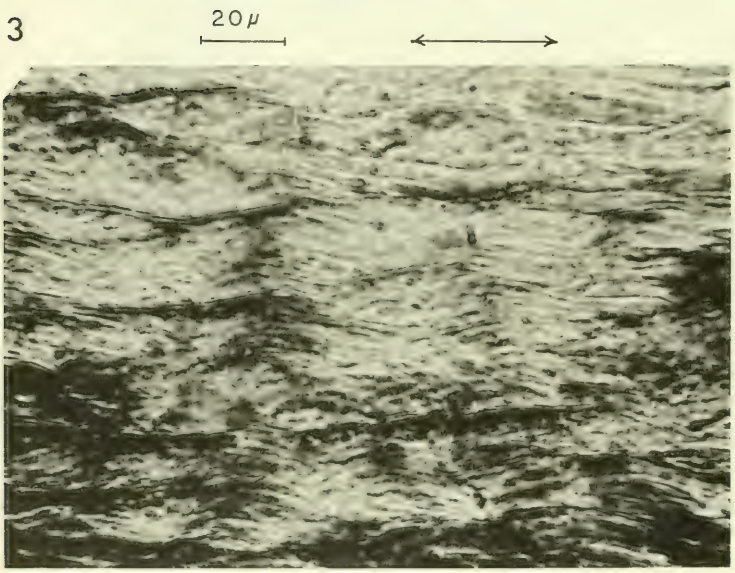
3
20 μ

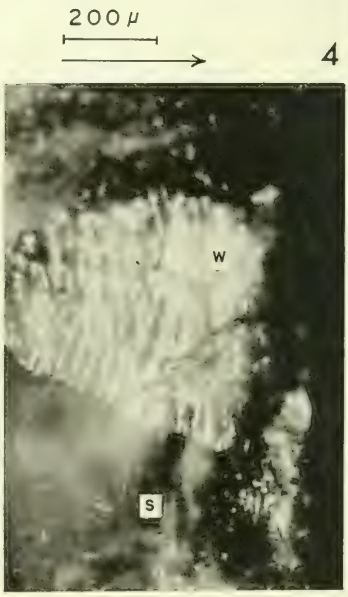
200 μ
4
W
S

EXPLANATION OF PLATE 14

Group 9 (figs. 1-4)

Figs. 1-4—*Patella mexicana*. Structure of shell layers: m + 3, radial crossed-foliated; m + 2, concentric crossed-foliated; m + 1, concentric crossed-lamellar. **1-3,** median sagittal section near posterior margin of shell; hypotype, UCMP no. 36487-a. **1, 2,** effect of the wavy structure on the appearance of first-order lamellae of the crossed-foliated layer (m + 2); arrow points anteriorly; ×32. **1,** under crossed nicols the boundaries between first-order lamellae are blurred; a small area at "a" is shown in figure 3. **2,** illuminated by low-angle incident light the first-order lamellae stand out clearly. **3,** enlarged area of first-order lamella (at "a" in figure 1) showing the wavy structure of second-order lamellae; double-headed arrow is parallel to growth lines; ×900. **4,** chip from layer m + 2 shows the inner surface (s) of the shell and the wavy structure (w) on the exposed dip surface of a second-order lamella; arrow points adapically; incident light; ×60; hypotype, UCMP no. 36487-c.

EXPLANATION OF PLATE 15

Group 9 (figs. 1, 2)

Figs. 1, 2—*Patella mexicana.* Structure of shell layers: m + 2, concentric crossed-foliated; m + 1, concentric crossed-lamellar; m, dependently prismatic; m — 1, complex crossed-lamellar. 1, median sagittal section showing optical dependence of myostracal prisms on the optical orientation of crystals within first-order lamellae of layer m + 1; arrow points anteriorly; ×500; hypotype, UCMP no. 36487-a. 2, vertical section nearly parallel to first-order lamellae of layer m + 1; note the vertically intertonguing relationship between first-order lamellae and overlying shell layer (m + 2); note also the decrease in dip angle of second-order lamellae from the dorsal to the ventral surface of layer m + 1; ×200; hypotype, UCMP no. 36487-b.

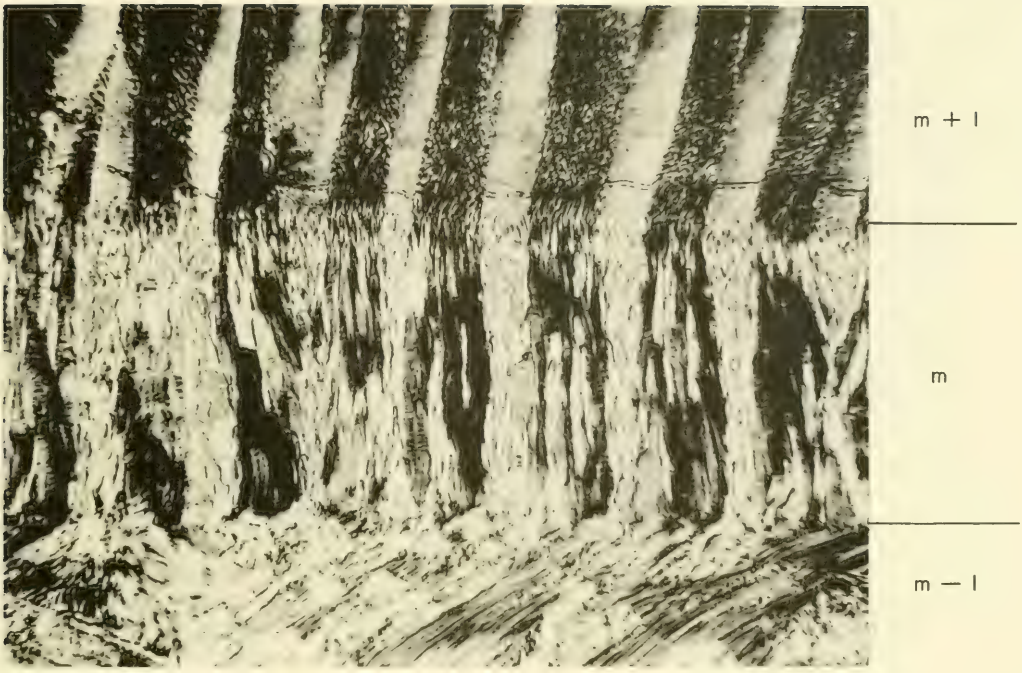

1

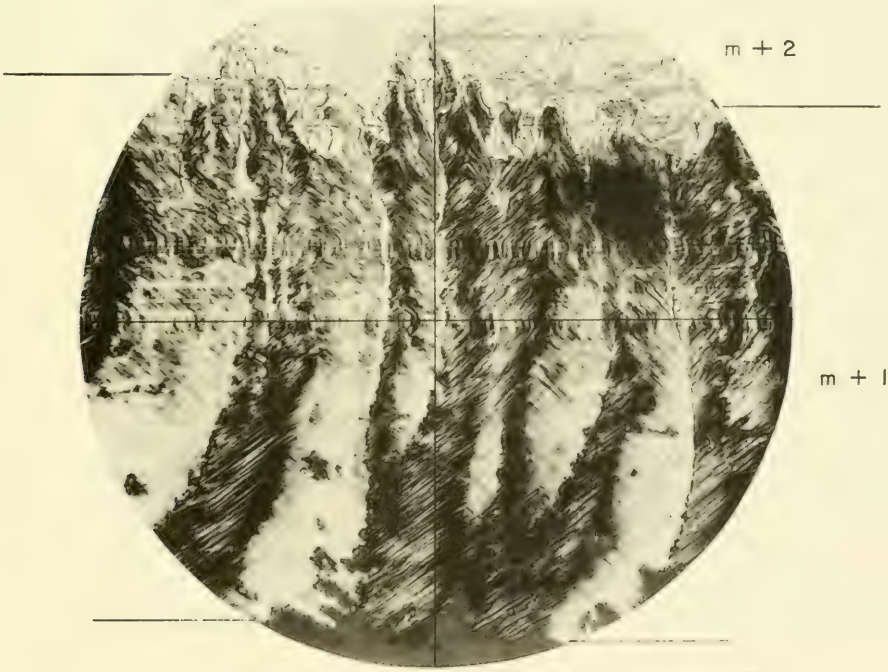

2

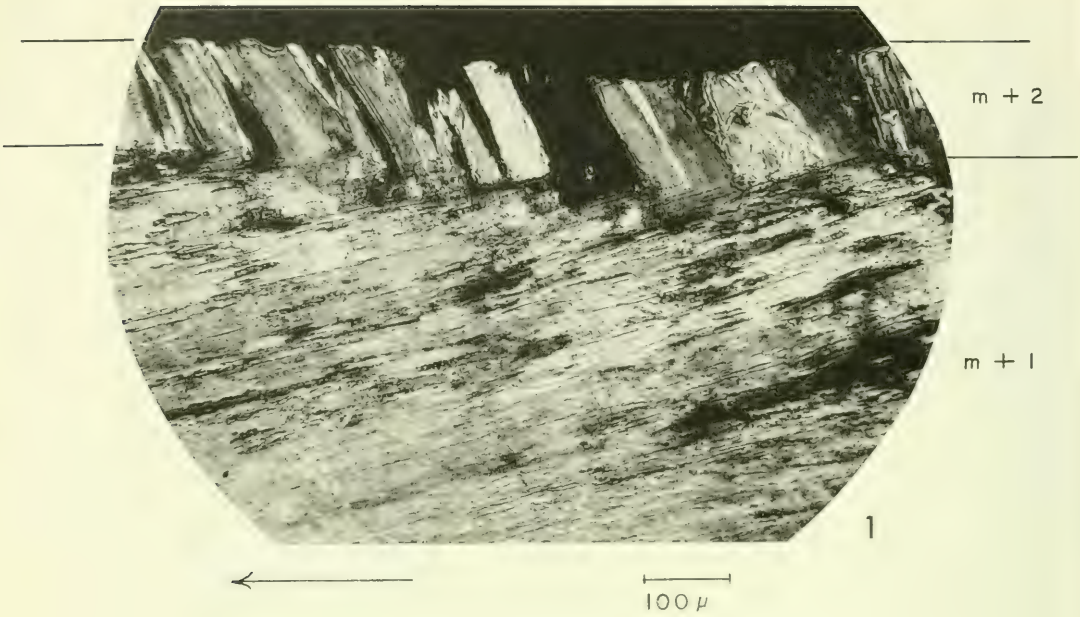
m + 2
m + 1
1
100 μ

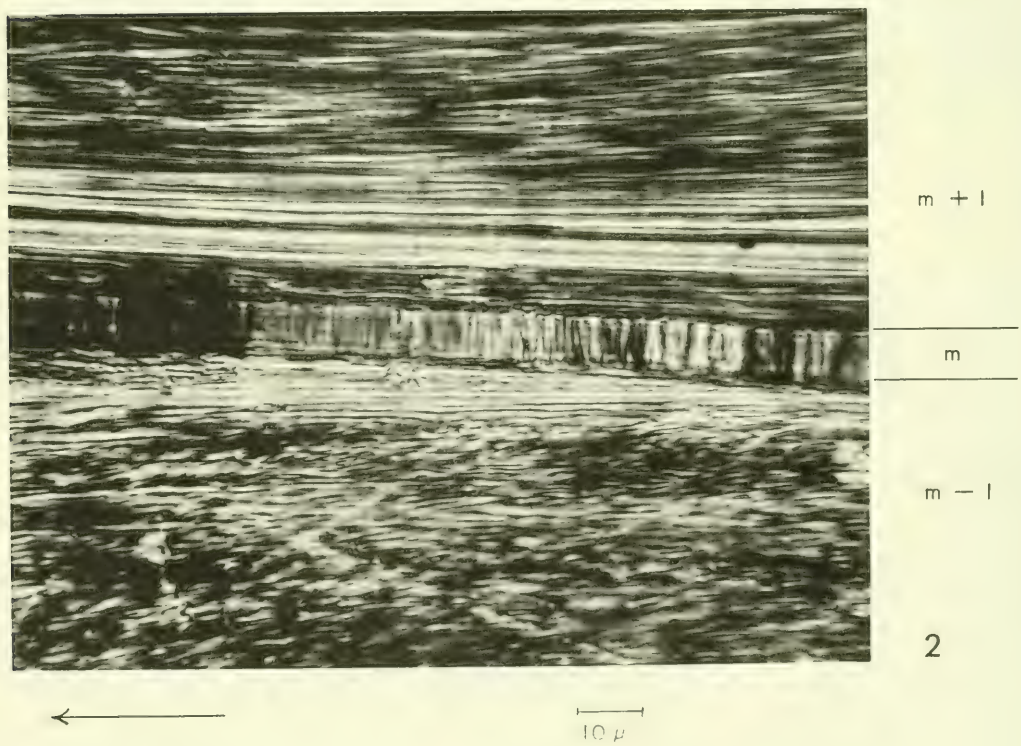
m + 1
m
m − 1
2
10 μ

EXPLANATION OF PLATE 16

Group 11 (figs. 1, 2)

Figs. 1, 2—*Nacella aenea;* median sagittal section. Structure of shell layers: m + 2, complex-prismatic; m + 1, foliated; m — 1, irregularly foliated; arrows point anteriorly; hypotype, UCMP no. 36486-a. **1,** optical dependence of folia on overlying prisms penetrates only a short distance into the foliated layer; ×200. **2,** section between apex of shell and pedal-retractor scar showing the thick foliated layers m + 1 and m — 1 in direct contact with the myostracum; ×900.

EXPLANATION OF PLATE 17

Group 11 (figs. 1, 2)

Figs. 1, 2—*Nacella aenea;* acetate peel of inner surface of shell showing outcrop pattern of folia; strike and dip of folia is indicated by the symbols at "s"; transmitted light; nicols uncrossed; ×200; hypotype, UCMP no. 36488-a. 1, foliated layer m + 1; arrow points adlaterally. 2, irregularly foliated layer m — 1; note the two areas where folia dip in nearly opposite directions.

1

100 μ

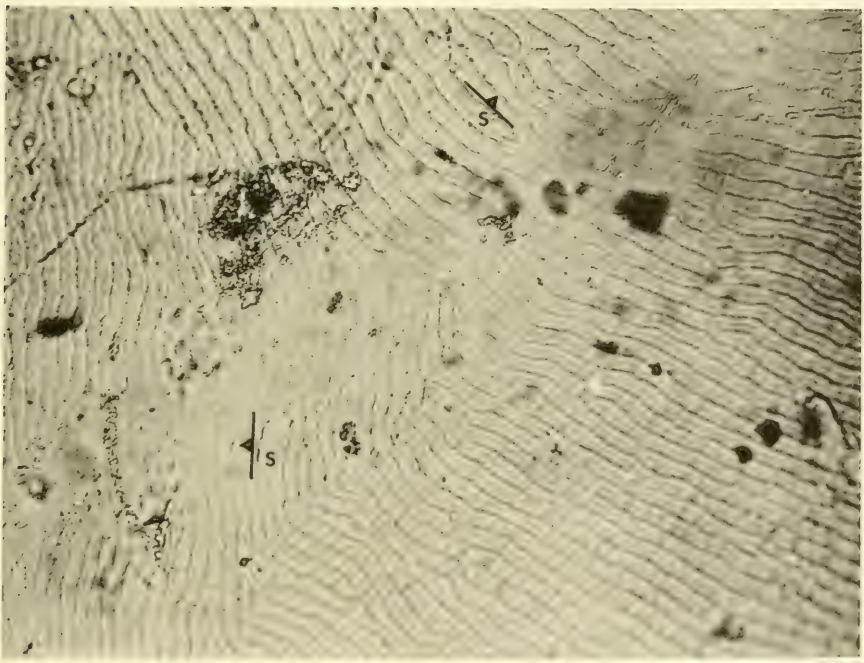

2

100 μ

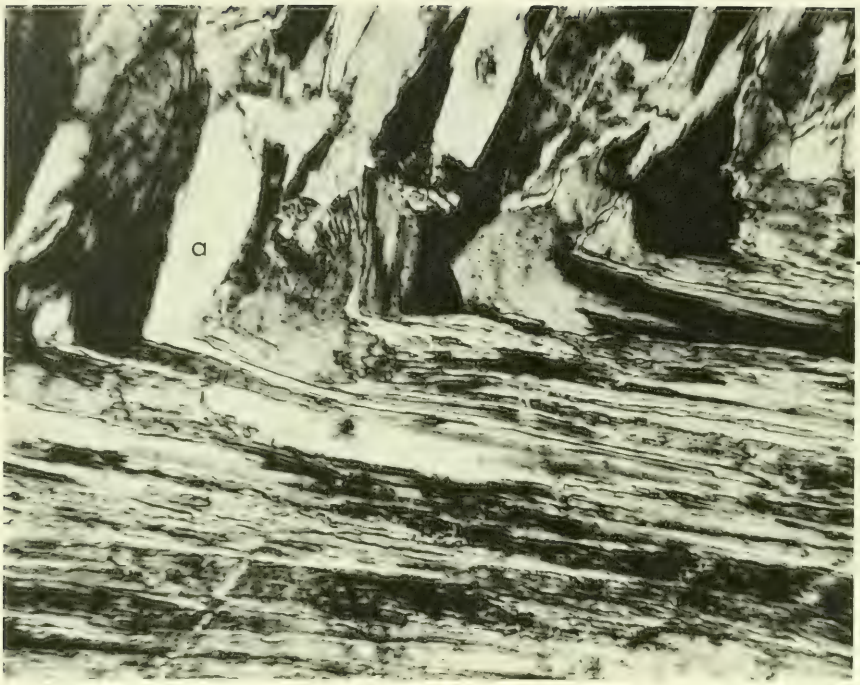
a
m + 3
m + 2
1
20 μ


m + 3
m + 2
2

EXPLANATION OF PLATE 18

Group 12 (figs. 1, 2)

Figs. 1, 2—*Cellana argentata;* median sagittal section. Structure of shell layers: m + 3, complex-prismatic; m + 2, foliated; section shows optical dependence of folia on the optic orientation of crystals in the complex-prismatic layer (m + 3); note particularly prism "a"; arrow points anteriorly; ×500; hypotype, UCMP no. 36484-a. 1, prism "a" and its optically dependent folia at nonextinction position. 2, prism "a" and its optically dependent folia at extinction position 30° from nonextinction position of figure 1.

EXPLANATION OF PLATE 19

Group 12 (figs. 1, 2), group 13 (figs. 3, 4)

Figs. 1, 2—*Cellana argentata;* median sagittal section between apex of shell and pedal-retractor scar. Structure of shell layers: m + 2, foliated; m + 1, radial crossed-lamellar; arrow points anteriorly; ×900; hypotype, UCMP no. 36484-a. 1, individual folia visible in foliated layer. 2, traces of blades superimposed on folia; stage rotated 22° from position shown in figure 1; note that in zone (a) where blades are parallel to the plane of the picture no blade traces can be seen.

Figs. 3, 4—*Cellana testudinaria;* median sagittal section. Structure of shell layers: m + 3, foliated; m + 2, irregularly tabulate foliated; m + 1, radial crossed-lamellar; m, dependently prismatic; m — 1, complex crossed-lamellar; thickness of myostracum shows inverse relationship to the width of the muscle scar generating it; arrows point anteriorly; ×200; hypotype, UCMP no. 36485-a. 3, thin myostracum generated by the wide pedal-retractor scar; note split in thin section between layers m + 2 and m + 3. 4, thick myostracum generated by the narrow anterior mantle-attachment scar.

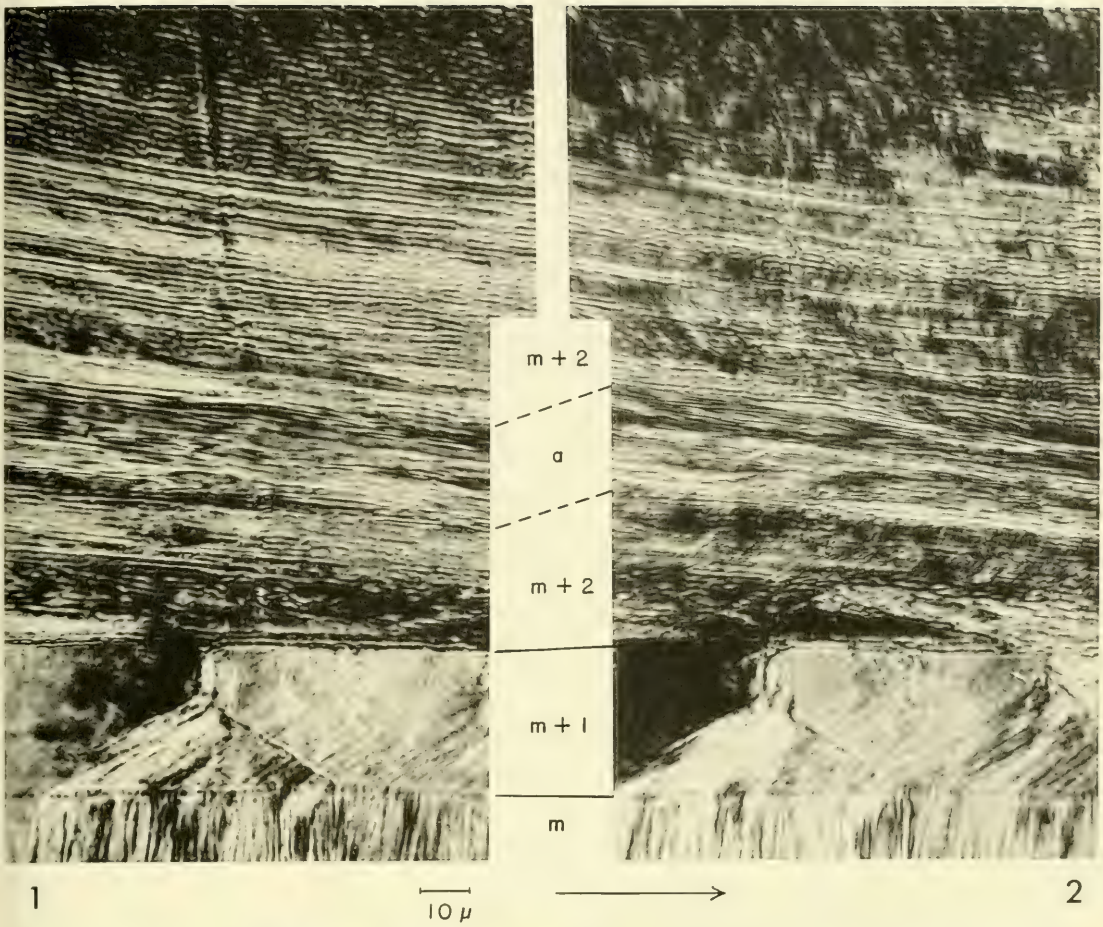
m + 2
a
m + 2
m + 1
m
1
10 μ
2

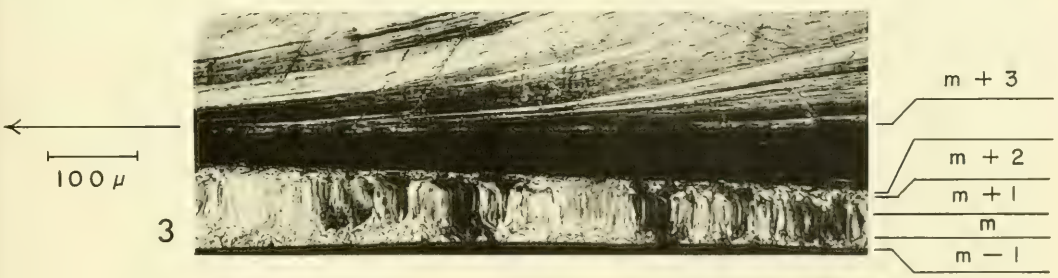
100 μ
3
m + 3
m + 2
m + 1
m
m − 1


m + 3
m + 2
m + 1
m
m − 1
100 μ
4

1

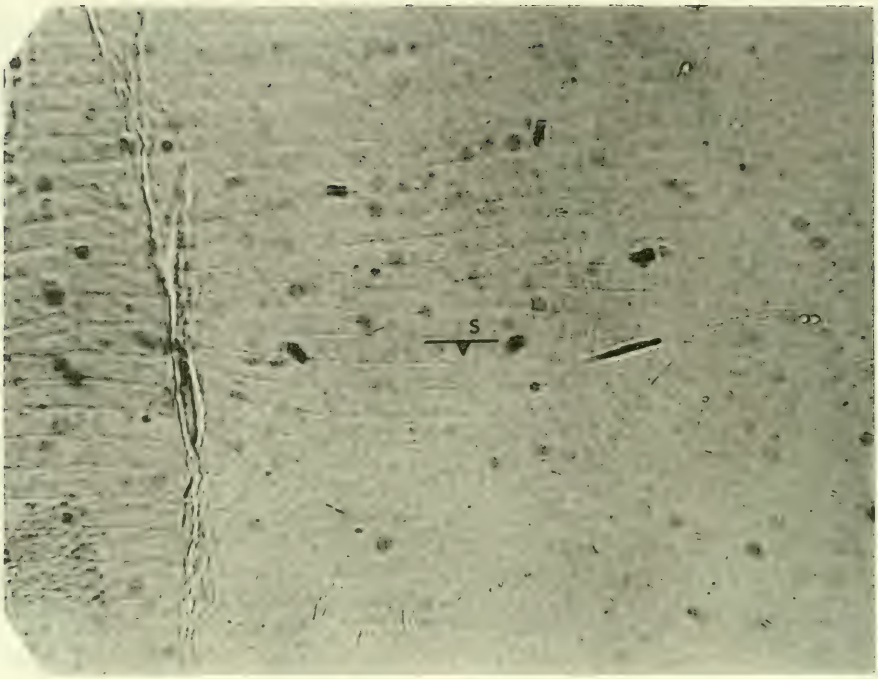

50 μ

2

EXPLANATION OF PLATE 20

Group 13 (figs. 1, 2)

Figs. **1, 2**—*Cellana testudinaria;* view, normal to growth surfaces, of small chip of the foliated layer (m + 3) from the ventral surface of the shell; arrow points adlaterally; ×500; hypotype, UCMP no. 36485-f. **1,** visible with the nicols uncrossed is the outcrop pattern of folia at the inner surface of the shell; note strike and dip symbol at "s." **2,** with nicols crossed, blade orientation as well as outcropping folia are visible.

EXPLANATION OF PLATE 21

Group 13 (figs. 1-10)

Figs. 1-10—*Cellana testudinaria*. 1-3, small chips from irregularly tabulate foliated layer (m + 2), viewed normal to folia. 1, 2, single chip showing two sets of tabulae; ×500; hypotype, UCMP no. 36485-d. 1, one set of tabulae at extinction. 2, the other set at extinction; stage rotated 7° from position shown in figure 1. 3, another chip; ×200; hypotype, UCMP no. 36485-e. 4-6, complex crossed-lamellar structure of layer m — 1. 4, median sagittal section showing an axial section of a major prism; ×500; hypotype, UCMP no. 36485-a. 5, 6, isolated cone removed from the ventral surface of the shell; the central axis of the cone is the central axis of the major prism from which it came; note third-order lamellae radiating from apex; low-angle incident light; ×150; hypotype, UCMP no. 36485-g. 5, dorsal view of cone. 6, side view of cone; base of cone is part of the ventral surface of the shell. 7-10, isolated folia from foliated layer (m + 3), viewed normal to folia. 7, 8, single fragment showing two sets of blades; relationship best seen in lower half of picture; ×500; hypotype, UCMP no. 36485-b. 7, one set of blades at extinction. 8, the other set at extinction; stage rotated 29° from position shown in figure 7. 9, folium showing insertion position of new blades along "growth lines"; ×500; hypotype, UCMP no. 36485-b. 10, single blades from two adjacent folia; blade "a" of one folium overlaps blade "b" of the adjacent folium; ×500; hypotype, UCMP no. 36485-c.

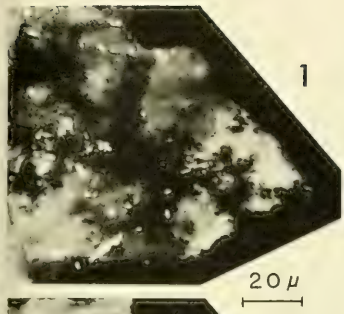
1
20 μ

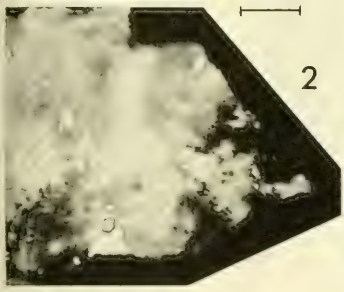
2


3
50 μ

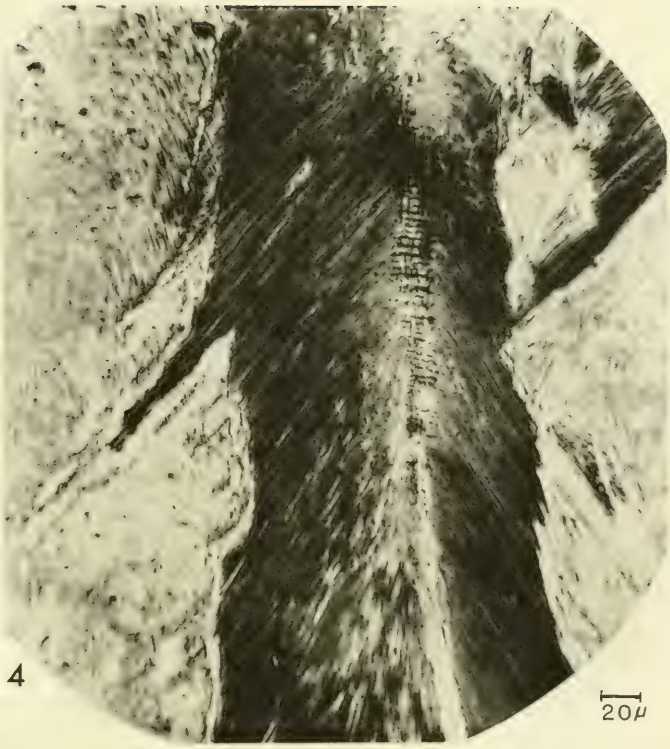
4
20μ

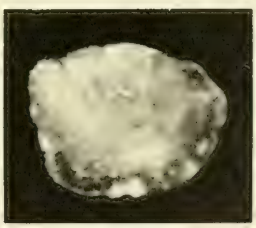
5

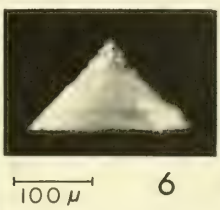
100 μ
6


20 μ
a
b


20 μ
9


7
20 μ


8

10

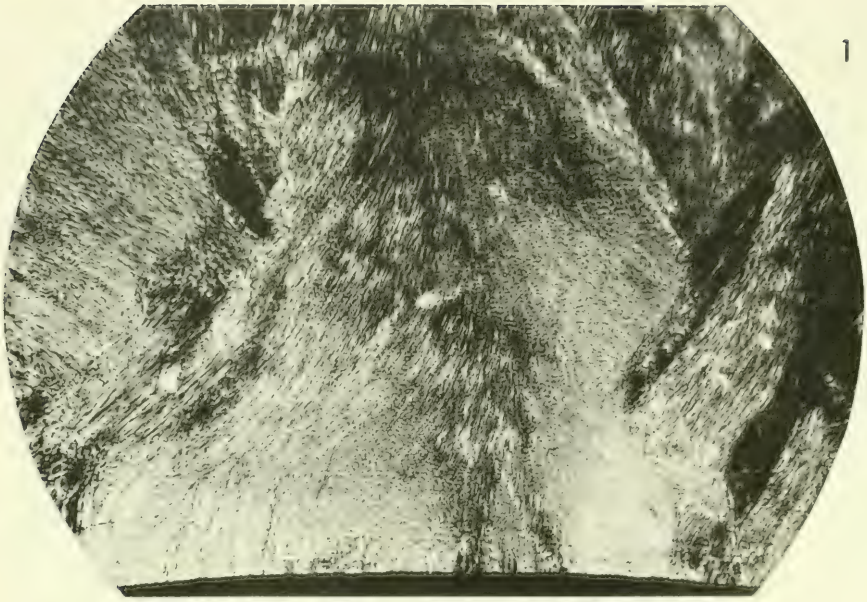

1

100 μ

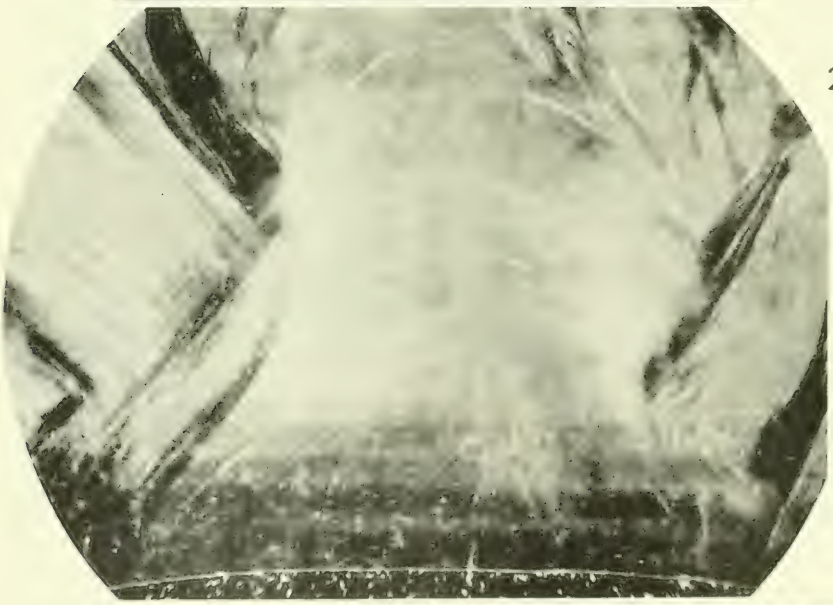

2

200 μ

3

EXPLANATION OF PLATE 22

Group 13 (figs. 1, 2), group 12 (fig. 3)

Figs. 1, 2—*Cellana testudinaria;* complex crossed-lamellar layer m — 1; median sagittal section through the flank of a major prism and parallel to the central axis of that prism; ×200; hypotype, UCMP no. 36485-a. 1, fan-shaped arrangement of traces of third-order lamellae; nicols partially uncrossed to 161°. 2, traces of conical second-order lamellae superimposed on traces of third-order lamellae; cone surfaces are visible only where a slight fracturing has taken place between cones; low-angle incident light.

Fig. 3—*Cellana radians;* vertically broken section through major prisms of the complex crossed-lamellar layer m — 1; low-angle incident light; ×60; hypotype, UCMP no. 36490-a.

EXPLANATION OF PLATE 23

Group 15 (figs. 1-4)

Figs. 1-4—*Acmaea mitra*. Structure of shell layers: m + 3, complex-prismatic; m + 2, foliated; m + 1, concentric crossed-lamellar. **1, 2,** section tangential to growth surfaces and normal to first-order prisms of the complex-prismatic layer m + 3; ×500; hypotype, UCMP no. 30797-b. **1,** one set of prisms at extinction. **2,** the other set of prisms at extinction; stage rotated 30° from the position shown in figure 1. **3, 4,** concentric section near margin of shell; arrows point anteriorly; hypotype, UCMP no. 30797-a. **3,** two sets of first-order prisms in layer m + 3; ×64. **4,** in this section parallel to blades of the foliated layer (m + 2), note that the folia are continuous (cf. Pl. 24, figs. 1, 2); note also the vertical intertonguing relationship between layers m + 2 and m + 1; ×200.

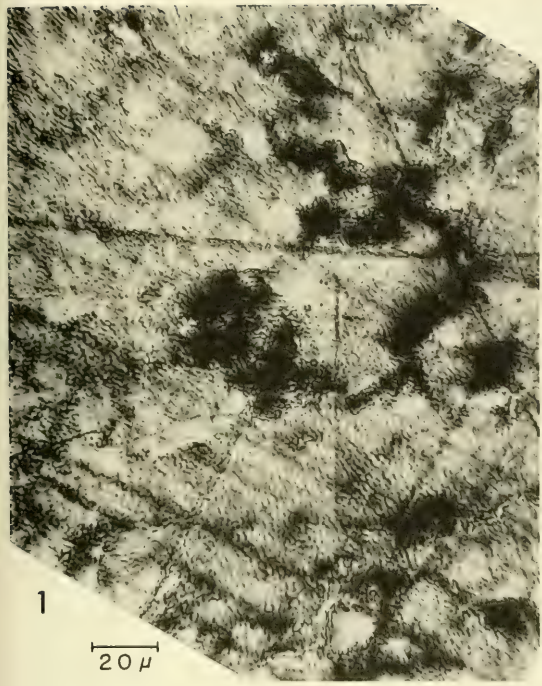
1
20 μ

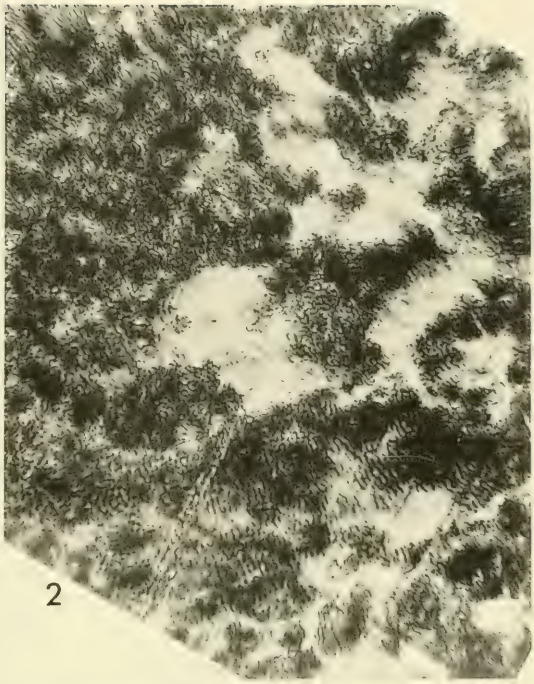
2


algae
m + 3
m + 2
500 μ
3

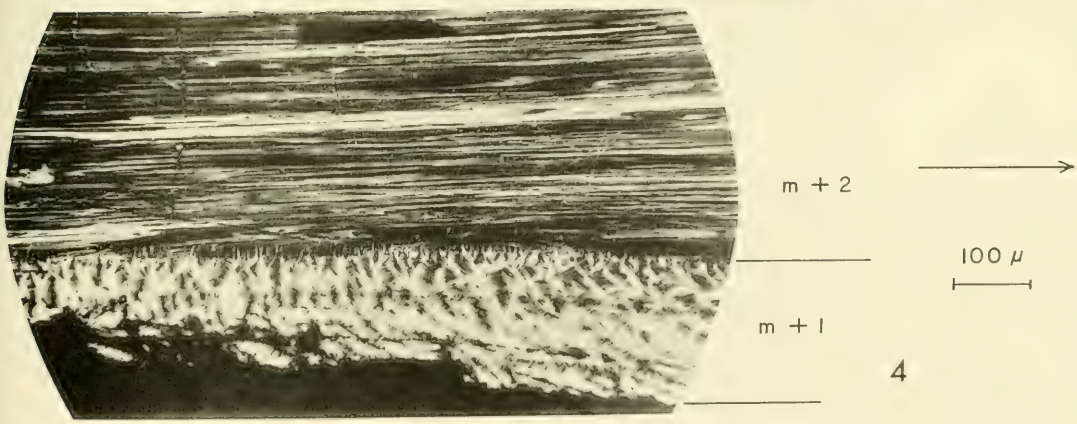
m + 2
100 μ
m + 1
4

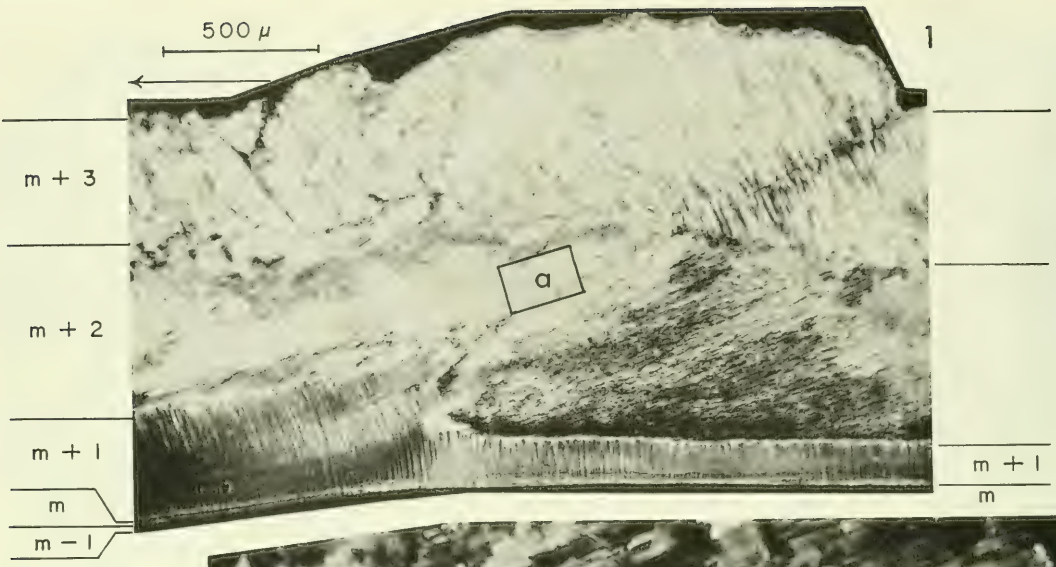
500 μ
1
m + 3
m + 2
m + 1
m
m − 1
a
m + 1
m


2
10 μ


3
20 μ

EXPLANATION OF PLATE 24

Group 15 (figs. 1-3)

Figs. 1-3—*Acmaea mitra*. Structure of shell layers: m + 3, complex-prismatic; m + 2, foliated; m + 1, concentric crossed-lamellar layer; m — 1, radial crossed-lamellar. **1, 2,** median sagittal section; hypotype, UCMP no. 30796-a. **1,** shell-layer sequence at the posterior part of the pedal-retractor scar; rectangular area at "a" is enlarged in figure 2; ×25.5. **2,** folia cut normal to the long axes of blades; note the "brick-wall" appearance caused by different extinction angles of blades; area enlarged from figure 1, a; ×360. **3,** section parallel to growth surfaces through foliated layer m + 2; note distinct, concentric trend of blades and the interrupted, but distinct trends of folia normal to the blade trend; double headed arrow indicates concentric direction; ×500; hypotype, UCMP no. 30797-b.

Fig. 1: contacts printed 1 mm too low.

EXPLANATION OF PLATE 25

Group 15 (figs. 1-3)

Figs. 1-3—*Lepeta concentrica;* median sagittal section. Structure of shell layers; m + 3, complex-prismatic; m + 2, foliated; m + 1, concentric crossed-lamellar; arrows point anteriorly; hypotype, UCMP no. 30798. **1,** section at anterior end of shell showing fan-shaped arrangement of fibrils in the complex-prismatic layer m + 3; ×200. **2, 3,** section near posterior end of shell showing the optical dependence of folia in layer m + 2 on the optical orientation of the prisms in layer m + 3; note that the dependence is expressed vertically through the foliated layer rather than laterally along folia (cf. Pl. 18, figs. 1, 2); ×500. **2,** one set of prisms and their optically dependent folia at or near extinction. **3,** the other set of prisms and folia at or near extinction; the stage is rotated 11° from the position shown in figure 2.

1

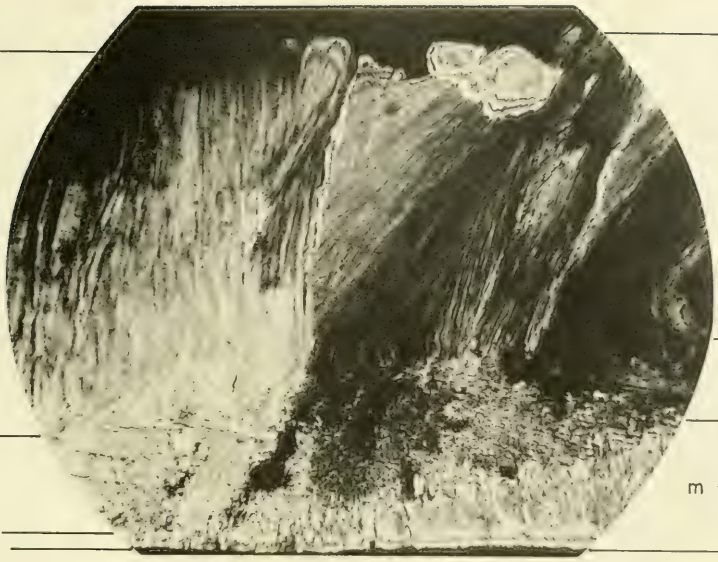

2

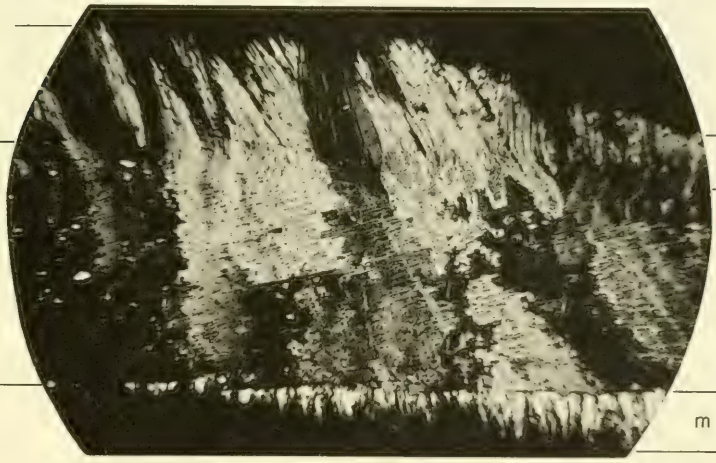

50 μ

3

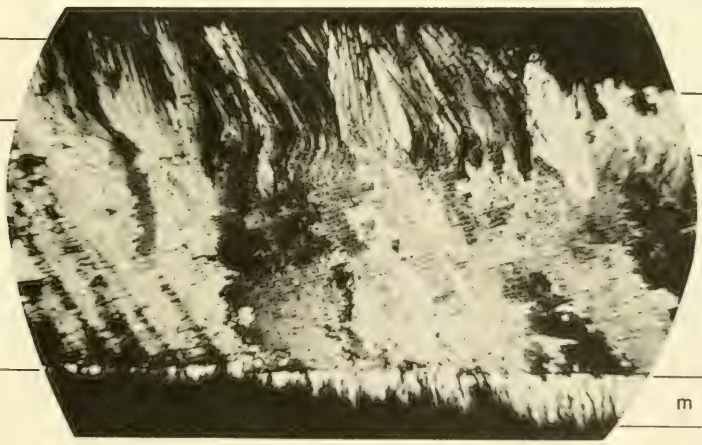

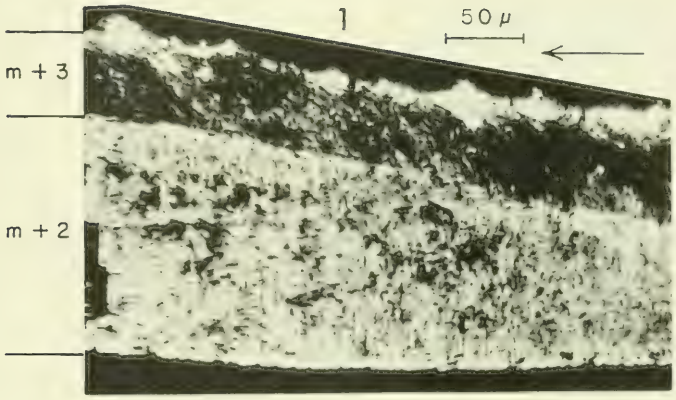
1
50 μ
m + 3
m + 2


m
m − 1
1 mm
3

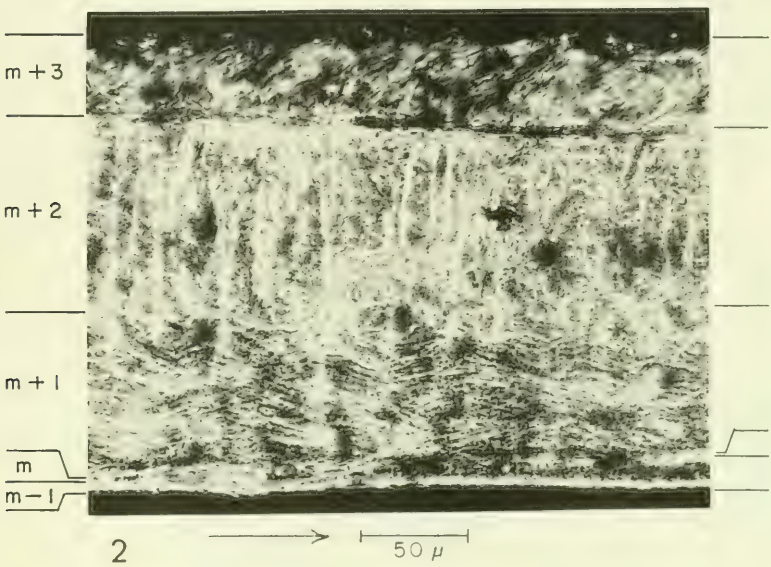
m + 3
m + 2
m + 1
m
m − 1
2
50 μ

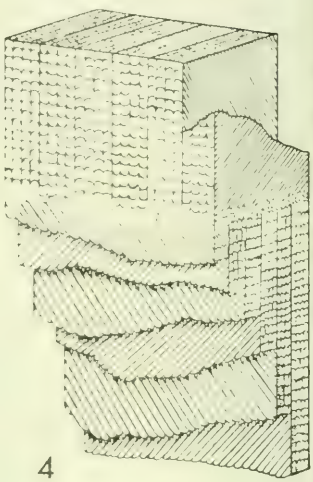
4

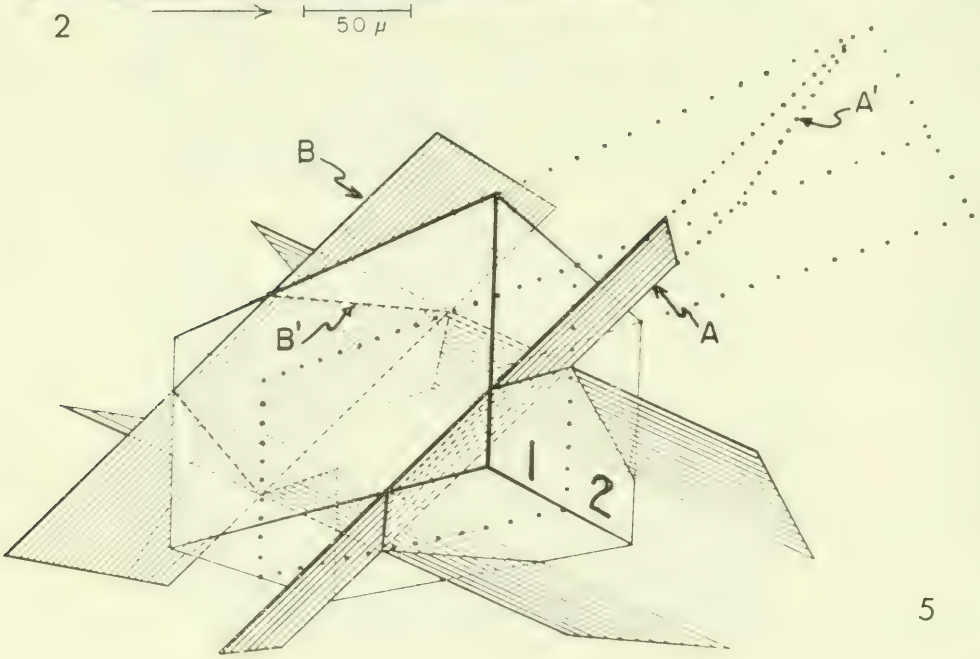
A'
B
B'
A
1
2
5

EXPLANATION OF PLATE 26

Group 17 (figs. 1, 2), group 10 (fig. 3), and early interpretations of the crossed-lamellar structure (figs. 4, 5).

Figs. 1, 2—*Proscutum elongatum;* vertical, radial section; arrows point adapically; hypotype, UCMP no. 34717. Structure of shell layers: m + 3, complex-prismatic?; m + 2, concentric crossed-lamellar; m + 1, radial crossed-lamellar; m — 1, radial crossed-lamellar. 1, section near margin of shell; ×80. 2, section between muscle scar and apex of shell; ×320.

Fig. 3—*Patella cochlear;* view of inner surface of shell showing part of a grooved ridge extending across pedal-retractor scar (m) at a constriction in the scar (see Text-fig. 68); incident light; ×36; hypotype, UCMP no. 36592.

Figs. 4, 5—Early interpretations of the crossed-lamellar structure. 4, after Nathusius-Königsborn (1877, Pl. 4, fig. 23, *fide* Biedermann, 1902, p. 93; 1914, Text-fig. 183); illustration shows two shell layers with first-order lamellae of one layer at right angles to first-order lamellae of the other. 5, after Thiem (1917b, Text-fig. 42); modified (with dotted lines) to show two adjacent *"Platten"* [first-order lamellae 1 and 2] and one extended *"Blättchen"* (A). As shown by the lines of intersection at A′ and B′ within *"Platten"* 1, *"Blättchen"* A and B are not parallel to each other.

EXPLANATION OF PLATE 27

Figs. 1-5—*Euphemites vittatus;* **1, 2,** tangential thin section comparing light source and observable structures; ×64; hypotype, USNM no. 144494-a. **1,** intertonguing first-order lamellae of the crossed-lamellar structure; low-angle incident light. **2,** same section showing only irregular patches of partially recrystallized shell; crossed nicols. **3,** small chip (viewed normal to growth surfaces) showing rectangular fretwork pattern at broken ends of first-order lamellae; low-angle incident light; ×120; hypotype, USNM no. 144494-c. **4, 5,** chip (viewed normal to growth surfaces) showing alternation of light-dark pattern of first-order lamellae with 180° change in light-source direction (see arrows); low-angle incident light; ×120; hypotype, USNM no. 144494-b. **4,** light from one direction. **5,** light from opposite direction.

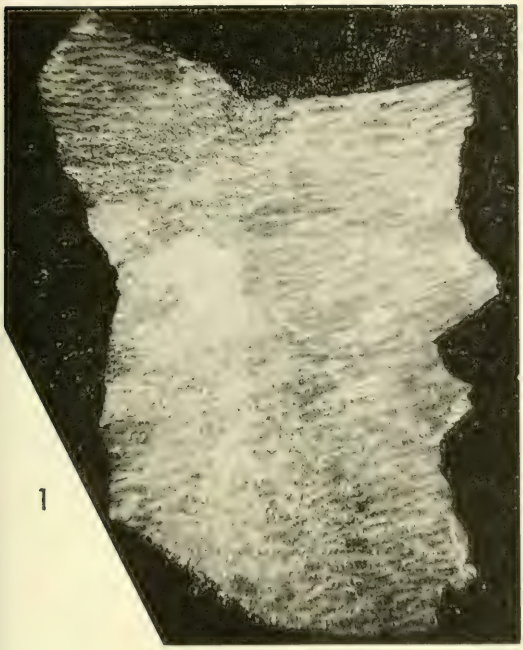

1

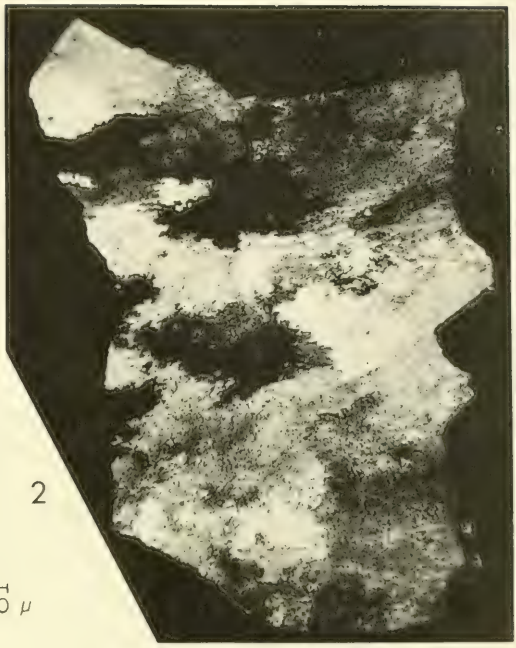

2

200 μ

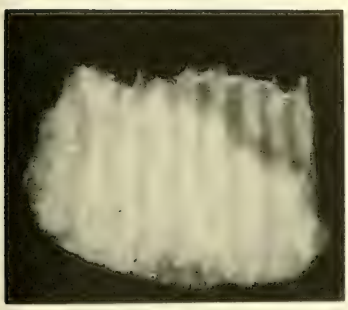

3

100 μ

4

100 μ

5

1

5 mm

S

S

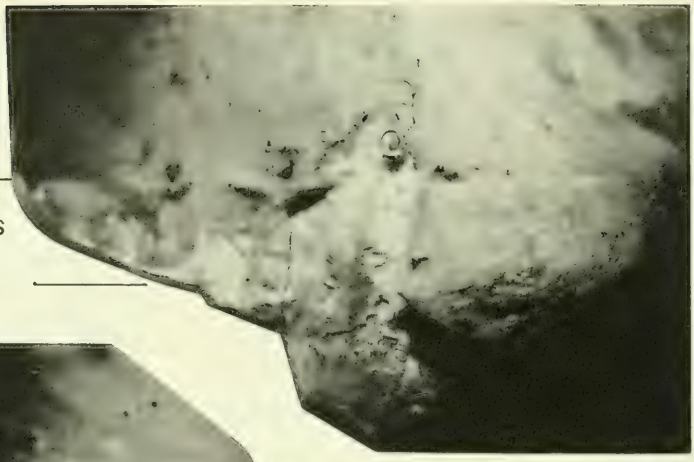

S

S

1 mm

2

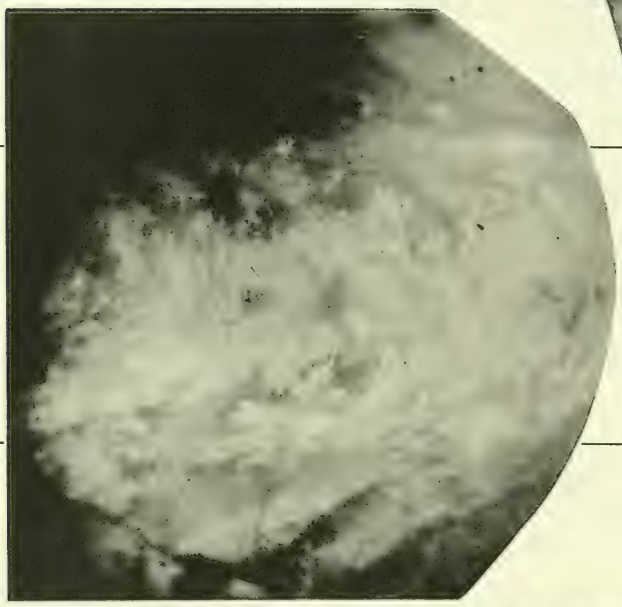

1 mm

S

S

3

EXPLANATION OF PLATE 28

Figs. 1-3—*Euphemites vittatus;* structural trends of first-order lamellae of the inner crossed-lamellar layer across the selenizone (s) at different depths in the shell; shell immersed in water; incident light; arrows point adaperturally; hypotype, USNM no. 144494. **1,** view of nearly whole shell including areas enlarged in figures 2 and 3; ×10. **2,** first-order lamellae forming a pattern concave adaperturally at the outer surface of the inner shell layer just under the thin perinductura (here ground away); ×30. **3,** first-order lamellae trending nearly straight across selenizone midway through inner shell layer; ×30.

EXPLANATION OF PLATE 29

Figs. 1-3—*Euphemites vittatus.* **1, 2,** polished tangential sections showing structural trends of first-order lamellae of the inner crossed-lamellar layer across the selenizone (s) at different depths in the shell; arrows point adaperturally; viewed from inside shell; low-angle incident light. **1,** central part of this polished section shows trend midway through the layer; here the first-order lamellae in and on either side of the selenizone form a pattern only slightly concave adaperturally; note that near the edges of the section, where the outer part of the inner layer is intersected, the trend becomes more concave adaperturally; ×32; hypotype, USNM no. 144495-b. **2,** central and adapical parts of this section, made one half a volution back from the aperture, show the trend at the inner surface of the layer to be sharply convex adaperturally; adaperturally this section intersects the outer parts of the inner shell layer and the pattern becomes, progressively, straight and then concave; ×32; hypotype, USNM no. 144495-a. **3,** weathered surface originally broken normal to shell surface and parallel to structural trend of first-order lamellae; note the intersecting dip angles of second-order lamellae; arrow points admedially; low-angle incident light; ×20; hypotype, USNM no. 144496-a.

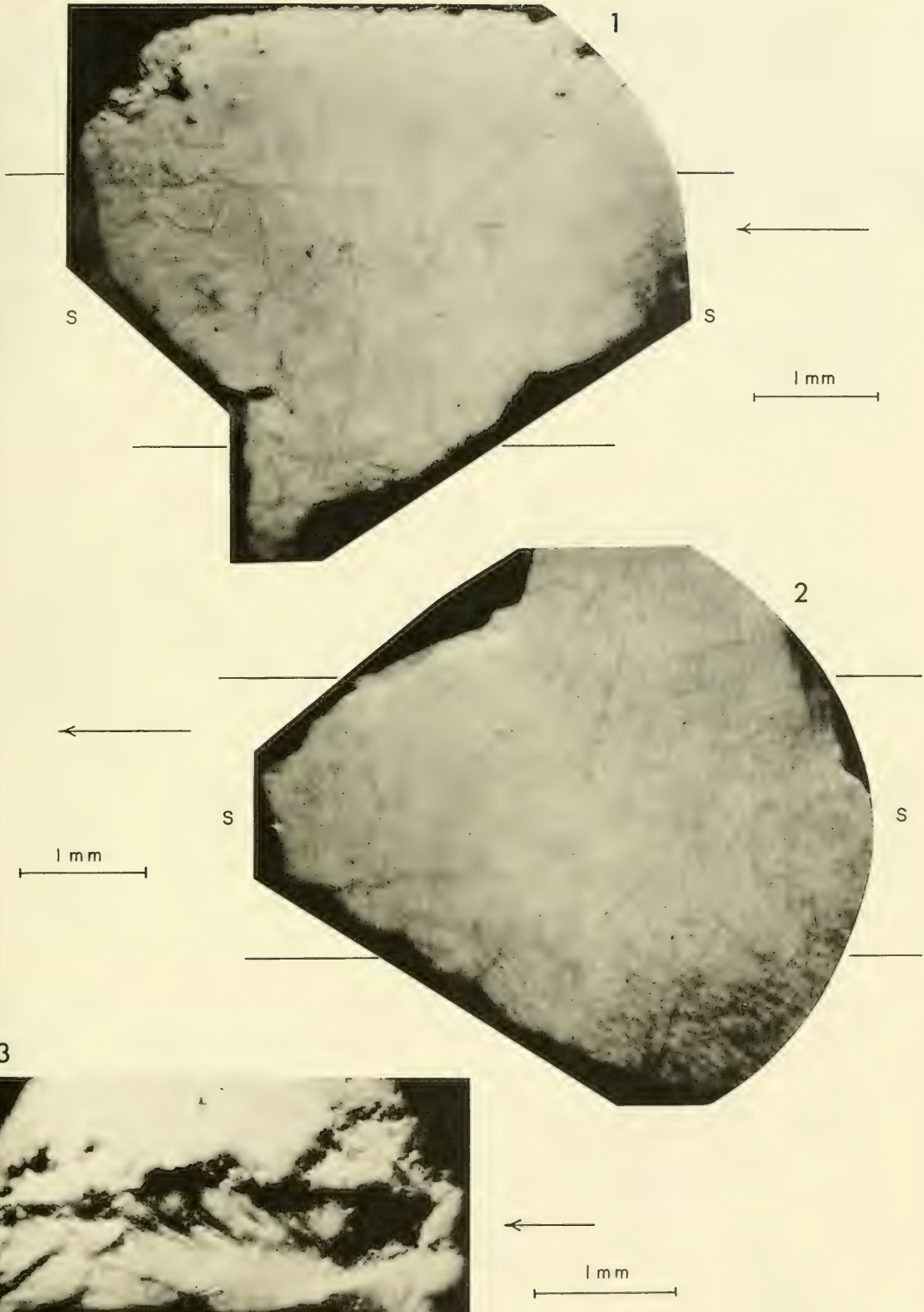
1
S
S
1 mm
2
S
S
1 mm
3
1 mm

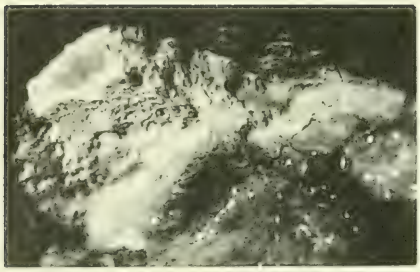

1

3 mm

100 μ

3

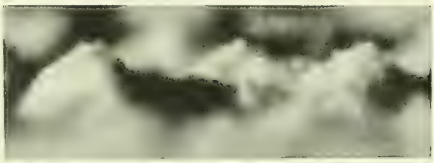

2

100 μ

100 μ

4

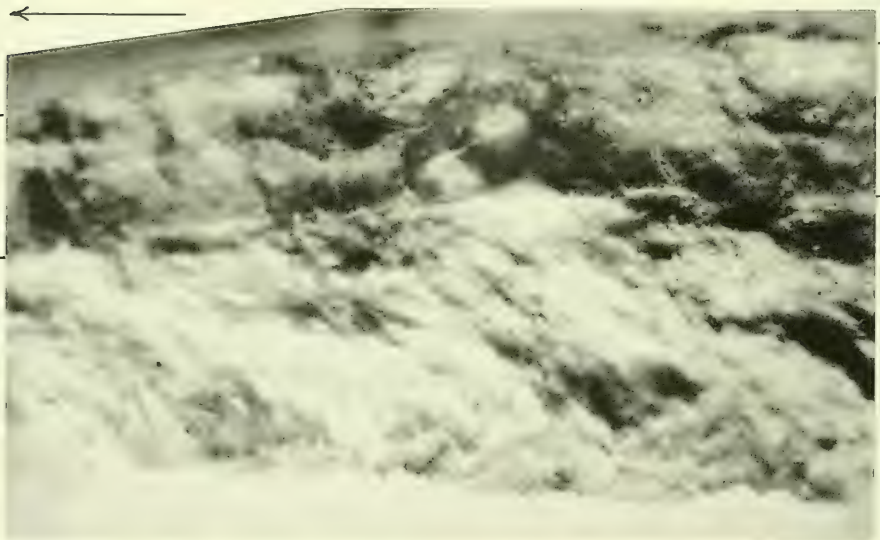

o

i

200 μ

o

i

5

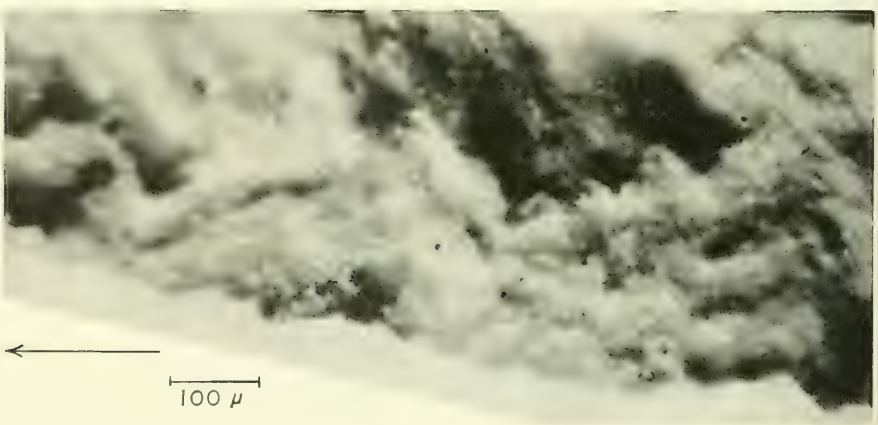

6

100 μ

EXPLANATION OF PLATE 30

Figs. 1-6—*Bellerophon (Pharkidonotus) percarinatus;* complex crossed-lamellar structure as observed in freshly broken area of one shell (see Text-fig. 126); incident light; hypotype, USNM no. 144498. **1,** general view of area; arrow points adapically; ×10. **2, 3,** side views of cones on growth surface; ×150. **2,** arrow points adapically. **3,** arrow points admedially. **4-6,** cross-sectional views of shell showing the chevron pattern which indicates the presence of conical second-order lamellae in major prisms. **4,** faintly visible chevron pattern in a single major prism; arrow points adapically; ×150. **5,** general cross-sectional view at right angles to the section seen in figure 4 but also showing the chevron pattern; a thin "homogeneous" outer layer (o) overlies the complex crossed-lamellar inner layer (i); note that the adlateral flanks of prism cones dominate the observable structure; arrow points admedially; ×60. **6,** enlargement of lower right hand part of the area seen in figure 5; ×150.

EXPLANATION OF PLATE 31

In figures 2-4 prism boundaries are emphasized by application of ink to shell.

Figs. 1, 2—*Bellerophon* (*Pharkidonotus*) *percarinatus;* complex crossed-lamellar structure viewed normal to freshly broken growth surfaces; low-angle incident light. 1, part of area shown in Pl. 30, fig. 1 looking down on sharply pointed conical ends of broken major prisms; ×150; hypotype, USNM no. 144498. 2, growth surface in upper part of complex crossed-lamellar layer (Text-fig. 126) showing "prismatic" appearance of major prisms; here the major prisms are rounded, not broken into sharp conical points; ×150; hypotype, USNM no. 144497.

Fig. 3—*Turbo marmoratus* Linnaeus: view of inner surface of shell along columellar lip showing contact between inner nacreous layer (n) and outer prismatic layer (p); low-angle incident light; ×60; hypotype, YPM no. 13372.

Fig. 4—*Bellerophon* (*Bellerophon*) sp.; view of outer surface of inner shell layer showing a "prismatic" pattern; low-angle incident light; ×150; hypotype, UCMP no. 30114.

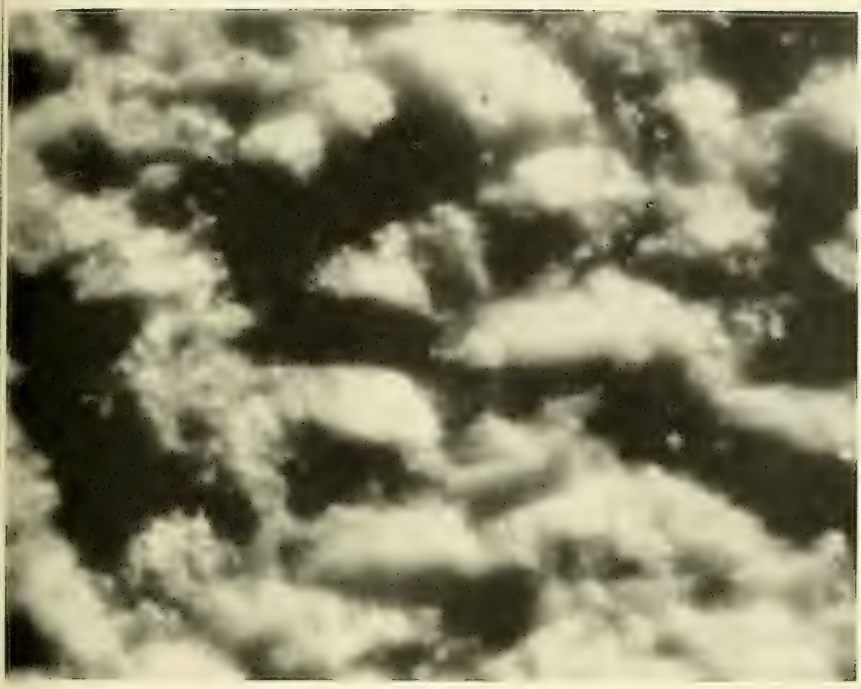

1

100 μ

200 μ

3

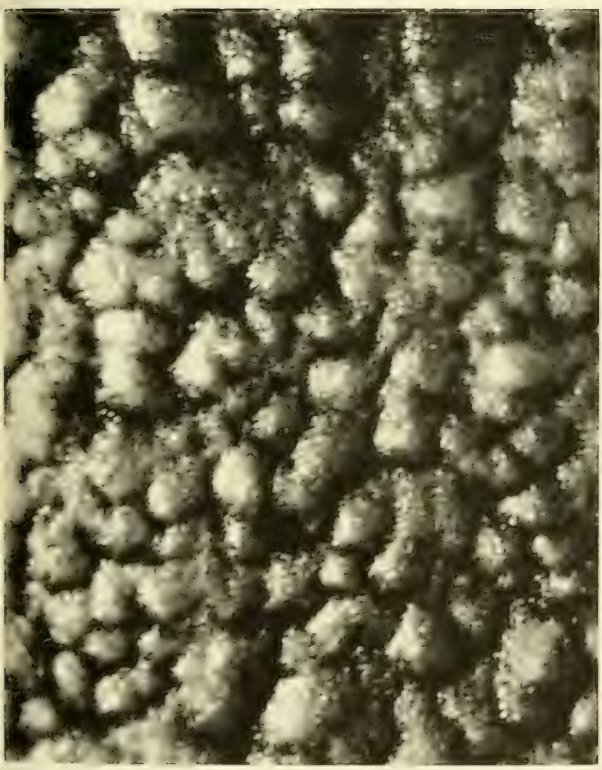

2

100 μ

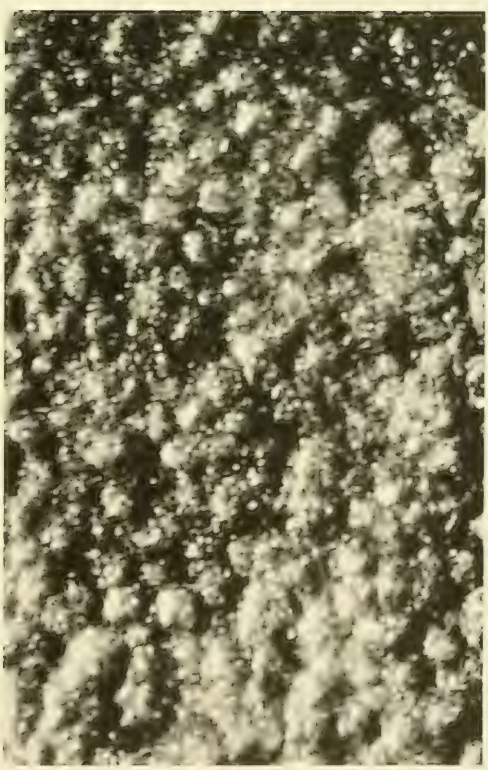

4

100 μ

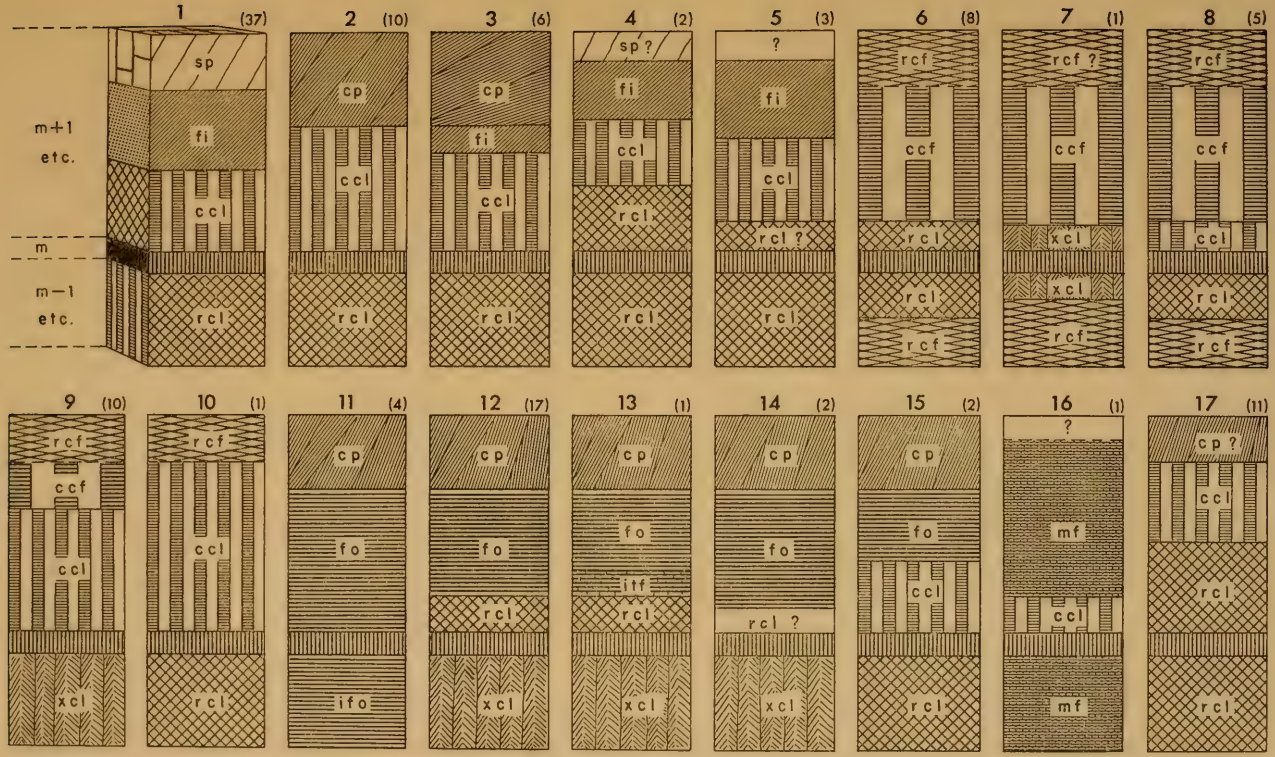

EXPLANATION OF PLATE 32

Generalized radial, columnar sections through patelloid shells (see Text-fig. 4; Table 5) comparing the 17 recognized shell-structure groups. The number of species examined per group is given in parentheses. Shell-layer thicknesses are approximately to scale except for very thin layers, such as the myostracum, where the vertical exaggeration is large. Group 1, illustrated in three dimensions, shows the related concentric section. Explanation of symbols is given below.

ccl, concentric crossed-lamellar
ccf, concentric crossed-foliated
cp, complex-prismatic
fi, fibrillar
fo, foliated
ifo, irregularly foliated
itf, irregularly tabulate foliated
m, myostracum (complex-prismatic structure)
m + 1 etc., shell layers dorsal to myostracum
m − 1 etc., shell layers ventral to myostracum
mf, modified foliated
rcf, radial crossed-foliated
rcl, radial crossed-lamellar
sp, simple-prismatic
xcl, complex crossed-lamellar